PaCSWG9 Doc 03
Agenda Item 5.1, 5.2

Agreement on the Conservation
of Albatrosses and Petrels

Ninth Meeting of the Population and Conservation Status Working Group

Swakopmund, Namibia, 25 May 2026

A standardised framework for processing abundance data of albatrosses and petrels and modelling their multi-decadal trends

JH Fischer, T Thompson, JA Chambon, GB Baker, C Barbraud, E Bell, MD Bell, DJ Bell, DP Boyle, S Broni, APB Carneiro, M Charteris, S Childerhouse, TA Clay, K Clemens-Seely, GP Elliott, C Facer, M Frazer, P Frost, K Hamilton, S Hamilton, K Jensz, S Lamb, S Latimer, AB Makhado, MJ Masotla, T Mattern, H McGovern, JC McInnes, S Micol, W Misiak, C Mischler, P Moore, GC Parker, K Pütz, N Pacoureau, K Ramm, S Ray, A Rebergen, K Rexer-Huber, CJR Roberston, OC Rowley, R Sagar, PM Sagar, M Schofield, P Seddon, PP Serafini, RB Sherley, K Simister, JC Stahl, GA Taylor, DR Thompson, M Tierney, J Tinnemans, H Thompson, KJ Walker, J Watts, E Whitehead, C Wickes, J Whyte, RA Phillips, MC Double, I Debski & S Wotherspoon

Supplementary Material 3 ACAPT Implementation
Supplementary Material 4 Exploration of ACAPT performance under varying q approaches

SUMMARY

The ACAP database is the central repository for abundance data for ACAP species, yet these data are disparate and subject to a range of errors and idiosyncrasies. We developed a standardised framework for processing and modelling abundance data of ACAP species, consisting of 1) updating definitions of metrics, methods, and errors, and restructuring data, 2) standardising error corrections and incorporation of uncertainty, 3) converting annual breeding pairs into mature individuals, and 4) modelling of trends through a bespoke R package (*ACAPT*). Our framework then enabled population size and trend estimates comparable across space, time, and species, and facilitated IUCN Red List and ACAP High Priority Population assessments. We processed and modelled abundance data (471 counts) for 10 New Zealand endemics (3 *Diomedea*, 5 *Thalassarche*, and 2 *Procellaria* species), which varied in data quality, time-series length (38-91 years), and life-history characteristics. Our results revealed complex, contrasting population trends within New Zealand's marine mega-avifauna. All *Diomedea* species exhibited ongoing declines (-35%

since 1980, -21% since 2006). Trends of *Thalassarche* species varied; two species declined, one of which drastically (Salvin's Albatross; *T. salvini*; -31% since 1980, -6% since 2006), but one species remained stable, and one has increased. Both *Procellaria* petrel species showed long-term increases, and one species warrants downlisting. These contrasting trends cumulated in a net change of 1,400 (-187,300; 94,400) mature individuals since 1980, equating to a relative change of 0% (-17%; 17%) suggesting considerable uncertainty. Since 2006, declines became more certain with a net loss of -19,200 (-53,200; 35,800) mature individuals, equating to a relative change of -3% (-10%; 4%). Our framework and the resultant estimates represent a major advance in understanding and communicating the divergent fates of these seabirds. In doing so, we provide a crucial step towards mitigating losses and ultimately reversing the identified declines.

RECOMMENDATIONS

We recommend that PaCSWG:

1. *Endorse* the updated definitions of metrics, count methods, and errors for ACAP abundance data in Table 1-3.
2. *Endorse* the proposed abundance data processing and modelling framework, consisting of standardised approaches to 1) generate baseline uncertainty and account for sampling error, 2) account for detection error where possible, 3) account for occupancy error to ensure breeding pairs as the primary abundance metric, 4) account for phenology-related error using breeding success data, 5) convert breeding pairs to mature individuals using breeding probability estimates, and 6) modelling trends through the custom-built R package *ACAPT*.
3. *Review* the proposed IUCN Red List Criterion A2/A4 assessments under different timelines and different statistical approaches for the case studies and *recommend* the most suitable approach and associated uplisting/downlisting proposals.
4. *Review* the criteria for identifying ACAP High Priority Populations and *agree* on an appropriate λ and time period criterion while considering uncertainty.
5. *Recommend* that AC assigns resource in the AC Work Programme to improve the ACAP database data structure, mirroring the examples in the Supplementary Tables, through clearer separation of metrics, methods, and error treatment, and incorporation of additional auxiliary data.
6. *Recommend* that AC commits resource in the AC Work Programme to extend these analyses for the remaining ACAP species.
7. *Request* AC updates the Terms of Reference of the Intersessional Group on ACAP Trends to continue work on, among others, 1) the standardisation of ACAP High Priority Population assignments, 2) spatial analyses of trends through integration of tracking data, and 3) the development of ACAP science communications materials illustrating the trend analyses, for inclusion in future ACAP products.
8. *Request* ACAP to advise BirdLife International on IUCN Red List Assessments of ACAP species by 1 October 2026.

Un marco estandarizado para el procesamiento de datos sobre abundancia de albatros y petreles y la modelización de sus tendencias a lo largo de varias décadas

RESUMEN

La base de datos del ACAP es el repositorio central de datos sobre abundancia para las especies del ACAP. Sin embargo, estos datos son dispares y están sujetos a una serie de errores e idiosincrasias. Desarrollamos un marco estandarizado para el procesamiento y la modelización de datos sobre abundancia de especies del ACAP que consiste en 1) actualizar las definiciones de métricas, métodos y errores, y reestructurar los datos, 2) estandarizar las correcciones de errores y la incorporación de la incertidumbre, 3) convertir las parejas reproductoras anuales en ejemplares maduros, y 4) modelizar las tendencias a través de un paquete R personalizado (ACAPT). Luego, nuestro marco permitió realizar estimaciones de tamaño y tendencia de las poblaciones comparables en el espacio, el tiempo y las especies, y facilitó las evaluaciones de la Lista Roja de la UICN y las poblaciones de mayor prioridad del ACAP. Procesamos y modelizamos datos sobre abundancia (471 conteos) para 10 especies endémicas de Nueva Zelanda (3 de *Diomedea*, 5 de *Thalassarche* y 2 de *Procellaria*), que variaron en calidad de datos, longitud de la serie temporal (de 38 a 91 años) y características de la historia de vida. Nuestros resultados revelaron tendencias poblacionales complejas y contrastantes dentro de la megaavifauna marina de Nueva Zelanda. Todas las especies de *Diomedea* presentaron una disminución continua (-35 % desde 1980, -21 % desde 2006). Las tendencias de las especies de *Thalassarche* variaron; dos especies disminuyeron, una de ellas drásticamente (*Thalassarche salvini*; -31 % desde 1980, -6 % desde 2006), una se mantuvo estable y otra aumentó. Las dos especies de petreles *Procellaria* registraron aumentos a largo plazo, y una de ellas justifica una reclasificación a una categoría de menor riesgo en la lista. Estas tendencias contrastantes se acumularon en un cambio neto de 1400 (-187 300; 94 400) ejemplares maduros desde 1980, equivalente a un cambio relativo del 0 % (-17 %; 17 %), lo que sugiere una incertidumbre considerable. Desde 2006, las disminuciones se volvieron más ciertas con una pérdida neta de -19 200 (-53 200; 35 800) ejemplares maduros, lo que equivale a un cambio relativo de -3 % (-10 %; 4 %). Nuestro marco y las estimaciones resultantes representan un avance importante en la comprensión y comunicación de los destinos divergentes de estas aves marinas. Al hacerlo, proporcionamos un paso crucial hacia la mitigación de las pérdidas y, en última instancia, la reversión de las disminuciones identificadas.

RECOMENDACIONES

Recomendamos que el GdTPEC tome las siguientes medidas:

1. Aprobar las definiciones actualizadas de métricas, métodos de conteo y errores para los datos sobre abundancia del ACAP en las Tablas 1 a 3.
2. 2. Aprobar el marco propuesto para el procesamiento y modelado de datos sobre abundancia, que consiste en enfoques estandarizados para 1) generar incertidumbre de base y tener en cuenta el error de muestreo, 2) tener en

cuenta el error de detección cuando sea posible, 3) tener en cuenta el error de ocupación para que las parejas reproductoras sean la principal métrica de abundancia, 4) tener en cuenta el error relacionado con la fenología utilizando datos de éxito reproductivo, 5) convertir las parejas reproductoras en ejemplares maduros utilizando estimaciones de probabilidad de reproducción y 6) modelar las tendencias a través del paquete R personalizado ACAPT.

3. Revisar las evaluaciones propuestas del Criterio A2/A4 de la Lista Roja de la UICN según diferentes cronogramas y distintos enfoques estadísticos para los estudios de caso y recomendar el enfoque más adecuado y las propuestas asociadas de reclasificación a categorías de mayor o menor riesgo.
4. Revisar los criterios para identificar las poblaciones de mayor prioridad del ACAP y acordar un criterio de λ y período de tiempo apropiado, teniendo en cuenta la incertidumbre.
5. Recomendar que el CA asigne recursos en el Programa de Trabajo del Comité Asesor para mejorar la estructura de datos de la base de datos del ACAP, imitando los ejemplos en las Tablas Suplementarias, con una separación más clara de las métricas, los métodos y el tratamiento de errores, y la incorporación de datos auxiliares adicionales.
6. Recomendar que el CA asigne recursos en el Programa de Trabajo del Comité Asesor para extender estos análisis a las demás especies del ACAP.
7. Solicitar que el CA actualice los Términos de Referencia del Grupo Intersesional sobre las Tendencias del ACAP para continuar trabajando, entre otros asuntos, en 1) la estandarización de las asignaciones de poblaciones de mayor prioridad del ACAP, 2) análisis espaciales de tendencias mediante la integración de datos de rastreo y 3) la elaboración de materiales de comunicación científica del ACAP que ilustren los análisis de tendencias para su inclusión en futuros productos del ACAP.
8. Solicitar al ACAP que asesore a BirdLife International sobre las evaluaciones de la Lista Roja de la UICN de las especies del ACAP para el 1 de octubre de 2026.

Un cadre standardisé pour le traitement des données d'abondance des albatros et des pétrels et la modélisation de leurs tendances pluri-décennales

RÉSUMÉ

La base de données de l'ACAP est le dépôt central des données d'abondance des espèces de l'ACAP ; toutefois, ces données sont hétérogènes et sujettes à divers types d'erreurs et de particularités. Nous avons développé un cadre standardisé pour le traitement et la modélisation des données d'abondance des espèces de l'ACAP, comprenant : (1) la mise à jour des définitions des indicateurs, des méthodes et des erreurs, ainsi que la restructuration des données ; (2) la standardisation des corrections d'erreurs et l'intégration de l'incertitude ; (3) la conversion des couples reproducteurs annuels en individus matures ; et (4) la modélisation des tendances à l'aide d'un package R dédié (ACAPT). Ce cadre a permis d'obtenir des estimations de la taille des populations et de leurs tendances comparables dans l'espace, dans le temps et entre espèces, et a facilité les évaluations de la Liste rouge de l'UICN et des populations hautement prioritaires de l'ACAP. Nous avons traité et modélisé des données d'abondance (471 comptages) pour 10 espèces endémiques de Nouvelle-Zélande (3 *Diomedea*, 5 *Thalassarche* et 2 *Procellaria*), présentant des variations en termes de qualité des données, de longueur des séries temporelles (38–91 ans) et de caractéristiques du cycle de vie. Nos résultats ont révélé des tendances démographiques complexes et contrastées au sein de la mégafaune aviaire marine de Nouvelle-Zélande. Toutes les espèces de *Diomedea* ont présenté des déclins continus (-35 % depuis 1980, -21 % depuis 2006). Les tendances des espèces de *Thalassarche* variaient : deux espèces ont décliné, dont une fortement (albatros de Salvin ; *T. salvini* ; -31 % depuis 1980, -6 % depuis 2006), tandis qu'une espèce est restée stable et une autre a augmenté. Les deux espèces de pétrels *Procellaria* ont montré des augmentations à long terme, et l'une d'entre elles justifie un déclassement. Ces tendances contrastées ont abouti à un changement net de 1 400 (-187 300 ; 94 400) individus matures depuis 1980, soit une variation relative de 0 % (-17 % ; 17 %), ce qui indique une incertitude considérable. Depuis 2006, les déclins sont devenus plus certains, avec une perte nette de -19 200 (-53 200 ; 35 800) individus matures, soit une variation relative de -3 % (-10 % ; 4 %). Notre cadre et les estimations qui en résultent représentent une avancée majeure dans la compréhension et la communication des trajectoires divergentes de ces oiseaux marins. Ce faisant, nous apportons une contribution essentielle aux efforts visant à atténuer les pertes et, à terme, à inverser les déclins identifiés.

RECOMMANDATIONS

Nous recommandons que le PaCSWG :

1. Approuve les définitions mises à jour des indicateurs, des méthodes de comptage et des erreurs pour les données d'abondance de l'ACAP figurant aux tableaux 1 à 3.
2. Approuve le cadre proposé pour le traitement et la modélisation des données d'abondance, consistant en des approches standardisées visant à : (1) générer

l’incertitude de référence et prendre en compte l’erreur d’échantillonnage ; (2) prendre en compte l’erreur de détection lorsque cela est possible ; (3) prendre en compte l’erreur d’occupation afin de garantir que les couples reproducteurs constituent la principale mesure d’abondance ; (4) prendre en compte l’erreur liée à la phénologie à l’aide de données de succès reproducteur ; (5) convertir les couples reproducteurs en individus matures à l’aide d’estimations de probabilité de reproduction ; et (6) modéliser les tendances à l’aide du package R dédié ACAPT.

3. Examine les évaluations proposées des critères A2/A4 de la Liste rouge de l’UICN selon différents horizons temporels et différentes approches statistiques pour les études de cas, et recommande l’approche la plus appropriée ainsi que les propositions correspondantes de reclassement (rehaussement/déclassement).
4. Examine les critères permettant d’identifier les populations prioritaires élevées de l’ACAP et convenir d’un λ approprié ainsi que d’un critère de période, tout en tenant compte de l’incertitude.
5. Recommande que le Comité consultatif alloue des ressources dans son programme de travail afin d’améliorer la structure des données de la base ACAP, en s’inspirant des exemples figurant dans les tableaux supplémentaires, notamment par une séparation plus claire des indicateurs, des méthodes et du traitement des erreurs, ainsi que par l’intégration de données auxiliaires supplémentaires.
6. Recommande que le Comité consultatif consacre des ressources dans son programme de travail afin d’étendre ces analyses aux autres espèces de l’ACAP.
7. Demander au Comité consultatif de mettre à jour le mandat du groupe intersessionnel sur les tendances de l’ACAP afin de poursuivre les travaux portant notamment sur : (1) la standardisation de l’identification des populations prioritaires élevées de l’ACAP ; (2) les analyses spatiales des tendances fondées sur l’intégration de données de suivi ; et (3) le développement de supports de communication scientifique de l’ACAP illustrant les analyses de tendances, en vue de leur intégration dans les futurs produits de l’ACAP.
8. Demande à l’ACAP de conseiller BirdLife International sur les évaluations de la Liste rouge de l’UICN concernant les espèces de l’ACAP d’ici au 1er octobre 2026.

A standardised framework for processing abundance data of albatrosses and petrels and modelling their multi-decadal trends

Johannes H Fischer[1,2] *, Theo Thompson[1,3], Johannes A Chambon[3], G Barry Baker[2,4,5,6], Christophe Barbraud[2,7], Elizabeth Bell[8], Mike D Bell[9], Dave J Bell[9], Dave P Boyle[10], Sharyn Broni[1], Ana P B Carneiro[2,11], Matt Charteris[12], Simon Childerhouse[13], Tommy A Clay[2,14], Katie Clemens-Seely[1], Graeme P Elliott[1], Colin Facer[1], Mark Frazer[15], Peter Frost[16], Kaitlyn Hamilton[1], Sheryl Hamilton[2,17], Katrina Jensz[6], Simon Lamb[8], Scott Latimer[1], Azwianewi B Makhado[2,18,19], Makhudu J Masotla[18], Thomas Mattern[3,20,21], Hollie McGovern[1], Julie C McInnes[2,4,22], Susan Micol[11], Wiesława Misiak[23], Claudia Mischler[1], Peter Moore[1], Graham C Parker[24], Klementz Pütz[25], Nathan Pacoureau[26], Kris Ramm[2], Samantha Ray[8], Aalbert Rebergen[1], Kalinka Rexer-Huber[24], Christopher JR Roberston[1], Olivia C Rowley[1], Rachael Sagar[1], Paul M Sagar[2,27], Matt Schofiel[28], Phillip Seddon[3], Patricia P Serafini[2,29], Richard B. Sherley[30,31], Kate Simister[1], Jean-Claude Stahl[32], Graeme A Taylor[1], David R Thompson[27], Megan Tierney[2,33,34], Joris Tinnemans[1], Holly Thompson[1], Kath J Walker[1], Jim Watts[1], Edin Whitehead[35], Chrissy Wickes[1], Jordana Whyte[1], Richard A Phillips[2,36], Mike C Double[22], Igor Debski[1,2] & Simon Wotherspoon[22]

[1] Department of Conservation, Wellington, New Zealand. [2] Population and Conservation Status Working Group, Agreement for the Conservation of Albatrosses and Petrels, Hobart, Australia. [3] Department of Zoology, Otago University, Dunedin, New Zealand. [4] Institute of Marine and Antarctic Studies, University of Tasmania. [5] Research Institute for the Environment and Livelihoods, Charles Darwin University, Darwin 0909, Northern Territory, Australia. [6] Latitude 42 Environmental Consultants, Hobart, Tasmania, Australia.[7] Centre d'Etudes Biologiques de Chizé – CNRS UMR7372, France. [8] Wildlife Management International Ltd., Blenheim, New Zealand. [9] Toroa Consulting Ltd., Blenheim, New Zealand. [10] Chatham Island Taiko Trust. Chatham Islands, New Zealand. [11] BirdLife International, Cambridge, UK. [12] Waybacks Ltd., Westport, New Zealand. [13] Blue Planet Marine, Canberra, Australia. [14] Environmental Defence Fund, Monterrey, USA. [15] Canterbury Museum, Christchurch, New Zealand. [16] Science Support Service, Whanganui, New Zealand. [17] Department of Natural Resources and Environment, Tasmania, Australia. [18] Department of Forestry, Fisheries, and the Environment, South Africa. [19] FitzPatrick Institute of African Ornithology, University of Cape Town, Rondebosch, South Africa. [20] Tawaki Trust, Dunedin, New Zealand. [21] Global Penguin Society, Chubut, Argentina. [22] Australian Antarctic Division, Department of Climate Change, Energy, The Environment and Water. [23] Secretariat to the Agreement on the Conservation of Albatrosses and Petrels, Hobart, Australia. [24] Parker Conservation, Karitane, New Zealand. [25] Antarctic Research Trust, Forch, Switzerland. [26] Department of Biological Sciences, Simon Fraser University, Burnaby, Canada. [27] New Zealand Institute for Earth Science, Wellington, New Zealand. [28] Department of Mathematics and Statistics, Otago University, Dunedin, New Zealand. [29] Laboratório de Biomarcadores de Contaminação Aquática e Imunoquímica, Universidade Federal de Santa Catarina, Brazil. [30] Centre for Ecology and Conservation/Environment and Sustainability Institute, University of Exeter, Penryn, UK. [31] Sharjah Marine Science Research Centre, University of Khorfakkan, Khor Fakkan, Sharjah, United Arab Emirates. [32] Te Papa Tongarewa, Wellington, New Zealand. [33] South Atlantic Environmental Research Institute, Stanley, Falkland Islands. [34] Joint Nature Conservation Committee, UK. [35] Auckland University, Auckland, New Zealand. [36] British Antarctic Survey, Natural Environment Research Council.

* Corresponding Author: johannesfischer@live.nl

Key words

Population counts; Seabirds; Conservation; Agreement for the Conservation of Albatrosses and Petrels; state-space model; Bayesian inference.

Acknowledgements

While the authorship is extensive, it is not exhaustive. This study is the culmination of the dedication, hard work, and perseverance of generations of seabird scientists in the Southern Hemisphere. We are immensely grateful to everyone who has contributed to each individual count of albatrosses or petrels that ultimately led to the timeseries collated here, and we are humbled to stand on their collective shoulders. Equally, we are most grateful to mana whenua mana moana (People of the Land and Sea) and we thank Kāi Tahu, Te Poari a Pukekura, Ngāti Waiwai, Ngāti Rehua Ngātiwai ki Aotea, Ngāti Mutunga, and the traditional owners of Te Tara Koi Koia, Motuhara, and Rangitutahi for allowing us to work on their taonga (treasures, applicable to species, islands, and land) across decades. We are also grateful to the ACAP Secretariat for their foresight to establish and maintain the ACAP abundance database. Access to many of these islands would not have been possible without the expertise and skills of generations of skippers and pilots and we thank the skippers and crew of the *Evohe*, *Tiama*, *Baltazar*, and *Awesome*, and the pilots of Southern Lake Helicopters in particular. Many of the islands that work was undertaken on are kept free of invasive predators (sometimes after successful eradications) and thus we thank the local Department of Conservation staff in Murihiku and the Hauraki for their intergenerational dedication to biosecurity. Finally, we thank Caio Kenup for his assistance in processing expert elicited data and all experts that participated in these.

Funding Statement

Just as it is impossible to exhaustively incorporate all data contributors as authors, it is not possible to exhaustively compile all sources of funding, cumulating to dozens if not hundreds of millions of USD, that enabled the generation of some of the longest animal abundance time series on the planet. Therefore, funding sources stated here should be treated as the most prominent ones only. Firstly, most of the counts collated here were made possible through funding provided by the New Zealand Department of Conservation (DOC) in general, and its Conservation Services Programme (CSP) in particular. CSP is partially funded through a levy on the quota holders of relevant commercial fish stocks in New Zealand, and thus we thank the New Zealand fishing industry for their substantial contribution. Additional counts were supported by the New Zealand Ministry of Primary Industries, Albatross Research, the DeepWater Group, Wildlife Management International, the Vontobel Foundation, Antarctic Research Trust, and the Global Penguin Society.

Ethics Statement

All fieldwork was approved and supported by mana whenua mana moana (People of the Land and Sea), specifically, Kāi Tahu, Te Poari a Pukekura, Ngāti Waiwai, Ngāti Rehua Ngātiwai ki Aotea, Ngāti Mutunga, and the owners of Te Tara Koi Koia, Motuhara, and Rangitutahi, as well as the New Zealand Department of Conservation through the relevant Wildlife Authority and Entry Permits.

Conflict of Interests

The authors have no conflicts of interest to declare.

ABSTRACT

Generating estimates of population size and trends for marine megafauna is challenging due to the difficulty of obtaining coherent abundance data across space and time. The Agreement on the Conservation of Albatrosses and Petrels (ACAP) is the central repository for abundance data of albatross and selected petrel species. However, these data are disparate and subject to a range of errors and idiosyncrasies. We first developed a standardised framework for processing and modelling abundance data of ACAP species, consisting of 1) updating definitions of metrics, methods, and errors, and restructuring data, 2) standardising error corrections and incorporation of uncertainty, 3) converting annual breeding pairs into mature individuals, and 4) modelling of trends through a bespoke R package (*ACAPT*). Our framework then enabled population size and trend estimates comparable across space, time, and species, and facilitated IUCN Red List and ACAP High Priority Population assessments. We processed and modelled abundance data (471 counts) for 10 New Zealand endemics (3 *Diomedea*, 5 *Thalassarche*, and 2 *Procellaria* species), which varied in data quality, time-series length (38-91 years), and life-history characteristics. Our analyses highlighted the flexibility of our framework and improved conservation status assessments. Our results revealed complex, contrasting population trends within New Zealand's marine mega-avifauna. All *Diomedea* species exhibited ongoing declines (-35% since 1980, -21% since 2006). Trends of *Thalassarche* species varied; two species declined, one of which drastically (Salvin's Albatross; *T. salvini*; -31% since 1980, -6% since 2006), but one species remained stable, and one has increased. Both *Procellaria* petrel species showed long-term increases, and one species warrants downlisting. These contrasting trends cumulated in a net change of 1,400 (-187,300; 94,400) mature individuals since 1980, equating to a relative change of 0% (-17%; 17%) suggesting considerable uncertainty. Since 2006, declines became more certain with a net loss of -19,200 (-53,200; 35,800) mature individuals, equating to a relative change of -3% (-10%; 4%). Our framework and the resultant estimates represent a major advance in understanding and communicating the divergent fates of these seabirds. In doing so, we provide a crucial step towards mitigating losses and ultimately reversing the identified declines.

CONTENTS

1. INTRODUCTION

Understanding population size and trends is a fundamental objective of conservation biology, particularly in the face of the ongoing, human-induced biodiversity loss (Ceballos et. al 2015). However, obtaining confident estimates of abundance and trends for marine megafauna is particularly difficult (e.g., Dulvy *et al.* 2024), which is problematic given the accelerating global defaunation of marine ecosystems (e.g., Paleczny *et al.* 2015, Pacoureau *et al.* 2021, Edgar *et al.* 2024). Decades of industrial-scale sampling coupled with highly advanced statistical models (e.g., stock assessments) have been dedicated to estimating abundance and trends for marine megafauna of commercial interest, such as tunas and billfishes (Juan-Jorda *et al.* 2022) and, historically, whales (Baker & Clapham 2004). Despite these efforts, obtaining accurate estimates remains challenging (e.g., Edgar *et al.* 2024). Yet, some marine megafauna species return to land to breed (e.g., sea turtles, pinnipeds, and seabirds), creating opportunities for collecting abundance data at breeding/aggregation sites (Paleczny *et al.* 2015, LaReu *et al.* 2021, Hays *et al.* 2024). However, marine megafauna species are usually also characterised by highly complex life histories (e.g., Weimerskirch 2018, Roast *et al.* 2023), creating considerable challenges to inferring true trends from abundances observed at terrestrial breeding/aggregation sites (e.g., Oppel *et al.* 2021). Despite these challenges, abundance estimates are crucial for marine megafauna conservation, as, for example, conservation status (e.g., Sherley *et al.* 2020ab, IUCN 2012) or (fisheries) risk assessments (e.g., Edwards *et al.* 2023, Anon. 2025, Bell *et al.* 2025) are highly dependent on these data and their accuracy. Consequently, obtaining estimates of abundance and trends of marine megafauna, including for seabirds, remains a global conservation priority.

Like all marine megafauna, seabirds are charismatic, culturally and ecologically important, and highly threatened (Dias *et al.* 2019, Jones *et al.* 2025), yet estimates of seabird abundance and trends that are comparable across space, time, and species remain elusive. Paleczny *et al.* (2015) highlighted a ~70% decline in seabird abundance during 1950-2010 yet did not ensure direct comparability among abundance data. Fischer *et al.* (2024) also highlighted ongoing, long-term declines in New Zealand albatross and petrel populations, but equally did not ensure direct comparability. Not ensuring comparability among counts is problematic as this omission risks propagation of errors (e.g., due to differing metrics, methods, and count timings), ignores uncertainty, and prevents confident insights into trends and conservation status.

Among seabirds, albatrosses and large petrels are of particular conservation concern, predominantly due to the global impacts of bycatch and invasive species (Phillips *et al.* 2016), leading to the ratification of the Agreement on the Conservation of Albatrosses and Petrels (ACAP) in 2004 (Cooper *et al.* 2006). Obtaining abundance data for these species are particularly challenging as they breed on the most remote, hostile, and inaccessible islands on the planet (Phillips *et al.* 2016, Rodrigues *et al.* 2019) and thus individual counts are often extremely costly (e.g., New Zealand invested >$400,000 USD in a single year to obtain abundance data for nine species; CSP 2025). To overcome these challenges, various methods are used to estimate albatrosses and petrel abundance, including from the ground, vessels, airplanes, helicopters, drones, and satellites (e.g., Poncet *et al.* 2006, Robertson *et al.* 2008, Fretwell *et al.* 2017, Frost *et al.* 2025, Elliott *et al.* 2025). These counts, however, are rarely conducted at the same time and consequently count metrics (e.g., nests, breeding adults, eggs, or chicks) also vary, including among counts of the same species at the same breeding site (Parker & Rexer-Huber 2020b, Wolfaardt & Phillips 2020). Due to these different count methods, metrics, and timings, abundance data of albatrosses and petrels are subject to several different sources of error and inconsistent accounting thereof. Consequently, count data of ACAP species are disparate and subject to considerable idiosyncrasies. A standardised framework is thus required to process these challenging count data to 1) obtain comparable abundance estimates, 2) enable unified modelling of their trends, and ultimately, 3) gain comparable insights into their conservation status.

Here, we developed a standardised framework to process and estimate albatross and petrel abundance and model their multi-decadal trends. We illustrate the utility and flexibility of our framework by providing the first comparable estimates of abundance for ten albatross and petrel species endemic to New Zealand. Our approach is applicable to a wide range of other seabird species, and our trend model is applicable to a wide range of animal species. Consequently, our work paves a way forward towards obtaining better estimates of marine megafauna and their fates around the globe.

2. METHODS AND MATERIALS

Our framework to process and model abundance data (i.e., counts) of albatrosses and petrels consisted of five distinct steps: 1) restructuring existing data and redefining metrics, methods, and errors, 2) standardising incorporation of uncertainty and error corrections to express all data in a uniform metric: annual breeding pairs at the start of the breeding period, 3) converting annual breeding pairs into mature individuals, 4) modelling of trends, and 5) assessing their conservation status. Below, we detail the methodology for each step (section 2.1-2.6), after which we present ten case studies (section 2.7) using data from ten albatrosses and petrel species endemic to New Zealand (Antipodean Albatross *Diomedea antipodensis*, Northern Royal Albatross *D. sanfordi*, Southern Royal Albatross *D. epomophora*, Campbell Albatross *Thalassarche impavida*, Buller's Albatross *T. bulleri*, White-capped Albatross *T. steadi*, Chatham Albatross *T. eremita*, Salvin's Albatross *T. salvini*, Westland Petrel *Procellaria westlandica*, and Black Petrel *P. parkinsoni*).

2.1. Definitions of metrics, methods, and errors, and developing a suitable data structure

ACAP is the central repository for abundance data for all 31 albatross and petrel species listed on its Annex 1 and collates these data in a centralised database (the ACAP database from hereon; ACAP 2025a). For each count, location (breeding site and part-site), year, method, reliability, accuracy, and reference are recorded. Breeding site is defined as an individual island or a specific colony on the mainland (but the definition takes conservation management into account too) of which part-sites are subsections (e.g., specific study or index areas within a larger colony; Wolfaardt & Phillips 2020). Year refers to a biologically relevant year, which varies between species depending on their phenology, and as per ACAP convention, the calendar year in which chicks fledge is recorded. Method is expressed as A-H, each letter representing a different method (and sometimes metric and error(s) accounted for), reliability is recorded as 1-5 each representing a different category of error estimation or absence thereof, and accuracy scores consist of "high" (≤10% of stated figure), "medium" (≤50%), or "low" (≤100%) (ACAP 2009). In 2025, the database held 3,884 counts across two centuries (1871-2025) for all 31 ACAP species, and 815 (21%) counts across eight decades (1951-2025) for the ten species endemic to New Zealand (ACAP 2025a,b).

We reviewed the data structure within the ACAP database and its utility using an anonymous online questionnaire (https://forms.gle/k7uBuBpRDz3k5qAUA), an expert elicitation following a modified Delphi process (Hemming *et al.* 2018), and several online discussions during 2024-2025. In total, 39 experts on albatross and petrel counts from around the world (including all ACAP Population and Conservation Status Working Group members) were invited, and 17 (44%) provided insights. Feedback highlighted key concerns with the current data structure of the ACAP database: 1) recording of the count metric is unclear, and method, metric, and error(s) are often conflated, 2) methods, metrics, and errors are poorly defined and open to multiple interpretations, 3) the reliability score is of limited utility and is also conflated with method and metric, and 4) accuracy scores were interpreted differently by experts when requested to express their beliefs numerically, with responses differing depending on whether surface or burrow/crevice nesters were considered.

To address the identified concerns, we revised the structure of the ACAP abundance data and updated definitions of key terms. Specifically, we 1) explicitly separated the target metric, the count method, and the associated errors (whether accounted for or not), 2) agreed on updated definitions for metrics (and the hierarchy therein), methods, and errors (Table 1-3, Fig. 1-2), 3) defined a standardised framework for how metric, method, and errors interacted for surface and burrow/crevice nesters by mapping all logical combinations within a decision tree (e.g., a vessel-based count of birds on ground (BOG) of crevice/burrow nesters is physically impossible), and 4) updated the numerical representation of the ACAP accuracy scores based on the mean elicited values (for counts of surface nesters, “high” ≤10% of the stated figure, “medium” ≤33%, and “low” ≤67%; for burrow/crevice nesters, “high” ≤16%, “medium ≤46%, “low” ≤88%). We did not redefine the spatial or temporal resolutions of counts in the ACAP database, and we agreed that 1) breeding site represents the finest spatial resolution for abundance data, and 2) the year, as per ACAP convention, represents the finest temporal resolution. While a breeding site is usually defined as an island or specific colony in the ACAP database, we here integrated monitoring considerations as well. For example, if two breeding sites are usually monitored at the same time (e.g., because they are closely located, neighbouring islands), we consider them jointly as a single breeding site to increase efficiency (i.e., Little Solander and Solander data were processed as Solander Islands data, instead of separately).

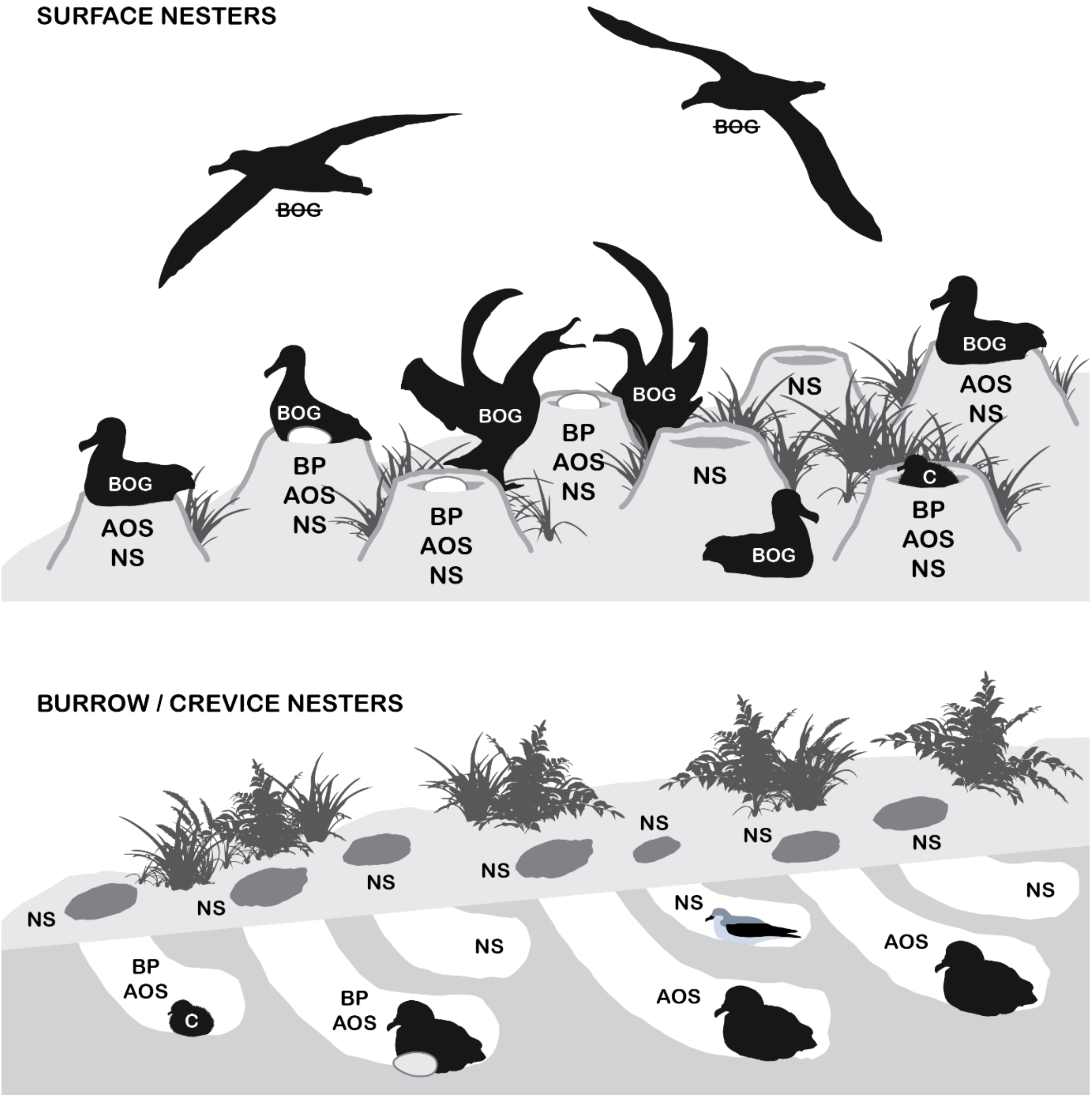

Fig. 1. Schematic illustrating the different metrics for both surface and burrow/crevice nesters and how they relate to each other, creating a hierarchy (Table 1). BP: annual breeding pairs, AOS: apparently occupied sites, BOG: birds on ground, NS: nest sites, C: chicks. Note the non-target *Pterodroma* petrel among the target *Procellaria* petrels to highlight the challenge of mixed-species colonies.

Following these adjustments to the structure of the ACAP database abundance data, we recorded annual abundance data at the breeding site level for the ten ACAP species endemic to New Zealand. For each record, we documented the metric in which the count originally was conducted and ultimately expressed in, method(s) applied, and errors accounted or unaccounted for, as well as the updated ACAP accuracy score, additional auxiliary data (e.g., date, relation to phenology, and breeding success (section 2.2.3), and breeding probability (section 2.3)), and references (Supplementary Tables 1-22). This reformatting exercise required revisiting the original publications or reports. In doing so, we regularly identified additional abundance data not currently captured in the ACAP database, which we then also included in our data. Specifically, we identified 177 additional counts for these ten species, leading to a total data set of 471 annual breeding site counts (note the ACAP database records counts of part-sites separately, while we combined these). Ultimately, our restructuring resulted in improved and more transparent datasets suitable for standardised processing and modelling of long-term trends and conservation status assessments (section 2.2-2.5).

Table 1. Updated, standardised definitions of metrics for counts of albatrosses and petrels. See Fig. 1 for a graphical representation.

Metric (acronym)	**Description**	**Example**
Annual Breeding pairs (BP)	The number of pairs successfully laying an egg in the year[A] the count is conducted. For this metric, the presence of an egg or chick will usually need to be confirmed systematically. This is the ACAP standard metric in which species abundance is expressed. This metric is sometimes referred to as occupied nest sites or expressed in number of eggs but to ensure consistency, is referred to as BP hereafter.	Wolfaardt & Phillips 2020, Elliott *et al.* 2025, Rexer-Huber *et al.* 2025
Apparently occupied nest sites (AOS)	The number of birds that appear to be breeding, e.g., because they are sitting on a nest or occupying a burrow, but the contents thereof have not been confirmed, in the year[A] the count is conducted. Nest site is defined as the location of where the adult bird sits on the egg or chick. This metric is sometimes referred to as apparently breeding adults, but to ensure consistency, is referred to as AOS hereafter.	Baker *et al.* 2023, Stevens *et al.* 2024
Birds on ground (BOG)	The number of birds on the ground present in the year[A] the count is conducted, regardless of 1) whether they are, or appear to be, breeding, 2) whether they are, or appear to be, associated with a nest site, and 3) regardless of their age (i.e., this metric can include immatures, prebreeders, non-breeders, and breeders).	Hayes *et al.* 2021
Nest sites (NS)	The number of nest sites (e.g., burrows) present in the year[A] the count is conducted regardless of their contents.	Parker & Rexer-Huber 2020b, Bell *et al.* 2017
Chicks (C)	The number of chicks present in the year[A] the count is conducted. Chicks are defined as young birds on the nest site between hatching and fledging age.	Frost 2017, 2024,

[A] Year refers to a biologically relevant year, which varies between species depending on the species' phenology. As per ACAP convention, the year stated reflects the year in which chicks fledge.

Table 2. Updated, standardised definitions of count methods for albatrosses and petrels.

Method (acronym)	**Definition**	**Example**
Ground count (GC)	Count of the target metric from the ground, including the use of aids such as tally counters, GPSs, burrowscopes, or RFID readers.	Waugh *et al.* 2020, Mischler *et al.* 2025,
Vantage point count (VPC)	Count of the target metric from a ground-based vantage point, including the use of aids such as binoculars or photography and orthomosaics.	Cuthbert & Sommer 2004, Stevens *et al.* 2024, Mischler *et al.* 2025
Aerial count – using fixed-wing (AC^{fw})	Count of the target metric on the ground from a fixed-wing plane including the use of aids such a photography and orthomosaics.	Fisher 1966, Robertson *et al.* 2008, Frost 2017
Aerial count – using helicopter (AC^{heli})	Count of the target metric from a helicopter including the use of aids such a photography and orthomosaics.	Baker *et al.* 2023, Frost *et al.* 2025
Aerial count – using UAV (AC^{UAV})	Count of the target metric from an unmanned aerial vehicle (UAV; e.g., drone or aerial kite), usually using photography and orthomosaics.	Rexer-Huber *et al.* 2025, Virtue *et al.* 2025
Aerial count – using satellite imagery (AC^{sat})	Count of the target metric under consideration from satellite imagery.	Fretwell *et al.* 2017, Attard *et al.* 2025
Vessel-based count (VBC)	Count of the target metric from a vessel at sea, including the use of aids such as binoculars or photography.	Poncet *et al.* 2006, Rexer-Huber *et al.* 2020

Table 3. Updated, standardised definitions of common[A] sources of error in counts of albatrosses and petrels. Overarching sources of error are indicated by Ψ, subcategories thereof are indicated by ψ. ↓ indicates an underestimate, ↑ indicates an overestimate.

Source of error (symbol)	**Definition**	**Impact on estimate**	**Example**
Sampling error (Ψ^{s})	The error associated with counting only a sample of the population and associated decisions (e.g., randomisation, representativeness, and coverage).	↓↑	Elliott *et al.* 2016
Detection error ($\Psi^{d}; \psi^{obs}$)	The error associated with the probability of not detecting the target metric, despite it being present, including obstruction error (ψ^{obs}) when the metric under consideration is being obstructed from view. When using some methods (e.g., AC^{sat}) false positives (objects incorrectly counted as birds) can also occur as well.	↓(↑)	Parker & Rexer-Huber 2020b
Occupancy error (Ψ^{o}; ψ^{ABA}, ψ^{BOG} & ψ^{occ})	The error associated with the probability of counting the target metric as a different metric. This error category consists of different sub-categories (Fig. 1 & 2): - Counting AOS (e.g., birds appearing to breed, while not actually breeding, sometimes referred to as pretend-breeders or triers) as BP (ψ^{ABA}). Relevant to both surface and burrow/crevice nesters. Example: BP ~ Bin(AOS, ψ^{ABA}). - Counting loafers (birds not associated with a nest site) as BP or AOS (ψ^{BOG}). Relevant to surface nesters only. Example: AOS ~ Bin(BOG, ψ^{BOG}); BP ~ Bin(BOG, $\psi^{BOG} \cdot \psi^{ABA}$). - Counting NS (e.g., burrows) as BP or AOS while not actually being occupied (ψ^{occ}). Relevant to both surface and burrow/crevice nesters. Example: AOS ~ Bin(NS, ψ^{occ}); BP ~ Bin(NS, $\psi^{occ} \cdot \psi^{ABA}$). For burrow/crevice nesters, ψ^{occ} (and ψ^{ABA}) are often quantified when assessing the proportion of counted nest sites/burrows that contain the target species and target metric (often referred to as burrow occupancy). In certain cases, this error can include other species (e.g., because burrow contents were not checked).	↑	Poncet *et al.* 2006, Robertson *et al.* 2008, Walker *et al.* 2020, Baker *et al.* 2023, Rexer-Huber *et al.* 2025
Phenology-related error ($\Psi^{p}; \psi^{lay}$ & ψ^{fail})	The error associated with the probability of not counting the target metric, because the nest failed prior to the count (ψ^{fail}) or because the egg had not been laid at the time of the survey (ψ^{lay}). Both sub-categories of phenology-related error can occur within the same count, if the count period spans a long enough time.	↓	Frederick *et al.* 2006, Poncet *et al.* 2006, Elliott *et al.* 2025

[A] Other sources of error raised included observer error (i.e., the error associated with different observers conducting counts; Parker & Rexer-Huber 2020b) and interpretation error (i.e., the error associated with the potential incorrect retrospective interpretation of the count data). While these errors do occur, they appear less common, and when the four common sources of error are accounted, the associated uncertainty should capture the less common sources of error as well.

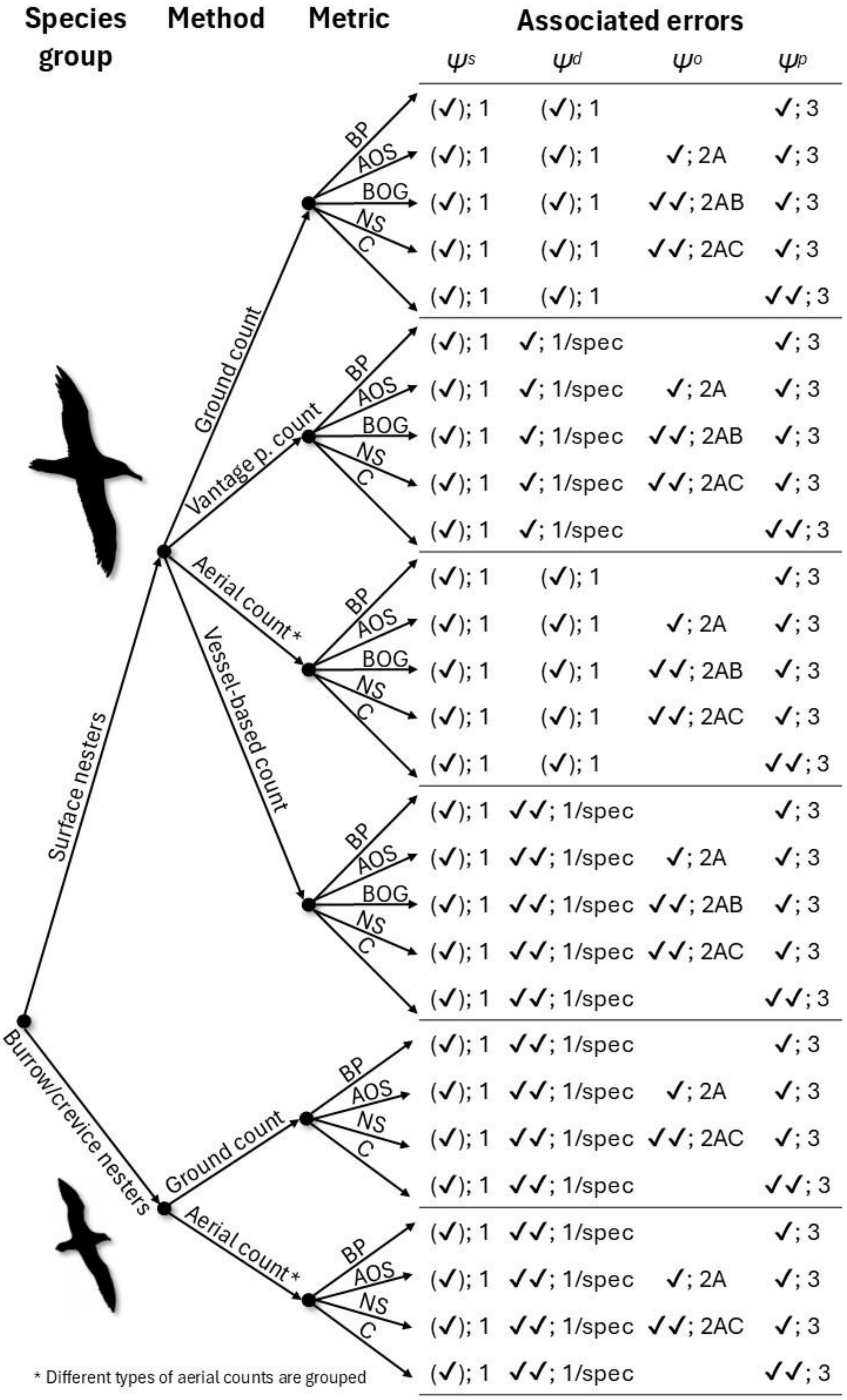

Species group	Method	Metric	ψ^s	ψ^d	ψ^o	ψ^p
Surface nesters	Ground count	BP	(✓); 1	(✓); 1		✓; 3
		AOS	(✓); 1	(✓); 1	✓; 2A	✓; 3
		BOG	(✓); 1	(✓); 1	✓✓; 2AB	✓; 3
		NS	(✓); 1	(✓); 1	✓✓; 2AC	✓; 3
		C	(✓); 1	(✓); 1		✓✓; 3
	Vantage p. count	BP	(✓); 1	✓; 1/spec		✓; 3
		AOS	(✓); 1	✓; 1/spec	✓; 2A	✓; 3
		BOG	(✓); 1	✓; 1/spec	✓✓; 2AB	✓; 3
		NS	(✓); 1	✓; 1/spec	✓✓; 2AC	✓; 3
		C	(✓); 1	✓; 1/spec		✓✓; 3
	Aerial count*	BP	(✓); 1	(✓); 1		✓; 3
		AOS	(✓); 1	(✓); 1	✓; 2A	✓; 3
		BOG	(✓); 1	(✓); 1	✓✓; 2AB	✓; 3
		NS	(✓); 1	(✓); 1	✓✓; 2AC	✓; 3
		C	(✓); 1	(✓); 1		✓✓; 3
	Vessel-based count	BP	(✓); 1	✓✓; 1/spec		✓; 3
		AOS	(✓); 1	✓✓; 1/spec	✓; 2A	✓; 3
		BOG	(✓); 1	✓✓; 1/spec	✓✓; 2AB	✓; 3
		NS	(✓); 1	✓✓; 1/spec	✓✓; 2AC	✓; 3
		C	(✓); 1	✓✓; 1/spec		✓✓; 3
Burrow/crevice nesters	Ground count	BP	(✓); 1	✓✓; 1/spec		✓; 3
		AOS	(✓); 1	✓✓; 1/spec	✓; 2A	✓; 3
		NS	(✓); 1	✓✓; 1/spec	✓✓; 2AC	✓; 3
		C	(✓); 1	✓✓; 1/spec		✓✓; 3
	Aerial count*	BP	(✓); 1	✓✓; 1/spec		✓; 3
		AOS	(✓); 1	✓✓; 1/spec	✓; 2A	✓; 3
		NS	(✓); 1	✓✓; 1/spec	✓✓; 2AC	✓; 3
		C	(✓); 1	✓✓; 1/spec		✓✓; 3

* Different types of aerial counts are grouped

Fig. 2. Decision tree illustrating the interaction of metric (Table 1), method (Table 2), and errors associated with counts of albatrosses and petrels (Table 3). BP: annual breeding pairs, AOS: apparently occupied sites, BOG: birds on ground, NS: nest sites, C: chicks (Fig. 1). Symbols indicate the importance of accounting for errors: (✓) = important, depending on context; ✓ important; ✓✓ crucially important. Numbers following tick marks indicate the equations in section 2.2 that should be applied. spec indicates that specific, custom, context-dependent approaches may be necessary, see case studies for examples thereof.

2.2. Standardised error corrections and incorporation of uncertainty

We applied a series of equations and models to standardise the disparate ACAP count data and prepare them for the standardised modelling of trends. Depending on how the target species was counted, through which metric the count was expressed, and following the decision tree in Fig. 2, we 1) incorporated baseline uncertainty and accounted for sampling error Ψ^s, 2) accounted for detection error Ψ^d where possible, 3) accounted for occupancy error Ψ^o when required, and 4) accounted for phenology-related error Ψ^p. This approach ensured that all adjusted counts were ultimately expressed in the standardised number of breeding pairs at the start of the breeding period while accounting for uncertainty. We completed step 1, 3, and 4 using a standardised approach consisting of several hierarchical models that were fit jointly to the data as required (see below). However, we could not develop a standardised methodology to account for Ψ^d (step 2), and as such, specific, custom, context-dependent approaches were included in our hierarchical framework where possible (see section 2.7). In our framework, we accounted for Ψ^o (step 3) and Ψ^p (step 4) separately but in parallel. This contrasts with some prevailing assumptions held on Ψ^o (e.g., AOS = BP, and ψ^{ABA} changes predictably over time; Poncet *et al.* 2006, Robertson *et al.* 2008, Baker *et al.* 2023) and we provide additional analyses in Supplementary Material 1 to justify our parallel approach. It should be noted that our standardised framework did not seek to overwrite any existing, already applied, efforts to account for errors (e.g., see Elliott *et al.* 2025, Rexer-Huber *et al.* 2025). Rather, our processing and standardisation steps are intended to enable the accounting for errors and incorporation of uncertainty where this has not yet been done, to ensure that abundance data are comparable, ultimately enabling estimates of trends. A glossary of all acronyms and symbols used in our framework can be found Table 4.

Table 4. Glossary of acronyms and symbols.

Acronym/symbol	Brief description (Section; Table; Figure)
Count metrics	
BP	Annual breeding pairs (2.1; Table 1; Figure 1, 3)
AOS	Apparently occupied sites (2.1; Table 1; Figure 1, 3)
BOG	Birds on ground (2.1; Table 1; Figure 1, 3)
NS	Nest sites (2.1; Table 1; Figure 1, 3)
C	Chicks (2.1; Table 1; Figure 1, 3)
Count methods	
GC	Ground count (2.1; Table 2)
VPC	Vantage point count (2.1; Table 2)
$\mathrm{AC}^{\mathrm{fw}}$/ $\mathrm{AC}^{\mathrm{heli}}$ / $\mathrm{AC}^{\mathrm{UAV}}$ /$\mathrm{AC}^{\mathrm{sat}}$	Aerial count from a fixed-wing plane / a helicopter / an unmanned aerial vehicle / a satellite (2.1; Table 2)
VBC	Vessel-based count (2.1; Table 2)
Errors	
Ψ^s	Sampling error (2.1; Table 3)
Ψ^d	Detection error (2.1; Table 3)
ψ^{obs}	Obstruction error, subcategory of Ψ^d (2.1; Table 3)
Ψ^o	Occupancy error (2.1; Table 3; Figure 3)
ψ^{ABA}	Counting AOS as BP, subcategory of Ψ^o (2.1; Table 3; Fig. 1 & 4)
ψ^{BOG}	Counting BOG as AOS or BP, subcategory of Ψ^o (2.1; Table 3; Fig. 1 & 4)
ψ^{occ}	Counting NS as AOS or BP, subcategory of Ψ^o (2.1; Table 3; Fig. 1 & 4)
Ψ^p	Phenology-related error (2.1; Table 3)
ψ^{fail}	Error caused by nests failing prior to count, subcategory of Ψ^p (2.1; Table 3; Fig. 5)
ψ^{lay}	Error caused by eggs being laid after count, subcategory of Ψ^p (2.1; Table 3)
Data processing	
$\rho_{t,i}$	Reported abundance of sample regardless of metric (2.2.1)
$\xi_{t,i}$	Proportion of the breeding site counted (2.2.1)
$P_{t,i}$	Extrapolated abundance of total breeding site regardless of metric (2.2.1)
$n_{t,i}$	Extrapolated abundance of total breeding site with standardised uncertainty regardless of metric (2.2.1; Table 4; Fig. 3)
$S(a_{t,i})$	Scaling factor associated with the ACAP accuracy score (2.2.1; Table 4; Fig. 3)
$\mathrm{bp}_{t,i}$	Number of nests for which egg/chick presence has been confirmed in (sub-)count (2.2.3)
$\mathrm{aos}_{t,i}$	Total number of AOS regardless of nest contents in (sub-)count (2.2.3)
$\mathrm{bog}_{t,i}$	Number of birds on the ground in (sub-)count (2.2.3)
$\mathrm{m}_{t,i}$	Number of apparent partners next to AOS (2.2.3)
$\mathrm{ns}_{t,i}$	Number of nest sites checked (2.2.3)
$\mathrm{n}^{\mathrm{bs}}_{t,i(,k)}$	Number of nests monitored for breeding success that were successful (2.2.4)
$\mathrm{o}^{\mathrm{bs}}_{t,i(,k)}$	Nests monitored for breeding success (2.2.4)
$f_{t,i(,k)}$	Annual breeding success (fecundity) (2.2.4; Figure 4)
$\theta_{t,i(,k)}$	Count timing in relation to the species' phenology (2.2.4; Fig. 5)
$\Theta_{i(,k)}$	Duration of total breeding period (or phenological stage *k*) (2.2.4; Fig. 5)
$\upsilon_{t,i(,k)}$	Start time of count in relation to the species' phenology (2.2.4)
$\omega_{t,i(,k)}$	End time of count in relation to the species' phenology (2.2.4)
$y_{i,t}$	Standardised abundance estimate, as derived from the data processing steps, expressed in BP at the start of the incubation period (2.2.5)
$\mathrm{M}_{i,t}$	Mature individuals (2.3)
$p^b_{i(,t)}$	Breeding probability (2.3)
$s_{i(,t)}$	Sex ratio (2.3)
Trend model	
$N_{t(,i)}$	Abundance of breeding site *i* in year *t* as derived through trend model Eq. 5 (2.4)
$\lambda_{t,i}$	Annual growth rate (2.4)
q	Mean log growth rate (2.4)
$x_{t,i}$	Logarithm of $N_{t,i}$ (2.4)
$r_{t,i}$	Logarithm of $\lambda_{t,i}$ (2.4)

Acronym/symbol	Brief description (Section; Table; Figure)
$\zeta_{i,t}$	Standardised component variance, as derived from the data processing (2.4)
Conservation assessments	
CR	Critically Endangered (2.5.1)
EN	Endangered (2.5.1)
VU	Vulnerable (2.5.1)
NT	Near Threatened (2.5.1)
LC	Least Concern (2.5.1)
GL	Generation length (2.5.1)
R_t	Fractional overall population change over predefined time period of 3 GL
T	Predetermined reference time interval based on GL
δ	Number of years within T during which abundance estimates are available
W	Time window (e.g., 2005-…)
Indexing	
t	Year: 1, 2, 3, … (the calendar year during which fledging occurs)
i	Breeding site: 1, 2, 3, …
k	Phenological stage: incubation, guard, post-guard

2.2.1. Incorporating baseline uncertainty and accounting for sampling error

Many counts of albatrosses and petrels (and seabirds in general) are recorded without explicit, consistent or comparable expressions of uncertainty. This is particularly common in abundance data, as absolute censuses of all breeding sites are essentially non-existent (Parker & Rexer-Huber 2020b, Wolfaardt & Phillips 2020). However, communicating uncertainty associated with counts of these species is challenging due to the idiosyncrasies associated with the data. Most counts of ACAP species consist of a single figure (e.g., Sagar & Stahl 2005, Mackley *et al.* 2025), though some estimates are paired with efforts to express uncertainty mathematically (e.g., Waugh *et al.* 2020, Frost *et al.* 2025). Even if uncertainty is expressed, some approaches represent only a subset of the uncertainty in the count methodology (e.g., a single assumption in the estimation process), rather than the full uncertainty surrounding the actual count (e.g., Moore *et al.* 2012, Elliott *et al.* 2025). Moreover, even if uncertainty is quantified, the resulting estimates may not be comparable across years (e.g., Elliott *et al.* 2016 vs. Elliott *et al.* 2025). Finally, many counts of albatrosses and petrels are conducted at smaller study or index sites, which are assumed to be representative of the larger breeding site population (e.g., Moore *et al.* 2012, Mischler *et al.* 2025), yet there is no standardised mechanism to incorporate information on what proportion of the overall population is counted (e.g., 1% vs. 10%), and how this proportion affects uncertainty surrounding the counts, i.e., sampling error Ψ^{S}.

Here, we formulate a standardised approach to incorporating baseline uncertainty surrounding counts of albatrosses and petrels in a consistent and comparable manner to overcome the challenges of the disparate data subject to varying idiosyncrasies while simultaneously accounting for Ψ^S. Specifically, we applied Eq. 1 to all counts, which leveraged 1) the accuracy scores within the ACAP database (ACAP 2025b) representing an existing semi-standardised mechanism that qualitatively reflects prior beliefs in uncertainty, and 2) knowledge on the proportion of a breeding site that is counted. This approach assumes that the proportion of the overall breeding site counted does not influence the accuracy score of the count. This assumption is appropriate, as high accuracy counts of small proportions are common in the ACAP database.

1.
$$P_{t,i} = \left(\frac{\rho_{t,i}}{\xi_{t,i}}\right)$$

$$n_{t,i} \sim \mathrm{N}(P_{t,i}, \tau^n_{t,i})$$

$$\tau^n_{t,i} = \frac{1}{S(a_{t,i}) \cdot P^2_{t,i} + \frac{(1-\xi_{t,i})}{\xi^2_{t,i}} \cdot P_{t,i}}$$

in which $P_{t,i}$ is the extrapolated abundance in year *t* at site *i* (irrespective of the metric the count is expressed in, see section 2.2.3), $\rho_{t,i}$ is the reported abundance, $\xi_{t,i}$ is the known proportion of the breeding site that has been counted, $n_{t,i}$ is the extrapolated abundance, truncated below $P_{t,i}$, with standardised uncertainty expressed through precision $\tau^n_{t,i}$, and $S(a_{t,i})$ is a scaling factor that was identified iteratively to define asymptotes matching prior beliefs associated with the ACAP accuracy scores (section 2.1, Table 5, Fig. 3). For example, for a count of 5,000 BP of a surface nester categorised as “High Accuracy”, our modified Delphi-expert elicitation (Hemming et al. 2018) identified that the true value of abundance should fall within 10% of the reported value, and thus, that uncertainty bounds should equate to 4,500-5,500 based on the held prior beliefs, provided a large enough proportion of the population was counted. We calculated the values of $S(a)$ reported in Table 5 iteratively in order to meet the identified prior beliefs assuming 100% of a population was counted. For a graphical representation, see Fig. 3.

Table 5. Scaling factors used in Eq. 1 to translate qualitative uncertainty into numerical uncertainty using the accuracy score categories within the ACAP database.

	Surface nesters		**Burrow/crevice nesters**	
Accuracy score	% within stated value (expert elicited)	*S(a)*	% within stated value (expert elicited)	*S(a)*
High	10%	0.0026	16%	0.0067
Medium	33%	0.0283	46%	0.0551
Low	67%	0.1169	88%	0.2016

Our approach leverages an asymptotic function that generates uncertainty around the count based on the pre-assigned accuracy category and proportion of the breeding site counted. This approach thus enables the generation of uncertainty in a standardised fashion, while adhering to the principle that counting a larger proportion of a breeding site reduces uncertainty (e.g., Elliott *et al.* 2016) - up to a certain extent - while retaining the prior information on count accuracy contained within the ACAP database. In most cases, we treated $\xi_{t,i}$ as fixed. However, in certain cases the fraction of the overall population was uncertain (e.g., Imber 1987, Bell *et al.* 2022), and we therefore constructed informed priors to incorporate the additional uncertainty surrounding $\xi_{t,i}$. We applied Eq. 1 to all counts to incorporate standardised baseline uncertainty, while simultaneously accounting for Ψ^s. As uncertainty was expressed as a function of ξ, we only included counts in which $\xi_{t,i} > 0.01$ (i.e., counts that covered more than 1% of the breeding site's population).

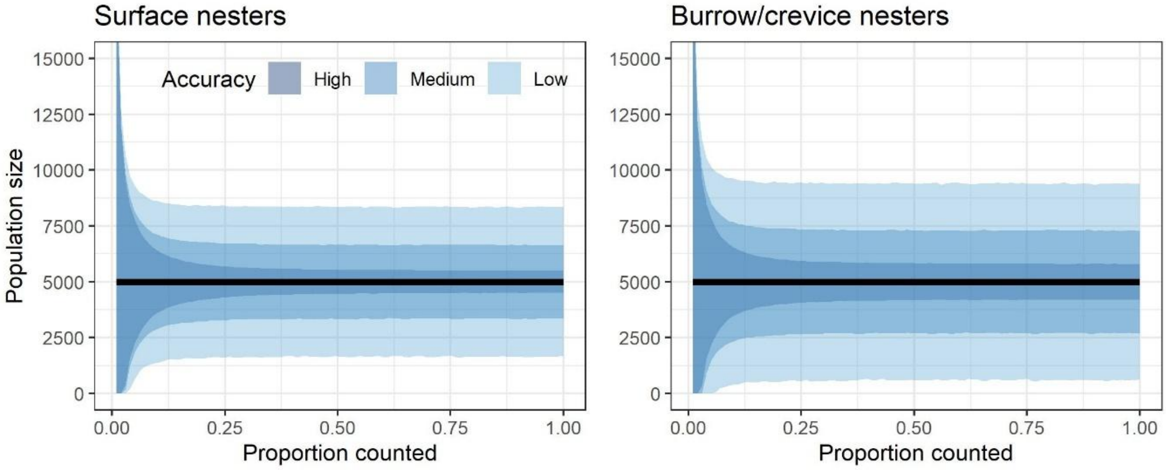

Fig. 3. Graphical representation of Eq. 1 applied to hypothetical counts of a surface and a burrow/crevice nester breeding site with a population size of 5,000 BP (horizontal black line). Shaded areas represent the uncertainty (represented by 95% CIs) as produced by Eq. 1 under varying ACAP accuracy scores ($S(a)$) and proportions of the population counted (ξ

2.2.2. Accounting for detection error

Imperfect detection of target metrics is an inherent, ubiquitous challenge in ecological monitoring, and is common for ACAP species, and thus, detection error Ψ^d is a common source of error associated with counts of albatrosses and petrels (Parker & Rexer-Huber 2020b, Wolfaardt & Phillips 2020). The target metric can be obscured from view during counts for various reasons, which are species-, site-, and context-dependent; thus, Ψ^{d} can be subject to considerable variation among counts. However, in general, Ψ^{d} is a more important consideration for the more cryptic burrow/crevice nesters (e.g., burrowing petrels; Parker & Rexer-Huber 2020b) than surface nesters (e.g., albatrosses; Wolfaardt & Phillips 2020) (Fig. 2), yet cliff-nesting albatrosses can also be subject to considerable detection challenges (Ryan *et al.* 2009). Common approaches to address Ψ^{d} for individual counts include distance sampling and repeat surveys in a mark-resight framework, comparing multiple methods (e.g. ground counts of an aerial-count block), or by perpendicular validation transects (Buckland *et al.* 2001, Walker & Elliott 2005, Frederick *et al.* 2006, Parker & Rexer-Huber 2020b).

However, to date, no approaches exist to account for Ψ^{d} retrospectively that effectively allows for improved comparability across counts, space, time, and species, and we were equally unable to identify an explicit standardised step in our framework to do this. It may be possible to infer Ψ^{d} for counts retrospectively when Ψ^{d} has been estimated for the same breeding site and species in previous/subsequent counts. Yet even if comparable information on Ψ^{d} exists, care needs to be taken to ensure that the area of extrapolation remains comparable (Parker & Rexer-Huber 2020b). However, if no prior data exists, quantifying Ψ^{d} may prove highly challenging due to the site-, species-, observer- and context-specific nature of this source of error (Parker & Rexer-Huber 2020b, Wolfaardt & Phillips 2020). Expert elicitations may provide some general solutions to estimate Ψ^{d} retrospectively (Fischer *et al.* 2020) including for a specific form of Ψ^{d}, obstruction error ψ^{obs}, but such approaches are time consuming and remain case- and context-specific.

We here follow the decision tree in Fig. 2 and we assume that the uncertainty incorporated through Eq. 1 is sufficient to account for Ψ^{d} for situations and species that inherently have a high detection probability (e.g., surface-breeding *Diomedea* albatrosses for which ground-counting Ψ^{d} has been shown to be >0.95; e.g., Walker & Elliott 2005, Rexer-Huber *et al.* 2024). In other cases (i.e., counts that are not ground or aerial counts of surface breeders), we either used averages of previously reported Ψ^{d} (e.g., Buller's Albatross VPCs; section 2.7.5) or count-specific modified Delphi expert elicitations (e.g., White-capped Albatross VBCs; section 2.7.6; Hemming *et al.* 2018, Fischer *et al.* 2020). Through this approach, we still attempted to account for Ψ^{d} where it was pressing to do so, while not overly inflating uncertainty for counts in contexts when detection is known to be high.

2.2.3. Accounting for occupancy error

Another common source of error associated with counts of albatrosses and petrels is occupancy error Ψ^o. The ACAP convention is to express abundance in annual breeding pairs (BP, i.e., the number of pairs successfully laying an egg in the year the count is conducted; Table 2; Wolfaardt & Phillips 2020). However, abundance of ACAP species can be expressed in range of other metrics (Fig. 1). For example, surface-nesters, like albatrosses, have the habit of being present on the breeding site, and even occupying nest sites, despite not actively breeding, and such individuals typically consist of a virtually indistinguishable mix of immatures, pre-breeders, non-breeders, and failed breeders (e.g., Stahl & Sagar 2006, Wolfaardt & Phillips 2020). This phenomenon is subject to local, diurnal, intra- and interannual variation (e.g., Poncet *et al.* 2006, Robertson *et al.* 2008, Walker *et al.* 2020, Baker *et al.* 2023). Consequently, counts of surface breeders, particularly from aerial, vantage point, or vessel-based counts, are often expressed in BOG or AOS, as it is not possible to confirm nest contents and therefore obtain a direct count in BP (Wolfaardt & Phillips 2020). Similar challenges occur for burrow/crevice nesters, like burrowing petrels (Parker & Rexer-Huber 2020b). While it is not possible to count these species as BOG, counts of nest sites with (AOS or BP) or without (NS) confirmation that the target species indeed occupies them are common (Fig. 1). Even when the target species has been confirmed to occupy the burrow, it is still required to confirm the presence of an egg or chick to obtain a count expressed in BP as, similar to surface nesters, burrow/crevice nesters can occupy nest sites without actively breeding (Parker & Rexer-Huber 2020b, Waugh *et al.* 2020). Thus, for both surface and burrow/crevice nesters, adjustments to any counts expressed in metrics other than BP are required to obtain uniform, directly comparable, abundance data.

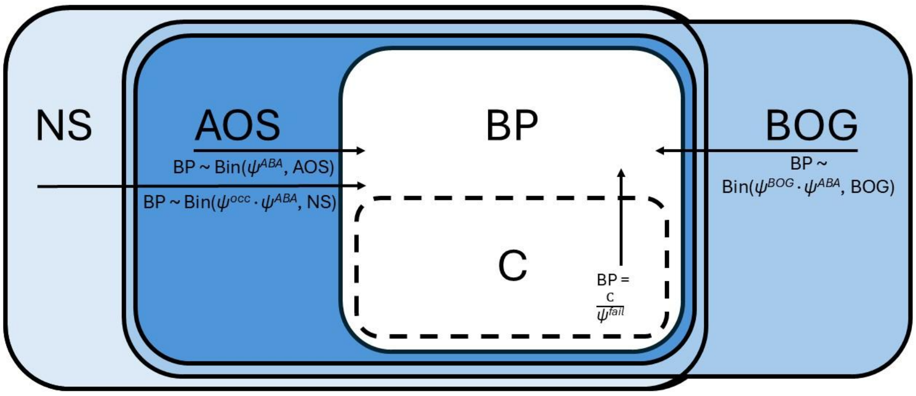

Fig. 4. Hierarchy of abundance metrics for ACAP species and how these can be converted to the standard, BP. BP: annual breeding pairs, AOS: apparently occupied sites, BOG: birds on ground, NS: nest sites, C: chicks. Equations illustrate Eq. 2ABC (and Eq. 3 for converting C into BP). Note, BOG is relevant to surface nesters only (Fig. 1).

To overcome the vexing challenge of Ψ^{o}, we leveraged the logical hierarchy of abundance metrics together with information contained in sub-counts associated with abundance counts to enable conversions of AOS, BOG, and NS into BP. The different abundance metrics are inter-related and follow a hierarchy (e.g., not all AOS equal BP, but all BP equal AOS; Fig. 4). This hierarchy logically guides conversions of other metrics into BP, provided information exists to enable these conversions. This information is typically collected in sub-counts associated with overall abundance counts. Examples of such sub-counts are ground transects of surface nesters concurrent to wider aerial counts to obtain a ratio of BP:AOS (e.g., Elliot *et al.* 2025, Frost *et al.* 2025, Rexer-Huber *et al.* 2025), close-up photographs during aerial counts to obtain a ratio of BOG:AOS (Baker *et al.* 2023), or burrow scoping transects/plots of burrow/crevice nesters during wider ground counts to obtain ratios of BP:NS or AOS:NS (e.g., Rexer-Huber *et al.* 2023). Here, we developed a hierarchical framework of binomial GLMMs (with logit-link functions) to leverage the information contained in such sub-counts to standardize accounting for Ψ^{o}. Specifically, we specified 1) a GLMM to adjust AOS to BP through estimates of ψ^{ABA} (Eq. 2A), which is relevant to both surface and burrow/crevice nesters, 2) a GLMM to adjust BOG to AOS through estimates of ψ^{BOG} (Eq. 2B), which is relevant to surface nesters only, and 3) a GLMM to adjust NS to AOS through estimates of ψ^{occ} (Eq. 2C), which is relevant to both surface and burrow/crevice nesters (Table 3, Fig. 1 & 4). We used these GLMMs in combination as required (e.g., to adjust NS to BP we combined Eq. 2A and 2C). Ψ^{o} is subject to breeding site, local, diurnal, intra- and interannual variation in an apparently not (fully) predictable manner (e.g., Supplementary Material 1; Poncet *et al.* 2006, Robertson *et al.* 2008, Stahl & Sagar 2006, Walker *et al.* 2020, Baker *et al.* 2023, Elliott *et al.* 2025, Rexer-Huber *et al.* 2025, Thompson 2025), and thus we simply indexed Eq. 2A-C per year *t* and breeding site *i* and modelled each conversion using random effects as following:

2A. $$\mathrm{bp}_{t,i} \sim \mathrm{Bin}\left(\mathrm{aos}_{t,i}, \psi_{t,i}^{ABA}\right)$$

$$\mathrm{logit}\left(\psi_{t,i}^{ABA}\right) = \alpha_{i}^{ABA} + \varepsilon_{t,i}^{ABA}$$

$$\varepsilon_{t,i}^{ABA} \sim \mathrm{N}\left(0, \sigma_{t,i}^{ABA^{-2}}\right)$$

in which $\mathrm{bp}_{t,i}$ is the number of nests in which the presence of an egg or chick has been confirmed in (sub-) count *c* (e.g., during ground transects; Frost *et al.* 2025), $\mathrm{aos}_{t,i}$ is the number of apparently occupied sites checked for the presence of an egg or chick in the same (sub-) count, $\psi_{t,i}^{ABA}$ is the count-specific adjustment for AOS to BP, α_i^{ABA} is the equation intercept, and $\varepsilon_{t,i}^{ABA}$ is a count-specific random effect with precision ${\sigma_{t,i}^{ABA}}^{-2}$ to be estimated from the data.

2B. $\mathrm{aos}_{t,i} \sim \mathrm{Bin}\left(\mathrm{bog}_{t,i} - \mathrm{m}_{t,i},\ \psi_{t,i}^{BOG}\right)$

$$\mathrm{logit}\left(\psi_{t,i}^{BOG}\right) = \alpha_i^{BOG} + \varepsilon_{t,i}^{BOG}$$

$$\varepsilon_{t,i}^{BOG} \sim \mathrm{N}\left(0, {\sigma_{t,i}^{BOG}}^{-2}\right)$$

in which $\mathrm{aos}_{t,i}$ is the number of apparently occupied sites in (sub-) count *c* (e.g., in close-up images; Baker *et al.* 2023), $\mathrm{bog}_{t,i}$ is the number of all birds on the ground in the same (sub-) count, $\mathrm{m}_{t,i}$ is the number of apparent partners to apparently occupied sites in the same sub-count, $\psi_{t,i}^{BOG}$ is the count-specific adjustment for BOG to AOS, α_i^{BOG} is the equation intercept, and $\varepsilon_{t,i}^{BOG}$ is a count-specific random effect with precision ${\sigma_{t,i}^{BOG}}^{-2}$ to be estimated from the data. Eq. 2B can be combined with Eq. 2A to adjust BOG to BP directly (e.g., Elliott *et al.* 2025, Rexer-Huber *et al.* 2025). Note, birds of unknown status should be excluded from Eq. 2B (e.g., Baker *et al.* 2023, Frost *et al.* 2025).

2C. $\mathrm{aos}_{t,i} \sim \mathrm{Bin}\left(\mathrm{ns}_{t,i},\ \psi_{t,i}^{occ}\right)$

$$\mathrm{logit}\left(\psi_{t,i}^{occ}\right) = \alpha_i^{occ} + \varepsilon_{t,i}^{occ}$$

$$\varepsilon_{t,i}^{occ} \sim \mathrm{N}\left(0, {\sigma_{t,i}^{occ}}^{-2}\right)$$

in which $\mathrm{aos}_{t,i}$ is the number of apparently occupied sites in (sub-) count *c* (e.g., burrow scoping transects), $\mathrm{ns}_{t,i}$ is the number of nest sites in the same (sub-)count, $\psi_{t,i}^{occ}$ is the count specific adjustment for NS to AOS, α_i^{occ} is the equation intercept, and $\varepsilon_{t,i}^{occ}$ is a count-specific random effect with precision ${\sigma_{t,i}^{occ}}^{-2}$. Eq. 2C can be fused with Eq. 2A to adjust NS directly to BP (e.g., Rexer-Huber *et al.* 2023). We used vague priors for all intercepts ($\alpha \sim$ N(0,0.001), where 0.001 refers to precision) and standard deviations ($\sigma_{t,i} \sim$ Uniform(0,3)). For breeding sites where the sub-count data covered ≤25% of the abundance count time series, we removed $\varepsilon_{t,i}$, as exploratory analyses highlighted that estimates with such limited data and high incidence of imputing became uninformative (e.g., $\psi_{t,i}^{ABA}$ ranged 0-1 when $\varepsilon_{t,i}^{ABA}$ was included).

Our approach to address Ψ^{o} overcomes shortfalls of using simple ratios derived from sub-counts, which are often based on small sample sizes and do not acknowledge uncertainty explicitly (e.g., Frost *et al.* 2025), and which have been used to correct abundance estimates in other years (e.g., see Walker *et al.* 2020 vs. Baker *et al.* 2023). Instead, our approach incorporates uncertainty surrounding Ψ^{o} (and therefore ψ_{c}^{ABA}, ψ_{c}^{BOG}, and ψ_{c}^{occ}), allows for inference of Ψ^{o} for abundance counts for which no data on Ψ^{o} was collected while increasing uncertainty, and vice-versa, enables for incorporation of information from years during which sub-counts did take place but no abundance counts were conducted (rarer but possible).

2.2.4. Accounting for phenology-related error

Albatrosses and petrels generally breed in remote locations that are difficult to reach, and this creates challenges to consistently conduct counts that coincide with the target species' ideal count time (i.e., early incubation; Wolfaardt & Phillips 2020). As the timing of counts often varies across years, this introduces another common source of error: phenology-related error Ψ^{p}. Most importantly, as nests fail over time from incubation onwards, the number of BP, AOS, NS, or C that can be counted is reduced relatively predictably: ψ^{fail} (e.g., Frederick *et al.* 2006, Rexer-Huber *et al.* 2020, Thompson 2025). We accounted for ψ^{fail} in a standardised manner by leveraging the principles of daily nest survival models (e.g., Fischer *et al.* 2021, Rexer-Huber *et al.* 2021, Thompson 2025), together with any data that was available on nests monitored to derive annual breeding success of the target species (i.e., the probability that a laid egg turned into a fledged chick), and insights into the timing of each specific count in relation to the target species' phenology. Note, nests monitored for breeding success usually consist of a smaller sample of overall abundance counts, so we necessarily assumed that the observed breeding success data was representative of the overall breeding site. Specifically, we applied the following binomial GLMM framework to account for ψ^{fail} for each breeding site *i* for each year *t* a count was conducted:

3A. $\mathrm{n}_{t,i}^{\mathrm{bs}} \sim \mathrm{Bin}\left(\mathrm{o}_{t,i}^{\mathrm{bs}}, f_{t,i}\right)$

$$\mathrm{logit}\left(f_{t,i}\right) = \alpha_{i}^{f} + \varepsilon_{t,i}^{f}$$

$$\varepsilon^{f}_{t,i} \sim \mathrm{N}\left(0, {\sigma^{f}_{t,i}}^{-2}\right)$$

$$\psi^{fail}_{t,i} = {f_{t,i}}^{\frac{\theta_{t,i}}{\Theta_i}}$$

$$\theta_{t,i} \sim \mathrm{U}\big(|\upsilon_{t,i} - 1|, \omega_{t,i} + 1\big)$$

in which $\mathrm{n}^{\mathrm{bs}}_{t,i}$ is number of nests monitored for breeding success that were successful (i.e., produced a fledgling), $\mathrm{o}^{\mathrm{bs}}_{t,i}$ is the total number of nests monitored for breeding success, $f_{t,i}$ is the breeding success (fecundity) estimate, α^{f}_{i} is the equation intercept, $\varepsilon^{f}_{t,i}$ is an annual random effect on breeding success with precision ${\sigma^{f}_{t,i}}^{-2}$ estimated from the data, Θ_i is the total breeding period (in weeks, rounded to the nearest integer, values for which were sourced from the literature), and $\theta_{t,i}$ is the timing the count took place in relation to the mean lay date of the breeding site of the target species (in weeks, rounded to the nearest non-negative integer), which was uniformly distributed between start time $\upsilon_{t,i}$ and end time $\omega_{t,i}$ of the count. We incorporated additional variation by subtracting 1 week of $\upsilon_{t,i}$ and adding one week to $\omega_{t,i}$, to acknowledge that species' breeding phenology can fluctuate from year to year (e.g., Lewis *et al.* 2012). We chose to express timings in weeks instead of days as to not portray an inflated level of precision. We used vague priors ($\alpha^{f}_{i} \sim$ N[0,0.001] and $\sigma^{f}_{t,i} \sim$ U[0,3]) unless otherwise stated (see section 2.7). In short, through Eq. 3 we first estimated breeding success *f* which we then used within a hazard function to estimate the likely nest failure that had occurred at the time the count took place (Fig. 5).

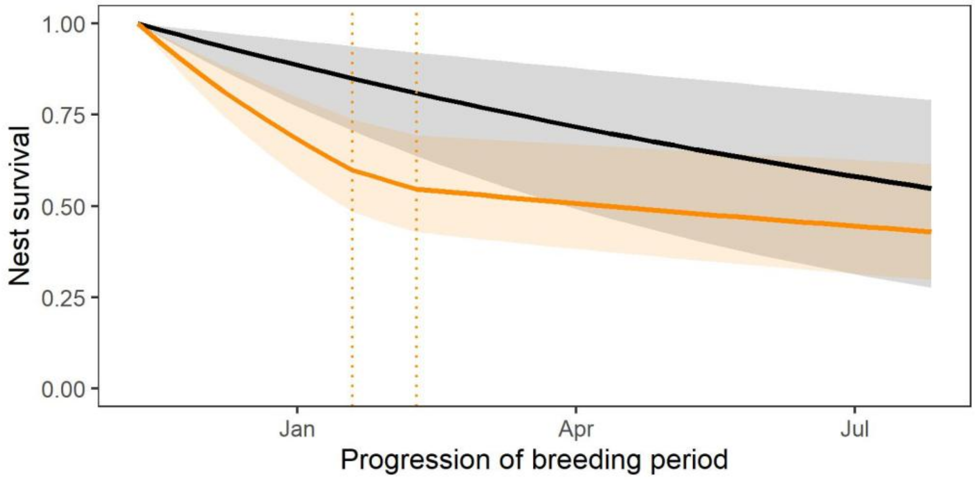

Fig. 5. Graphical representation of Eq. 3A (black) and Eq. 3B (orange). Dotted lines indicate changes between phenological stages with differing f_k for Eq. 3B.

Equation 3A relies on the assumption of an exponential hazard function, meaning that the rate of breeding failure is considered a consistent function of time (Fig. 5). In many cases, this assumption may have been violated (e.g., due to increased failures during adverse weather events or during specific phenological stages; Cleeland *et al.* 2020, Rexer-Huber *et al.* 2021). Occasionally, sufficient monitoring data exists to obtain survival estimates for individual phenological stages (i.e., incubation, guard, or post-guard respectively; Rexer-Huber *et al.* 2021, Thompson 2025). When such data exists, Eq. 3A can be adapted to estimate $\psi_{t,i}^{fail}$ as a product of the different stage-specific survival estimates $f_{k,j}$, enabling the incorporation of differing rates of breeding failure for each phenological stage (Fig. 5; Thompson 2025) as:

3B.
$$\mathrm{n}_{t,i,k}^{\mathrm{bs}} \sim \mathrm{Bin}\left(\mathrm{o}_{t,i,k}^{\mathrm{bs}}, f_{t,i,k}\right)$$
$$\mathrm{logit}\left(f_{t,i,k}\right) = \alpha_{i,k}^{f} + \varepsilon_{t,i,k}^{f}$$
$$\varepsilon_{t,i,k}^{f} \sim \mathrm{N}\left(0, {\sigma_{t,i,k}^{f}}^{-2}\right)$$
$$\psi_{t,i,k}^{fail} = {f_{t,i,k}}^{\frac{\theta_{t,i,k}}{\Theta_{i,k}}}$$
$$\theta_{t,i,k} \sim \mathrm{U}\left(|\upsilon_{t,i,k} - 1|, \omega_{t,i,k} + 1\right)$$
$$\psi_{t,i}^{fail} = \prod_{k} \psi_{t,i,k}^{fail}$$

Our approach to address Ψ^{p} thus leverages existing data on species' breeding success and knowledge on phenology. Additionally, the approach in both Eq. 3A and Eq. 3B allows for inference of breeding success for years during which no specific breeding success monitoring took place, but for which abundance counts are available, and vice-versa, allows for incorporation of information for years during which breeding success monitoring took place, but no abundance counts were conducted. We applied Eq. 3AB to all counts of albatross and petrel species, where possible, depending on whether the required data were available (see section 2.7, Table 7). It should be noted that when both active and failed nests are reported, Eq. 3 should be only fit to active nests (e.g., Sagar *et al.* 2014), as it would otherwise result in double-accounting for failed nests. Eq. 3 can be extended with additional fixed effects on f to incorporate additional nuance, e.g., known environmental impacts (see Northern Royal Albatross, section 2.7.2, for an example). For breeding sites where breeding success data covered ≤25% of the abundance count time series, we removed $\varepsilon_{t,i}^{f}$, as preliminary analyses highlighted that estimates with such limited data and high incidence of imputing became uninformative (i.e., $f_{t,i}$ ranged 0-1 when $\varepsilon^{f}_{t,i}$ was included). In scenarios where abundance was expressed in both BP/AOS + failed nests (e.g., Bell *et al.* 2017, Bell 2022), we excluded counts of failed nests, as it is unclear for how long failed nests remain noticeable, and once Eq. 3 is applied to BP/AOS, all failures will be accounted for. Where no breeding success data existed, we used informative priors for $f_{t,i}$ either based on published figures, or closely related species where necessary. Species- and breeding-site-specific approaches are detailed in Table 4. For our rationale on why we applied Ψ^{o} (Eq. 2) and (Eq. 3) in parallel, see Supplementary Material 1.

Through Eq. 3AB we developed a standardised solution for counts that were conducted at varying times after mean laying, ψ^{fail}. However, a different form of Ψ^{p} can occur: the error that is associated when counts are conducted prior to all eggs having been laid, ψ^{lay} (Wolfaardt & Phillips 2020). In scenarios where counts are conducted around laying, but prior to mean lay dates, conversions using the count date and the mathematical distribution of the lay period of the species and breeding site can be applied to adjust the count (e.g., Elliott *et al.* 2025, Rexer-Huber *et al.* 2025). As counts subject to ψ^{lay} are relatively rare, we adhere to the count-specific approach applied to such instances instead of developing a second standardised model for ψ^{lay}.

2.2.5. Hierarchical modelling to account for various sources of error

In our standardised abundance processing framework, various sources of error can be accounted for simultaneously. Specifically, after accounting for Ψ^{s} to incorporate baseline uncertainty, and obtaining an abundance estimate of the total breeding site in the original metric at the time of the count through Eq. 1, i.e., $n_{t,i}$, the outputs of Eq. 2 and 3, and, if applicable, appropriate estimates of Ψ^{d} can be combined to convert $n_{t,i}$ into the desired standardised measure of abundance for ACAP species, i.e., BP at the beginning of the breeding season, $y_{t,i}$, as following:

4. $$y_{t,i} = \frac{\frac{n_{t,i}}{\Psi^{d}_{t,i}} . \Psi^{o}_{t,i}}{\Psi^{p}_{t,i}}$$

In which $\Psi_{t,i}^{d}$ is either considered 1.000 if it warrants to do so (i.e., if Eq. 1 has already provided sufficient uncertainty) or estimated through a custom approach (section 2.2.2), $\Psi_{t,i}^{o}$ is expressed as either $\psi_{t,i}^{ABA}$ (e.g., for a AC of AOS of albatrosses), $\psi_{t,i}^{BOG}$ (e.g., for a VPC of BOG of albatrosses), $\psi_{t,i}^{occ}$ (e.g., for a GC of NS of a burrow-nesting petrel), or a combination thereof (section 2.2.3), and $\Psi_{t,i}^{p}$ is usually expressed as $\psi_{t,i}^{fail}$ (section 2.2.4). While Eq. 4 here is formulated to sequentially account for Ψ^{d}, then for Ψ^{o}, and then for Ψ^{p}, conversions of $n_{t,i}$ to $y_{t,i}$ will produce the same result if Eq. 4 is formulated in a different order. The order as in Eq. 4 however is beneficial in scenarios where breeding success has traditionally been estimated through metrics other than BP (e.g., Robertson 1991, Scofield 2011) as this approach allows for first adjusting to BP, then calculate $f_{i,t}$, and thus $\psi_{t,i}^{fail}$, and then estimating $y_{t,i}$ if so required (e.g., Section 2.7.2). Through this equation, the various equations accounting for errors are combined hierarchically within the same modelling framework. Ultimately, our approach enabled us to convert all counts of ACAP species into abundance data truly comparable across time, space, and species.

2.3. Conversions from annual breeding pairs to mature individuals

Abundance data on albatrosses and petrels is recorded in annual breeding pairs (ideally, or derivatives thereof; Table 1) as per ACAP convention, yet other global conservation processes require abundance to be expressed in mature individuals, including BirdLife International and the International Union for the Conservation of Nature (IUCN) Red List (IUCN 2012, BirdLife International 2025). Mature individuals are defined as individuals known, estimated or inferred to be capable of producing offspring, excluding juveniles, senescent individuals, suppressed individuals, or individuals in subpopulations whose densities are too low for fertilization to occur (BirdLife International 2025). Note, this definition does not allow for gradual exclusion of senescent individuals a function of age (e.g., Froy et al. 2013), but we did not seek to update this widely used definition. To elevate the utility of the abundance data collated in the ACAP database for wider global conservation processes, including Red List assessments (IUCN 2012) and fisheries risk assessments (e.g., Edwards *et al.* 2023, Anon. 2025), we also transformed the standardised annual breeding pair estimate, $y_{t,i}$, (see section 2.2) into an estimate of mature individuals as part of our overall framework.

Albatrosses and petrels have some of the most complex life histories of all bird species (Carneiro *et al.* 2020, Oppel *et al.* 2022, Richards *et al.* 2024), and as such, transforming annual breeding pairs into mature individuals requires careful consideration. For example, at least 32% of ACAP species are semi-biennial or biennial breeders once mature, and thus, transformations to mature individuals requires incorporation of breeding probability (the probability than an adult female lays an egg in a given year; Edwards *et al.* 2023). Furthermore, some species exhibit skewed sex-ratios due to sex-specific impacts on adult survival (Weimerskirch et al. 2005, Awkerman et al. 2007, Gianuca et al. 2019, Richard et al. 2024), which requires further consideration beyond breeding probabilities within these transformations. Building upon the approach by Edwards *et al.* (2023), we established two equations for transformations of annual breeding pairs (i.e., the metric in which $\mathrm{y}_{t,i}$ is expressed) to mature individuals M:

5A. $\mathrm{M}_{t,i} = \frac{2\cdot \mathrm{y}_{t,i}}{p_i^b}$

5B. $\mathrm{M}_{t,i} = \frac{(\frac{1}{s_i})\cdot \mathrm{y}_{t,i}}{p_i^b}$

In which p_i^b refers to the annual breeding probability (which can be indexed on *t* if such data exist, see below), and s_i is the sex ratio (which also can be indexed on *t* if such data exist). *s* should be skewed towards the less abundant sex, so that if there is a deviation from a 50:50 ratio, $s < 0.5$. To establish an approach for conversions to M suitable for application within our wider standardised framework, we evaluated both equations using data on Antipodean Albatross (*D. a. antipodensis*) from the Antipodes and Gibson's Albatross (*D. a. gibsoni*) from Adams Island, two biennially breeding taxa with a skewed sex ratio that has become evident after a population crash in 2005 (e.g., Richards *et al.* 2024) for which conversions to M are not straightforward.

To evaluate both conversions, we relied on the long-term capture-mark-recapture (CMR) data for Antipodean Albatross (including the Gibson's Albatross subspecies) and contrasted M estimates derived thereof using multi-state modelling (Elliott *et al.* 2025, Rexer-Huber *et al.* 2025) with estimates derived from Eq. 4A and 4B. We sourced BP from the ACAP database and extracted CMR-based estimates of $p_{t,i}^b$ (i.e., annually varying) and estimates of s_i pre- and post-2005 from Elliott *et al.* (2025) and Rexer-Huber *et al.* (2025) which we used to construct informative priors, specified via mean and precision ($s_{\leq 2005}^{antips} \sim$ N(0.491, 10000); $s_{\geq 2006}^{antips} \sim$ N(0.403, 2500); $s_{\leq 2005}^{gibsons} \sim$ N(0.487, 7500); $s_{\geq 2006}^{gibsons} \sim$ N(0.423, 1500)). Annual variation captured in $p^{b}_{t,i}$ is a product of in-depth multi-event CMR modelling and such information is not available for all populations of albatrosses and petrels. We therefore also repeated both equations with a fixed p^{b}_{i} using informative priors for the periods pre- and post-2005: ($p^{b\,antips}_{\leq 2005}$ ~ N(0.501, 1500); $p^{b\,antips}_{\geq 2006}$ ~ N(0.450, 150); $p^{b\,gibsons}_{\leq 2005}$ ~ N(0.583, 150); $p^{b\,gibsons}_{\geq 2006}$ ~ N(0.600, 300)).

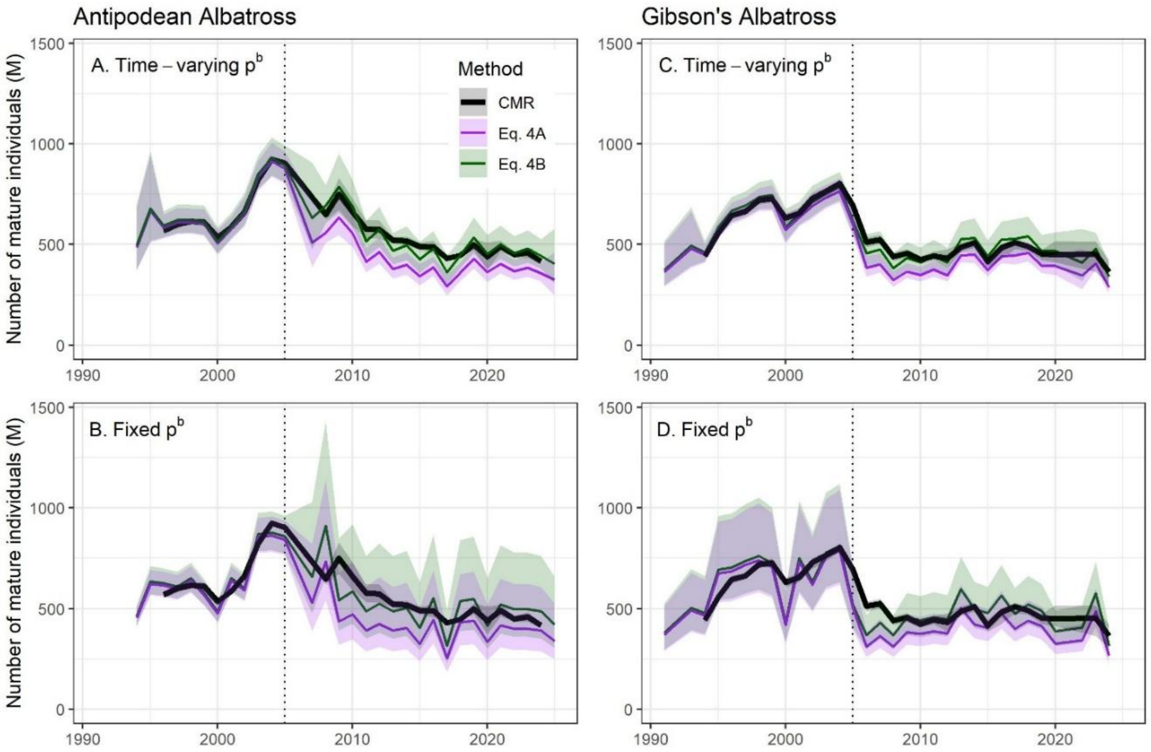

Fig. 6. Comparison of CMR-derived estimates of M (black lines) with two BP-to-M conversions using time-varying (AC) and fixed p^b (BD) for Antipodean (AB) and Gibson's Albatross (CD). The dotted vertical line indicates the population crash in both breeding sites after which a different *s* was applied.

The results of our evaluation (Fig. 6) indicated that, if a population has an even sex ratio, the simpler conversion, Eq. 4A, provides adequate approximations for M, but if a skewed sex ratio is present, Eq. 4A results in an underestimate of M, and Eq. 4B provides a more adequate estimate. Both conversions could be readily applied to years for which CMR-based M estimates did not exist (early 1990s), enabling longer time series, while incorporating uncertainty. However, when using fixed p^b instead of time-varying p^b estimates, uncertainty increased substantially, to the extent that the improvements provided by incorporation of *s* were no longer beneficial, resulting in an arguably lower performance of Eq. 4B. Based on this evaluation, we converted BP into M using Eq. 4A if no evidence exists for a skewed sex ratio, or using Eq. 4B, if such evidence exists and time-varying p^b estimates were available.

It should be noted that these estimates of M do not incorporate juveniles and pre-breeders (sub-adults) as per the definition of mature individuals (BirdLife International 2025). To incorporate those life-stage classes, further advanced modelling approaches, such as matrix population models (Waugh *et al.* 2015, Pardo et al, 2017) or integrated population models (e.g., Ventura et al. 2021, Oppel *et al.* 2022, Richard *et al.* 2024), are required, for which the necessary data is generally sparser.

2.4. Standardised modelling of trends

Once the albatross and petrel abundance data was adjusted to be comparable across time, space, and species, we fit custom Bayesian state-space models to timeseries of each breeding site of each species to obtain standardised trend estimates. Specifically, we developed a bespoke Bayesian state-space trend model that we fit through the custom R package *ACAPT*, which allowed for the necessary flexibility and considerations when working with extremely long-lived species such as albatrosses and petrels (Bird *et al.* 2020), which we built on the generalised state-space decision support tool *JARA* (Winker *et al.* 2020, Sherley *et al.* 2020a,b). Fundamentally, both *JARA* and our own state-space model enable the modelling of trends of multiple abundance timeseries simultaneously even if those timeseries span different time periods, contain missing values, and have different scales through a hierarchical process that separates process variation from observation error (Winker *et al.* 2020). Our trend model was structured as follows:

6. $N_{(t+1),i} = \lambda_{t,i} \cdot N_{t,i}$

$$\lambda_{t,i} \sim \mathrm{LogN}(q, \sigma_q^2)$$

$$N_t = \sum_i N_{t,i}$$

In which $N_{t,i}$ is the trend model estimated population size for breeding site *i* and year *t* (expressed as either BP or M), $\lambda_{t,i}$ is the annual growth rate, with mean log growth rate q that is constant and common to all breeding sites, constant variance σ_q^2, and total population size N_t. In log space, our trend model can be expressed in the form of a normal random walk:

$$x_{(t+1),i} = x_{t,i} + r_{t,i}$$

$$r_{t,i} \sim \mathrm{N}(q, \sigma_q^2)$$

$$y_{t,i} \sim \mathrm{LogN}(x_{t,i}, \sigma_y^2 + \zeta_{t,i}^2)$$

In which $x_{t,i}$ equals Log($N_{t,i}$), $r_{t,i}$ equals Log($\lambda_{t,i}$), $y_{t,i}$ is the standardised abundance estimate as derived through the steps detailed in sections 2.2-2.3 for breeding site *i* at year *t* with mean $x_{t,i}$ and variance consisting of the count-specific variance $\zeta_{t,i}^2$ as derived through the processes in sections 2.2-2.3, and additional variance common to all surveys σ_y^2. We used vague priors, specified via mean and precision ($q \sim \mathrm{N}(0, 0.01)$, $\sigma_q^{-2} \sim \mathrm{Gamma}(0.01, 0.01)$, and $\sigma_y^{-2} \sim \mathrm{Gamma}(0.01, 0.01)$) and the initial year in each timeseries was specified as $x_{t_0 i} \sim \mathrm{N}(\mu_{t_0 i}, \tau_{t_0 i}^{-1})$. We assumed that q as constant over time. In exploratory analyses, we varied our model specification by defining q either as an additional random walk, a smoothed cubic spline, or a linear model. These variations of our model became problematic with intermittent data (i.e., unrealistically high extents of uncertainty), a feature that is common of ACAP abundance data, and thus the simplest formulation in which q_t was treated as constant was considered the most appropriate. Our trend model up to this point is essentially identical to the trend model implemented through *JARA* (Winker *et al.* 2020, Sherley *et al.* 2020a,b), but our approach as implemented through *ACAPT* deviates when estimating overall population change for the conservation status assessments as we do not implement the lognormal bias correction that *JARA* uses (see section 2.5). Our trend model can be freely accessed and used through the custom R package *ACAPT* via https://github.com/SWotherspoon/ACAPT. For more information on *ACAPT*, see Supplementary Material 3 & 4.

We fit our trend model in Eq. 5 to all our standardised breeding site timeseries of the ten case studies both in terms of BP and M to estimate trends in both metrics and through summing the estimates of individual breeding sites, we provide estimates of current population size in BP and M per species regardless of the duration since the last count at a given breeding site. Furthermore, to evaluate overall trends on a genus level, we reran our trend model across the breeding sites of *Diomedea*, *Thalassarche*, and *Procellaria* species in our case studies jointly (M only). Finally, to provide overall insights into the fate of New Zealand's endemic large Procellariiform community, we reran our trend model across all breeding sites jointly (M only). Consequently, our flexible trend model provided the opportunity to obtain unprecedented insights into multi-decadal fates of ACAP species and has the potential to facilitate various conservation status assessments.

2.5 Conservation status assessments

2.5.1 IUCN Red List assessments

The IUCN Red List is the world's most comprehensive conservation status assessment, providing key insights into species' extinction risk and through this, guide conservation prioritisation and policy (IUCN 2025). IUCN Red List categories are assigned through several objective criteria relevant to populations and their extinction risk (IUCN 2012). The categories Critically Endangered (CR; extremely high risk of extinction), Endangered (EN; very high risk), and Vulnerable (VU; high risk) jointly indicate that a species is threatened, in contrast with Near Threatened (NT; not threatened now, but is likely at risk in the near future) and Least Concern (LC; not threatened). A key assessment criterion, Criterion A, is population trend over three generation lengths (GL; the average age of parents of the current cohort). The other criteria evaluate geographic range in the form extent of occurrence and/or area of occupancy (Criterion B), small population size in decline (Criterion C), very small population (Criterion D), and direct estimates of extinction probability (Criterion E). Each criterion consists of several sub-criteria, which for Criterion A revolve around the causes of population reduction and period over which the reduction is estimated (Table 6).

Table 6. Overview of IUCN Red List Criterion A, its four sub-criteria, and what percentage of population reduction results in what Red List category (IUCN 2012). GL = generation length, CR = Critically Endangered, EN = Endangered, VU = Vulnerable, NT = Near Threatened.

Sub-criteria	**Brief description**	**CR**	**EN**	**VU**	**NT**
A1	Population reduction estimated over 3 GL in the past, for which causes are clearly reversible and understood and have ceased.	≥90%	≥70%	≥50%	≥25%
A2	Population reduction estimated over 3 GL in the past, for which causes may not have ceased or may not be understood or may not be reversible.	≥80%	≥50%	≥30%	≥20%
A3	Population reduction projected to be met over 3 GL in the future.	≥80%	≥50%	≥30%	≥20%
A4	Estimated and/or projected population reduction over 3 GL, where the time period mst include both the past and the future, and for which causes may not have ceased or may not be understood or may not be reversible.	≥80%	≥50%	≥30%	≥20%

All ACAP species have been assessed on the IUCN Red List, but most are due for re-assessment (BirdLife International 2025) and to address this shortcoming, we built upon *JARA* (Winker *et al.* 2020, Sherley *et al.* 2020ab) and modelled population trends within our R package *ACAPT* in such a fashion that our results also provided insights into IUCN Red List re-assessment against Criterion A. For ACAP species, Criterion A is the most crucial criterion as 1) most species are showing long-term, ongoing, and concerning declines and causes thereof have generally not yet ceased (Fischer *et al.* 2024, ACAP 2025b), 2) ACAP species range extremely widely and thus geographic range is mostly relevant to single island endemics, 3) most populations exceed 10,000 (VU under Criterion C) and thus also 1,000 (VU under Criterion D) (ACAP 2025b), and 4) direct estimates of extinction probability only exist for a select few species (e.g., Genovart *et al.* 2016, Oppel *et al.* 2022, Richard *et al.* 2024). We focussed on assessing species against Criterion A4 (Table 6) as this 3 GL "moving window" is the most flexible of the four sub-criteria and the most relevant for species with extremely long GLs that usually are not fully covered by the available timeseries (e.g., 3 GL for Antipodean Albatross approximate a century; Table 7). However, for some species, very long timeseries that cover 3 GL do exist, enabling assessments against Criterion A2. Specifically, we modelled population change in mature individuals M to facilitate the Criterion A assessments as following:

7. $$R_t = \left(\frac{M_t}{M_{t-\delta}}\right)^{\frac{T}{\delta}}$$

$$t \in W$$

In which R_t is the (fractional) overall population change over a predetermined reference time interval T based on GL (e.g., 75 based on a GL of 25), δ is the number of years within T for which abundance estimates as derived through the trend model are available (e.g., 20), and W is the time window (e.g., 2005-2080). We specified three different W to facilitate three different Red List assessment approaches: 1) the full timeseries available up to 3 GL and inferred forwards to obtain 3 GL (if 3 GL were fully covered, this equated to an assessment against Criterion A2), 2) the last GL and then inferred for the next 2 GL (Criterion A4), and 3) the last 20 years and then inferred forward up to 3 GL (Criterion A4). We included the latter assessment approach as 20 years is the ACAP standard time period to provide statements on population change; ACAP 2025b). We sourced GL estimates for each of our case study species directly from BirdLife International (2025) after an update of Bird *et al.*

(2020) (Table 7). These calculations were conducted in our custom R package *ACAPT*. We report both the median of R_t as well as the density-based approach (c.f. *JARA*; Winker *et al.* 2020) to facilitate discussion on what the most appropriate Red List category assignment would be per species (noting that preliminary data explorations highlighted that the zero-bound on the lower end, and the absence of a boundary on the upper end of R_t had the potential to bias category assignments either towards CR or LC in cases of high uncertainty).

Our approach to calculating population change and assigning Red List categories against Criterion A slightly diverges from the approach in *JARA* (Winker *et al.* 2020, Sherley *et al.* 2020a,b). Specifically, our approach deviates from *JARA* in the projection component required for Eq. 7. The projection approach incorporated in *JARA* ignores the propagated uncertainty for individual abundance estimates yet results in unrealistically high uncertainty unless the lognormal bias correction is applied. We favoured a projection approach grounded in the observed trend from the known history when projecting, acknowledging the uncertainty of individual abundance estimates, without a lognormal bias correction. We believe that this approach provides more transparency, even if it ultimately comes at the cost of higher uncertainty.

2.5.2 ACAP High Priority Population assessments

Next to the IUCN Red List conservation status assessments, ACAP has its own conservation prioritisation mechanism in which it identified High Priority populations of ACAP species (ACAP 2025b). A population (i.e., breeding site) can be considered an ACAP High Priority population if it 1) holds ≥10% of the world population of the species, 2) is at risk of fisheries bycatch, and crucially, 3) has been declining at a rate ≥3% per annum for 20 years (ACAP 2025b). While these criteria are objective, ACAP High Priority populations have not uniformly been identified in a standardised fashion, and designation has largely been driven by ACAP Members making a case for candidate High Priority populations. Our standardised modelling of trends of ACAP species provides an opportunity for standardised designation of ACAP High Priority populations as well, and we showcase this through our case studies. Specifically, we identified which breeding sites hold ≥10% (Table 7), consulted the literature to identify which species are at risk from fisheries bycatch, and most importantly, adapted W and T in Eq. 6 to reflect the last 20 years, applying the equation at the breeding site level rather than the species level. If a population met the first two criteria and the median of R_{20}

fell below 45.6% (3% population decline means $\lambda_{t,i}$ = 0.970, and 1-0.970^{20} = 0.456), we proposed that this population be considered an ACAP High Priority population.

2.6 Model implementation

We completed the Bayesian modelling underpinning our framework in two steps. The first step, the series of hierarchical models enabling the standardised error corrections, explicit incorporation of uncertainty (section 2.3), and the conversion into M (section 2.4), was completed in OpenBUGS (Spiegelhalter *et al.* 2014). Within this first step, we ran our hierarchical models for 100,000 iterations using two MCMC chains with a burn-in of 50,000 iterations. Evaluation of trace plots and $\hat{R} < 1.05$ indicated successful convergence of all monitored parameters. We then extracted median, SD (which we converted into CV), and 95% credible intervals (CrI) from the 100,000 posterior samples for each standardised count for $y_{t,i}$ (so BP) and $M_{i,t}$. We used the median and the CV for the second modelling step, the modelling of trends and the subsequent conservation prioritisations assessments through the custom R package *ACAPT*. This second step was implemented using the Bayesian modelling programme JAGS (Plummer 2003) within R (R Core Team 2024). Within this second step, trend models were run for 10,000 iterations using four MCMC chains with a burn-in of 5,000 iterations, which were sufficient to achieve model convergence, confirmed through posterior predictive checks. We report medians and 95% CrIs from the 20,000 posterior samples for all trend estimates obtained through *ACAPT*. We explicitly chose to separate the hierarchical modelling in OpenBUGS and the trend modelling in *ACAPT*, rather than fully integrate these two, to ensure that 1) any of the preparatory steps did not have possibly overly inflated impacts on the overall trend estimates and 2) that *ACAPT* remained a more general trend modelling package like its predecessor *JARA* (Winker *et al.* 2020).

For reporting purposes, population changes are initially presented as changes over the full time series, since 1980 (as not all time series started at of prior to 1970, which would have been the preferred staring point, e.g., see Pacoureau et al. 2021, Juan-Jorda et al. 2022, Dulvy et al. 2024), and since 2006 (i.e., the last 20 years as per ACAP convention; ACAP 2025b). However, for the evaluations against IUCN Red List Criterion A, changes are presented over the full time series up to 3GL, the last GL, and since 2006. For the ACAP High Priority Population evaluation, change was only assessed since 2006 as per ACAP convention (ACAP 2025b).

2.7 Case studies

We illustrate the utility of our framework to process and model abundance data of albatrosses and petrels using ten New Zealand endemics from 22 breeding sites (Fig. 7). These case studies vary in terms of data availability, quality, and time span (39-91 years, mean = 53 years) as well as life history characteristics, such as breeding probability (e.g., Carneiro *et al.* 2020, Edwards *et al.* 2023), and generation length (e.g., Bird *et al.* 2020). Thus, these case studies enable a thorough evaluation of how the framework could overcome different challenges associated with idiosyncratic and disparate abundance data of a range of species. Below, we provide overviews of each case study (Table 4). We refer to place names of breeding sites at first mention using both te reo Māori/traditional names and English. Thereafter, we will revert to the former whenever possible (e.g., there is no known te reo Māori name for Disappointment Island or the Western Chain islets as a collective).

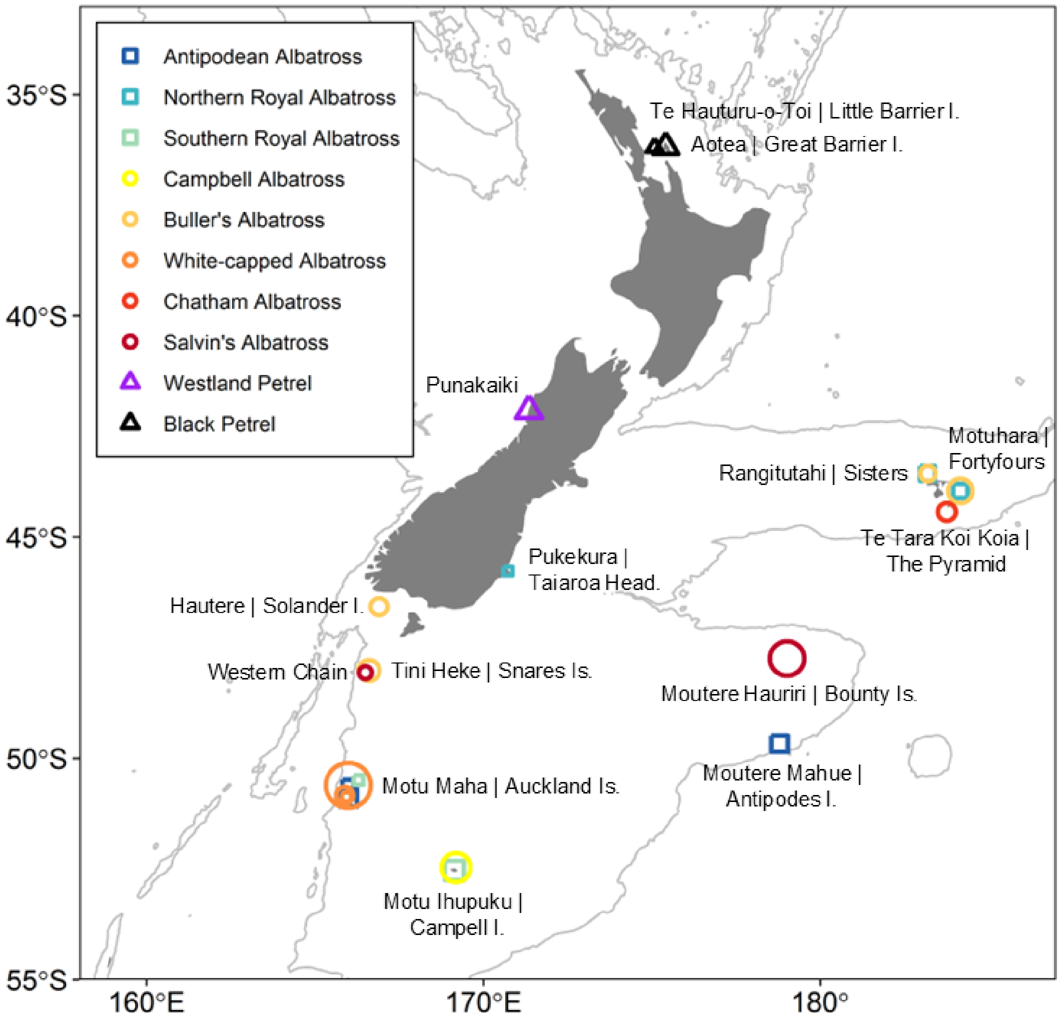

Fig. 7. Breeding sites of *Diomedea* albatrosses (squares), *Thalassarche* albatrosses (circles), and *Procellaria* petrels (triangles) endemic to New Zealand (in relation to the 2,000 m depth contour; grey lines). Symbol size approximates relative colony size; place names are given in te reo Māori/traditional names | English.

2.7.1. Antipodean Albatross (Diomedea antipodensis)

The Antipodean Albatross is arguably the best studied seabird species in New Zealand. We collated data for this species from the three key breeding sites (Moutere Mahue | Antipodes Island for ssp. *antipodes*, Adams and Disappointment Island for ssp. *gibsoni*) across 1969-2025, which jointly cover >99% of the overall population (Table 4; Supplementary Table 1-3). Counts for this species have largely been conducted annually following standardised protocols since the mid-1990s using GCs at designated study and index sites on Moutere Mahue and Adams Island (representing 2.8-14.9% and 2.6-9.5% of the breeding sites, depending on study site combinations, respectively). These counts have documented concerning declines in both breeding sites from the mid-2000s onwards (e.g., Elliott *et al.* 2025, Rexer-Huber *et al.* 2025), which resulted in the species being listed as EN on the IUCN Red List in 2018 (BirdLife International 2025) and the Moutere Mahue population as an ACAP High Priority Population in 2017 (Walker & Elliott 2017). Full island counts, however, are rare and were only conducted in the 1960s, 1970s and 1990s (Robertson 1975, Walker & Elliott 1999, 2005), and recently, when the world's largest AC$^{\mathrm{UAV}}$ enabled the total breeding site estimates on Moutere Mahue and Adams Island (Elliott *et al.* 2024, 2025, Rexer-Huber *et al.* 2024, 2025). In contrast, the Disappointment Island colony has only been counted three times, through a combination of GC, VPC, and AC$^{\mathrm{heli}}$ (Robertson 1975, Baker & Jensz 2014a). This species also breeds on Motu Ihupuku | Campbell Island and Rangihaute / Rangiāuria | Pitt Island, but both populations are very small (<1% of the world population combined) and counts are irregular and incomplete (Miskelly *et al.* 2008, Mischler *et al.* 2025), so we did not include these data in our analyses.

Most Antipodean Albatross counts required minimal adjustments, as most of the reported counts were already aligned with our framework in the original references (e.g., Elliott *et al.* 2025, Rexer-Huber *et al.* 2025). As typically $\Psi^{d} > 0.950$ for this species (Walker & Elliott 2005), we did not explicitly account for detection and assumed that Eq. 1 would suffice to address this error. Moutere Mahue counts were not adjusted for Ψ^{p} during 1978-2023, while the Adams Island counts were not adjusted for Ψ^{p} during 1973-1996. Consequently, we used an annually varying model (Eq. 3A) to make the necessary adjustments for ψ^{fail}. The Disappointment Island counts required adjustments for Ψ^{o} and Ψ^{p}, for which we used the intercepts of the Adams Island models (Eq. 2AB & 3A, respectively). Both the Moutere Mahue and Adams Island populations have a known history of skewed sex-ratios (Elliott *et al.* 2025, Rexer-Huber *et al.* 2025), and, as data enabling insights on time-varying p^b exist for both, we applied conversions from $y_{t,i}$ to $M_{t,i}$ that specifically accounted for these factors (Eq. 5B). No p^b data for Disappointment Island exists and thus we used the model intercept for Adams Island for the conversions on Disappointment Island (Eq. 5A).

2.7.2. Northern Royal Albatross (D. sanfordi)

We collated count data for the three Northern Royal Albatross breeding sites, the privately-owned Motuhara | Forty-fours and Rangitutahi | Sisters archipelagos within the Chatham Islands and the Pukekura | Taiaroa Head colony on the Otago Peninsula – the world's only "mainland" albatross colony (jointly comprising >99% of the world population), over a remarkably long period: 1936-2026 (Table 4; Supplementary Table 4-6). Pukekura is small (<1% of the global population), but its accessibility has resulted in a truly unique time-series: a virtually continuous GC census of >90 years, documenting every breeding attempt since the establishment of the breeding site in the 1930's (Richdale 1939, Robertson 1993, DOC unpubl. data). This breeding site is subject to concerted management and breeding success is maximised through targeted interventions (e.g., predator control, artificial incubation, and cross fostering; Robertson 2001, Richard *et al.* 2015). Both Chatham Islands breeding sites on the other hand are challenging to access, but hold >99% of the species' population. Both sites have been counted intermittently, with periods of concerted effort during the 1970s, 1990s, 2000s, and 2020s. Counts are predominantly completed as AC^{fw}, with both breeding sites counted simultaneously, but GCs do occur (e.g., Frost 2017, 2024, Bell 2024). Therefore, counts are expressed in BP, AOS, BOG, and C. In 1985, a severe storm stripped most soil and vegetation from the Motuhara (and to a lesser extent, Rangitutahi), caused near-complete breeding failure, and disrupted the alternating cycle of this biennial breeder, making trends difficult to detect, at least for a period (Roberston 1991, 1998). Both sites have been subjected to multiple counts within years to compare counting methods (e.g., GCs vs AC^{fw} vs AC^{sat}), which included the establishment of study quadrats representing 11% of the breeding site, but direct comparability between methods remained challenging (e.g., Scofield 2011, Baker *et al.* 2017, Bell 2021, Frost 2022). Despite irregularity, environmental stochasticity, and differing methods, these data indicated concerning declines over time (e.g., Bell *et al.* 2018), resulting in the species being listed as EN in 2000 (BirdLife International 2025).

Uniquely, the Pukekura time-series represents continuous monitoring of all breeding attempts and is thus expressed as all BP at the start of the breeding period for the entire breeding site. Therefore, no adjustments were required apart from applying Eq. 1. For the

Chatham Island breeding sites, we first selected the counts that required the least data processing for years during which >1 count was conducted. Then, as Bell *et al.* (2018) estimated $\Psi^d > 0.950$ (on Rangitutahi), as is typical for *Diomedea* albatrosses, we did not explicitly account for imperfect detection and assumed that Eq. 1 would suffice. Less than 25% of counts on both the Motuhara and Rangitutahi provided explicit data on ψ^{BOG} despite BOG being the common metric of counting this species and thus we used an intercept only model to first transform BOG into AOS through Eq. 2B. Only two counts provided explicit data on ψ^{ABA} and thus we used these two data points to generate a uniform prior to then transform AOS into BP as per Eq. 2A. The traditional metric to express counts of Northern Royal Albatrosses on the Chatham Islands is not BP, and f is estimated through whole breeding site counts of chicks (e.g., Robertson 1991, Frost 2017), and thus, obtaining accurate estimates of f was not straightforward. Pukekura estimates could not be used as this site is subject to management targeted to maximize f (e.g., DOC Coast Otago Operations 2026). Consequently, we first transformed all counts into BP, and then used the BP estimates at the time of the count and whole island counts of chicks to obtain f. We then included a fixed effect for the years 1989-2000 to capture the substantial impacts of the severe storm on the productivity of both sites (Roberston 1991, Scofield 2011, Bell *et al.* 2018). After these steps, we successfully applied Eq. 3A to estimate BP at the start of the breeding season for both breeding sites, i.e., $y_{t,i}$. Finally, as the only information on p^b for this species is based on the Pukekura long-term CMR dataset, we used the information contained in Richard *et al.* (2015) and Edwards *et al.* (2025) to first devise an informative prior for years without storm impacts (N[0.567,125]). We then used the long-term f estimate during 1989-2000 of both Chatham Island sites with the estimates p^b of failed and successful breeders in Richard *et al.* (2015) to devise a second informative prior for p^b for years with storm impacts for both Chatham Island sites during 1989-2000 (N[0.664,125]). No evidence exists for skewed sex ratios in this species and thus we applied Eq. 5A to convert $y_{t,i}$ to $M_{t,i}$ for all three breeding sites.

2.7.3. Southern Royal Albatross (D. epomophora)

We collated count data for two Southern Royal Albatross breeding sites, Motu Ihupuku | Campbell Island and Enderby Island (jointly comprising >99% of the world population) over a notably long period: 1943-2025 (Table 4; Supplementary Table 7-8). These two breeding sites contrast in size, with Motu Ihupuku holding >99% of the overall population and Enderby Island holding <1%. This contrast is reflected in the count data, with Enderby Island GCs typically covering the entire site, and being repeated almost annually since 1993 (Childerhouse *et al.* 2003), while Motu Ihupuku counts (GCs, sometimes combined with VPCs) were more intermittent and irregular, with full island counts being conducted roughly every decade until the mid-2000s (Moore *et al.* 1997, 2012). However, standardised study and index site GCs (representing 2.5-25.7% of the Motu Ihupuku population, depending on combinations) provided additional, more regular data since the late 1980s up to 2026, which recently highlighted a substantial population decline (Mischler *et al.* 2025). This species also breeds on Adams Island, but the population is minute (<1% of the world population) and counts are irregular and incomplete (Elliott *et al.* 2025), so we did not include these data in our analyses.

To standardise the Southern Royal Albatross data, we first selected the counts that required the least amount of adjustment in the few years that several counts were conducted on Enderby and then we fit Eq. 1 to both the Enderby and the Motu Ihupuku time series. Various studies have shown that $\Psi^d > 0.950$ for GCs of this species (e.g., Moore *et al.* 1997, 2012, Mischler *et al.* 2025) and thus for GCs, we did not explicitly account for imperfect detection and assumed that Eq. 1 would suffice. However, $\Psi^d < 0.950$ for VPCs on Motu Ihupuku (Moore *et al.* 1997, 2012), and thus we used the few estimates that exist to construct an informative prior for ψ^d_{VPC} (U[0.720-1.000]) to account for imperfect detection in VPCs (1958-1983 and 1995). Similarly, those older VPCs did not account for Ψ^o and these counts consisted of an indistinguishable mix of BP, AOS, and BOG. Data on ψ^{ABA} and ψ^{BOG} for this species is rare (e.g., Baker *et al.* 2014, 2020) thus, we used an intercept-only formulations of Eq. 2A and 2B to estimate ψ^{ABA} and ψ^{BOG}, respectively. Some counts from Motu Ihupuku were paired with explicit estimates of ψ^{fail} (Moore *et al.* 2012), and these original adjustments were carried over. Where no adjustments had been made, we fit a time-varying model to existing f data from Motu Ihupuku to estimate annually varying ψ^{fail} through Eq. 3A. However, no detailed data on f exist from Enderby (Childerhouse *et al.* 2003) and thus we used the f intercept estimate from the Campbell data to adjust the Enderby Island counts. Information on p^b for this species is limited, and thus we used the little information contained in Waugh *et al.* (1997), Moore *et al.* (2012), and Edwards *et al.* (2025) to construct an informative prior (N[0.515,100]), and as no evidence exists for a skewed sex ratios in this species, we applied Eq. 5A to convert $y_{t,i}$ to $M_{t,i}$ for all three breeding sites.

2.7.4. Campbell Albatross (Thalassarche impavida)

TBC

2.7.5. Buller's Albatross (T. bulleri)

We collated data for the four major Buller's Albatross colonies, Hautere | Solander and Tini Heke | Snares Islands in the New Zealand Subantarctic (ssp. *bulleri*) and the Motuhara and Rangitutahi in the Chatham Island archipelago (ssp. *platei*) (jointly comprising >99% of the world population) across 1969-2025 (Table 4, Supplementary Table 10-13). The Tini Heke population has been studied intensively since 1948 (e.g., Sagar *et al.* 2000, Francis & Sagar 2012). Population counts, consisting of a combination of GCs and VPCs started in 1969, but varied across years depending on what sections were counted (study and index areas on North East Island cover 1.4-18.5% depending on their combination), and full archipelago counts have been intermittent (i.e., 1969, 1992, 1997, 2002, 2014, 2019, and 2020; Sagar *et al.* 1999, Sagar & Stahl 2005, Sagar 2014, Thompson & Sagar 2020). The remote and difficult to access Hautere, Motuhara, and Rangitutahi populations, the latter two of which are privately-owned, have been counted sporadically using a variety of approaches (GCs, VPCs, AC^{heli} and AC^{fw}; e.g., Baker *et al.* 2017, Bell 2021, Frost *et al.* 2025). Of these three, only Motuhara holds established index plots (representing 1.8-3.9%; Bell 2021, 2023, 2026), while the other two breeding sites are largely counted at a full island or archipelago level. Buller's Albatrosses also breed on Rosemary Rock in the Three Kings archipelago (ssp. *platei*; Rayner *et al.* 2020), but the population is minute (<1% of the world population) and counts are irregular, so we did not include these data in our analyses.

For Hautere and Tini Heke counts (i.e., ssp. *bulleri*), we incorporated baseline uncertainty and extrapolated all counts to breeding site level through Eq. 1. Attempts have been made to estimate Ψ^{d} for various Hautere counts (0.900-0.960) and Tini Heke VPCs (0.900-0.950) (Sagar & Stahl 2005, Thompson *et al.* 2017, Thompson & Sagar 2020) and so we incorporated these estimates explicitly through informed uniform priors. For the Tini Heke, we separated the sections of each count that were conducted using GCs and those that were conducted using VPCs using Thompson & Sagar (2020) and Sagar (unpubl. data) and adjusted the latter only. Most of the AC from Hautere were already adjusted from BOG to AOS in the original references (e.g., Frost *et al.* 2025), but none accounted for ψ^{ABA} and so we sourced data on Hautere transect counts (Baker & Jensz 2014b, Thompson *et al.* 2017, Frost *et al.* 2025) and applied Eq. 2A to these data to account for ψ^{ABA} retrospectively while incorporating further uncertainty as all transect counts were based on small sample sizes

(Frost *et al.* 2025). As no direct data on ψ^{ABA} from Tini Heke was directly available (despite the detailed work on this topic; Stahl & Sagar 2006), we used the intercept estimate from Hautere to adjust the Tini Heke VPCs (as these produced data expressed in AOS as well). Subsequently, we sourced the data on f from Hautere (JC Stahl unpubl. data) and Tini Heke (Sagar & Stahl 2005) and applied Eq. 3A to these data to account for ψ^{fail} for all Hautere counts and the Tini Heke VPCs only. We did not adjust the GCs on Tini Heke as signs of failed nests (e.g., eggshells, dead chicks etc.) remain in place for an unusually long time under the forest canopy on this breeding site and thus data had already been adjusted for this source of error (P. Sagar pers. comm.). Finally, we formulated an informative prior based on Edwards *et al.* (2025) for p^b (N[0.800, 250]), which was based on the information contained in Fu & Sagar (2016). We then used this prior to transform $y_{t,i}$ into $M_{t,i}$ through Eq. 5A for both breeding sites, as there is no indication for a sex bias in any population and no further information to differentiate p^b among sites.

For Motuhara and Rangitutahi counts (i.e., ssp. *platei*), we did not adjust for Ψ^d as the habitat on these islands differs considerably from Hautere and Tini Heke and Bell *et al.* (2018) estimated Ψ^d at 0.996-0.999 on Rangitutahi. As such, for these two islands, we assumed that the uncertainty incorporated through Eq. 1 was sufficient. Motuhara and Rangitutahi counts have been expressed in virtually all possible metrics over the years and as such it was necessary to estimate ψ^{ABA}, ψ^{BOG}, and ψ^{occ}, but data for the estimation of these parameters were sparse, partially as potentially definitions of failed and empty nests differed between teams (alternatively the situation has changed on the islands over time; e.g., Fraser *et al.* 2010 vs. Bell 2026). We sourced five estimates with data for ψ^{ABA}, three for ψ^{BOG}, and four for ψ^{occ} (Fraser *et al.* 2010, Baker *et al.* 2017, Bell 2026). Based on how these were distributed among the years in the timeseries, we used Eq. 2A (ψ^{ABA}) and Eq. 2C (ψ^{occ}) while accounting for annual variation for Motuhara but used an intercept-only model for Eq. 2B (ψ^{BOG}) for Motuhara. As almost all data on Ψ^o originated from Motuhara instead of Rangitutahi, we used intercept only models for Eq. 2ABC for the latter breeding site. Information on f for Motuhara and Rangitutahi is exceptionally sparse and only one estimate that covers the entire breeding period exists (fused from two different sources; Bell 2021, Frost *et al.* 2021), which we used to construct a mildly informed prior (N[0.510,50]) for integration into Eq. 3A. We then used the same approach (i.e., the same prior for p^b within Eq. 5A) as for Hautere and Tini Heke, as no information for Motuhara or Rangitutahi on p^b exists, nor is there any indication for a sex imbalance. Subsequently, all counts were expressed in $y_{t,i}$ and $M_{t,i}$ suitable for the our trend modelling steps.

2.7.6. White-capped Albatross (T. steadi)

Population counts and trends of this species, the most numerous albatross species in New Zealand, have been subject to considerable debate, as trend estimates vary considerably depending on how error adjustments are applied (see Walker *et al.* 2021 vs. Baker *et al.* 2023). We collated data for the three major White-capped Albatross colonies, Disappointment Island, Southwest Cape on Maukahuka | Auckland Island, and Logan Point on Adams Island (jointly comprising >99% of the world population), across 1973-2021 (Table 4, Supplementary Table 14-16). All three colonies are difficult to survey, and counts have been conducted intermittently and irregularly (although regular counts did occur during 2007-2018; Baker *et al.* 2023), using a variety of different methods, including GCs, VPCs, VBCs, AC^{heli} and AC^{UAV}. While a study area exists on the largest colony (Castaway Bay representing ~4.7% of the Disappointment Island colony), this area is not fully geographically demarcated, is largely used for demographic studies, and has not been widely used as an index count site (Walker *et al.* 2021, Parker *et al.* 2024). White-capped Albatrosses also breed on Bollon's Island off Antipodes Island (Tennyson *et al.* 1998), the Western Chain Islets (Miskelly *et al.* 2001), and Motuhara (Bell *et al.* 2017), but these populations are very small (<1% of the world population) and counts are very rare, so we did not include these data in our analyses. Furthermore, we note that this species recently bred on the Diego Ramirez archipelago in Chile (Suazo *et al.* 2024), but we continue to treat this species as a New Zealand breeding endemic here.

We fit Eq. 1 to all White-capped Albatross counts under the assumption that the incorporated uncertainty would also cover the associated Ψ^d. However, the 1973 VBCs, some which were combined with GCs and VPCs, were documented with rough uncertainty estimates (Robertson 1975), but required further Ψ^d adjustments due to the influence of this error on VBCs (Fig 2; e.g., Rexer-Huber *et al.* 2020). To address this gap, we completed an online modified Delphi expert elicitation (https://forms.gle/kXCoSfzbGkAPzYvZ9; Hemming *et al.* 2018) with 11 experts familiar with the breeding sites. After round two, we aggregated the provided four-point estimates to derive priors following Fischer *et al.* (2022) for the Disappointment Ψ^d_{VBC}: β(9.044, 2.681) and the Southwest Cape Ψ^d_{VBC}: β(6.388, 2.585) (corresponding to modes of 0.771 and 0.711, respectively). Due to the small population size and considerable uncertainty surrounding the Logan Point VBC in 1973, no attempts were made to infer Ψ^{d} for this count. We then used all available data on ψ^{ABA} (Walker *et al.* 2021, Parker *et al.* 2022, Elliott *et al.* 2023) and ψ^{BOG} (Walker *et al.* 2021, Parker *et al.* 2022, Baker *et al.* 2023, Elliott *et al.* 2023) to fit to Eq. 2A and Eq. 2B, respectively, each while accounting for interannual effects. As virtually all information on ψ^{ABA} and ψ^{BOG} were obtained on Disappointment Island, we followed the approach from Baker et al (2023) and considered these values representative for the other breeding sites as well. Despite this shortcoming, this approach still allowed us to transform counts expressed in BOG or AOS into BP while incorporating uncertainty explicitly. We collated all available data on f (e.g., Thompson & Sagar 2008ab, Francis 2012, Frost 2026) and fit Eq. 3A to these. As only three of the six years for which data on f were available covered years in the abundance timeseries (i.e., <25% of the time series), we used an intercept only model to obtain $y_{t,i}$. Again, we did not differentiate between different breeding sites due to data limitations. Finally, we sourced the only available estimate of p^{b} for White-capped Albatross from Francis (2012), and constructed an informative prior (N[0.680, 250]) to convert the generated $y_{t,i}$ into $M_{t,i}$ using Eq. 5A to obtain both standardised abundance metrics required for our trend models.

2.7.7. Chatham Albatross (T. eremita)

Counts of this species, the rarest of the New Zealand endemic albatrosses, are rare and intermittent. In general, this species is one of the least studied albatross species globally, which is in part caused by the extreme difficulty of accessing its main breeding site, Te Tara Koi Koia | the Pyramid within the Chatham Islands archipelago, which is privately owned (Bell *et al.* 2017, Bell 2026). We collated the intermittent and irregular abundance data for this breeding site across 1965-2026 (Table 4, Supplementary Table 17). Data were predominantly collected between 2000 and 2026 during GCs with a small proportion of VPCs (Bell *et al.* 2017), aside from two early counts, a VBC in 1965 (Dawson 1973) and an AC^{fw} in 1973 (Robertson *et al.* 1991). All counts covered the entire island, and no abundance index sites exist (although there are two study areas for demographic studies; Bell *et al.* 2017). During 2014-2018, the site was visited to translocate pre-fledging chicks to main Chatham Island in order to establish a second colony, but no abundance data were collected during these visits, and ultimately, no second colony was established through these translocations, as all chicks that survived to maturity recruited back to the source site (or the Western Chain; Bell 2026, P Sagar unpubl. data). A few Chatham Albatross pairs also breed on the Western

Chain islets (Miskelly *et al.* 2001), but their number is so small (<1% of the world population) and counts are rare, so we did not include these data in our analyses.

Chatham Albatross counts were almost entirely expressed in NS rather than BP, despite indications that NS do not equal BP (Robertson *et al.* 2003, Bell *et al.* 2017). For 2000-2026, Ψ^{d} was considered sufficiently high that we did not explicitly account for detection and assumed that Eq. 1 would suffice. For these counts, the proportion counted through VPCs was known and thus this was subtracted to derive ξ for Eq. 1 and simplify subsequent steps. The 1965 VBC and 1973 AC^{fw} each had existing Ψ^{d} estimates, but these were potentially inaccurate (Dawson 1973, Robertson *et al.* 1991). We therefore completed an online modified Delphi expert elicitation (https://forms.gle/79gRwTEzwEViXgUD6; Hemming *et al.* 2018) with nine experts familiar with the breeding site. We aggregated the obtained four-point estimates following Fischer *et al.* (2022), including the original Ψ^{d} estimates (obtaining a total of six estimates), to derive updated beta-distributed priors for the Ψ^{d} associated with the VBC and AC^{fw} (β[7.119, 4.079], β[18.200, 2.870], corresponding to modes of 0.636 and 0.864, respectively). While interpretation of empty vs. failed nests appeared to have changed over time, all GCs recorded nest contents (e.g., Fraser *et al.* 2011, Bell *et al.* 2017, Bell 2026), enabling direct interpretation of BP, and thus no adjustments of Ψ^{o} for these data were required. However, the VBC and AC^{fw} presumably recorded AOS (as no landings took place) and to convert these into BP in the absence of species-specific data, we calculated the mean of the intercept estimates for ψ^{ABA} for both White-capped and Salvin's Albatross as the most closely related species, and then used this estimate in Eq. 2A. Similarly, no breeding success data exists for Chatham Albatross, but it may mirror the closely related Salvin's Albatross, which also breeds on similar substrates (Bell *et al.* 2017). Thus, to account for ψ^{fail}, we generated an informative prior using all available data on f for Salvin's Albatross (N[0.352,250]); Thompson 2025), after which we fit Eq. 3 to all Chatham Albatross counts. Finally, also no data p^{b} exists for Chatham Albatross and thus we used the informative priors we had generated for p^{b} for the two most closely-related species, White-capped and Salvin's Albatross (N[0.680, 250]), and N[0.927,100], respectively) and averaged these, after which we fit Eq. 4A to all counts. Following these steps, all Chatham Albatross data were in a suitable, comparable format to enable the coherent modelling of trends.

2.7.8. Salvin's Albatross (T. salvini)

Counts of this species, the second-most numerous albatross species in New Zealand, are uncommon and intermittent, and depending on how early counts are interpreted, trend estimates vary considerably, leading to contrasting conservation status assessments (IUCN Red List = VU, New Zealand Threat Classification System = CR; BirdLife International 2025, Robertson *et al.* 2021). We collated data for the two major Salvin's Albatross breeding sites, the Bounty Islands | Moutere Hauriri, and the Western Chain Islets (jointly comprising >99% of the world population) across 1979-2026 (Table 4; Supplementary Table 18-19). Salvin's Albatross breeding sites are characterised as densely populated, but barren, isolated granite rock stacks that are extremely difficult to access and survey, and thus various methods have been used to obtain abundance data, ranging from GCs, to AC^{fw} and AC^{heli}, to more recently, AC^{UAV} (Thompson 2025). The largest Salvin's Albatross population is located on Moutere Hauriri (97% of the global population), and while whole archipelago counts have been conducted (as ACs), there has been a focus on Proclamation Island in some years due to the accessibility of this islet (10.3% of the breeding site) (Parker & Rexer-Huber 2020a, Mattern 2022, 2024ab). The smaller breeding site, the Western Chain islets, consists of two main islets (Toru; 66.7%; and Rima; 33.3%) which have largely been counted through GCs (Sagar *et al.* 2014, Thompson 2025). Salvin's Albatrosses also breed on Te Tara Koi Koia, but in such low numbers (<1% of the world population; Bell *et al.* 2017) that we did not include these data in our analyses. Furthermore, we note that this species also breeds on Penguin Island and Apôtres Island in the Crozet Archipelago, but these populations are extremely small (<1%) (Jouventin 1990; Weimerskirch et al. 2018), and thus we continue to treat this species as a New Zealand breeding endemic here.

While almost all counts of Salvin's Albatross could be processed and adjusted relatively straightforwardly through our standardised framework, the 1979 Bounty Islands GC needed additional consideration. Specifically, Robertson & van Tets (1982) estimated a density of 0.5 BP/m^2 and then extrapolated across all suitable areas (15.3 ha). This approach may have produced an overestimate due to sampling in high density areas only, the assumption of uniform density, and an absence of high-resolution maps to enable fine-scale delineation of suitable areas (Amy & Sagar 2013, Thompson 2025). It was not possible to re-evaluate the densities in 1979. Instead, we updated the delineation of suitable areas by placing a 2 m^2 circular buffer around each manually identified Salvin's Albatross BOG in high-resolution UAV footage of the entire archipelago collected in 2023 and 2025 (Mattern 2022, 2024a, 2024b), merging all buffers, recalculating the mean area between both years (9.85 ha), and ultimately repeating the original extrapolation (see Thompson 2025 for details). We then assigned the lowest ACAP accuracy score to this count to further acknowledge the continuing, unsurmountable uncertainty.

After this additional work, we followed our framework step by step as outlined above. Salvin’s Albatross breeding sites are barren in nature, and Amey & Sagar (2013) estimated Ψ^d > 0.990 on Moutere Hauriri, so we did not explicitly account for detection and assumed that Eq. 1 would suffice. We then collated all information on Ψ^o obtained through transects or close-up photographs (e.g., Amey & Sagar 2013, Baker & Jensz 2018) and fit Eq. 2A and Eq. 2B to the collated data on ψ^{ABA} and ψ^{BOG}, respectively, allowing us to convert BOGs into BPs, while allowing for annual variation. All counts from the Western Chain were obtained during GCs and expressed in BP and thus this step was not necessary for this breeding site. As Salvin’s Albatross is one of the few species for which stage-specific f values have been quantified, we were able to account for Ψ^p through Eq. 3B (Thompson 2025). However, the number of years for which f_k has been quantified are few, and thus, we used the mean f_k across years to account for Ψ^p. Specifically, we used the information in Thompson (2025) on T_k and f to construct informative priors ($f_{\text{inc}} = \text{N}[0.562{,}125]$, $f_{\text{guard}} = \text{N}[0.960{,}30000]$, $f_{\text{post-guard}} = \text{N}[0.697, 600]$) and use these in Eq. 3B. Information on f has been obtained from Moutere Hauriri only and to date no estimates for the Western Chain are available, and thus we used Moutere Hauriri f to adjust both sites. Finally, the only information available on p^b for Salvin’s Albatross is based on three years of research on Toru islet (Sagar *et al.* 2011). We used the data contained in Sagar *et al.* (2011) to fit a binomial GLMM with a logit-link function to estimate p^b and construct an informative prior (N[0.927,100]), which we included in Eq. 5A to estimate M for all counts (Thompson 2025). Following these steps, all Salvin’s Albatross data were in a suitable format to allow for the modelling of trends.

2.7.9. Westland Petrel (Procellaria westlandica)

We collated data covering 1974-2019 for the sole breeding site Westland Petrels, Punakaiki, on the Te Waipounamu | the South Island of New Zealand (Table 4, Supplementary Table 20). The species breeds in a rugged area across ~28 sub-colonies that can be difficult to access, define, and may change over time (Waugh *et al.* 2020). Due to these challenges, population counts for this species are rare and gaps in the timeseries are common and long. Counts can only realistically be conducted as GCs, but despite this commonality, differences between counts remained in terms of timing, correction for Ψ^o, and subsequent extrapolation steps (Wood & Otley 2013, Baker *et al.* 2020, Waugh *et al.* 2020). Consequently, considerable uncertainty surrounded most data. Nevertheless, Waugh & Wilson (2017) successfully argued that the species should be uplisted to EN on the IUCN Red List due to the perceived impact of extreme weather events on the fragmentation of breeding habitat.

Westland Petrel GCs during 2002-2005 and 2010, were not documented with sufficient information to disentangle individual count years, and thus we used 2003 as a mid-point for these counts (Wood & Otley 2013). No Westland Petrel GCs explicitly accounted for Ψ^d (e.g., through distance sampling) and since we were unable to identify a unified mechanism to incorporate Ψ^d retrospectively, we attempted to acknowledge the absence of accounting for this error by downscaling the accuracy of all counts by one category. All Westland Petrel GCs have been accompanied with some efforts to account for Ψ^o. However, some GCs explicitly accounted for ψ^{ABA} and ψ^{occ} (2003 and 2019; Wood & Otley 2013, Waugh *et al.* 2020), while the other GCs only accounted for ψ^{occ} (e.g., Baker *et al.* 2020). Consequently, we used the data reported in Baker *et al.* (2020) to model ψ^{ABA} and information in Waugh *et al.* (2020) to construct an informative prior (N[0.480,200]), which we then fused into an overall estimate for Westland Petrel ψ^{ABA} = 0.658 (0.570-0.743). We then used this overall estimate within Eq. 2A to adjust all counts that had not explicitly accounted for this source of error. Breeding success in this species may have changed over time (Bartle 1985, Freeman & Wilson 2002, Waugh *et al.* 2006, 2020) and thus we used the available information on multi-year averages in Freeman & Wilson (2002) to generate an informative prior for $f_{1974\text{-}1975}$ (N[0.390, 100]), Waugh *et al.* (2006) to generate a prior for f_{2003} (N[0.620, 700]), and Waugh *et al.* (2020) to generate a prior for $f_{2007\text{-}2019}$ (N[0.685, 80]). We then used these different estimates to account for Ψ^P in Eq. 3A, while explicitly incorporating change in f over time. Only limited information was available on Westland Petrel p^b. Specifically, two, quite different deterministic estimates were available (Waugh *et al.* 2015, Waugh & Wilson 2017), which we used to construct a uniform prior (U[0.460,0.768]) and estimate M for the 1974-2011 counts. However, recently, more data has been collected due to the perception that p^b has changed and thus we used recent (2021-2024) intensive burrow monitoring data (K Simister unpubl. data) together with a binomial GLMM with a logit-link function to obtain an updated estimate for p^b = 0.706 (0.693-0.720) and estimate M for the 2019 count. No evidence exists for a skewed sex ratio in this species (e.g., Waugh *et al.* 2015) and thus we used Eq. 5A for all estimates of M. Following these steps, all Westland Petrel data (both in $y_{t,i}$ and $M_{t,i}$) were in a suitable format to allow for the modelling of trends.

2.7.10. Black Petrel (P. parkinsoni)

This species has been subject to a long-standing and ongoing population study at its largest breeding site, Aotea | Great Barrier Island, since 1996 (Bell *et al.* 2025), rendering it one of the best studied species of its genus, rivalled only by White-chinned Petrel (*P. aequinoctialis*) studies in other ocean basins (e.g., Dasnon *et al.* 2022). We collated data across 1977-2025 for the two Black Petrel breeding sites, Aotea | Great Barrier Island (~87%) and Te Hauturu-o-toi | Little Barrier Island (~13%) which jointly hold 100% of the world population (Table 4; Supplementary Table 21-22). Note, the first count for both sites was here labelled as 1977 as a midpoint of the 1972-1975, 1977, 1979, and 1982-1983 counts that could not be disentangled (Imber 1987). The two breeding sites contrast in their data availability, with Aotea having been monitored annually for >20 years (e.g., Bell & Sim 2000, Bell *et al.* 2025), while only two data points exist for Hauturu (Imber 1987, Bell *et al.* 2016). Only one comprehensive effort to estimate the true population of the entirety of Aotea exists, spanning three years of GCs (2019-2021; Bell *et al.* 2022), which we here used to scale all other counts (i.e., calculate ξ). Aside from this effort, GCs on Aotea are usually conducted using nine census squares within the traditional Mt Hirakimata study area (ξ = 2.3%). However, during 1996-1998, only three census grids existed, representing <1% of the breeding site population, which we therefore excluded from processing in our framework (see section 2.2.1). Occasionally, stratified transect GCs have been conducted throughout the wider study area (ξ = 53%), and these data have provided contrasting results when directly compared to data from the census grids (e.g., Bell *et al.* 2013, 2018). When both were available, we favoured counts that represented a larger proportion of the breeding site, i.e., transects. We excluded area-based extrapolations using the census-grids only due to the known bias of these grids towards high-density areas (e.g., Bell & Sim 2000, Bell *et al.* 2013, 2018). The two data points that exist for Hauturu were both obtained through GCs, of which only the latter consisted of concerted efforts using transects and dog surveys (Bell *et al.* 2016). Other Black Petrel work has taken place on Hauturu (e.g., Bell *et al.* 2011, 2015), most of which involved using existing study burrows, but as the proportion study burrows represent is unknown, we could not collate additional abundance data for this site. Using two data points to estimate trends is far from optimal, but we include the Hauturu data here for completeness' sake (and posterior predictive checks did not indicate any poor fit of the trend model).

Modern Black Petrel GCs explicitly accounted for Ψ^d, e.g., through distance sampling (Bell *et al.* 2022) and several other counts have gone through great lengths to maximize Ψ^d, e.g., through the use of petrel detection dogs (e.g., Bell *et al.* 2015, 2016). As we did not identify a unified mechanism to incorporate Ψ^d retrospectively, we did not explicitly account for this error. However, we did adjust the ACAP accuracy score of some counts to reflect the lack of specific accounting for Ψ^d. Specifically, following comparison with the latest transect counts (Bell *et al.* 2022), the 2005 and 2010 transect counts in the 35 ha study area were re-categorised *Low* accuracy and the 2013 and 2017 transect counts in the same area were re-categorised as *Medium* accuracy. Furthermore, to acknowledge the uncertainty of the 1977 Aotea and Hauturu counts (Imber 1987), we used expert judgement to adjust ξ using uniform priors (ξ_{Aotea} = U[0.333-0.531], $\xi_{Hauturu}$ = U[0.250-0.500]). Black Petrel GCs on both Aotea and Hauturu have always been accompanied with concerted efforts to count BP directly while accounting for Ψ^o ($\psi^{occ} \cdot \psi^{ABA}$ specifically; Bell *et al.* 2016, 2022, 2025), and thus the original efforts were carried over for both sites rather than applying retrospective adjustments through Eq. 2AC. However, generally, Black Petrel counts were not adjusted for Ψ^p, even though virtually all counts from Aotea and even some Hauturu counts are accompanied with data on f (Bell *et al.* 2016, 2025). Consequently, we fit a time-varying model to f data from Aotea and to estimate annually varying ψ^{fail} through Eq. 3A. Due to the limited data for Hauturu, we only used the f intercept estimate to adjust the one Hauturu count that needed it (2016). Concerted population modelling has been conducted for Black Petrels as well (e.g., Zhang *et al.* 2020), but annual estimates of p^b, not conditional on breeding success, are not currently available. Thus, we used information contained in Zhang *et al.* (2020) to construct an informative prior (N[0.719,7000]). As no evidence exists for a skewed sex ratios in this species, we applied Eq. 5A to convert $y_{t,i}$ to $\mathrm{M}_{t,i}$ for both breeding sites.

Table 6. Overview of data and processing steps for the ten New Zealand endemic albatrosses and petrels that are listed on ACAP Annex 1. Proportions of total population are based on the most recent estimates. For definitions of acronyms see Table 4. **Bold** breeding sites indicate that they contain ≥10% of the species' population. Numbers in brackets indicate equations applied (see main text and Table 3). ~ O indicates that original approaches in the source references were carried over, ~ t indicates that time-sensitive models were used to apply year-specific estimates to make corrections/transformations, ~ α indicates that mean estimates from models were applied due to limited data, ~ U indicates the application of uniform priors, ~ N indicates the application of normal priors, ~ β indicates the application of beta-distributed priors. GL is based on a BirdLife International (2025) update of Bird *et al.* 2020. For further details, see the Supplementary Tables for each species.

Species	**Breeding site**	**Prop. pop.**	**Time series**	**No. counts**	**Metric**	**Method**	Ψ^d	Ψ^o (Eq. 2)	Ψ^p (Eq. 3AB)	p^b (Eq. 5AB)	*s* (Eq. 5B)	**GL**
Antipodean Albatross	**Moutere Mahue | Antipodes I.**	42%	1969-2025	32	BP, BOG	GC, VPC, AC^{UAV}	-	$\psi^{BOG}\cdot\psi^{ABA}$ ~ O	ψ^{fail} ~ O (1969, 2024-2025) ψ^{fail} ~ t (1978-2023) (3A)	~ t (5B)	~U (pre- & post-2005)	31
	Adams I.	54%	1973-2025	34	BP, BOG	GC, VPC, AC^{UAV}	-	$\psi^{BOG}\cdot\psi^{ABA}$ ~ O	ψ^{fail} ~ t (1973-1996) (3A) ψ^{fail} ~ O (1997- 2025)	~ t (5B)	~U (pre- & post-2005)	
	Disappointment I.	4%	1973-2014	3	BP, AOS	GC, VPC, AC^{heli}	-	$\psi^{BOG}\cdot\psi^{ABA}$ ~ α (Adams; 2AB)	ψ^{fail} ~ α (Adams; 3A)	~ α (Adams; 5A)	-	
Northern Royal Albatross	**Motuhara | Fortyfours**	38%	1972-2026	30	BP, AOS, BOG, C	GC, AC^{fw}, AC^{sat}	-	ψ^{ABA} ~ U (2A) ψ^{BOG} ~ α (2B)	ψ^{fail} ~ t + fixed effect for storm impacts (3A)	~N (with/ without storm impacts (5A)	-	28
	Rangitutahi | Sisters	61%	1972-2025	30	BP, AOS, BOG, C	GC, AC^{fw}, AC^{sat}	-	ψ^{ABA} ~ U (2A) ψ^{BOG} ~ α (2B)	ψ^{fail} ~ t + fixed effect for storm impacts (3A)	~N (with/ without storm impacts (5A)	-	
	Pukekura | Taiaroa head	<1%	1938-2026	91	BP	GC	-	-	-	~N (5A)	-	
Southern Royal Albatross	**Motu Ihupuku | Campbell I.**	>99%	1958-2026	29	BP, AOS	GC, VPC	ψ^{d}_{vpc} ~ U	ψ^{ABA} ~ α (2A) ψ^{BOG} ~ α (2B)	ψ^{fail} ~ O (1995-1996, 2005-2009) ψ^{fail} ~ t (1958-1994, 1997-1999, 2020-2026) (3A)	~N (5A)	-	27
	Enderby I.	<1%	1943-2026	41	BP, AOS	GC, AC^{heli}	-	-	ψ^{fail} ~ α (3A)	~N (5A)	-	
Campbell Albatross	**Motu Ihupuku | Campbell I.**	100%	1943-2025	TBC	TBC	TBC	TBC	TBC	TBC	TBC	-	21
Buller's Albatross	**Hautere | Solander I.**	13%	1985-2024	6	AOS, BOG, C	GC, VPC, AC^{heli}	ψ^{d}_{vpc} ~ U	ψ^{ABA} ~ t (2A)	ψ^{fail} ~ t (3A)	~N (5A)	-	24
	Tini Heke | Snares Is.	28%	1969-2025	39	BP, AOS,	GC, VPC	ψ^{d}_{vpc} ~ U	$\psi^{ABA}{}_{\text{VPC}}$ ~ α (2A)	$\psi^{\text{fail}}{}_{\text{VPC}}$ ~ t (3A)	~N (5A)	-	

Species	Breeding site	Prop. pop.	Time series	No. counts	Metric	Method	Ψ^{d}	Ψ^{o} (Eq. 2)	Ψ^{p} (Eq. 3AB)	p^{b} (Eq. 5AB)	s (Eq. 5B)	GL
	Motuhara | Fortyfours	49%	1972-2026	11	BP, BOG, AOS, NS	GC, VPC, AC^{fw}	-	$\psi^{ABA} \sim t$ (2A) $\psi^{BOG} \sim \alpha$ (2B) $\psi^{occ} \sim t$ (2C)	$\psi^{fail} \sim N$ (3A)	~N (5A)	-	
	Sisters | Rangitutahi	9%	1972-2018	6	BP, AOS, BOG, NS	GC, AC^{fw}	-	$\psi^{ABA} \sim \alpha$ (2A) $\psi^{BOG} \sim \alpha$ (2B) $\psi^{occ} \sim \alpha$ (2C))	$\psi^{fail} \sim N$ (3A)	~N (5A)	-	
White-capped Albatross	**Disappointment I.**	95%	1973-2018	16	BOG	GC, VPC, AC^{heli}, VBC	$\psi^{d}_{VBC} \sim \beta$	$\psi^{ABA} \sim t$ (2A) $\psi^{BOG} \sim t$ (2B)	$\psi^{fail} \sim \alpha$ (3A)	~N (4A)	-	22
	Southwest Cape	5%	1973-2021	15	BOG	GC, VPC, AC^{heli}, AC^{UAV}, VBC	$\psi^{d}_{VBC} \sim \beta$	$\psi^{ABA} \sim t$ (2A) $\psi^{BOG} \sim t$ (2B)	$\psi^{fail} \sim \alpha$ (3A)	~N (4A)	-	
	Adams I.	<1%	1973-2018	13	BOG	GC, VPC, AC^{heli}, VBC	-	$\psi^{ABA} \sim t$ (2A) $\psi^{BOG} \sim t$ (2B)	$\psi^{fail} \sim \alpha$ (3A)	~N (4A)	-	
Chatham Albatross	**Te Tara Koi Koia | Pyramid**	100%	1965-2026	14	AOS, NS	GC, VPC, AC^{fw}, VBC	$\psi^{d}_{VBC} \sim \beta$, $\psi^{d}_{AC} \sim \beta$	$\psi^{ABA} \sim \alpha$ (1965-1974) (2A)	$\psi^{fail} \sim N$ (3A)	~N (4A)	-	21
Salvin's Albatross	**Moutere Hauriri | Bounty Is.**	97%	1979-2025	11		GC, AC^{fw}, AC^{UAV}	-	$\psi^{ABA} \sim t$ (2A) $\psi^{BOG} \sim t$ (2B)	$\psi_{k}^{fail} \sim N$ (3B)	~N (4A)	-	21
	Western Chain	3%	1977-2026	8		GC, AC^{fw},	-	-	$\psi_{k}^{fail} \sim N$ (3B)	~N (4A)	-	
Westland Petrel	**Punakaiki**	100%	1974-2019	8	BP, AOS, NS	GC	-	$\psi^{ABA} \sim (N \cdot \alpha)$ (1974-1975, 2007-2011) (2A) $\psi^{occ} \sim O$ (1974-1975, 2007-2011) (2C) $\psi^{occ} \cdot \psi^{ABA} \sim O$ (2003, 2019) (2AC)	$\psi^{fail} \sim N$ (1974-1975, 2003, 2007-2019, separately) (3A)	~ U (1974-2011) (4A) ~ α (2019) (4A)	-	18
Black Petrel	**Aotea| Great Barrier I.**	85%	1977-2025	31	BP, NS	GC	-	$\psi^{occ} \cdot \psi^{ABA} \sim O$	$\psi^{fail} \sim t$ (3A)	~ N (4A)	-	16
	Hauturu | Little Barrier I.	15%	1977-2016	2	BP, NS	GC	-	$\psi^{occ} \cdot \psi^{ABA} \sim O$	$\psi^{fail} \sim \alpha$ (3A)	~ N (4A)	-	

3. RESULTS

Our standardised framework to process and model abundance data of ACAP species performed well, with the necessary flexibility, and ensured that all abundance data available for our case studies were subjected to standardised error corrections resulting in unified expression of data in BP at the start of the breeding season (Supplementary Table 1-22), after which data were converted into M, both of which allowed for the standardised modelling of trends.

3.1 Population trends

3.1.1. Diomedea *albatrosses*

Antipodean Albatross abundance declined from an estimated 21,594 (10,857; 45,216) breeding pairs (BP) in 1969 to 8,425 (7,180; 10,037) BP in 2025, which equated to a net change of -36,162 (-86,242; -13,356) mature individuals (M), or a relative change of -49.1 (-66.4; -29.3) %, over the entire timeseries, and a net change of -11,168 (-13,398; -9,359) M, or a relative change of -23.0 (-23.4; -22.5) % in the last 20 years (Fig. 8AB; Table 7). This collapse was predominantly driven by large declines on Adams Island between the 1970s and 1990s, followed by further declines on both Adams Island and Moutere Mahue in the mid-2000s.

Northern Royal Albatross abundance changed from an estimated 5,067 (1,678; 10,605) BP in 1936 to a peak in abundance at 6,502 (4,601; 8,729) BP in 1993, after which a decline became apparent, leaving 3,981 (2,779; 5,351) BP in 2026 (Fig. 8DC). The trend equated to a net change of 4,835 (-17,356; 8,557) M. or a relative change of 48.5 (-47.3; 291.0) %, over the entire timeseries, indicating that this species most likely increased since the beginning of last century, but that there is a possibility of a considerable decline as well. However, in the last 20 years, Northern Royal Albatrosses suffered a net change of -2,817 (-2,994; -2,626) M, equating to a relative change of -16.0 (-18.6; -13.4) % (Table 7). This decline was pronounced on Motuhara in particular, but the Rangitutahi population declined as well.

Similar to its northern sister species, Southern Royal Albatross abundance changed from an estimated 1,679 (693; 3,955) BP in 1943 to a peak in abundance at 8,396 (6,969; 10,156) BP in 2005, after which a decline became apparent, leaving 6,450 (5,250; 7,948) BP in 2026 (Fig. 8EF). The trend equated to a net increase of 19,394 (16,741; 18,894) M, or a relative change of 208.8 (42.5; 578.6) %, over the entire timeseries. However, Southern Royal Albatrosses suffered a net change of -6,336 (-6,525; -5,852) M, or a relative change of -19.8 (-

25.0; -14.9) %, in the last 20 years (Table 7). This decline was predominantly driven by declines on Motu Ihupuku, while the small Enderby population continued to slowly increase.

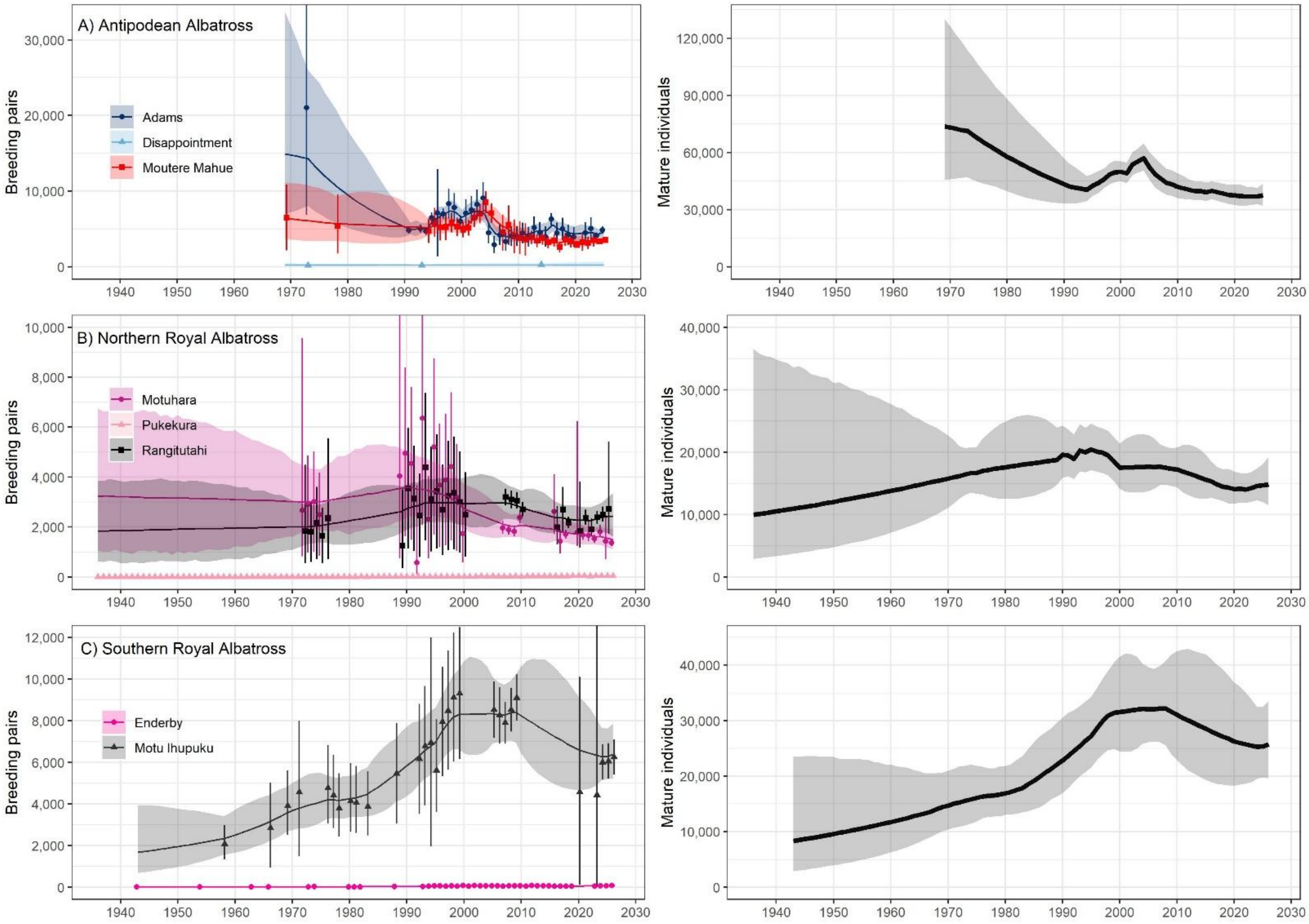

Fig. 8. Standardised abundance and trend estimates of Antipodean (AB), Northern Royal (CD), and Southern Royal Albatross (EF) expressed in breeding pairs per breeding site (ACE) and total mature individuals (BDF). Symbols with error bars (ACE) represent $y_{t,i}$ (annual breeding pairs) estimates produced through the standardised processing and modelling framework (step 2.2) expressed in medians with 95% CrIs. Trend lines and translucent ribbons represent *ACAPT* trend model estimates (also expressed in medians with 95% CrIs). Note y-axes vary between species.

Table 7. Absolute (net) and relative change in mature individuals (M) since 1980 and 2006 (i.e., the last 20 years), per species, genus, and overall (in median; 95% CrIs).

Species	**Absolute change since 1980**	**Rel. change since 1980 (%)**	**Absolute change since 2006**	**Rel. change since 2006 (%)**
Antipodean Albatross	-20,316 (-44,369; -7,422)	-35.1 (-50.4; -18.7)	-11,168 (-13,398; -9,359)	-23.0 (-23,4; -22,5)
Northern Royal Albatross	-2,769 (-5,613; -1,003)	-15.7 (-22.6; -8.0)	-2,817 (-2,994; -2,626)	-16.0 (-18,6: -13.4)
Southern Royal Albatross	8,796 (6,569; 11,692)	52.0 (50.3; 53.6)	-6,336 (-6,525; -5,852)	-19.8 (-25.0; -14.9)
Diomedea total	-14,289 (-43,412; 3,266)	-15.5 (-28.4; -2.8)	-20,321 (-22,917; -17,837)	-20.7 (-22.6; -18.7)
Buller's Albatross	26,107 (15,400; 29,172)	45.9 (19.1; 68.9)	13,212 (10,737; 15,484)	18.9 (17.7; 19.2)
Campbell Albatross	TBC	TBC	TBC	TBC
White-capped Albatross	7,585 (-23,691; 21,864)	3.3 (-6.6; 14.4)	-23,228 (-39,540; 1,577)	-8.8 (-18.6, 0.05)
Chatham Albatross	1,561 (-3,511; 3,514)	13.1 (-16.7; 52.0)	1,793 (819; 3,594)	15.4 (8.6; 25.9)
Salvin's Albatross	-47,416 (-146,577; -7,701)	-31.3 (-9.4; 52.0)	-7,150 (-7,524; -4,908)	-6.2 (-6.4; -4.9)
Thalassarche total	-12,162 (-158,379; 46,848)	-2.7 (-30.5; 21.2)	-15,373 (-35,507; 15,746)	-3.4 (-9.1, 2.3)
Westland Petrel	14,833 (6,407; 24,338)	331.1 (180.3; 406.7)	9,125 (2,690; 18,401)	89.6 (50.8; 94,7)
Black Petrel	13,026 (8,053; 19,986)	205.6 (110.2; 348.1)	7,394 (2,485; 19,498)	61.8 (31.5; 104.6)
Procellaria total	27,859 (14,460; 44,324)	257.6 (140.1; 371.8)	16,519 (5,175; 37,899)	74.6 (39.3; 99.6)
Total	**1,408** **(-187,331; 94,438)**	**0.3** **(-16.6; 16.9)**	**-19,175** **(-53,248; 35,808)**	**-3.3** **(-10.1; 3.9)**

3.1.2. Thalassarche *albatrosses*

Buller's Albatross abundance increased from an estimated 19,408 (11,629; 34,792) BP in 1969 to 32,958 (26,056; 41,989) BP in 2026 (Fig. 9AB). This trend equated to a net increase of 31,263 (16,114; 35,078) M, or a relative change of 60.3 (20.2; 96.2) %, over the entire time series and 13,212 (10,737; 15,484) M, or 18.9 (17.7; 19.2) %, in the last 20 years (Table 7). While generally all four Buller's Albatross breeding sites showed increases across the entire time series, for Tini Heke, this increase sharply stagnated around the mid-2000s and reverted to a slow decline, contrasting with the other breeding sites.

White-capped Albatross abundance changed from an estimated 78,906 (44,751; 137,867) BP in 1973 to a peak in abundance of 93,410 (70,642; 129,510) BP in 2002, after which a shallow decline may have become apparent, leaving 81,625 (57,533; 116,719) BP in 2021 (Fig. 9DC). The trend equated to a net change of 7,333 (-55,915; 35,177) M, or a relative change of 3.2 (-14.3; 25.4) %, over the entire timeseries, highlighting considerable uncertainty around the fate of this species. However, uncertainty decreased more recently, and White-capped Albatrosses suffered a net change of -23,228 (-39,540; 1,577) M, or a relative change of -8.8 (-18.6; 0.05) %, in the last 20 years (Table 7). This decrease was predominantly driven by declines on Disappointment Island, but the Southwest Cape population appeared in decline as well.

Contrasting with most other species, Chatham Albatross abundance on the sole breeding site at Te Tara Koi Koia remained nearly unchanged, with an estimated 4,273 (2,238; 8,066) BP in 1965 and an estimated 5,388 (4,189; 6,871) BP 2026, equating to a net change of 2,777 (-2,935; 4,760) M, or a relative change of 26.1 (-14.4; 86.3) %, over the entire time series, and 1,793 (819; 3,593) M, or a relative change of 15.4 (8.6; 25.9) %, in the last 20 years (Fig. 9EF, Table 7).

Salvin’s Albatross abundance declined from an estimated 72,098 (36,342; 146,793) BP in 1973 to 48,285 (35,107; 66,763) BP in 2026 (Fig. 9GH), which equated to a net change of -49,747 (-174,483; -3,819) M, or a relative change of -32.4 (-4.9; -54.3) %, over the entire timeseries, and a net change of -7,150 (-7,524; -4,908) M, or a relative change of -6.2 (-6.4; -4.9) %, in the last 20 years (Table 7). This concerning decrease was predominantly driven by declines on the large Moutere Hauriri population, but the small Western Chain population has shown declines since the mid-1990s as well.

3.1.3. Procellaria *petrels*

Westland Petrel abundance increased from an estimated 1,909 (912; 4055) BP in 1974 to 6,430 (3,981; 13,255) BP in 2019 (Fig. 10AB). This growth equated to a net increase of 15,802 (6,553; 29,071) M, or a relative change of 450.2 (331.7; 458.7) %, over the entire timeseries, and 9,058 (2,688; 17,094) M, or a relative change of 89.6 (50.8; 61.8) %, in the last 20 years (Table 7). This increase appeared to be predominantly driven by the count in 2019 and considerable uncertainty surrounded the trajectory of this species.

Black Petrel abundance changed from an estimated 1,691 (822; 3,540) BP in 1977 to 6,883 (4,439; 10,834) BP in 2026 (Fig. 10AB). This growth equated to a net increase of 13,466 (8,366; 20,307) M, or a relative change of 228.4 (113.9; 418.2) %, over the entire timeseries, and 7,393 (2,485; 19,498) M, or a relative change of 61.8 (31.5; 99.6) %, in the last 20 years (Table 7). This increase was surrounded by considerable uncertainty, similar to its sister species, yet the uncertainty surrounding the Black Petrel population trajectory was driven by the low representativeness of counts rather than low temporal resolution.

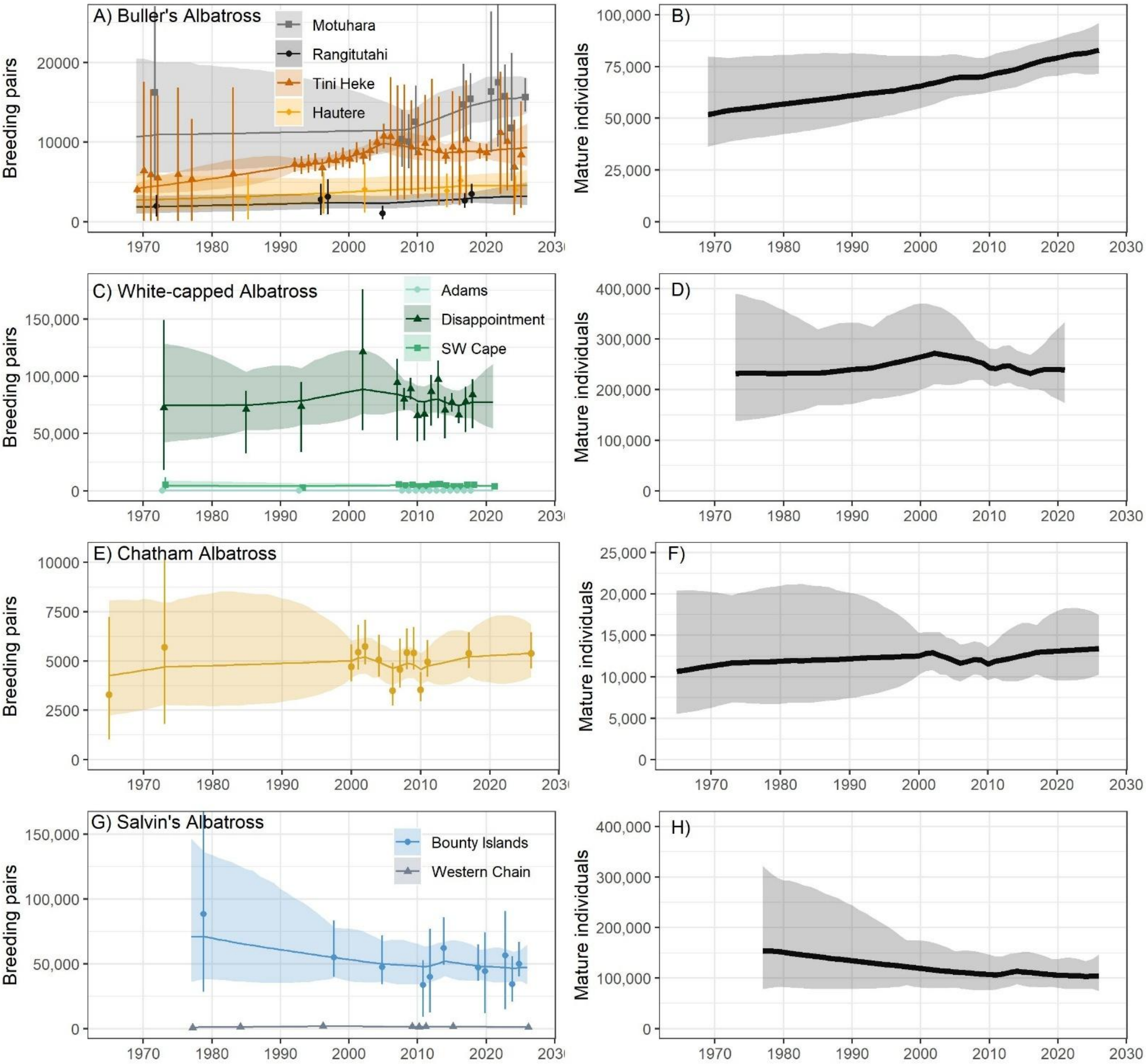

Fig. 9. Standardised abundance and trend estimates of Buller's (AB), White-capped (CD), Chatham (EF), and Salvin's Albatross (GH), expressed in breeding pairs per breeding site (ACEG) and total mature individuals (BDFH). Symbols with error bars (ACEG) represent $y_{t,i}$ (annual breeding pairs) estimates produced through the standardised processing and modelling framework (step 2.2) expressed in medians with 95% CrIs. Trend lines and translucent ribbons represent *ACAPT* trend model estimates (also expressed in medians with 95% CrIs). Note y-axes vary between species.

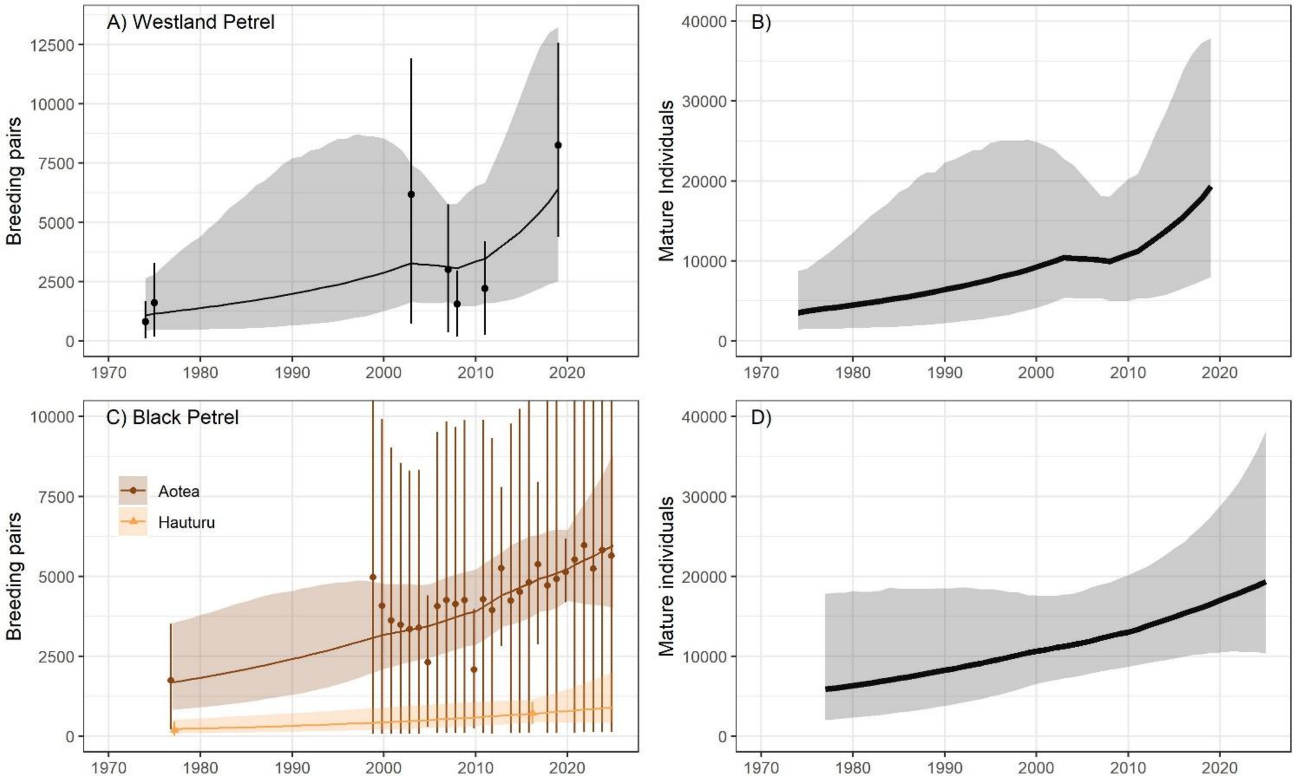

Fig. 10. Standardised abundance and trend estimates of Westland (AB) and Black Petrel (CD) expressed in breeding pairs per breeding site (AC) and total mature individuals (BD). Symbols with error bars (AC) represent $y_{t,i}$ estimates produced through the standardised processing and modelling framework (step 2.2) expressed in medians with 95% CrIs. Trend lines and translucent ribbons represent *ACAPT* trend model estimates of mature individuals (also expressed in medians with 95% CrIs). Note y-axes vary slightly between species.

3.2 Conservation assessments

3.2.1. IUCN Conservation status

When evaluating each species against IUCN Red List Criterion A, different species fell into different categories depending on what section of the timeseries in the past was considered and what statistical approach was used to identify the right category. Some species' timeseries were sufficiently long enough to enable evaluation against Criterion A2 (Northern and Southern Royal Albatross, Campbell Albatross, and Black Petrel), but as most evaluations were made against Criterion A4, results refer to this criterion unless explicitly stated otherwise. For evaluations of species against other criteria, see Table 8.

Antipodean Albatross (currently EN) was evaluated as EN, both when using a density-based or a median approach, for each of the different observation periods used in the assessment (Fig. 11), highlighting a high degree of certainty associated with the species' conservation status. The timeseries for Northern Royal Albatross (EN) was sufficiently long to enable assessments against Criterion A2 and against this criterion, the species' status was evaluated as LC. Under Criterion A4, the species' status was categorised as EN when using the last 20 years of observed data in the assessment (both for the density-based and median approach). The timeseries for Southern Royal Albatross (VU) was also sufficiently long to enable evaluations against Criterion A2, under which, the species was categorised as LC. Under Criterion A4, the species was also evaluated as LC regardless of the statistical approach and period used in the assessment, despite the recent onset of considerable declines, highlighting the uncertainty that surrounds the number of mature individuals of this species (possibly driven by limited information on p^b).

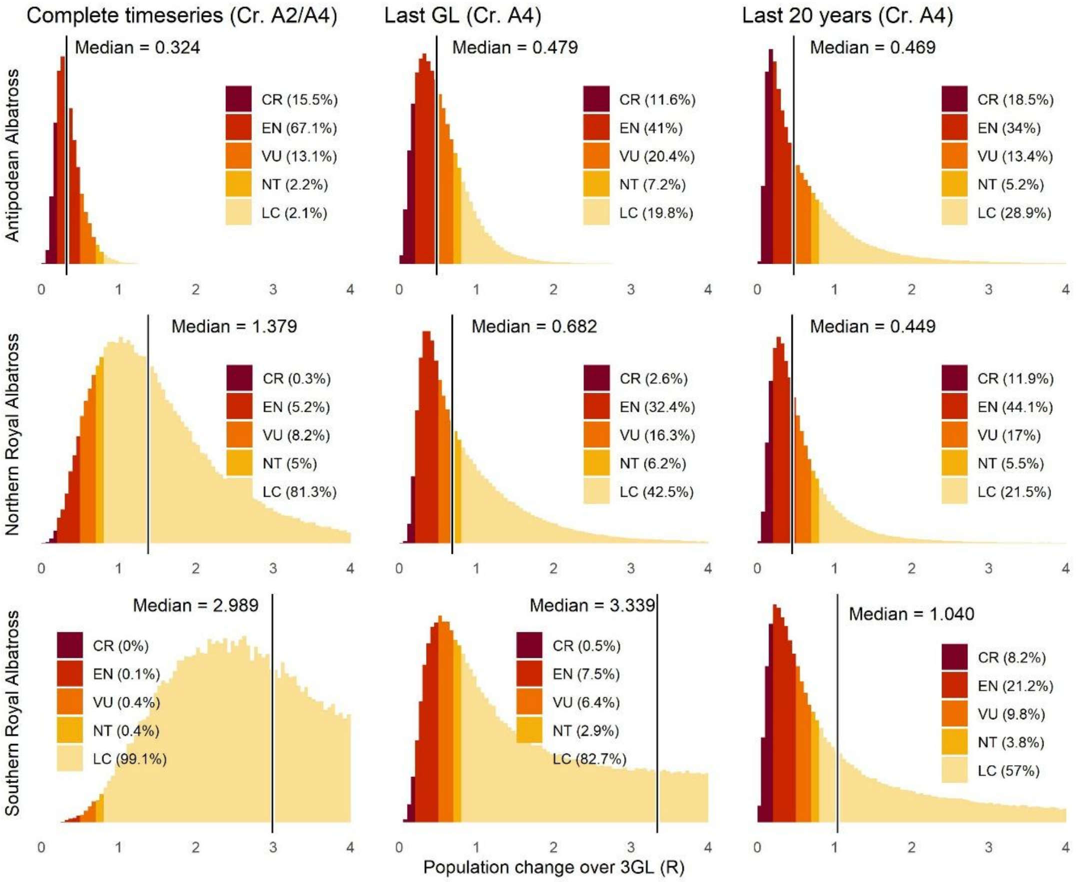

Figure 11. IUCN Red List evaluations using Criterion A for Antipodean (top row), Northern Royal (middle row), and Southern Royal Albatross (bottom row) based on population change evaluated over the entire timeseries available up until 3 generation lengths (GL) (left column), over the last GL (middle column), or over the last 20 years (right column). Legends provide percentual allocation of densities into IUCN Red List categories; vertical lines represent medians. The total timeseries for Northern and Southern Royal Albatross were long enough (>3GL) to enable evaluation against Criterion A2, while for Antipodean Albatross, evaluation using the total timeseries represents another assessment approach under Criterion A4, as the timeseries did not cover the full 3GL.

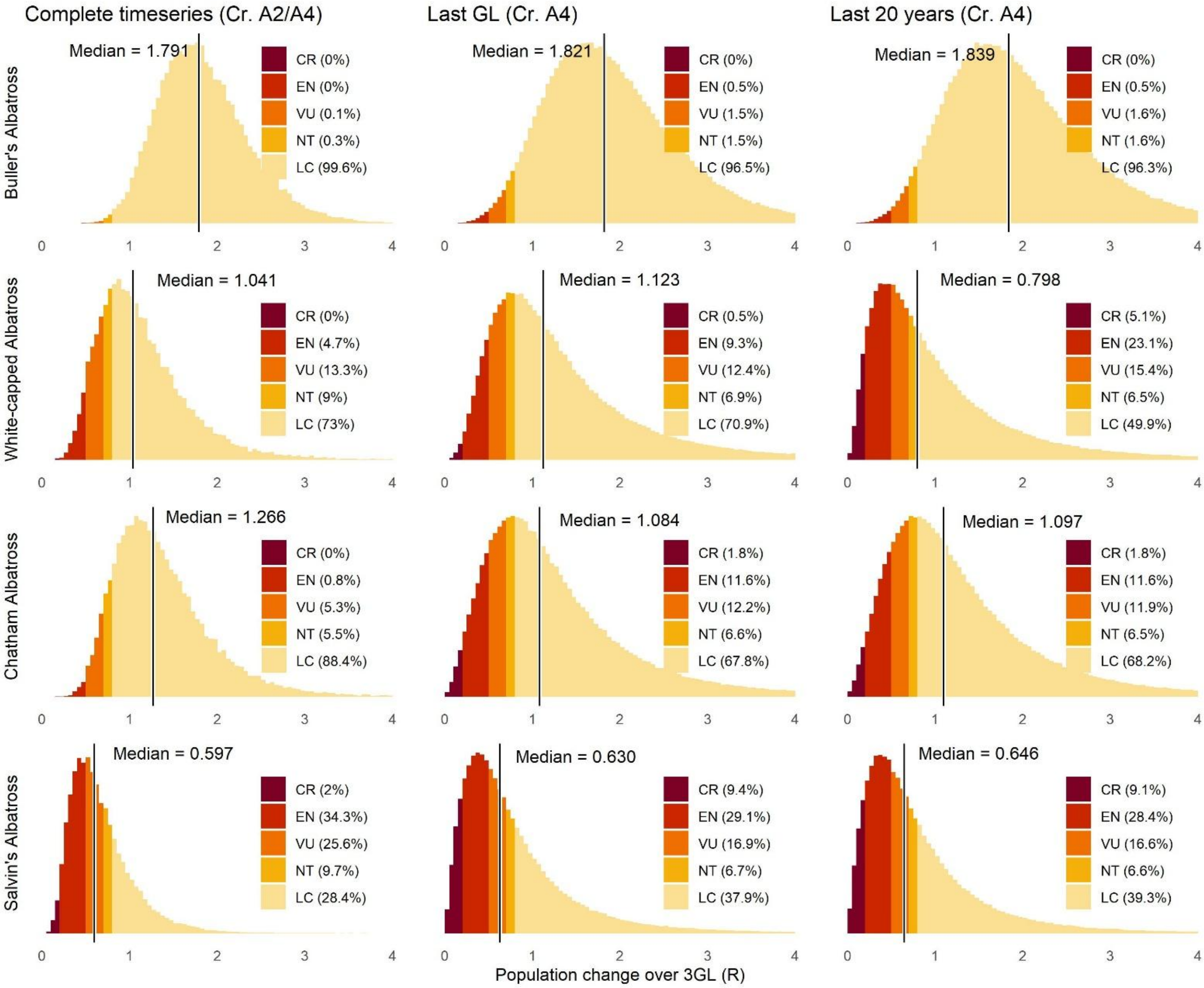

Figure 12. IUCN Red List evaluations using Criterion A for Buller's (top row), White-capped (second row), Chatham (third row), and Salvin's Albatross (bottom row) based on population change evaluated over the entire timeseries available up until 3 generation lengths (GL) (left column), over the last GL (middle column), or over the last 20 years (right column). Legends provide percentual allocation of densities into IUCN Red List categories; vertical lines represent medians. The total timeseries for all species were insufficiently long to cover full 3GL and thus all evaluation approaches fall under Criterion A4.

Buller's Albatross (currently NT) was evaluated as LC regardless of the period of observations under Criterion A2 and the statistical approach employed (Fig. 12), highlighting the long-term stability and increases in this species (bar the recently declining Tini Heke population). White-capped Albatross (NT) was evaluated as LC regardless of the period of observations used under the density-based approach. However, when using the median approach and the last 20 years of data, the species was evaluated as NT, capturing the recent onset of a shallow decline. Chatham Albatross (VU) was evaluated as LC regardless of the period of data used and the statistical approach employed, highlighting the long-term stability of this species at its sole breeding site. Salvin's Albatross (VU) was evaluated as EN when using the density-based approach for the entire timeseries, but as LC when using more recent sections of the timeseries. When using the median approach, the species was evaluated as VU regardless of the section of the timeseries used.

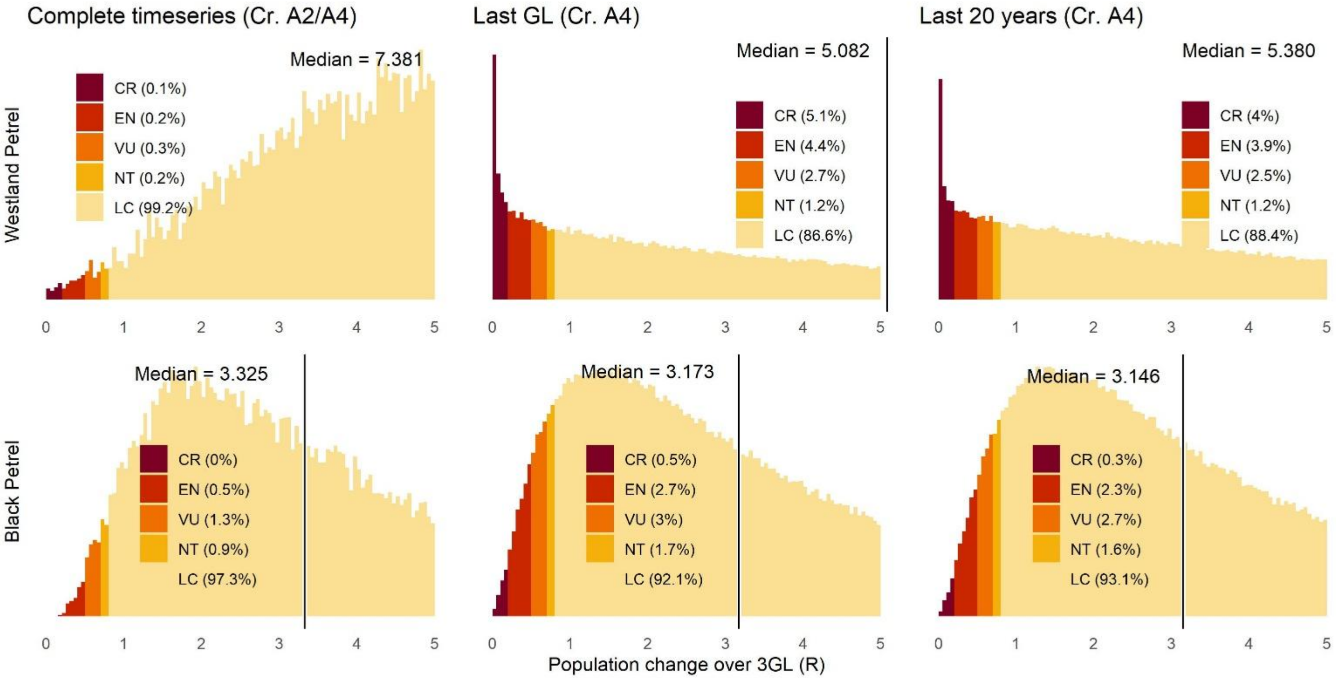

Figure 13. IUCN Red List evaluations using Criterion A for Westland (top row) and Black Petrel (bottom row) based on population change evaluated over the entire timeseries available up until 3 generation lengths (GL) (left column), over the last GL (middle column), or over the last 20 years (right column). Legends provide percentual allocation of densities into IUCN Red List categories; vertical lines represent medians. The total timeseries for Black Petrels was long enough (>3GL) to enable evaluation against Criterion A2, while for Westland Petrel, the evaluation using the total timeseries represents another assessment approach under Criterion A4, as the timeseries did not cover the full 3GL.

Westland Petrel (currently EN) was evaluated as LC category regardless of the period under assessment and the statistical approach (Fig. 13). However, Fig. 13 also highlighted the high degree of uncertainty associated with this species, despite the reasonable confidence in an increasing trend. The timeseries for Black Petrel (VU) was sufficiently long to enable assessments against Criterion A2 and against this criterion, the species' status was evaluated as LC regardless of the statistical approach. Under Criterion A4, Black Petrel (VU) also fell into the LC category regardless of the period under consideration or the statistical approach employed.

Table 8. IUCN Red List categories per species under each Criterion.

Species	**Current Status (key crit.)**	**Highest cat. under A2 (median; density)**	**Highest cat. under A4 (median; density)**	**B**	**C**	**D**	**E**	**Proposed category**
Antipodean Albatross	EN (A4)	-	EN; EN	TBC	TBC	TBC	TBC	EN
Northern Royal Albatross	EN (A4, B2)	LC; LC	EN; EN	TBC	TBC	TBC	TBC	EN
Southern Royal Albatross	VU (D2)	LC; LC	LC; LC	TBC	TBC	TBC	TBC	
Campbell Albatross	VU (D2)	TBC	TBC	TBC	TBC	TBC	TBC	
Buller's Albatross	NT (D2)	-	LC; LC	TBC	TBC	TBC	TBC	
White-capped Albatross	NT (A4)	-	NT; LC	TBC	TBC	TBC	TBC	NT
Chatham Albatross	VU (D2)	-	LC; LC	TBC	TBC	TBC	TBC	VU
Salvin's Albatross	VU (D2)	-	VU; EN	TBC	TBC	TBC	TBC	
Westland Petrel	EN (B2)	-	LC; LC	TBC	TBC	TBC	TBC	VU
Black Petrel	VU (D2)	LC; LC	LC; LC	TBC	TBC	TBC	TBC	VU

Criterion A is not the sole Criterion under consideration when assessing species for the IUCN Red List and the restricted nature of several species assessed here also need to be taken into consideration (Table 8). For example, Southern Royal Albatross, Chatham Albatross, Westland Petrel, and Black Petrel all warrant listing as VU under … TBC.

3.2.2. ACAP High Priority Populations

TBC

4. DISCUSSION

We here present the most comprehensive and coherent approach to evaluate albatross and petrel abundance in New Zealand to date, which provided fully comparable insights across space, time, and species, while incorporating uncertainty explicitly, thereby providing a considerable advancement in our ability to understand the fates of these species. By 1) incorporating prior information on count accuracy, 2) adjusting for imperfect detection where needed, 3) transforming different proxy metrics into the primary abundance metric (annual breeding pairs), and 4) inferring the proportion of failed nests, our abundance data processing framework ensured that each individual count was transformed into the number of breeding pairs at the beginning of the breeding period. Using further auxiliary information on breeding probability, we then provided abundance data expressed in mature individuals as well, as required for conservation (IUCN 2012) and fisheries risk assessments (e.g., Edwards *et al.* 2023, Anon. 2025). Following the generation abundance estimates, comparable across species, time, and space, we formulated a flexible trend model through our bespoke R package *ACAPT* that enabled us to infer population trends for each breeding site and therefore species, while incorporating uncertainty associated with individual counts. Our trend models have documented, in unprecedented detail, the dynamics of the albatrosses and large petrels endemic to New Zealand, highlighting the complex fates of these species. Our results in part provide further documentation of the extinction crisis as announced by ACAP in 2025 (ACAP 2025c), have great relevance to conservation assessments, and add to the insights necessary to reverse the documented declines. Furthermore, the framework we developed here provides the stepping stone towards obtaining similarly detailed insights into the population trajectories of all 31 ACAP species, and perhaps, ultimately, all seabird species.

4.1 Abundance data processing and insights into future monitoring and reporting

Our abundance processing framework mirrors the modelling approach used in integrated population models by utilising various related sources of information, through which analysis results are greater than the sum of all parts. Integrated population models fuse different datasets across potentially different timeseries to enable more coherent insights into the dynamics of populations while incorporating uncertainty, accounting for covariance among demographic parameters, and providing a flexible platform for integrating further auxiliary information to capture relevant biological information, including environmental variables, effects of inbreeding, and/or density-dependence (e.g., Schaub & Abadi 2000, Zipkin & Saunders 2018, Armstrong *et al.* 2021, Richard *et al.* 2024). Similarly, leveraging data beyond abundance ensured a high level of confidence in our estimates while retaining flexibility within our analysis approach. Sub-models within our framework leveraged 1) available information on the status of individuals to enable the transformation of proxy metrics to annual breeding pairs while incorporating uncertainty, even for years during which no direct data were available, 2) data on number of fledged chicks to estimate breeding success and back-cast to estimate the number of annual breeding pairs at the start of the breeding period, and 3) information on the number of breeding individuals to estimate breeding probability and ultimately, the number of mature individuals in the population, while acknowledging the biennial nature of some of the species under consideration. These sub-models proved highly flexible, enabling the integration of nuanced information to achieve higher accuracy where required. For example, we accounted for the development of a skewed sex ratio in Antipodean Albatross populations (Elliott *et al.* 2025) when estimating mature individuals. We also flexibly accounted for the temporary impact of a catastrophic storm event on Northern Royal Albatross demographics (Robertson 1991, 1998). Similarly, we capitalised on the unique data available for Salvin's Albatross stage-specific breeding success (Thompson 2025) when adjusting for nest failure. However, data in many cases were limited and thus we had to resort regularly to using informative priors. While the use of informative priors is not unusual (e.g., Edwards *et al.* 2023, Anon. 2025), parameter estimates rooted in data are certainly preferred. Considering the comprehensive nature of our analyses, our framework provides opportunities to reflect on current data availability and what monitoring and reporting considerations for these species are relevant for the future.

ACAP has guidelines for counts of both surface nesters (Wolfaardt & Phillips 2020) and burrow/crevice nesters (Parker & Rexer-Huber 2020b), both of which are valuable resources, and our analyses of abundance data here build on this advice. Specifically, the optimum recommended approach consists of annual monitoring (including counts) of representative study sites/plots/quadrats in combination with full breeding site counts every 5-10 years (Wolfaardt & Phillips 2020). Our modelled trajectories support this recommendation as still the best approach for obtaining the ideal abundance data. However, our results suggest that the representative study sites should exceed 10% of the breeding site population due to the nature of decreasing uncertainty under the asymptote specified in Eq. 1 (which mirrors the Poisson error distribution patterns, equally inflecting around 10%; Elliott *et al.* 2016). The impact of the uncertainty generation for counts that only represent small fractions is particularly evident for Buller's Albatross on Tini Heke and Black Petrel on Aotea (Fig 9A & 10A), both of which would benefit from increased coverage of their representative study sites (at least for abundance data). Some of the species analysed here are monitored annually, but not for abundance (e.g., Westland Petrels; Simister *et al.* 2023) and thus would benefit from the establishment of abundance study sites as well (e.g., in the form of plots or quadrats). Our work also revealed which species and sites should be considered the highest priority for obtaining updated abundance estimates to reduce uncertainty, White-capped Albatrosses at Disappointment Island and Westland Petrels at Punakaiki. Furthermore, it should be noted that when annual abundance monitoring is not possible, it is preferable to conduct counts in several successive years at larger time intervals rather than single counts over smaller time intervals, partially due to the impact breeding probability variation can have on single counts (Wolfaardt & Phillips 2020), and partially due to decrease in uncertainty as propagated through our trend model. ACAP also recommends to clearly record the unit (or metric) of counts (Wolfaardt & Phillips 2020), but despite this recommendation, it remained a challenge to interpret some counts due to the lack of detail. Ideally, each count has an exact description of what was counted and how the count metric(s) fit into the definitions of abundance metrics presented here. Finally, Wolfaardt & Phillips (2020) and Parker & Rexer-Huber (2020b) recommended to count albatrosses and petrels as closely as possible to the end of laying, and this recommendation is supported by our work here as well. As such, our work here supports previous recommendations through increased statistical rigor, which will hopefully reduce uncertainty in the future.

The ACAP database (ACAP 2025b) has been fundamental to our analyses, and while our study underscores its importance, it also revealed several avenues for improving this crucial resource and ensuring its continued relevance and utility. Our work suggests that the database is not exhaustive, even for some very well studied species. Specifically, 38% of the counts collated here were not in the ACAP database and as such further effort for other species and breeding sites are required to ensure comprehensive coverage. More pressingly though, the current data structure within the ACAP database is not fully fit for the purpose of transparently archiving abundance data. The most problematic aspect of the current data structure appeared to be the conflation of metric, method, and errors accounted or not accounted for. Clear, coherent definitions of metrics, methods, and errors were also lacking. Further challenges included the limited utility of the reliability score (which also is conflated with method and metric) and differing numerical interpretations of the ACAP accuracy score. Our framework has provided solutions to each of these challenges. We coin more transparent definitions of metrics, methods, and errors (Table 1-3), which subsequently allow for clear separation between the three in the data structure (Supplementary Table 1-22). Furthermore, while we discarded the reliability score, we formulated a numerical approach using the ACAP accuracy score to communicate prior beliefs on uncertainties associated individual counts. The approach in Eq. 1 appeared a promising avenue going forward, with applications extending beyond solely ACAP species, but the accuracy scores still rely on being entered consistently by those archiving counts. Further improvements could consist of providing clear definitions of what *Low*, *Medium*, and *High* counts consist of (i.e., what combination of metric, method, and timing, and other additional considerations would result in which score). Our data structure allowed for more transparent recording of metadata as well. The current ACAP database does not have the option to record count dates (and how these relate to the species' phenology) or how representative (i.e., ξ) a count is, and both should be considered crucial additions. Finally, our formulated data structure also enabled the recording of auxiliary data that proved the strength of our modelling approach.

To capitalise on the power that the joint modelling of abundance and demographic information beyond abundance in our framework highlighted, recording relevant auxiliary data in the ACAP database should be considered as well. Key additional data could include 1) the number of NS/BOGs/AOS/BPs counted in transects (e.g., Frost *et al.* 2025), close-up photographs (e.g., Baker *et al.* 2023), or burrow inspections (Bell *et al.* 2025) for each species, site, and count where possible. Recording this information would enable more precise estimation of BP even if abundance is recorded in other metrics (i.e., through Eq. 2 or future adaptions thereof). Similarly, recording the number of nests monitored and number of chicks that have fledged from these (or eggs hatched, chicks survived till post-guard, and subsequently fledged for higher resolution data; Fischer *et al.* 2021, Thompson 2025) for each species, site, and year where possible. Such records would not only provide a clear record of breeding success within the ACAP database but would also allow for more precise back-casting of abundance to the start of the breeding period c.f. Eq. 3. ACAP already recommends assessing nest failure in sample plots alongside counts (Wolfaard & Phillips 2020) and thus integrating data obtained through these into the ACAP database would present a logical next step. Finally, additional recording of the number of individuals in a population as estimated through mark-resight/capture-mark-resight modelling (Elliott *et al.* 2025, Rexer-Huber *et al.* 2025) would be beneficial to more precise estimation of p^b as well through Eq. 5, but such estimates rely on significant amounts of data and considerable analysis efforts. However, if such data are available, and the mark-resight/capture-mark-resight analyses are undertaken for other purposes, reporting the estimated number of adults in the study population (Elliott *et al.* 2025, Rexer-Huber *et al.* 2025) would be highly beneficial for further integration of different data sources in abundance analyses such as ours.

To enable recording of auxiliary data in the ACAP database in the most useful manner, data should be reported as data summaries, rather than reported estimates alone. Particularly challenging are estimates presented as multi-year means only or conditional estimates. It may not be possible to properly integrate the latter into the current formulation of our analysis framework (e.g., p^b for successful or failed breeders, without reporting overall p^b; e.g., Waugh *et al.* 2015, Fu & Sagar 2016). Similarly, compound estimates, e.g., recording NS and BP only for burrow/crevice nesters for informing $\psi^{occ} \cdot \psi^{ABA}$ only in combination (Rexer-Huber *et al.* 2023) or BOG and BP only for surface nesters informing $\psi^{BOG} \cdot \psi^{ABA}$ only in combination (Elliott *et al.* 2025, Rexer-Huber *et al.* 2025), should be avoided where possible, as such reporting misses a step in the occupancy metric hierarchy (Fig. 4). However, we recognize that this may be challenging in certain scenarios (e.g., Thompson 2025). Ideally, summaries are recorded to the finest resolution possible (e.g., for Ψ^o: 967 BOG, 865 AOS, 850 BP; c.f. Baker *et al.* 2017) alongside estimates, as this would enable the inclusion of these auxiliary data in the ACAP database in a manner that would allow for direct integration into the data processing steps clarified here.

Finally, we also identified a key area for future study and improvement of our data standardisation and processing framework. Firstly, despite our best efforts, we were unable to formulate a standardised approach that enables accounting for Ψ^d in counts that have not done so originally. We have attempted to overcome this challenge by using informative priors when other counts reported Ψ^d estimates (e.g., Sagar & Stahl 2005), by increasing uncertainty surrounding counts through downscaling the associated ACAP accuracy score in Eq. 1, or by applying custom adjustments for specific counts through formal expert elicitations (Hemming *et al.* 2018). While these custom approaches are powerful (e.g., Fischer *et al.* 2020), they are also time consuming and place considerable burden on experts and thus are only suitable when it is most pressing to account for Ψ^d, e.g., for VBCs. Ideally, a similar standardised approach mirroring our process for accounting for Ψ^o (Eq. 2) and Ψ^p (Eq. 3) would be developed for Ψ^d, enabling retrospective adjustments. Secondly, we formulated the proportion of the population ξ being directly representative of the population of the breeding site to enable extrapolation in Eq. 1. However, extrapolation is often based on density calculations and surface area estimations particularly with burrow/crevice nesters, which can be particularly sensitive to various considerations including 2D vs. 3D surface extrapolations

(Parker & Rexer-Huber 2020b). Our approach's strength is its simplicity, yet future work could investigate how to integrate density-based estimation processes into our framework, which may hold a potential solution to the challenge of retrospectively accounting for Ψ^d (e.g., by integrating distance-sampling; Buckland *et al.* 2001).

4.2 Trend modelling through *ACAPT*

TBC

4.3 Long-term albatross and petrel trends in New Zealand

Our analyses build upon previous multi-species work (e.g., Fischer *et al.* 2024) and underscore the concerning, long-term, and ongoing declines of several ACAP species endemic to New Zealand, but also provide improved nuance. Previous work had not integrated uncertainty in both the underlying abundance data and the trend models, and as such, our overall results appear less severe than those reported in Fischer *et al.* (2024). Nevertheless, our results have several commonalities with previous work, and while the underlying causes of the documented trends were not a focus of our analyses, some insights can be gained from the literature and will hopefully guide future work to provide detailed insights into causes, and, ultimately, conservation actions.

A common theme of both our and previous work is the continuing collapse of the *Diomedea* albatross populations in New Zealand. While the ongoing and dire status of the Antipodean Albatross has been well documented and studied (e.g., Richard et al. 2024, Rowley et al. 2024, Elliott et al. 2025, Rexer-Huber et al. 2025), the more recent, but apparently equally severe declines of Northern and Southern Royal Albatross has received less attention. The demise of the Antipodean Albatross is tightly linked to bycatch in pelagic longline fisheries, particularly in the high seas of the Tasman Sea and the southwestern Pacific east of New Zealand (Richard et al. 2024, Rowley et al. 2024, Anon. 2025). However, the impact of bycatch of royal albatrosses in pelagic longline fisheries is less well understood, and direct links may be more difficult to establish as these species are susceptible to bycatch in both trawl fisheries and longline fisheries (Edwards et al. 2023), including off the Patagonian Shelf (Jimenez et al. 2014, Tamini et al. 2020) and South Africa (Petersen et al. 2009, Rollinson et al. 2017). In addition, the distribution of both species is circumpolar (Morten et al. 2025) and as such, both species may encounter various fleets in various jurisdictions around the Southern Ocean that jointly impact upon their populations.

Irrespective of the pelagic causes of their declines, what is clear is that the conservation gains achieved for Southern Royal Albatross through the invasive species eradications on Motu Ihupuku and the resultant restoration of this breeding site (Towns & Broome 2010, Brown et al. 2023), are now coming undone. Similarly, both Chatham Island strongholds for Northern Royal Albatrosses have now recovered from the impacts of the severe storm in the 1980s (Roberston 1991, 1998, Bell 2026) and while sufficient time has passed for demographic impacts from this storm to be no longer evident, both populations are still declining. Clearly, more concerted monitoring of all three species, as well as more concerted efforts to mitigate bycatch in the relevant fleets is required to stem the current declines. The key fleets that impact Antipodean Albatross are known (Richard et al. 2024, Rowley et al. 2024), but they are not for the two royal albatrosses, and this should be seen as a research and conservation priority.

Contrasting with the *Diomedea* albatrosses, not all *Thalassarche* albatrosses exhibited declines, and some species showed stable or increasing trends. Of the four *Thalassarche* species evaluated, Salvin's Albatross exhibited the most severe decline. In terms of net abundance loss, this species may be the most impacted of all New Zealand endemic ACAP species. Yet, despite our best efforts to align challenging, historic records (e.g., Robertson & van Tets 1982) with modern counts, the extent of loss remains surrounded by uncertainty, and the population on Moutere Hauriri continues to show considerable interannual variation. Notably, the latest count on the smaller Western Chain Islets also suggested further concerning declines. The underlying causes of the suspected demise of this species are uncertain. Neither breeding site suffers from the presence of any invasive species, and the species is not commonly caught in pelagic longline fisheries, unlike the *Diomedea* albatrosses, but can be subject to considerable trawl bycatch (Adamse et al. 2019, Edwards et al. 2023, Anon. 2025). It is possible that the use of net-sonde cables in trawl fisheries in the 1980s and 1990s underpinned the decline of this species, which would align with the apparent semi-stabilisation of the species' trend following the ban of these cables in New Zealand in 1992 (Bartle 1991, Adamse et al. 2019). However, most of the observed mortalities associated with net-sonde cables in the New Zealand trawl fleet were assigned to the White-capped Albatrosses (Bartle 1991), so uncertainty remains prominent. White-capped Albatrosses are the most abundant albatross species in New Zealand, and their trends have been subject to considerable debate in the literature, with some analyses showing non-significant declines, while others indicated a catastrophic population collapse (e.g., Walker et al. 2021 vs. Baker et al. 2023). Our analyses provide a more nuanced understanding of the fate of this species, suggesting that the species may recently have started to decline, i.e., a middle ground between previous analyses. However, the last count of this species at its stronghold on Disappointment Island dates to 2018 (Baker et al. 2023). Mortality estimates in New Zealand domestic fisheries alone exceed 2,600 adults annually (Edwards et al. 2023) to which several thousand mortalities caused by high seas fisheries should be added (e.g., Rollinson et al. 2017, Peatman et al. 2019, Anon. 2025). Therefore, reigniting previous efforts to quantify the species' abundance (next to demographics; Parker et al. 2024) appears a global research priority. Contrasting with its two sister species, the small Chatham Albatross population has remained remarkably stable for the entire ~60-year time series available, indicating that this species is potentially at carrying capacity at its sole breeding ground, and is not too impacted by bycatch in New Zealand (Edwards et al. 2023) or South American waters (Quinones et al. 2022). Of the four *Thalassarche* species analysed here, Buller's Albatross has shown the most positive trend, but this trend, at least in recent years, appears largely driven by the Chatham Island breeding sites. In contrast, the Tini Heke population has apparently been in decline since the mid-2000s, showing a similar population trajectory as both Antipodean Albatross populations, albeit less severe. Adult survival continues to be low for this population (Sagar et al. 2025) and thus continuing declines appear likely for this population. The contrasting trend of the Tini Heke population further highlights the challenges that seabird bycatch in the Tasman Sea (where this population forages more prominently than the other populations; Fischer et al. 2023) is causing for New Zealand ACAP species (Anon. 2025).

A surprising result of our analyses were the consistent, long-term increases of the two endemic *Procellaria* species. Both species are considered at a reasonably high risk of suffering population level impacts due to bycatch (Edwards et al. 2023), and thus these trends contradict current perceptions. While trends for both species evaluated here remain surrounded by considerable uncertainty, there is supporting evidence for increasing trends in both species. For both species, adult survival is reasonably high, particularly Westland Petrels (Waugh et al. 2015). Additionally, for both species, terrestrial threats appeared to have decreased over the last 50 years. Westland Petrel chicks were harvested at least until the mid-1950's (Wilson 2016, Waugh & Wilson 2017), a practice which since has ceased. Black Petrels may have benefited from improved predator control on Aotea and the complete eradication of invasive predators from Hauturu (Veitch 2001, Wade & Veitch 2019).

Furthermore, considerable efforts have been invested into reducing seabird bycatch in demersal longline fisheries, at least in the north of New Zealand, to relieve pressure on Black Petrels (Goad & Williamson 2015, Goad & Debski 2017). Consequently, it is not unlikely that the presented trends are a true reflection of reality, but ideally, our abundance trends are corroborated with supporting demographic studies (e.g., an update of Zhang et al. 2020) and further, high-quality abundance estimates in the near-future, to reduce uncertainty.

The abundance trends presented here provide a stepping stone to better understand and communicate the fate of these charismatic species. Our results are a considerable improvement on previous studies (e.g., Fischer et al. 2024). Our approach offers the opportunity to improve the nature of seabird abundance assessments and bring understanding of seabird abundance closer in line with abundance insights into other marine megafauna communities (e.g., Pacoureau et al. 2021, Juan-Jorda et al. 2022, Dulvy et al. 2024). Next steps should clearly focus on expanding our analyses to all ACAP species to provide complete and coherent insights into the population trajectories of all albatrosses and large petrels. Furthermore, considering similar efforts that have been completed for other species-groups (e.g., Che-Castaldo et al. 2017, Talis et al. 2023, Sherley et al. 2019, 2024) obtaining continuous time-series for all seabird species, may be possible, and would indeed result in seabird abundance assessments mirroring those of other marine mega-fauna communities. An additional future opportunity includes the provision of these continuous timeseries to fisheries risk assessments to disentangle the improvements that bycatch mitigation may afford species from the reduced number of individuals available for capture due to the decline of populations (e.g., Anon. 2025). Perhaps more importantly though, our trends estimates provide more tangible and communicable metrics to the general publics to illustrate the on-water impact of the current extinction crisis (ACAP 2025c).

4.4 Conservation status assessments

Our work also resulted in the most detailed IUCN Red List assessments of these 10 New Zealand endemics to date. However, despite the documentation of concerning, long-term declines of these long-lived, highly *k*-selected species (e.g., Bird et al. 2020), no direct IUCN Red List changes have become evident either through the density-based approach or the median approach for assigning categories. The most prominent change may be the proposal to downlist Westland Petrels from EN to VU, as the species appears to be increasing and the argument fragmentation of the breeding sites should not be used under Criterion B for a wide-ranging species like a seabird (Waugh & Wilson 2017). The lack of obvious uplisting candidates may be caused by the challenges of assigning IUCN Red List Categories while incorporating uncertainty. The combination of a left-hand zero-bound, the lack of a right-hand bound, and uneven categories renders assigning categories probabilistically challenging, particularly when uncertainty abounds. This challenge is particularly obvious for Southern Royal Albatross, an extremely long-lived species which may has lost ~20% of its population in the last 10-20 years (i.e., <1 GL), yet our assignments do not exceed VU. This apparent contradiction may be caused by the lack of information on p^b causing uncertainty to increase rapidly, particularly when forecasting. As such, further integration of abundance data and demographic data should be encouraged to reduce uncertainty (and where data do not exist, as is the case for Southern Royal Albatrosses, data collection should be prioritised). Similar challenges and apparent contradictions between the documented declines and the suggested IUCN Red List statuses are evident for Salvin's and White-capped Albatrosses, and both should be prioritised for future data collection and model updates. It should be noted that *JARA* included an additional measure to address the challenges posed by probabilistic allocation of IUCN Red List categories. Specifically, *JARA* assigns NT in cases where threatened categories contain >50% of the iterations but LC contains the highest percentual allocation (Winker et al. 2020). It does not appear that this rule would have applied in any of our case studies, yet it would be worth considering including such a step for *ACAPT* as well. An alternative explanation for the apparent contradiction between lack of uplisting and documented declines could be that the previous IUCN Red List assignments have been too pessimistic and only now that populations have declined further, do they warrant the status that they had already been assigned. This may be the case for, for instance, Northern Royal Albatross (Fig. 9). Finally, our conservation status assessments through *ACAPT* also bear relevance and opportunities for local Red List assessments (e.g., Roberston et al. 2021).

ACAP High Priority Populations. TBC

6. CONCLUSION

We presented the most comprehensive abundance assessment of albatrosses and petrels in New Zealand to date. Our work built upon decades in the field across the most remote and inhospitable islands on the planet, representing the investment of generations of scientists into the understanding of these seabirds. We coined updated definitions, designated an improved data structure, designed a novel data processing framework, and developed a flexible trend model implemented through our bespoke R package. These combined advancements resulted in trend estimates and assessments of conservation status comparable across space, time, and species, illuminating over half a century of abundance change in the seabird capital of the world. Our work illustrated and quantified the concerning, long-term, and ongoing declines affecting *Diomedea* albatrosses and Salvin’s Albatross, and placed these declines alongside other, less impacted, species that appeared to have benefited from decades of conservation investments (e.g., predator eradications and improvements in bycatch mitigation). These estimates provide a path towards improved monitoring, reporting, research prioritisations, further expansions of the analyses presented here, and investigations into the underlying causes of uncovered trends. Most importantly however, our work presents the opportunity to both communicate the current fate of these species and to develop and enforce strategies that reverse declines to once again ensure that all albatrosses and petrels species thrive.

7. REFERENCES

ACAP. 2009. ACAP species assessment: Southern Royal Albatross *Diomedea epomophora*. https://www.acap.aq/. Agreement on the Conservation of Albatrosses and Petrels. Accessed 1 December 2025.

ACAP. 2025a. Agreement on the Conservation of Albatrosses and Petrels – Data Portal. https://data.acap.aq/. Agreement on the Conservation of Albatrosses and Petrels. Accessed 1 December 2025.

ACAP. 2025b. ACAP Priority Conservation Actions for 2026-2028. Eight Meeting of Parties, Dunedin, New Zealand. Agreement on the Conservation of Albatrosses and Petrels.

ACAP. 2025c. Agreement on the Conservation of Albatrosses and Petrels: Report of the eighth session of the meeting of parties. Dunedin, New Zealand.

Adamse LM, Canales CM & Adamse NA. 2019. Incidental seabird mortality and discarded catches from trawling off far southern Chile (39-57**°S).** ICES Journal of Marine Science 76: 848-858.

Amey J & Sagar P. 2013. Salvin's albatross population trend at the Bounty Islands, 1997-2011. Conservation Services Programme, Department of Conservation, Wellington, New Zealand.

Anon. 2025. CCSBT collaborative risk assessment for seabird bycatch with surface longlines in the Southern Hemisphere 2025. CCSBT, Canberra, Australia.

Armstrong DP, Parlato EH, Egli B, Dimond WJ, Berggren A, McCready M, Parker KA & Ewen JG. 2021. Capturing the dynamics of small populations: a retrospective assessment using long-term data for an island reintroduction. Journal of Animal Ecology 90: 2915-2927.

Attard MRG, Phillips RA, Oppel S, Bowler E & Fretwell PT. 2025. Feasibility of using very high-resolution satellite imagery to monitor Tristan albatrosses *Diomedea dabbenena* on Gough Island. Endangered Species Research 56: 187-199.

Awkerman JA, Westbrock MA, Huyvaert KP & Anderson DJ. 2007. Female-biased sex ratio arises after parental care in the sexually dimorphic Waved Albatross (*Phoebastria irrorata*). The Auck 124: 1336-1346.

Baker BG, Jensz K, Bell M, Fretwell PT & Phillips RA. 2017. Seabird Population Research, Chatham Islands 2016/17 aerial photographic survey. Conservation Services Programme, Department of Conservation, Wellington, New Zealand.

Baker CS & Clapham PJ. 2004. Modelling the past and future of whales and whaling. Trends in Ecology and Evolution 19: 365-371.

Baker GB & Jensz K. 2014a. Gibson's Albatross at Disappointment Island - Analysis of aerial photographs. Conservation Services Programme, Department of Conservation, Wellington, New Zealand.

Baker GB & Jensz K. 2014b. Buller's albatross aerial survey at the Solander Islands 2014. Conservation Services Programme, Department of Conservation, Wellington, New Zealand.

Baker GB & Jensz K. 2019. Aerial survey of Salvin's albatross at the Bounty Islands. Conservation Services Programme, Department of Conservation, Wellington, New Zealand.

Baker GB, Elliott GP, French RK, Jensz K, Muller CG & Walker KJ. 2020. Development of aerial monitoring techniques to estimate population size of great albatrosses (Diomedea spp.). Notornis 67: 321-331.

Baker GB, Hedley G, Cunningham R & Waugh S. 2020. Estimated population size of the Westland Petrel 2007-2011. New Zealand Aquatic Environment and Biodiversity Report No. 242. Fisheries New Zealand, Wellington, New Zealand.

Baker GB, Jensz K & Hamer D. 2014. Southern royal albatross at Enderby Island – analysis of aerial photographs 2014. Conservation Services Programme, Department of Conservation, Wellington, New Zealand.

Baker GB, Jensz K, Bell M, Fretwell PT & Phillips RA. 2017. Seabird population research, Chatham Islands; 2016/17 aerial photographic survey. Conservation Services Programme, Department of Conservation, Wellington, New Zealand.

Baker GB, Jensz K, Cunningham R, Robertson G, Sagar P, Thompson TR & Double MC. 2023. Population assessment of White-capped Albatross *Thalassarche steadi* in New Zealand. Emu – Austral Ornithology 123: 60-70.

Bartle JA 1985. Report on research on Westland black petrels 1969-83 with an outline of future objectives and a brief summary of management problems. Unpublished report of the National Museum of New Zealand, Wellington, New Zealand.

Bartle JA. 1991. Incidental capture of seabirds in the New Zealand subantarctic squid trawl fishery, 1990. Bird Conservation International 1: 351-359.

Bell E & Sim J. 2000. Surveying and monitoring of black petrels on Great Barrier Island, 1997/1998. Conservation Services Programme, Department of Conservation, Wellington, New Zealand.

Bell E, Lamb S, Ray S. 2022. Population trends and breeding population size of black petrels (*Procellaria parkinsoni*) – 2020/2021 operational report. New Zealand Aquatic Environment and Biodiversity Report No. 280. Fisheries New Zealand, Wellington, New Zealand.

Bell EA, Lamb S & Ray S. 2025. Key demographic parameters and population trends of tākoketai/black petrels (*Procellaria parkinsoni*) on Aotea/Great Barrier Island: 2024/25. Conservation Services Programme, Department of Conservation, Wellington, New Zealand.

Bell EA, Mischler C & Sim JL. 2015. Preliminary survey and population monitoring of black petrels (Procellaria parkinsoni) on Hauturu-o-toi/Little Barrier Island, 2014,15. Conservation Services Programme, Department of Conservation, Wellington, New Zealand.

Bell EA, Mischler CP, MacArthur N & Sim JL. 2016. Black petrel (*Procellaria parkinsoni*) population study on Hauturu-o-Toi/Little Barrier Island, 2015/16. Conservation Services Programme, Department of Conservation, Wellington, New Zealand.

Bell EA, Sim J, Scofield P, Francis C & Landers T. 2013. At-sea distribution and population parameters of the black petrels (*Procellaria parkinsoni*) on Great Barrier Island (Aotea Island), 2012/13. Conservation Services Programme, Department of Conservation, Wellington, New Zealand.

Bell EA, Sim JL, Bull L, Pierre J, Torres L & Shaffer S. 2011. At-sea distribution of the black petrels (*Procellaria parkinsoni*) on Great Barrier Island (Aotea Island), 2009/10: Part 1 – environmental variables. Conservation Services Programme, Department of Conservation, Wellington, New Zealand.

Bell JB, Fischer JH, Carneiro APB, Griffiths S, Bielli A, Jimenez S, Oppel S, Phillips RA, Wade HM, Yates O & Reeves SA. 2025. Evaluating the effectiveness of seabird mitigation measures for pelagic longlines in the South Atlantic. Biological Conservation 302: 110981.

Bell M, Bell D, Boyle D & Tuanui-Chisholm. 2018. Rangitatahi Seabird Research: December 2017. Conservation Services Programme, Department of Conservation, Wellington, New Zealand.

Bell M. 2021. Motuhara seabird research: field trip report January 2021. Conservation Services Programme, Department of Conservation, Wellington, New Zealand.

Bell M. 2023. Motuhara seabird research: field trip report Dec 2022. Conservation Services Programme, Department of Conservation, Wellington, New Zealand.

Bell M. 2024. Motuhara seabird research: field trip report January 2024. Conservation Services Programme, Department of Conservation, Wellington, New Zealand.

Bell M. 2026. Seabird research – Chatham Islands. Conservation Services Programme, Department of Conservation, Wellington, New Zealand.

Bell MD, Bell DJ & Boyle DP. 2017. Chatham Island Mollymawk research on Te Tara Koi Koia: November 2016. Conservation Services Programme, Department of Conservation, Wellington, New Zealand.

Bird JP, Martin R, Akcakaya HR, Gilroy J, Burfield IJ, Garnett ST, Symes A, Taylor J, Sekercioglu CH & Butchart SHM. 2020. Generation lengths of the world's birds and their implications for extinction risk. Conservation Biology 34: 1252-1261.

BirdLife International. 2025. BirdLife International Data Zone. BirdLife DataZone. Accessed 1 December 2025.

Brown DA, Cox FS & Fergus AJ. 2022. The eradication of Campbell Island sheep and subsequent ecological responses. New Zealand Journal of Ecology 46: 3483.

Buckland ST, Anderson DR, Burnham KP, Laake JL, Borchers DL & Thomas L. 2001. Introduction to distance sampling: estimating abundance of biological populations. Oxford University Press.

Carneiro APB *et al.* 2020. A framework for mapping the distribution of seabirds by integrating tracking, demography and phenology. Journal of Applied Ecology 57: 514-525.

Ceballos G, Ehrlich PR, Barnosky AD, Garcia A, Pringle PM & Palmer TM. 2015. Accelerated modern human-induced species losses: Entering the sixth mass extinction. Science Advances 1: 1400253.

Che-Castaldo C, Jenouvrier S, Youngflesh C, Shoemaker KT, Humphries G, McDowall P, Landrum L, Holland MM, Li Y, Ji R & Lynch HJ. 2017. Pan-Antarctic analysis aggregating spatial estimates of Adelie penguin abundance reveals robust dynamics despite stochastic noise. Nature Communications 8: 832.

Childerhouse S, Robertson CJR, Hockley W & Gibbs NJ. 2003. Royal Albatross (*Diomedea epomophora*) on Enderby Island, Auckland Islands. Department of Conservation, Wellington, New Zealand.

Cleeland JB, Pardo D, Raymond B, Terauds A, Alderman R, McMahan CR, Phillipps RA, Lea MA & Hindell MA. 2020. Introduced species and extreme weather as key drivers of reproductive output in three sympatric albatrosses. Scientific Reports 10: 8199.

Cooper J, Baker GB, Double MC, Gales R, Papworth W, Tasker ML & Waugh SM. 2006. The agreement on the conservation of albatrosses and petrels: rationale, history, progress and the way forward. Marine Ornithology 34: 1-5.

CSP. 2025. Conservation Services Programme Annual Plan 2025/26. Conservation Services Programme, Department of Conservation, Wellington, New Zealand.

Cuthbert RJ & Sommer ES. 2004. Population size and trends of four globally threatened seabirds at Gough Island, South Atlantic Ocean. Marine Ornithology 32: 97-103.

Dasnon A, Delord K, Chaigne A & Barbraud C. 2022. Fisheries bycatch mitigation measures as an efficient tool for the conservation of seabird populations. Journal of Applied Ecology 59: 1674-1685.

Dawson EW. 1973. Albatross populations at the Chatham islands. Notornis 20: 210–230.

Department of Conservation Coastal Otago District Operations. 2026. Pukekura annual report. 2024/25 Season. Department of Conservation, Dunedin, New Zealand.

Dias MP, Martin R, Pearmain EJ, Burfield IJ, Small C, Phillips RA, Yates O, Lascelles B, Borboroglu PG & Croxall JP. 2019. Threats to seabirds: a global assessment. Biological Conservation 237: 525-537.

Dulvy NK, Pacoureau N, Matsushiba JH, Yan HF, Vanderwright WJ, Rigby CL, Finucci B, Sherman CS, Jabado RW, Carlson JK, Carlson JK, Pollom RA, Charvet P, Pollock CM, Hilton-Taylor C & Simpfendorfer CA. 2024. Ecological erosion and expanding extinction risk of sharks and rays. Science 386: 6726.

Edgar GJ, Bates AE, Krueck NC, Baker SC, Stuart-Smith RD & Brown CJ. 2024. Stock assessment models overstate sustainability of the world's fisheries. Science 385: 860-865.

Edwards CTT, Peatman T, Fischer J & Gibson W. 2025. Inputs to the 2024 seabird risk assessment for the Southern Bluefin Tuna surface longline fishery. Fisheries New Zealand, Wellington, New Zealand.

Edwards CTT, Peatman T, Goad D & Webber DN. 2023. Update to the risk assessment for New Zealand seabirds. New Zealand Aquatic Environment and Biodiversity Report No. 314. Fisheries New Zealand, Wellington, New Zealand.

Elliot G, Walker K, Rexer-Huber K, Tinnemans J, Long J, Sagar S, Osborne J & Parker G. 2024. Gibson's wandering albatross: demography, satellite tracking and census. Conservation Services Programme, Department of Conservation, Wellington, New Zealand.

Elliott G, Waker K, Rexer-Huber K, Tinnemans J, McDonald A, Rawlence T & Parker G. 2025. Gibson's wandering albatross: drone-based population estimate, demography and at-sea distribution. Conservation Services Programme, Department of Conservation, Wellington, New Zealand.

Elliott G, Walker K, Parker G & Rexer-Huber K. 2016. Gibson's wandering albatross census and population study 2015/16. Conservation Services Programme, Department of Conservation, Wellington, New Zealand.

Elliott G, Walker K, Rexer-Huber K & Parker G. 2023. White-capped Albatross population study: February 2023. Conservation Services Programme, Department of Conservation, Wellington, New Zealand.

Fischer JH, Bell M, Frost P, Sagar PM, Thompson DR, Middlemiss KL, Debski I & Taylor GA. 2023. Year-round GLS tracking of Northen Buller's Albatross and comparison with Southern Buller's Albatross. Conservation Services Programme, Wellington, New Zealand.

Fischer JH, Carneiro A, Rowley O & Debski I. 2024. An update on the New Zealand large-scale monitoring and tracking programme with improved insights into trends and distribution. Eight meeting of the Population and Conservation Status Working Group, Agreement for the Conservation of Albatrosses and Petrels, Lima, Peru.

Fischer JH, Taylor GA, Cole R, Debski I, Armstrong DP & Wittmer HU. 2020. Population growth estimates of a threatened seabird indicate necessity for additional management following invasive predator eradications. Animal Conservation 23: 94-103.

Fischer JH, Wittmer HU, Kenup CF, Parker KA, Cole R, Debski I, Taylor GA, Ewen JG, Armstrong DP. 2022. Predicting harvest impact and establishment success when translocating highly mobile and endangered species. Journal of Applied Ecology 59: 2071-2083.

Fischer JH, Wittmer HU, Taylor GA, Debski I & Armstrong DA. 2021. Preparing for translocations of a Critically Endangered petrel through targeted monitoring of nest survival and breeding biology. Oryx 55: 564-572.

Fisher HI. 1966. Aerial census of Layan Albatrosses breeding on Midway Atoll in December, 1962. The Auk 83: 670-673.

Francis RIC & Sagar PM. Modelling the effect of fishing on southern Buller's albatross using a 60-year dataset. New Zealand Journal of Zoology 39: 3-17.

Francis RICC. 2012. Fisheries risks to the population viability of White-capped Albatross *Thalassarche steadi*. Fisheries New Zealand, Wellington, New Zealand.

Fraser M, Cameron N, Scofield P, Robertson CJRR. 2010A. Population assessment of Northern Buller's Albatross and Northern Giant Petrels at the Fortyfours, Chatham Islands, 1-8 December 2009. Ministry of Fisheries, Wellington, New Zealand.

Fraser M, Henderson G, Robertson CJR & Scofield P. 2011. Population dynamics of the Chatham Albatross at the Pyramid, 19 November – 2 December 2010. Ministry of Fisheries, Wellington, New Zealand.

Frederick PC, Heath JA, Bennetts R & Hafner H. 2006. Estimating nests not present at the time of breeding surveys: an important consideration in assessing nesting populations. Journal of Field Ornithology 77: 212-219.

Freeman AND & Wilson K-J. 2002. Westland petrels and hoki fishery waste: opportunistic use of a readily available resource. Notornis 49: 139-144.

Fretwell PT, Scofield P & Phillips RA. 2017. Using super-high resolution satellite imagery to census threatened albatross. Ibis 159: 481-490.

Frost PGH, Baker GB, Fischer JH & Sagar PM. 2025. Population survey of Southern Buller's Albatross *Thalassarche bulleri bulleri* on the Solander Islands | Hautere, March 2024. Marine Ornithology 53: 361-371.

Frost PGH, Bell MD & Taylor GA. 2021. Trial-camera assessment of the fates of Northern Royal Albatross and Northern Buller's Mollymawk chicks: 2021 breeding season, Motuhara. Conservation Services Programme, Department of Conservation, Wellington, New Zealand.

Frost PGH. 2017. Aerial census of Northern Royal Albatross (*Diomedea sanfordi*) fledglings on Rangitatahi (The Sisters) and Motuhara (Fortyfours), July 2017. Conservation Services Programme, Department of Conservation, Wellington, New Zealand.

Frost PGH. 2021. Status of Northern Royal Albatross Diomedea sanfordi nesting on the Chatham Islands, December 2020, Conservation Services Programme, Department of Conservation, Wellington, New Zealand.

Frost PGH. 2022. A census of Northern Royal Albatross nesting on the Chatham Islands, February 2022. Conservation Services Programme, Department of Conservation, Wellington, New Zealand.

Frost PGH. 2024. Aerial survey of Northern Royal Albatross | Toroa (*Diomedea sanfordi*) populations on the Chatham Islands, December 2023. Conservation Services Programme, Department of Conservation, Wellington, New Zealand.

Frost PGH. 2026. Trail-camera monitoring of White-capped Albatross (Thalassarche steadi) on Disappointment Island: 2018, 2022 and 2023) breeding seasons. Conservation Services Programme, Department of Conservation, Wellington, New Zealand.

Froy H, Phillips RA, Wood AG, Nussey DH & Lewis S. 2013. Age-related variation in reproductive traits in the wandering albatross: evidence for terminal improvement following senescence. Ecology Letters 16: 642-649.

Fu D & Sagar P. 2016. The 2014 demographic assessment of the Snares islands population of Southern Buller's albatross (*Diomedea bulleri bulleri*). New Zealand Aquatic Environment Biodiversity Report 165. Ministry for Primary Industries, Wellington, New Zealand.

Genovart M, Arcos MJ, Alvarez D, McMinn M, Meier Rm Wynn RB, Guilford T & Oro D. 2016. Demography of the critically endangered Balearic Shearwater: the impact of fisheries and time to extinction. Journal of Applied Ecology 53: 1158-1168.

Gianuca D, Votier SC, Pardo D, Wood AG, Sherley RB, Ireland L Choquet R, Townley S, Forcada J, Tuck GN & Phillips RA. 2019. Sex-specific effects of fisheries and climate on the demography of sexually dimorphic seabirds. Journal of Animal Ecology 88: 1366-1378.

Goad D & Debski I. 2017. Bird-scaring line designs for small longline vessels. Eighth Meeting of the Seabird Bycatch Working Group, Agreement on the Conservation of Albatrosses and Petrels, Wellington, New Zealand.

Goad D & Williamson J. 2015. Improving and documenting seabird bycatch mitigation practices in the North Eastern New Zealand longline fishery. Conservation Services Programme, Wellington, New Zealand.

Hayes M, Gray PC, Harris G, Sedgwick WC, Crawford VD, Chazal N, Crofts S & Johnston DW. 2021. Drones and deep learning produce accurate and efficient monitoring of large-scale seabird colonies. Ornithological Applications 123: duab022.

Hays GC, Schofield G, Papazekou M, Chatzimentor A, Katsanevakis S & Mazaris AD. 2024. A pulse check for trends in sea turtle numbers across the globe. iScience 27: 109071.

Hemming V, Burgman MA, Hanea AM, McBride MF & Wintle BC. 2018. A practical guide to structured expert elicitation using the IDEA protocol. Methods in Ecology & Evolution 9: 169-180.

Imber MJ. 1987. Breeding ecology and conservation of the black petrel (*Procellaria parkinsoni*). Notornis 34: 19–39.

IUCN. 2012. IUCN Red List categories and criteria, version 3.1, second edition. IUCN Species Survival Commission, IUCN, Cambridge, UK.

Jimenez S, Phillips RA, Brazeiro A, Defeo O & Domingo A. 2014. Bycatch of great albatrosses in pelagic longline fisheries in the Southwest Atlantic: Contributing factors and implications for management. Biological Conservation 171: 9-20.

Jones HP, Appoo J, Benkwitt CE, Borrelle SB, Dunn RE, Epstein HE, Fowlke LA, Holmes ND, Jeannot LL, Malhi Y, Ranking LL, Steibl S, Wails CN, Will DJ & Graham NAJ. 2025. The circular seabird economy is critical for oceans, islands and people. Nature Reviews Biodiversity 1: 689-702.

Jouventin P. 1990. Shy albatrosses Diomedea cauta salvini breeding on Penguin Island, Crozet Archipelago, Indian Ocean. Ibis 132: 126-127.

Juan-Jorda MJ, Murua H, Arrizablaga H, Merino G, Pacoureau N & Dulvy NK. 2022. Seventy years of tunas, billfishes, and sharks as sentinels of global ocean health. Science 378: 6620.

LaRue M, Salas L, Nur N, Ainley D, Stammerjohn S, Pennycook J, Dozier M, Saints J, Stamatiou K, Barrington L & Rotella J. 2021. Insights form the first global population estimate of Weddell seals in Antarctica. Science Advances 7: 3674.

Lewis S, Nussey DH, Wood AG, Croxall JP & Phillips RA. 2012. Intrinsic determinants of a population trend in timing of breeding in the wandering albatross. Oikos 121: 2061-2071.

Mackley EK, Poncet S, Black A, Black J, Floyd K, Hall RM, Holmes EE, Manthorpe SJ, Passfield K, Bennison A & Phillips RA. 2025. Endurance or extinction: long-term declines in albatrosses at South Georgia highlight threats from South Atlantic fisheries and climate change. Endangered Species Research 57: 437-451.

Mattern T. 2022. Tawaki Project: Bounty-Antipodes expedition 2022.

Mattern T. 2024a. Tawaki Project: Antipodes-Bounty expedition 2023/24.

Mattern T. 2024b. Tawaki Project: Bounty-Antipodes expedition 2024.

Mischler C, Moore P, Thompson H, Hamilton K & Pryde M. 2025. Campbell Island Seabird Research. Conservation Services Programme, Department of Conservation, Wellington, New Zealand.

Miskelly CM, McNally N, Seymour R, Gregory-Hunt D & Lanauze J. 2008. Antipodean wandering albatross (*Diomedea antipodensis*) colonising the Chatham Islands. Notornis 55: 89-95.

Miskelly CM, Sagar PM, Tennyson AJD & Scofield RP. 2001. Birds of the Snares Islands, New Zealand. Notornis 48: 1-40.

Moore PJ, Larsen EJ, Chateris M & Pryde M. 2012. Southern Royal Albatross on Campbell Island/Motu Ihupuku; Solving a band injury problem and population survey 2004-08. DOC Research and Development Series 333, Department of Conservation, Wellington, New Zealand.

Moore PJ, Scott JJ, Joyce LJ & Peart M. 1997. Southern royal albatross *Diomedea epomophora epomophora* census on Campbell Island, 4 January – 6 February 1996. Science & Research Series 101. Department of Conservation, Wellington, New Zealand.

Morten JM, et al. 2025. Global marine flyways identified for long-distance migrating seabirds from tracing data. Global Ecology and Biography 34: e70004.

Oppel S, Clark BL, Risi MM, Horswill C, Converse SJ, Jones CW, Osborne AM, Stevens K, Perold V, Bond AL, Wanless RM, Cuthbert R, Cooper J & Ryan PG. 2022. Cryptic population decrease due to invasive species predation in a long-lived seabird supports need for eradication. Journal of Applied Ecology 59: 2059-2070.

Oppel S, Clark BL, Risi MM, Horswill C, Converse SJ, Jones CW, Osborne AM, Stevens K, Perold V, Bond AL, Wanless RM, Cuthbert R, Cooper J & Ryan PG. 2021. Cryptic population decrease due to invasive species predation in a long-lived seabird supports need for eradication. Journal of Applied Ecology 59: 2059-2070.

Pacoureau N, Rigby CL, Kyne PM, Sherly RB, Winker H, Carlson JK, Fordham SV, Barreto R, Fernando D, Francis MP, Jabado RW, Herman KB, Liu KM, Marshall AD, Pollom RA, Romanov EV, Simpfendorfer CA, Yin JS, Kindsvater HK & Dulvy NK. 2021. Half a century of global decline in oceanic sharks and rays. Nature 589: 567-571.

Paleczny M, Hammill E, Karpouzi V & Pauly D. 2015. Population trend of the world's monitored seabirds, 1950-2010. PLoS ONE 10: e0129342.

Pardo D, Forcada J, Wood AG, Tuck GN, Ireland L, Pradel R, Croxall JP & Phillips RA. 2017. Additive effects of climate and fisheries drive ongoing declines in multiple albatross species. PNAS 114: E10829-10837.

Parker G & Rexer-Huber K. 2020a. Drone-based Salvin's albatross population assessment: feasibility at the Bounty Islands. Conservation Services Programme, Department of Conservation, Wellington, New Zealand.

Parker GC & Rexer-Huber K. 2020b. Guidelines for designing population surveys of burrowing petrels. Agreement for the Conservation of Albatrosses and Petrels.

Parker GC, Elliott G, Walker K & Rexer-Huber K. 2022. Gibson's albatross and white-capped albatross in the Auckland Islands 2021-2022. Conservation Services Programme, Department of Conservation, Wellington, New Zealand.

Parker GC, Osborne J, Sagar R, Schultz H & Rexer-Huber K. 2024. White-capped albatross population study, Disappointment Island 2024. Conservation Services Programme, Department of Conservation, Wellington, New Zealand.

Parker GC, Osborne J, Sagar R, Schultz H, Rexer-Huber K. 2024. White-capped Albatross population study, Disappointment Island 2024. Conservation Services Programme, Wellington, New Zealand.

Peatman T, Abraham E, Ochi D, Webber D & Smith N. 2019. Project 68: estimation of seabird mortality across the WCPFC Convention Area. Fifteenth regular session of the Scientific Committee of the Western and Central Pacific Fisheries Commission, Pohnpei, Federated States of Micronesia.

Petersen SL, Honig MB, Ryan PG & LG Underhill. 2010. Seabird bycatch in the pelagic longline fishery off Southern Africa. African Journal of Marine Science 31: 191-204.

Phillips RA, Gales R, Baker GB, Double MC, Favero M, Quintana F, Tasker ML, Weimerskirch H, Uhart M & Wolfaardt A. 2016. The conservation status and priorities for albatrosses and large petrels. Biological Conservation 201: 169-183.

Plummer M. 2003. JAGS: A program for analysis of Bayesian graphical models using Gibbs sampling. Proceedings of the 3rd international workshop on distributed statistical computing. 124: 1-10.

Poncet S, Robertson G, Phillips RA, Lawton K, Phalan B, Trathan PN & Croxall JP. 2006. Status and distribution of wandering, black-browed and grey-headed albatrosses breeding at South Georgia. Polar Biology 29: 772-781.

QGIS.org. 2025. QGIS geographic information system. http://www.qgis.org

Quinones J, Romero C, Mangel JC, Alfaro-Shigueto J, Moreno C & Zavalaga C. 2022. At-sea surveys reveal new insights of fine-scale behaviour and foraging behaviour of Chatham Albatrosses (Thalassarche eremita) in central southern Peru. Notornis 69: 72-78.

R Core Team. 2024. R: A language and environment for statistical computing. R Foundation for Statistical Computing, Vienna Austria.

Rayner MJ, Parker KA, Neho T & Hvid T. 2020. Buller's mollymawk (*Thalassarche bulleri platei*) count at Rosemary Rock, Manawatāwhi (Three Kings Islands). Notornis 67: 580-582.

Rexer-Huber K, Parker G, Elliott G & Walker K. 2023. Antipodes Island white-chinned petrel population size and survival study setup. Conservation Services Programme, Department of Conservation, Wellington, New Zealand.

Rexer-Huber K, Parker G, Sager P & Thompson D. 2021. Salvin's Albatross breeding dates and productivity: nest-camera analysis. Conservation Services Programme, Department of Conservation, Wellington, New Zealand.

Rexer-Huber K, Parker KA & Parker GC. 2020. Campbell Island seabirds: Operation Endurance November 2019. Conservation Services Programme, Department of Conservation, Wellington, New Zealand.

Rexer-Huber K, Walker KJ, Elliott GP, Baker GB, Debski I, Jensz K, Sagar PM, Thompson DR & Parker GC. 2020. Population trends of light-mantled sooty albatross (*Phoebetria palpebrata*) at Adams Island and trial of ground, boat, and aerial methods for population estimates. Notornis 67: 341-355.

Rexer-Huber K, Whitehead E, Parker G, Patterson E, Walker K, Welch J & Elliott G. 2024. Antipodean wandering albatrosses and white-chinned petrels 2024. Conservation Services Programme, Department of Conservation, Wellington, New Zealand.

Rexer-Huber K, Whitehead E, Walker K & Elliott G. 2025. Antipodean wandering albatrosses and white-chinned petrels 2025. Conservation Services Programme, Department of Conservation, Wellington, New Zealand.

Richard Y, Berkenbusch K, Crawford E, Tornquist M, Walker K, Elliott G, & Tremblay-Boyer L. 2024. Antipodean Albatross multi-threat risk assessment. New Zealand Aquatic Environment and Biodiversity Report No. 332. Fisheries New Zealand, Wellington, New Zealand.

Richard Y, Perriman L, Lalas C & Abraham ER. 2015. Demographic rates of northern royal albatross at Taiaroa Head, New Zealand. PeerJ 3:e906.

Richdale LE 1939. A Royal Albatross nesting on the Otago Peninsula, New Zealand. Emu 38: 467-488.

Roast MJ, Martins S, Fernandez-Peralta L, Beaz JC, Diame A, March D, Ouled-Cheikh, Marco A, Gonzales-Solis & Cardona Luis. 2023. Hidden demographic impacts of fishing and environmental drivers of fecundity in a sea turtle population. Conservation Biology 37: e 14110.

Robertson CJR & van Tets GF. 1982. The status of birds at the Bounty Islands. Notornis 29: 311-336.

Robertson CJR, Bell D & Scofield P. 2003. Population Assessment of the Chatham Albatross at The Pyramid, December 2001. DOC Science Internal Series 91. Department of Conservation, Wellington.

Robertson CJR. 1975. Report on the distribution, status, and breeding biology of the Royal Albatross, Wandering Albatross and White-capped Mollymawk on the Auckland Islands. In Yaldwyn JC (ed). Preliminary Results of the Auckland Islands Expedition 1972-1973. Department of Lands and Survey, Wellington, New Zealand.

Robertson CJR. 1991. Questions on the harvesting of Toroa in the Chatham Islands. Science & Research Series 35. Department of Conservation, Wellington.

Robertson CJR. 1993. Survival and longevity of the Northern Royal Albatross *Diomedea epomorphora sanfordi* at Taiaroa Head 1937-93. Emu 93: 269-276.

Robertson CJR. 1998. Factors influencing the breeding performance of the Northern Royal Albatross. In: Robertson G & Gales R. (eds), Albatross biology and conservation, pp. 99-104. Surrey Beatty & Sons, Chipping Norton, Australia.

Robertson CJR. 2001. Effects of intervention on the royal albatross population at Taiaroa Head, Otago, 1937-2001. DOC Science Internal Series 23. Department of Conservation, Wellington, New Zealand.

Robertson G, Moreno CA, Lawton K, Kirkwood D & Valencia J. 2008. Comparison of census methods for Black-browed Albatrosses breeding at Ildefonso Archipelago, Chile. Polar Biology 31: 153-162.

Robertson HA, Baird KA, Elliott GP, Hitchmough RA, McArthur NJ, Makan TD, Miskelly CM, O'Donnell CFJ, Sagar PM, Scofield RP, Taylor GA & Michel P. 2021. Conservation status of birds in Aotearoa New Zealand, 2021. Department of Conservation, Wellington, New Zealand.

Rodriguez A, Arcos JM, Bretagnolle V, Dias MD, Holmes ND, Louzao M, Provencher J, Raine AF, Ramirez F, Rodriguez B, Ronconi RA, Taylor RS, Bonnaud E, Borrelle SB, Cortes V, Descamps S, Friesen VL, Genovart M, Hedd A, Hodum P, Humpries GRW, Le Corre M, Lebarbenchon C, Martin R, Melvin EF, Montevecchi WA, Pinet P, Pollet IL, Ramos R, Russel JC, Ryan PG, Sanz-Aguillar A, Spatz DR, Travers M, Votier SC, Wanless RM, Woehler E, Chiaradia A. 2019. Future directions in conservation research on petrels and shearwaters. Frontiers in Marine Science 6: https://doi.org/10.3389/fmars.2019.00094

Rollinson DP, Wanless RM & Ryan PG. 2017.Patterns and trends in seabird bycatch in the pelagic longline fishery off South Africa. African Journal of Marine Science 39: 9-25.

Rowley O, Waipoua TA, Debski I, Elliott G, Parker G, Rexer-Huber K, Walker K & Fischer J. 2024. Fine scale overlap analysis of Antipodean and Gibson's albatross with pelagic longline fishing effort. Joint Twelfth meeting of the Seabird Bycatch Working Group and Eight meeting of the Population and Conservation Status Working Group, Agreement for the Conservation of Albatrosses and Petrels, Lima, Peru.

Ryan PG, Jones MGW, Dyer BM, Upfold L & Crawford RJM. 2009. Recent population estimates and trends in numbers of albatrosses and giant petrels breeding at the sub-Antarctic Prince Edward Islands. African Journal of Marine Science 31: 409-417.

Sagar P, Charteris M & Scofield P. 2014. Salvin's albatross population size and survival at the Snares Western Chain. Conservation Services Programme, Department of Conservation, Wellington, New Zealand.

Sagar P, Rexer-Huber K, Schultz H, Simister K, Thompson D & Parker G. 2025. Population studies of southern Buller's Albatross at Tini Heke | The Snares Islands. Conservation Services Programme, Wellington, New Zealand.

Sagar P. 2014. Population studies of Southern Buller's Albatrosses on the Snares. Conservation Services Programme, Department of Conservation, Wellington, New Zealand.

Sagar PM & Stahl J-C. 2005. Increases in the numbers of breeding pairs in two populations of Buller's Albatross (*Thalassarche bulleri bulleri*). Emu – Austral Ornithology 105: 49-55.

Sagar PM, Molloy J, Weimerskirch H & Warham J. 2000. Temporal and age-related changes in survival rates of Southern Buller's Albatrosses (*Thalassarche bulleri bulleri*) at the Snares, New Zealand, 1948-1997. The Auk 117: 699-708.

Sagar PM, Stahl J-C, Molloy J, Taylor GA & Tennyson AJD. 1999. Population size and trends within the two populations of Southern Buller's Albatross *Diomedea bulleri bulleri*. Biological Conservation 89: 11-19.

Schaub M & Abadi F. Integrated population models: a novel analysis framework for deeper insights into population dynamics. Journal of Ornithology 152: 227-237.

Scofield P. 2011. Data collection of demographic, distributional, and trophic information on selected seabird species to allow estimation of effects of fishing on populations viability. Ministry of Fisheries, Wellington, New Zealand.

Sherley RB, Crawford RJM, de Blocq AD, Dyer BM, Geldenhuys D, Hagen C, Kemper J, Makhado AB, Pichegru L, Tom D, Upfold L, Visagie J, Waller LJ & Winker H. 2020a. The conservation status and population decline of the African penguin deconstructed in space and time. Ecology and Evolution 10: 8506-8516.

Sherley RB, Winker H, Rigby CL, Kyne PM, Pollom Rm Pacoureau N, Herman K, Carlson JK, Yin JS, Kndsvater HK & Dulvy NK. 2020b. Estimating IUCN Red List population reduction: JARA – A decision-support tool applied to pelagic sharks. Conservation Letters 13: e12688.

Sherley RB, Makhado AB, Crawford RJM, Hagen C, Kemper J, Ludynia K, Masolta MJ, McInnes A, Pichegru L, Tom D, Upfold L & Waller LJ. 2024. The African Penguin *Spheniscus demersus* should be considered Critically Endangered. Ostrich 95: 181-187.

Sherley RB, Crawford RJM, Dyer BM, Kemper J, Makhado AB, Masotla M, Pichegru L, Pistorius PA, Roux JP, Ryan PG, Tom D, Upfold L & Winker H. 2019. The status and conservation of the Cape Gannet *Morus capensis*. Ostrich 90: 335-346.

Spiegelhalter D, Thomas A, Best N, Lunn D. 2014. OpenBUGS user manual version 3.2.3. MCR Biostatistics Unit, Cambridge, UK.

Stahl JC & Sagar PM. 2006. Behaviour and patterns of attendance of non-breeding birds at the breeding colony in a Buller's Albatross *Thalassarche bulleri* population at The Snares. Notornis 53: 327-338.

Stevens KL, Altwegg R, Connan M & Ryan P. 2024. Population growth of the grey-headed albatross population on Marion Island inferred using three analysis methods. Antarctic Science 36:1-11.

Suazo CG, Anguita C, Letelier CG, Martinez A & Quillfeldt P. 2024. The white-capped albatross: a new breeding record from the Diego Ramirez Islands, Chile. Polar Biology 47: 771-777.

Talis EJ, Che-Castaldo C, Hart T, McRae L & Lynch HJ. 2023. Penguindex: a living planet index for Pygoscelis species penguins identifies key areas of population change. Polar Biology 46: 707-718.

Tamini LL, Chaves LN, Dellacasa RF, Crawford R & Frere E. 2021. Incidental capture of seabirds in Argentinean side-haul trawlers. Bird Conservation International 31: 591-604.

Tennyson A, Imber M & Taylor R. 1998. Numbers of Black-browed Mollymawk (*Diomedea m. melanophrys*) and White-capped Mollymawk (*D. cauta steadi*) at the Antipodes Islands in 1994-1995 and their population trends in the New Zealand region. Notornis 45: 157-166.

Thompson D & Sagar P. 2008a. Annual report 2006/07: A population and distributional study of white-capped albatross (Auckland Islands). Conservation Services Programme, Department of Conservation, Wellington, New Zealand.

Thompson D & Sagar P. 2008b. Annual report 2007/08: A population and distributional study of white-capped albatross (Auckland Islands). Conservation Services Programme, Department of Conservation, Wellington, New Zealand.

Thompson D & Sagar P. 2020. Population studies of southern Buller's albatrosses on the Snares Islands | Tini Heke. Conservation Services Programme, Department of Conservation, Wellington, New Zealand.

Thompson D, Sagar P, Baker B & Jensz K. 2017. Southern Buller's Albatross survey at Solander Islands 2016. Conservation Services Programme, Department of Conservation, Wellington, New Zealand.

Thompson T. 2025. Advancing remote monitoring of albatrosses through emerging technologies to inform conservation. MSc thesis. University of Otago, Dunedin, New Zealand.

Towns DR & Broome KG. 2003. From small Maria to massive Campbell: forty years of rat eradications from New Zealand islands. New Zealand Journal of Zoology 30: 377-398.

Veitch CR. 2001. The eradication of feral cats (*Felis catus*) from Little Barrier Island, New Zealand. New Zealand Journal of Zoology 28: 1-12.

Ventura F, Lukacs PM, Granadeiro JP, Matano R & Catry P. 2021. Demographic responses to environmental change of black-browed albatross, sentinel of the Patagonian Shelf Large Marine Ecosystem. Marine Ecology Progress Series 668: 107-120.

Virtue J, Turner D, Williams G, Zeliadt S & Lucieer A. 2023. Thermal drone observations capture fine-scale population decline of short-tailed shearwaters. Remote Sensing in Ecology and Conservation https://doi.org/10.1002/rse2.70020

Wade R & Veitch CR. 2019. Costs and benefits for biodiversity following rat and cat eradication on the Hauturu-o-toi/Little Barrier Island. Island invasives: scaling up to meet the challenge 62: 558.

Walker K & Elliott G. 1999. Population changes and biology of the wandering albatross *Diomedea exulans gibsoni* at the Auckland Islands. Emu 99: 239-247.

Walker K & Elliott G. 2005. Population changes and biology of the Antipodean wandering albatross. Notornis 52: 206-214.

Walker K & Elliott G. 2017. ACAP priority population assessment: Antipodean Albatross at Antipodes Island. Fourth Meeting of the Population and Conservation Status Working Group, Wellington, New Zealand. Agreement on the Conservation of Albatrosses and Petrels.

Walker KJ, Elliott GP, Rexer-Huber K, Parker GC, Sagar PM & McClelland PJ. 2021. Shipwrecks and mollymawks: an account of Disappointment Island Birds. Notornis 67: 213-245.

Waugh SM & Wilson KJ. Threats and threat status of the Westland Petrel *Procellaria westlandica*. Marine Ornithology 45: 195-203.

Waugh SM, Barbraud C, Adams L, Freeman AND, Wilson K-J, Wood G, Landers TJ & Baker GB. 2015. Modelling the demography and population dynamics of a subtropical seabird, and the influence of environmental factors. The Condor: Ornithological Applications 117: 147-164.

Waugh SM, Barbraud C, Delord K, Simister KLJ, Baker GB, Hedley GK, Wilson K-J & Rands DRD. 2020. Trends in density, abundance, and response to storm damage for Westland Petrels *Procellaria westlandica*, 2007-2019.

Waugh SM, Doherty PF, Freeman AND, Adams L, Wood GC, Bartle JA & Hedley GK. 2006. 2006. Demography of Westland Petrels (*Procellaria westlandica*), 1995–2003. Emu 106: 219-226.

Waugh SM, Sagar PM & Paull D. 1997. Laying dates, breeding success and annual breeding of southern royal albatrosses *Diomedea epomophora* at Campbell Island during 1964–69. Emu 97: 194–199.

Weimerskirch H, Delord K, Barbraud C, Le Bouard F, Ryan PG, Fretwell P & Marteau C. 2018. Status and trends of albatrosses in the French Southern Territories, Western Indian Ocean. Polar Biology 41: 1963-1972.

Weimerskirch H, Lallemand J & Martin J. 2005. Population sex ratio variation in a monogamous long-lived bird, the wandering albatross. Journal of Animal Ecology 74: 285-291.

Weimerskirch H. 2018. Linking demographic processes and foraging ecology in wandering albatross – Conservation implications. Journal of Animal Ecology 87: 945-955.

Wilson KJ. 2016. A review of the biology and ecology and evaluation of threats to the Westland Petrel *Procellaria westlandica*. Unpublished report.

Winker H, Pacoureau N & Sherley RB. 2020. JARA: 'Just Another Red-list Assessment'. BioRxiv: https://doi.org/10.1101/672899.

Wolfaardt A & Phillips R. 2020. Guideline census methodologies for albatrosses and petrels. Agreement on the Conservation of Albatrosses and Petrels.

Wood GC & Otley HM. 2013. An assessment of the breeding range, colony sizes and population of the Westland Petrel (*Procellaria westlandica*). New Zealand Journal of Zoology 40: 186–195. Marine Ornithology 48: 273-281.

Zhang J, Bell EA & Roberts JO. 2020. Demographic assessment of black petrels (*Procellaria parkinsoni*) on Great Barrier Island (Aotea Island). New Zealand Aquatic Environment and Biodiversity Report N. 244. Fisheries New Zealand, Wellington, New Zealand.

Zipkin EF & Saunders SP. 2018. Synthesising multiple data types for biological conservation using integrated population modelling. Biological Conservation 217: 240-250.

SUPPLEMENTARY MATERIAL 1.

Are there predictable intra-annual patterns in the proportion of apparently occupied sites that can be integrated into the abundance data processing framework?

In our abundance data processing framework, we apply Ψ^o and Ψ^P in parallel (Fig. 2) where relevant (e.g., counts of AOS conducted after mean laying). This contrasts with a widespread assumption that Ψ^o and Ψ^p are inherently linked, particularly for ψ^{ABA}. Various studies on albatrosses have argued that the number of apparently occupied sites may increase over time as a function of nest failure (e.g., Poncet *et al.* 2006, Robertson *et al.* 2008, Baker *et al.* 2023, Frost *et al.* 2025). Some studies have attempted to investigate the influence of various factors on the proportion of non-breeders, apparently breeding adults, and/or BOGs present on colonies throughout the breeding period to better understand intra-annual change in ψ^{ABA}. For example, Stahl & Sagar (2006) showed that the proportion of Buller's Albatross BPs compared to BOGs ($\psi^{BOG} \cdot \psi^{ABA}$) remained stable during incubation and chick-rearing despite the onset of nest failures. Walker *et al.* (2020) illustrated that annual variation, not intra-annual variation, had the greatest influence on the proportion of White-capped Albatross BP compared to AOS (ψ^{ABA}). Elliott *et al.* (2024, 2025) and Rexer-Huber *et al.* (2024, 2025) illustrated that the proportion of BPs compared to BOGs ($\psi^{BOG} \cdot \psi^{ABA}$) also does not vary in a predicable manner for both subspecies of Antipodean Albatross. Thus, a range of studies have indicated the importance of considering species-specific, diurnal, and interannual variation as well as any intra-annual variation in occupancy error, but no study has been able to show conclusively that the proportion of non-breeders, apparently breeding adults, and/or BOGs present on colonies changes predictably throughout the breeding period.

We leveraged all the information we collated on Ψ^o for our case studies (Supplementary Tables 1-22) to explicitly investigate if Ψ^o is subject to predictable intra-annual patterns. Specifically, we used data from 48 albatross sub-counts quantifying BP as a proportion of AOS (ψ^{ABA}) to fit a Bayesian binomial GLMM with a logit-link function:

1.
$$\mathrm{bp}_c \sim \mathrm{Bin}(\mathrm{aos}_c,\ \psi_c^{ABA})$$
$$\mathrm{logit}(\psi^{ABA}) = \alpha_{ABA} + \theta_s^{\beta^{ABA}} \cdot s_{s,c} \cdot t_c + \varepsilon_{y,c}^{ABA}$$

In which bp_c is the number of BP counted per sub-count c investigating Ψ^o, aos_c is the number of AOS counted per sub-count, α_{ABA} is the model intercept, $\theta_s^{\beta^{ABA}}$ is a design-matrix of species-specific fixed effects on intra-annual variation, $s_{s,c}$ is the species under consideration, t_c is the timing (in relation to species-specific phenology of the count), and $\varepsilon_{y,c}^{ABA}$ is a random annual effect. Thus, we leveraged the information-sharing ability of Bayesian statistics, while investigating if there are general patterns in intra-annual variation in ψ^{ABA}.

The results of this supplementary analysis are illustrated in Supplementary Figure 1., which highlight that the majority of the species included in this analysis did not show any significant intra-annual patterns in ψ^{ABA} and highlighted uncertainty above all. Antipodean Albatross did show a significant intra-annual pattern in ψ^{ABA} , in which the proportion of BP in relation to AOS increases as the breeding period progresses, presumable as pre-breeders become less common on the colony. Salvin’s Albatross showed a similar significant pattern, but this potentially requires more investigation and the Salvin’s Albatross sample size was particularly small <5 data points.

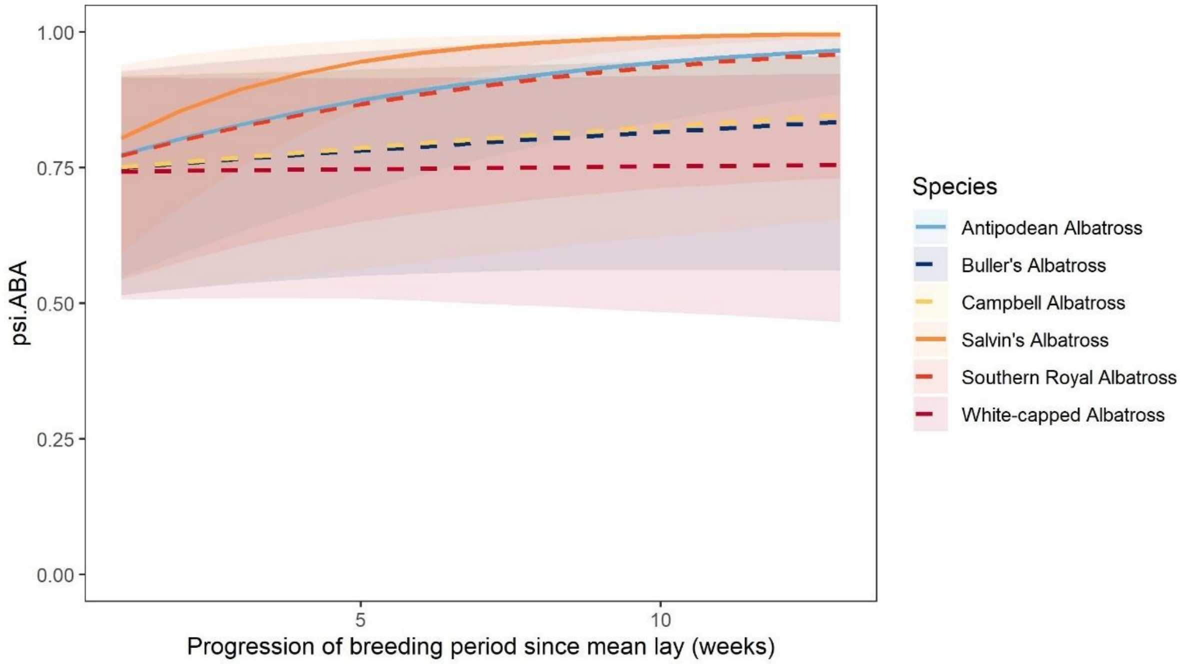

Supplementary Figure 1. Model estimates of the proportion breeding pairs in relation to apparently occupied sites (ψ^{ABA}) over the course of the breeding period for six species of albatross. Dashed lines indicate non-significance.

Our additional analysis in combination with the pre-existing body of evidence illustrates the lack of strong evidence for predictable intra-annual patterns in ψ^{ABA}. Consequently, the most parsimonious approach to account for ψ^{ABA} (and by extension Ψ^{o}) is to use random effects within relatively simple binomial GLMMs that adjust individual counts using model estimates of ψ^{ABA} without additional attempts to incorporate intra-annual effects, i.e., as per Eq. 2ABC. Naturally, there are clear, predictable intra-annual patterns in Ψ^{p} (Fig. 4), and thus, we account for this source of error while incorporating intra-annual patterns. Ultimately, we therefore accounted for these two counter-acting sources of error (Ψ^{o} results in overestimation, Ψ^{p} results in underestimation) in parallel, but separately.

References

Baker GB, Jenzs K, Cunningham R, Robertson G, Sagar P, Thompson TR & Double MC. 2023. Population assessment of White-capped Albatross *Thalassarche steadi* in New Zealand. Emu – Austral Ornithology 123: 60-70.

Elliot G, Walker K, Rexer-Huber K, Tinnemans J, Long J, Sagar S, Osborne J & Parker G. 2024. Gibson's wandering albatross: demography, satellite tracking and census. Conservation Services Programme, Department of Conservation, Wellington, New Zealand.

Elliott G, Walker K, Rexer-Huber K, Tinnemans J, McDonald A, Rawlence T & Parker G. 2025. Gibson's wandering albatross: drone-based population estimate, demography and at-sea distribution. Conservation Services Programme, Department of Conservation, Wellington, New Zealand.

Frost PGH, Baker GB, Fischer JH & Sagar PM. 2025. Population survey of Southern Buller's Albatross *Thalassarche bulleri bulleri* on the Solander Islands | Hautere, March 2024. Marine Ornithology 53: 361-371.

Poncet S, Robertson G, Phillips RA, Lawton K, Phalan B, Trathan PN & Croxall JP. 2006. Status and distribution of wandering, black-browed and grey-headed albatrosses breeding at South Georgia. Polar Biology 29: 772-781.

Rexer-Huber K, Whitehead E, Parker G, Patterson E, Walker K, Welch J & Elliott G. 2024. Antipodean wandering albatrosses and white-chinned petrels 2024. Conservation Services Programme, Department of Conservation, Wellington, New Zealand.

Rexer-Huber K, Whitehead E, Walker K & Elliott G. 2025. Antipodean wandering albatrosses and white-chinned petrels 2025. Conservation Services Programme, Department of Conservation, Wellington, New Zealand.

Robertson G, Moreno CA, Lawton K, Kirkwood D & Valencia J. 2008. Comparison of census methods for Black-browed Albatrosses breeding at Ildefonso Archipelago, Chile. Polar Biology 31: 153-162.

Stahl JC & Sagar PM. 2006. Behaviour and patterns of attendance of non-breeding birds at the breeding colony in a Buller's Albatross *Thalassarche bulleri* population at The Snares. Notornis 53: 327-338.

Walker KJ, Elliott GP, Rexer-Huber K, Parker GC, Sagar PM & McClelland PJ. 2021. Shipwrecks and mollymawks: an account of Disappointment Island Birds. Notornis 67: 213-245.

SUPPLEMENTARY MATERIAL 2. DATA TABLES

Antipodean Albatross

Supplementary Table 1. Antipodes Island counts of Antipodean Albatross (ssp. *antipodensis*), including count methods, metrics, and error specifications, as well as subsequent standardised data $y_{i,t}$ expressed in BP at the start of the breeding season (for which superscript numbers refer to equations in main text applied). * Indicates counts not (yet) included in the ACAP database.

Year	Method	Counted metric	Part site	Reported raw count	Count date	Weeks post μ lay[A]	*f*	p^{b}	Ψ^{s}	Ψ^{d}	Ψ^{p}	Ψ^{o}	π[B]	Acc. category	Reported adjusted count	Reported adjusted metric	Standardised abundance ($y_{i,t}$)	References
1969*	VPC & GC	BOG & BP	Antipodes I.	1,867	7 Feb – 1 Mar	2-5	NA	NA	NA	0.688[C]	✓; ?	0.333[C]	1.000	Unknown (low)	5,000-8,000[C]	BP	6,500 (2,170-10,840)	Warham & Bell 1979; Walker & Elliott 2005
1978*	GC	C	Antipodes I.	1,096	Nov-Dec	40-49	NA	NA	-	-	-	NA	0.333[C]	Unknown (low)	3,800[C]	BP	5,384 (1,776-9,604)	Bell 1978; Walker & Elliott 2005
1994	GC	BP	Antipodes I.	4,635	Feb	1-5	0.748	NA	NA	-	-	NA	1.000	Medium	-	-	4,727 (3,175-6,283)	Walker & Elliott 2005
1995	GC	BP	Antipodes I.	5,757	Feb	1-5	0.748	NA	NA	-	-	NA	1.000	Medium	-	-	5,858 (3,921-7,795)	Walker & Elliott 2005
1996	GC	BP	Antipodes I.	5,148	Feb	1-5	0.791	0.538	NA	-	-	NA	1.000	Medium	-	-	5,234 (3,496-6,967)	Walker & Elliott 2005
1997	GC	BP	Antipodes I.	3,167	Feb	1-5	0.797	0.497	-	-	-	NA	0.612	Medium	-	-	5,258 (3,511-7,004)	Walker & Elliott 2005
1998	GC	BP	SA, MCBA	694	5-19 Feb	2-4	0.748	0.535	-	(0.985[D])	-	NA	0.121	High	5,736	BP	5,845 (4,535-7,146)	Walker & Elliott 2005
1999	GC	BP	SA, MCBA	621	5-19 Feb	2-4	0.626	0.472	-	(0.985[D])	-	NA	0.121	High	5,132	BP	5,271 (4,037-6,514)	Walker & Elliott 2005
2000	GC	BP	SA, B32, MCBA	711	5-19 Feb	2-4	0.774	0.472	-	(0.985[D])	-	NA	0.148	High	4,740	BP	4,890 (3,891-5,876)	Walker & Elliott 2005
2001	GC	BP	SA, B32, MCBA	744	5-19 Feb	2-4	0.784	0.571	-	(0.985[D])	-	NA	0.147	High	4,960	BP	5,147 (4,120-6,177)	Walker & Elliott 2005
2002	GC	BP	SA, B32, MCBA	931	5-19 Feb	2-4	0.678	0.448	-	(0.985[D])	-	NA	0.147	High	6,207	BP	6,487 (5,286-7,679)	Walker & Elliott 2005
2003	GC	BP	SA, B32, MCBA	1,009	5-19 Feb	2-4	0.731	0.518	-	(0.985[D])	-	NA	0.147	High	6,727	BP	7,004 (5,758-8,251)	Walker & Elliott 2005
2004	GC	BP	SA, B32, MCBA	1,220	5-19 Feb	2-4	0.719	0.474	-	(0.985[D])	-	NA	0.146	High	8,133	BP	8,535 (7,089-9,979)	Walker & Elliott 2005
2005	GC	BP	SA, B32, MCBA	1,010	5-19 Feb	2-4	NA	0.483	-	(0.985[D])	-	NA	0.146	High	6,733	BP	7,086 (5,811-8,371)	Walker & Elliott 2005
2007	GC	BP	SA, B32	246	Feb	1-5	0.575	-	-	-	-	NA	0.056	High	4,393	BP	4,530 (2,147-6,909)	Elliott & Walker 2017
2008	GC	BP	SA, B32	300	Feb	1-5	0.655	0.618	-	-	-	NA	0.056	High	5,357	BP	5,490 (2,894-8,105)	Elliott & Walker 2017

Year	Method	Counted metric	Part site	Reported raw count	Count date	Weeks post μ lay[A]	f	p^b	Ψ^s	Ψ^d	Ψ^p	Ψ^o	π [B]	Acc. category	Reported adjusted count	Reported adjusted metric	Standardised abundance ($y_{i,t}$)	References
2009	GC	BP	SA, B32	218	Feb	1-5	0.550	0.283	-	-	-	NA	0.056	High	3,893	BP	4,016 (1,798-6,253)	Elliott & Walker 2017
2010	GC	BP	SA, B32	207	Feb	1-5	0.660	0.366	-	-	-	NA	0.056	High	3,696	BP	3,788 (1,658-5,959)	Elliott & Walker 2017
2011	GC	BP	SA, B32	196	Feb	1-5	0.517	0.413	-	-	-	NA	0.056	High	3,500	BP	3,618 (1,506-5,738)	Elliott & Walker 2017
2012	GC	BP	SA, B32, MCBA	544	Feb	1-5	0.557	0.397	-	-	-	NA	0.144	High	3,627	BP	3,896 (3,001-4794)	Elliott & Walker 2017
2013	GC	BP	SA, B32, MCBA	478	Feb	1-5	0.567	0.466	-	-	-	NA	0.144	High	3,187	BP	3,425 (2,596-4,247)	Elliott & Walker 2017
2014	GC	BP	SA, B32, MCBA	535	Feb	1-5	0.681	0.453	-	-	-	NA	0.143	High	3,567	BP	3,831 (2,943-4,718)	Elliott & Walker 2017
2015	GC	BP	SA, B32, MCBA	450	Feb	1-5	0.527	0.412	-	-	-	NA	0.143	High	3,000	BP	3,253 (2,447-4,068)	Elliott & Walker 2017
2016	GC	BP	SA, B32, MCBA	483	Feb	1-5	0.667	0.532	-	-	-	NA	0.143	High	3,220	BP	3,457 (2,632-4,297)	Elliott & Walker 2017
2017	GC	BP	SA, B32, MCBA	369	5-10 Feb	2	0.804	0.365	-	-	-	NA	0.142	High	2,460	BP	2,628 (1,915-3,336)	Elliott & Walker 2017
2018	GC	BP	SA, B32, MCBA	509	5-10 Feb	2	0.660	0.564	-	-	-	NA	0.142	High	3,393	BP	3,644 (2,780-4,502)	Elliott & Walker 2018
2019	GC	BP	SA, B32, MCBA	471	5-10 Feb	2	0.590	0.458	-	-	-	NA	0.142	High	3,140	BP	3,384 (2,562-4,205)	Elliott & Walker 2019
2020	GC	BP	SA	75	15-28 Mar	7-9	0.615	0.397	-	-	-	NA	0.028	High	2,679	BP	2,876 (75-6,758)	Elliott & Walker 2020
2021	GC	BP	SA, B32, MCBA	307	5-10 Feb	2	0.625	0.465	-	-	-	NA	0.096	High	3,198	BP	3,259 (2,087-4,421)	Walker & Elliott 2022
2022	GC	BP	SA, B32, MCBA	438	5-10 Feb	2	0.723	0.497	-	-	-	NA	0.141	High	2,920	BP	3,148 (2,359-3,943)	Walker & Elliott 2022
2023	GC	BP	SA, B32, MCBA	487	6-12 Feb	2	0.711	0.466	-	-	-	NA	0.140	High	3,247	BP	3,528 (2,678-4,383)	Parker et al. 2023
2024*	GC & AC^{UAV}	AOS	Antipodes I.	2,766	2 Feb – 2 Mar	2-5	0.681	0.500	-	(0.980[D])	✓[E]	ψ^{ABA} = 0.698 (0.489; 0.872)[E]	0.824	High	3,383 (3,182; 3,585)[F]	BP	3,384 (3,044-3,723)	Rexer-Huber et al. 2024
2025*	GC & AC^{UAV}	AOS	Antipodes I.	4,389	25 Jan-10 Feb	0-2	NA	NA	-	-	✓[E]	ψ^{ABA} = 0.600 (0.324; 0.723)[E]	0.985	High	3,546 (3,048; 4,044)[F]	BP	3,546 (3,192-3,901)	Rexer-Huber et al. 2025

[A] Mean lay is ~24 Jan and breeding period is considered ~50 weeks. [B] Proportion of breeding site based on retrospective assessment based on full island drone counts in Rexer-Huber et al. 2024, 2025.[C] Retrospectively estimated in Walker & Elliott 2005. [D] E_d estimated but deemed negligible and not included in reported adjusted count. [E] Day-specific $\psi^{lay} \cdot \psi^{fail}$ estimates were included for each daily count. [F] Based on habitat-related extrapolation.

Appendix Table 2. Adams Island counts of Antipodean Albatross (ssp. *gibsoni*), including count methods, metrics, and error specifications, as well as subsequent standardised data $y_{i,t}$ expressed in BP at the start of the breeding season (for which superscript numbers refer to equations in main text applied). * Indicates counts not (yet) included in the ACAP database.

Year	Method	Counted metric	Part site	Reported raw count	Count date	Weeks post μ lay[A]	f	p^b	Ψ^s	Ψ^d	Ψ^p	Ψ^o	π [B]	Acc. category	Reported adjusted count	Reported adjusted metric	Standardised abundance ($y_{i,t}$)	References
1973*	GC	BP	Adams I.	7,000	Early Feb	3-4	NA	NA	-	0.195[C]	-	NA	1.000	Unknown (low)	20,000[C]	BP	21,040 (6,928-35,150)	Robertson 1975, Walker & Elliott 2002
1991	GC & VPC	BP	RR, AA, AB	3,531	Early Feb	3-4	0.648	NA	-	-	-	✓; ?	0.754	High	-	-	4,832 (4,337-5,329)	Walker & Elliott 2002
1993	GC & VPC	BP	RR, AA, AB	3,746	Early Feb	3-4	0.778	NA	-	-	-	✓; ?	0.754	High	-	-	5,066 (4,551-5,583)	Walker & Elliott 2002
1994	GC & VPC	BP	RR, AA, AB	3,433	Early Feb	3-4	0.713	0.606	-	-	-	✓; ?	0.754	High	-	-	4,667 (4,187-5,149)	Walker & Elliott 2002
1995	GC, VPC & AC^{heli}	BP & AOS	RR, AA, AB	4,750	Early Feb	3-4	0.634	0.704	-	-	-	✓; ?	0.754	High	-	-	6,510 (5,850-7,173)	Walker & Elliott 2002
1996	GC	BP	SA	200	Early Feb	3-4	0.644	0.618	-	-	-	NA	0.029	High	-	-	7,119 (1,342-12,880)	Walker & Elliott 2002, Elliott et al. 2016
1997	GC, VPC & AC^{heli}	BP & AOS	Adams I.	6,993	23-31 Jan	2-3	0.676	0.622	NA	(0.994)[D]	$\psi^{lay} \cdot \psi^{fail} = 0.944$	✓; ?	1.000	High	8,414	BP	6,992 (6,293-7,689)	Hamilton et al. 2000, Walker et al. 2002, Elliott et al. 2016
1998	GC	BP	RR, AA, FS	791	25 Jan – 20 Feb	2-6	0.637	0.604	-		$\psi^{lay} \cdot \psi^{fail} = 0.991$	NA	0.095	High	8,436	BP	8,324 (6,358-10,300)	Walker et al. 2002, Elliott et al. 2016
1999	GC	BP	RR, AA, FS	743	3 Jan – 6 Feb	0-4	0.612	0.564	-	-	$\psi^{lay} \cdot \psi^{fail} = 0.996$	NA	0.095	High	7,886	BP	7,818 (5,907-9,720)	Walker & Elliott 2005, Elliott et al. 2016
2000	GC	BP	RR, AA, AB, FS	1,556	Jan	0-3	0.521	0.404	-	✓; ?	$\psi^{lay} \cdot \psi^{fail} = 0.982$	NA	0.259	High	4,904[E]	BP	6,010 (5,225-6,792)	Walker & Elliott 2005, Elliott et al. 2016
2001	GC	BP	RR, AA, FS	675	Jan	0-3	0.650	0.684	-	-	$\psi^{lay} \cdot \psi^{fail} = 0.956$	NA	0.095	High	7,463	BP	7,106 (5,301-8,909)	Walker & Elliott 2005, Elliott et al. 2016
2002	GC	BP	RR, AA, FS	714	Jan	0-3	0.620	0.513	-	-	$\psi^{lay} \cdot \psi^{fail} = 0.965$	NA	0.095	High	7,822	BP	7,510 (5,649-9,373)	Walker & Elliott 2005, Elliott et al. 2016
2003	GC	BP	RR, AA, FS	784	Jan	0-3	0.530	0.604	-	-	$\psi^{lay} \cdot \psi^{fail} = 0.991$	NA	0.095	High	8,362	BP	8,255 (6,299-10.220)	Walker & Elliott 2005, Elliott et al. 2016
2004	GC	BP	RR, AA, FS	862	Jan	0-3	0.540	0.603	-	-	$\psi^{lay} \cdot \psi^{fail} = 0.975$	NA	0.095	High	9,345	BP	9,072 (6,990-11,150)	Walker & Elliott 2005, Elliott et al. 2016
2005	GC	BP	RR, AA, FS	429	Jan	0-3	0.379	0.476	-	-	$\psi^{lay} \cdot \psi^{fail} = 0.949$	NA	0.095	High	4,778	BP	4,518 (3,118-5,908)	Walker & Elliott 2005, Elliott et al. 2016
2006	GC	BP	RR, AA, FS	279	Jan	0-3	0.255	0.460	-	-	$\psi^{lay} \cdot \psi^{fail} = 0.818$	NA	0.095	High	3,605	BP	2,940 (1,834-4,039)	Elliott & Walker 2013, Elliott et al. 2016
2007	GC	BP	RR, AA, FS	400	Jan	0-3	0.243	0.533	-	-	$\psi^{lay} \cdot \psi^{fail} = 0.930$	NA	0.095	High	4,545	BP	4,206 (2,865-5,554)	Elliott & Walker 2013, Elliott et al. 2016
2008	GC	BP	RR, AA, FS	318	Jan	0-3	0.326	0.570	-	-	$\psi^{lay} \cdot \psi^{fail} = 0.933$	NA	0.095	High	3,605	BP	3,345 (2,156-4,533)	Elliott & Walker 2013, Elliott et al. 2016
2009	GC	BP	RR, AA, FS	386	Jan	0-3	0.242	0.634	-	-	$\psi^{lay} \cdot \psi^{fail} = 0.906$	NA	0.095	High	4,503	BP	4,060 (2,742-5,381))	Elliott & Walker 2013, Elliott et al. 2016
2010	GC	BP	RR, AA, FS	383	Jan	0-3	0.310	0.656	-	-	$\psi^{lay} \cdot \psi^{fail} = 0.977$	NA	0.095	High	4,144	BP	4,031 (2,726-5,338)	Elliott & Walker 2013, Elliott et al. 2016

Year	Method	Counted metric	Part site	Reported raw count	Count date	Weeks post µ lay[A]	f	p^b	Ψ^s	Ψ^d	Ψ^p	Ψ^o	π [B]	Acc. category	Reported adjusted count	Reported adjusted metric	Standardised abundance $(y_{i,t})$	References
2011	GC	BP	RR, AA, FS	425	Jan	0-3	0.432	0.624	-	-	$\psi^{lay} \cdot \psi^{fail} = 0.970$	NA	0.095	High	4,630	BP	4,472 (3,100-5,858)	Elliott & Walker 2013, Elliott et al. 2016
2012	GC	BP	RR, AA, FS	379	Jan	0-3	0.417	0.665	-	-	$\psi^{lay} \cdot \psi^{fail} = 0.907$	NA	0.095	High	4,419	BP	3,988 (2,685-5,289)	Elliott & Walker 2013, Elliott et al. 2016
2013	GC	BP	RR, AA, FS	492	23-31 Jan	2-3	0.497	0.696	-	-	$\psi^{lay} \cdot \psi^{fail} = 0.948$	NA	0.095	High	5,486	BP	5,181 (3,680-6,692)	Elliott & Walker 2013, Elliott et al. 2016
2014	GC	BP	RR, AA, FS	430	23-31 Jan	2-3	0.302	0.553	-	-	$\psi^{lay} \cdot \psi^{fail} = 0.909$	NA	0.095	High	5,000	BP	4,529 (3,126-5,922)	Elliott & Walker 2014, Elliott et al. 2016
2015	GC	BP	RR, AA, FS	381	23-31 Jan	2-3	0.419	0.661	-	-	$\psi^{lay} \cdot \psi^{fail} = 0.938$	NA	0.095	High	4,292	BP	4,012 (2,702-5,315)	Walker & Elliott 2015, Elliott et al. 2016
2016	GC	BP	RR, AA, AB, FS	1,628	23 Jan – 9 Feb	2-5	0.676	0.656	-	✓; ?	$\psi^{lay} \cdot \psi^{fail} = 0.952$	$(\psi^{BOG} \cdot \psi^{ABA} = 0.740)$[F]	0.259	High	5,385[E]	BP	6,283 (5,477-7,101)	Elliott et al. 2016, Baker et al. 2017
2017	GC	BP	RR, AA, FS	424	23-31 Jan	2-3	0.677	0.529	-	-	$\psi^{lay} \cdot \psi^{fail} = 0.946$	NA	0.095	High	4,736	BP	4,461 (3,070-5,842)	Walker et al. 2017
2018	GC	BP	RR, AA, FS	475	Jan	0-3	0.576	0.574	-	-	$\psi^{lay} \cdot \psi^{fail} = 0.971$	NA	0.095	High	5,169	BP	4,999 (3,533-6,479)	Rexer-Huber et al. 2019
2019	GC	BP	RR, AA, FS	403	23-31 Jan	2-3	0.544	0.636	-	-	$\psi^{lay} \cdot \psi^{fail} = 0.953$	NA	0.095	High	4,471	BP	4,243 (2,902-5,592)	Rexer-Huber et al. 2019
2020	GC	BP	RR, AA, FS	376	23-31 Jan	2-3	NA	0.478	-	-	$\psi^{lay} \cdot \psi^{fail} = 0.962$	NA	0.095	High	4,133	BP	3,959 (2,659-5,248)	Rexer-Huber et al. 2020
2022	GC	BP	RR, AA, FS	428	23-31 Jan	2-3	0.736	NA	-	-	$\psi^{lay} \cdot \psi^{fail} = 0.953$	NA	0.095	High	4,746	BP	4,505 (3,120-5,888)	Parker et al. 2022
2023	GC & AC^{UAV}	BP	RR, AA, FS	481	23-31 Jan	2-3	0.599	0.749	-	-	$\psi^{lay} \cdot \psi^{fail} = 0.960$	$(\psi^{ABA} = 0.729)$[G]	0.095	High	5,296	BP	5,063 (3,583-6,551)	Walker et al. 2023
2024	AC^{UAV}	BOG	Adams I.	5,559	21 Jan – 25 Feb	2-7	0.468	0.533	-	-	✓[G]	$\psi^{BOG} \cdot \psi^{ABA} = 0.540$ (0.350; 0.880)[H]	0.794	High	4,130 (3,904-4,361)	BP	4,130 (3,715-4,539)	Elliott et al. 2024
2025*	AC^{UAV}	BOG	Adams I.	-	13 Jan-2 Feb	0-3	NA	NA	-	-	✓[G]	$\psi^{BOG} \cdot \psi^{ABA} = 0.670$ (0.360-0.900)[H]	0.590	High	4,865 (4,793-4,929)	BP	4,864 (4,377-5,350)	Elliott et al. 2025

[A] Mean lay is ~10 Jan and breeding period is considered ~50 weeks. [B] Proportion of breeding site based on full island counts completed in 1997 and then updated in 2025 (Elliott et al. 2025). [C] Retrospectively estimated by Walker & Elliott 2002 by repeating the methodology in 1997. [D] Estimated but considered negligible. [E] Estimated but without the counts at AB included in the extrapolation. [F] Estimated during aerial survey trials. [G] Estimated during drone trials. [H] Day-specific $\psi^{lay} \cdot \psi^{fail}$ estimates were included for each daily count.

Appendix Table 3. Disappointment Island counts of Antipodean Albatross (ssp. *gibsoni*), including count methods, metrics, and error specifications, as well as subsequent standardised data $y_{i,t}$ expressed in BP at the start of the breeding season (for which superscript numbers refer to equations in main text applied). * Indicates counts not (yet) included in the ACAP database.

Year	**Method**	**Counted metric**	**Part site**	**Reported raw count**	**Count date**	**Weeks post μ lay**[A]	f	p^b	Ψ^s	Ψ^d	Ψ^p	Ψ^o	π	**Acc. category**	**Reported adjusted count**	**Reported adjusted metric**	**Standardised abundance** $(y_{i,t})$	**References**
1973	GC	BP	Disappointment I.	200	6 Jan & 15 Feb	0-5	NA	NA	-	-	-	-	1.000	Unknown (Low)	-	-	207 (68-346)^{1,2}	Robertson 1975
1993	GC & VPC	BP & AOS	Disappointment I.	-	17-18 Jan	1	NA	NA	-	-	-	0.911	1.000	Medium	226	BP	229 (154; 305)^{1,2}	Walker et al. 2021
2014	AC^{heli}	AOS	Disappointment I.	463	20 Jan	1	NA	NA	-	-	-	($\psi^{BOG} \cdot \psi^{ABA}$ = 0.560)[B]	1.000	Unknown (Low)	452	AOS	293 (97; 497)^{1,2,3}	Baker & Jensz 2014A

[A] Mean lay is ~10 Jan and breeding period is considered ~50 weeks. [B] Ψ^o measured on Adams Island on the same day but not included in this count (Walker et al. 2021).

Northern Royal Albatross

Table 4. Motuhara | Fortyfours counts of Northern Royal Albatross, including count methods, metrics, and error specifications, as well as subsequent standardised data $y_{i,t}$ expressed in BP at the start of the breeding season (for which superscript numbers refer to equations in main text applied). * Indicates counts not (yet) included in the ACAP database. **Bold** indicates count selected for inclusion in the data processing framework in scenarios where >1 counts were completed in a year.

Year	Method	Counted metric	Part site	Reported raw count	Count date	Weeks post µ lay^{A}	f	p^b	Ψ^s	Ψ^d	Ψ^p	Ψ^o	π^{B}	Acc. category	Reported adjusted count	Reported adjusted metric	Standardised abundance ($y_{i,t}$)	References
1954*	GC	BP	Motuhara	2,000	1 Feb		-	-	-	-	-	NA	1.000	Unknown (Low)	-	-		Dawson 1955, Robertson 1991
1972*	AC^{fw}	C	Motuhara	1,752^{C}	Sep	42-46	-	-	NA	-	-	NA	1.000	Unknown (Low)	-	-		Robertson 1991, Rebergen 2000
1973*	AC^{fw}	BOG	Motuhara	3,285	28 Nov	2	0.557^{D}	-	NA	-	-	$\psi^{BOG} = 0.688^{E}$	1.000	Unknown (Low)	-	-		Robertson 1991, Rebergen 2000
1974*	AC^{fw}	BOG	Motuhara	3,450^{F}	24 Oct	0	0.446^{D}	-	NA	-	-	$\psi^{BOG} = 0.688^{E}$	1.000	Unknown (Low)	-	-		Robertson 1991
1975*	AC^{fw}	BOG	Motuhara	2,846	28 Nov	2	0.609^{D}	-	NA	-	-	$\psi^{BOG} = 0.688^{E}$	1.000	Unknown (Low)	-	-		Robertson 1991, Rebergen 2000
1989*	AC^{fw}	C	Motuhara	719	25 Sep	45	-	-	NA	-	-	NA	1.000	Unknown (Low)	-	-		Robertson 1991, Rebergen 2000
1990*	AC^{fw}	BOG	Motuhara	4,562	2 Dec	3	0.027^{D}	-	NA	-	-	$\psi^{BOG} = 0.650^{E}$	1.000	Unknown (Low)	-	-		Robertson 1991, Rebergen 2000
1991*	AC^{fw}	BOG	Motuhara	4,520	2 Dec	3	0.091^{D}	-	NA	-	-	$\psi^{BOG} = 0.650^{E}$	1.000	Unknown (Low)	-	-		Robertson 1991, Rebergen 2000
1992*	AC^{fw}	C	Motuhara	118	28 Aug	41	-	-	NA	-	-	-	1.000	Unknown (Low)	-	-		Rebergen 2000
1993*	AC^{fw}	BOG	Motuhara	5,982	3 Dec	3	0.038^{D}	-	NA	-	-	-	1.000	Unknown (Low)	-	-		Rebergen 2000
1994*	AC^{fw}	BOG	Motuhara	2,178	20 Dec	5	-	-	NA	-	-	-	1.000	Unknown (Low)	-	-		Rebergen 2000
1995*	AC^{fw}	BOG	Motuhara	5,542	1 Dec	2	0.133^{D}	-	NA	-	-	-	1.000	Unknown (Low)	-	-		Rebergen 2000
1996*	AC^{fw}	BOG	Motuhara	3,828	5 Dec	3	0.181^{D}	-	NA	-	-	-	1.000	Unknown (Low)	-	-		Rebergen 2000
1997*	AC^{fw}	BOG	Motuhara	3,893	5 Dec	3	0.098^{D}	-	NA	-	-	-	1.000	Unknown (Low)				Rebergen 2000
1998*	AC^{fw}	BOG	Motuhara	4,893	30 Nov	2	0.344^{D}	-	NA	-	-	-	1.000	Unknown (Low)				Rebergen 2000
1999*	AC^{fw}	BOG	Motuhara	3,570	23 Nov	1	0.254^{D}	-	NA	-	-	-	1.000	Unknown (Low)				Rebergen 2000
2000*	AC^{fw}	BOG	Motuhara	1,957	27 Dec	2	0.449^{D}	-	NA	-	-	-	1.000	Unknown (Low)				Rebergen 2000
2007	AC^{fw}	BOG	Motuhara	1,879	10 Dec	4	0.542^{D}	-	NA	-	-	-	1.000	High	-	-		Scofield 2011

Year	Method	Counted metric	Part site	Reported raw count	Count date	Weeks post µ lay[A]	*f*	p^b	Ψ^s	Ψ^d	Ψ^p	Ψ^o	π [B]	Acc. category	Reported adjusted count	Reported adjusted metric	Standardised abundance $(y_{i,t})$	References
2008	**GC**	BP	Motuhara	2,125	29 Nov	2	0.479	-	NA	-	-	$\psi^{ABA} \cdot \psi^{BOG}$ = 0.961	1.000	High	-	-		Scofield 2011
	AC^{fw}	BOG		2,212	29 Nov	2	0.460[D]	-	-	-	-	-	1.000	High	-	-		
2009	AC^{fw}	BOG	Motuhara	2,055	28 Nov	2	0.504[D]	-	NA	-	-	-	1.000	High	-	-		Scofield 2011
2010	AC^{fw}	BOG	Motuhara	2,692	28 Nov	2	0.402[D]	-	NA	-	-	-	1.000	High	-	-		Scofield 2011
2016	AC^{sat}	BOG	Motuhara	2,632	12-19 Feb	13-14	-	-	NA	-	-	-	1.000	Medium	-	-		Fretwell et al. 2017
2017	AC^{fw}	BOG	Motuhara	1,803	23 Nov	1	0.580[G]	-	NA	-	-	ψ^{BOG} = 0.943[H] ψ^{BOG} = 0.864[I]	1.000	Medium	1,581 (1,502-1,661)	AOS		Baker et al. 2017, Frost 2017
	GC	BP	Motuhara	1,400	8 Dec	3	0.716	-	NA	-	-	ψ^{ABA} =0-916-0.957	1.000	Medium	-	-		M Bell et al. 2017B
	AC^{sat}	BOG	Motuhara	2,533	20 Dec	5	-	-	NA	-	-	-	1.000	Medium	-	-		
2018	AC^{fw}	BOG	Motuhara	1,850	4 Dec	3	0.667 [G]	-	NA	-	-	ψ^{BOG} = 0.967[H]	1.000	High	1,789 (1,704-1,874)	AOS		Frost 2019, 2021A
2020	AC^{fw}	C	Motuhara	1,059	15 Sep	44	-	-	NA	-	✓[J]	NA	1.000	High	1,203	C		Frost 2021A
2021	**AC^{fw}**	BOG	Motuhara	1,782	18 Dec	5	-	-	NA	-	-	ψ^{BOG} = 0.954[H]	1.000	High	1,696 (1,616-1,779)	AOS		Frost 2021B
	GC	BP	NRA1-5	146	28 Jan	11	-	-	-	-	-	-	0.110	High	-	-		Bell 2021
2022	GC	BP	NRA1-5	148	29 Jan	11	-	-	-	-	-	NA	0.110	High	-	-		Bell 2022
	AC^{fw}	BOG	Motuhara	1,705	1 Feb	11	-	-	NA	-	-	ψ^{BOG} = 0.957[H]	1.000	High	1,604 (1,501-1,704)	AOS		Frost 2022
2023	**GC**	BP	Motuhara	1,498	13 Dec	4	0.804	-	NA	-	-	NA	1.000	High	-	-		Bell 2023
	AC^{fw}	BOG	Motuhara	2,366	20 Dec	5	0.692[G]	-	NA	-	-	ψ^{BOG} = 0.748[H]	1.000	High	1,744 (1,461-2,041)	AOS		Frost 2024A
2024	**AC^{fw}**	BOG	Motuhara	2,178	9 Dec	4	-	-	NA	-	-	ψ^{BOG} = 0.944[H]	1.000	High	1,853 (1,770-1,939)	AOS		Frost 2024B
	GC	BP	Motuhara	1,472	20 Jan	10	-	-	NA	-	-	NA	1.000	High	-	-		Bell 2024
2025*	GC	C	NRA1-5	134	24 Feb	15	-	-	NA	-	-	NA	0.110	High	-	-		M Bell unpub.
2026*	GC	BP	Motuhara	1,344	1 Dec	2	-	-	NA	-	-	NA	1.000	High	-	-		Bell 2026

[A] Mean lay date ~ 14 Nov and breeding period is considered ~46 weeks (Robertson & Richdale 1993). [B] Proportion represented by aerial study grids NRA1-5 based on 2023-2024 averages (Bell 2023, Frost 2024A, Bell 2024). [C] Robertson (1991) only reports C for all Chatham Islands breeding sites in 1972, so mean proportion between breeding sites over 1973-1975 was used to allocate chicks to breeding sites. [D] Calculated using BOG rather than BP. [E] Robertson (1991) applies two estimates of ψ^{BOG} based on Pukekura data as an academic exercise, but these estimates were not based on local data, and counts are considered expressed in BOG. [F] Disagreement between Robertson (1991) and Rebergen (2000) on this count and we favoured the original count here. [G] Calculated using AOS rather than BP. [H] Based on close-up photographs. [I] Based on ground transects. [J] Adjustments made based on Pukekura fledging curve (Frost 2021A).

Table 5. Sisters counts of Northern Royal Albatross, including count methods, metrics, and error specifications, as well as subsequent standardised data $y_{i,t}$ expressed in BP at the start of the breeding season (for which superscript numbers refer to equations in main text applied). * Indicates counts not (yet) included in the ACAP database. **Bold** indicates count selected for inclusion in the data processing framework in scenarios where >1 counts were completed in a year.

Year	Method	Counted metric	Part site	Reported raw count	Count date	Weeks post μ lay^A	f	p^b	Ψ^s	Ψ^d	Ψ^p	Ψ^o	π^B	Acc. category	Reported adjusted count	Reported adjusted metric	Standardised abundance $(y_{i,t})$	References
1954*	GC	BP	Little Sister	1,000	26 Dec		-	-	-	-	-	NA	0.395	Unknown (Low)	-	-		Dawson 1954, Robertson 1991
1972*	AC^{fw}	C	Little & Big Sister	848^C	Sep	42-46	-	-	NA	-	-	NA	1.000	Unknown (Low)	-	-		Robertson 1991
1973*	AC^{fw}	BOG	Little & Big Sister	1,996	28 Nov	2	0.261^D	-	NA	-	-	ψ^{BOG} = 0.688^E	1.000	Unknown (Low)	-	-		Robertson 1991, Rebergen 2000
1974*	AC^{fw}	BOG	Little & Big Sister	2,500^F	24 Oct	0	0.517^D	-	NA	-	-	ψ^{BOG} = 0.688^E	1.000	Unknown (Low)	-	-		Robertson 1991, Rebergen 2000
1975*	AC^{fw}	BOG	Little & Big Sister	1,868	28 Nov	2	0.417^D	-	NA	-	-	ψ^{BOG} = 0.688^E	1.000	Unknown (Low)	-	-		Robertson 1991
1976*	AC^{fw}	C	Little Sister	446	?	37-46^G	-	-	-	-	-	NA	0.395	Unknown (Low)	-	-		Robertson & Gales 1998
1989*	AC^{fw}	C	Little & Big Sister	380	25 Sep	45	-	-	NA	-	-	NA	1.000	Unknown (Low)	-	-		Robertson 1991, Rebergen 2000
1990*	AC^{fw}	BOG	Little & Big Sister	3,763	2 Dec	3	0.204^D	-	NA	-	-	ψ^{BOG} = 0.650^E	1.000	Unknown (Low)	-	-		Robertson 1991, Rebergen 2000
1991*	AC^{fw}	BOG	Little & Big Sister	3,380	2 Dec	3	0.270^D	-	NA	-	-	ψ^{BOG} = 0.650^E	1.000	Unknown (Low)	-	-		Robertson 1991, Rebergen 2000
1992*	AC^{fw}	BOG	Little Sister	1,101	30 Nov	1	0.262^D	-	NA	-	-	-	1.000	Unknown (Low)	-	-		Robertson & Gales 1998, Rebergen 2000
1993*	AC^{fw}	BOG	Little & Big Sister	4,428	3 Dec	3	0.096^D	-	NA	-	-	-	1.000	Unknown (Low)	-	-		Robertson & Gales 1998, Rebergen 2000
1994*	AC^{fw}	BOG	Little & Big Sister	3,133	20 Dec	5	0.227^D	-	NA	-	-	-	1.000	Unknown (Low)	-	-		Robertson & Gales 1998, Rebergen 2000
1995*	AC^{fw}	BOG	Little & Big Sister	3,816	1 Dec	2	0.343^D	-	NA	-	-	-	1.000	Unknown (Low)	-	-		Robertson & Gales 1998, Rebergen 2000
1996*	AC^{fw}	BOG	Little & Big Sister	2,902	5 Dec	3	0.268^D	-	NA	-	-	-	1.000	Unknown (Low)	-	-		Rebergen 2000
1997*	AC^{fw}	BOG	Little & Big Sister	3,535	5 Dec	3	0.292^D	-	NA	-	-	-	1.000	Unknown (Low)				Rebergen 2000
1998*	AC^{fw}	BOG	Little & Big Sister	3,764	30 Nov	2	0.351^D	-	NA	-	-	-	1.000	Unknown (Low)				Rebergen 2000
1999*	AC^{fw}	BOG	Little & Big Sister	3,396	23 Nov	1	0.221^D	-	NA	-	-	-	1.000	Unknown (Low)				Rebergen 2000
2000*	AC^{fw}	BOG	Little & Big Sister	2,774	27 Dec	2	0.293^D	-	NA	-	-	-	1.000	Unknown (Low)				Rebergen 2000
2007	AC^{fw}	BOG	Little & Big Sister	3,509	10 Dec	4	0.439^D	-	NA	-	-	-	1.000	High	-	-		Scofield 2011

Year	Method	Counted metric	Part site	Reported raw count	Count date	Weeks post μ lay[A]	f	p^b	Ψ^s	Ψ^d	Ψ^p	Ψ^o	π[B]	Acc. category	Reported adjusted count	Reported adjusted metric	Standardised abundance ($y_{i,t}$)	References
2008	AC^{fw}	BOG	Little & Big Sister	3,389	29 Nov	2	0.213[D]	-	NA	-	-	-	1.000	High	-	-		Scofield 2011
2009	AC^{fw}	BOG	Little & Big Sister	3,397	28 Nov	2	0.288[D]	-	NA	-	-	-	1.000	High	-	-		Scofield 2011
2010	AC^{fw}	BOG	Little & Big Sister	3,052	28 Nov	2	0.404[D]	-	NA	-	-	-	1.000	High	-	-		Scofield 2011
2016	AC^{sat}	BOG	Little & Big Sister	1,805	29 Dec	13-14	-	-	NA	-	-	-	1.000	Medium	-	-		Fretwell et al. 2017
2017	**AC^{fw}**	BOG	Little & Big Sister	3,269	23 Nov	1	0.394[H]	-	NA	-	-	ψ^{BOG} = 0.932[I]	1.000	Medium	2,824 (2,718-2,931)	AOS		Baker et al. 2017, Frost 2017
	AC^{sat}	BOG	Little & Big Sister	2,578	20 Dec	5	-	-	NA	-	-	-	1.000	Medium		-		
2018	**GC**	BP	Little & Big Sister	2,092	30 Nov-4 Dec	2-3	0.457	-	NA	1.000	-	ψ^{ABA} = 0.941	1.000	High	-	-		M Bell et al. 2018
	AC^{fw}	BOG	Little & Big Sister	2,165	4 Dec	3	0.448[H]	-	NA	-	-	ψ^{BOG} = 0.982[J] ψ^{BOG} = 0.970[K]	1.000	High	2,130	AOS		Frost 2019, 2021A
2020	AC^{fw}	C	Little & Big Sister	739	15 Sep	44	-	-	NA	-	✓[K]	NA	1.000	High	840	C		Frost 2021A
2021	AC^{fw}	BOG	Little & Big Sister	2,392	18 Dec	5	-	-	NA	-	- -	ψ^{BOG} = 0.953[J] ψ^{BOG} = 0.959[K]	1.000	High	2,298 (2,168-2,435)	AOS		Frost 2021B
2022	AC^{fw}	BOG	Little & Big Sister	1,841	1 Feb	11	-	-	NA	-	-	ψ^{BOG} = 0.944[J] ψ^{BOG} = 0.942[K]	1.000	High	1,668 (1,517-1,843)	AOS		Frost 2022
2023	AC^{fw}	BOG	Little & Big Sister	2,733	20 Dec	5	0.569[H]	-	NA	-	-	ψ^{BOG} = 0.741[J] ψ^{BOG} = 0.844[K]	1.000	High	2,405 (1,922-2,991)	AOS		Frost 2024A
2024	AC^{fw}	BOG	Little & Big Sister	2,795	9 Dec	4	-	-	NA	-	-	ψ^{BOG} = 0.906[J] ψ^{BOG} = 0.953[K]	1.000	High	2,469 (2,333-2,609)	AOS		Frost 2024B
2025*	GC	C	Little Sister	517	26 Aug	41	-	-	-	-	-	NA	0.395	High	-	-		Bell 2026

[A] Mean lay date ~ 14 Nov and breeding period is considered ~46 weeks (Robertson & Richdale 1993). [B] Proportions between both islands based on 2007-2024 average. [C] Robertson 1991 only reports C for all Chatham Islands breeding sites in 1972, so mean proportion between breeding sites over 1973-1975 was used to allocate chicks to breeding sites. [D] Calculated using BOG rather than BP. [E] Robertson (1991) applies two estimates of ψ^{BOG} based on Pukekura data as an academic exercise, but these estimates were not based on local data, and counts are considered expressed in BOG. [F] Disagreement between Robertson (1991) and Rebergen (2000) on this count and we favoured the original count here. [G] Without information on count date, assumed to have occurred between 1 Aug and 30 Sep. [G] Calculated using AOS rather than BP. [H] Estimated using close-up photographs. [I] Estimated on Big Sister using close-up photographs. [J] Estimated on Little Sister using close-up photographs. [K] Adjustments made based on Pukekura fledging curve (Frost 2021A).

Table 6. Pukekura counts of Northern Royal Albatross, including count methods, metrics, and error specifications, as well as subsequent standardised data $y_{i,t}$ expressed in BP at the start of the breeding season (for which superscript numbers refer to equations in main text applied). * Indicates counts not (yet) included in the ACAP database.

Year	Method	Counted metric	Part site	Reported raw count	Count date	Weeks post μ lay^A	f	p^b	Ψ^s	Ψ^d	Ψ^p	Ψ^o	π	Acc. category	Reported adjusted count	Reported adjusted metric	Standardised abundance ($y_{i,t}$)	References
1936*	GC	BP	Pukekura	1	Continuous ^{B}	0	-	-	NA	-	-	NA	1.000	High	-	-		DOC unpub.
1937*	GC	BP	Pukekura	1	Continuous ^{B}	0	-	-	NA	-	-	NA	1.000	High	-	-		DOC unpub.
1938*	GC	BP	Pukekura	2	Continuous ^{B}	0	-	-	NA	-	-	NA	1.000	High	-	-		DOC unpub.
1939*	GC	BP	Pukekura	4	Continuous ^{B}	0	-	-	NA	-	-	NA	1.000	High	-	-		DOC unpub.
1940*	GC	BP	Pukekura	5	Continuous ^{B}	0	-	-	NA	-	-	NA	1.000	High	-	-		DOC unpub.
1941*	GC	BP	Pukekura	3	Continuous ^{B}	0	-	-	NA	-	-	NA	1.000	High	-	-		DOC unpub.
1942*	GC	BP	Pukekura	5	Continuous ^{B}	0	-	-	NA	-	-	NA	1.000	High	-	-		DOC unpub.
1943*	GC	BP	Pukekura	2	Continuous ^{B}	0	-	-	NA	-	-	NA	1.000	High	-	-		DOC unpub.
1944*	GC	BP	Pukekura	3	Continuous ^{B}	0	-	-	NA	-	-	NA	1.000	High	-	-		DOC unpub.
1945*	GC	BP	Pukekura	6	Continuous ^{B}	0	-	-	NA	-	-	NA	1.000	High	-	-		DOC unpub.
1946*	GC	BP	Pukekura	0	Continuous ^{B}	0	-	-	NA	-	-	NA	1.000	High	-	-		DOC unpub.
1947*	GC	BP	Pukekura	3	Continuous ^{B}	0	-	-	NA	-	-	NA	1.000	High	-	-		DOC unpub.
1948*	GC	BP	Pukekura	3	Continuous ^{B}	0	-	-	NA	-	-	NA	1.000	High	-	-		DOC unpub.
1949*	GC	BP	Pukekura	4	Continuous ^{B}	0	-	-	NA	-	-	NA	1.000	High	-	-		DOC unpub.
1950*	GC	BP	Pukekura	5	Continuous ^{B}	0	-	-	NA	-	-	NA	1.000	High	-	-		DOC unpub.
1951*	GC	BP	Pukekura	6	Continuous ^{B}	0	-	-	NA	-	-	NA	1.000	High	-	-		DOC unpub.
1952*	GC	BP	Pukekura	7	Continuous ^{B}	0	-	-	NA	-	-	NA	1.000	High	-	-		DOC unpub.
1953*	GC	BP	Pukekura	4	Continuous ^{B}	0	-	-	NA	-	-	NA	1.000	High	-	-		DOC unpub.
1954*	GC	BP	Pukekura	6	Continuous ^{B}	0	-	-	NA	-	-	NA	1.000	High	-	-		DOC unpub.
1955*	GC	BP	Pukekura	6	Continuous ^{B}	0	-	-	NA	-	-	NA	1.000	High	-	-		DOC unpub.
1956*	GC	BP	Pukekura	6	Continuous ^{B}	0	-	-	NA	-	-	NA	1.000	High	-	-		DOC unpub.
1957*	GC	BP	Pukekura	6	Continuous ^{B}	0	-	-	NA	-	-	NA	1.000	High	-	-		DOC unpub.
1958*	GC	BP	Pukekura	6	Continuous ^{B}	0	-	-	NA	-	-	NA	1.000	High	-	-		DOC unpub.
1959*	GC	BP	Pukekura	6	Continuous ^{B}	0	-	-	NA	-	-	NA	1.000	High	-	-		DOC unpub.
1960*	GC	BP	Pukekura	3	Continuous ^{B}	0	-	-	NA	-	-	NA	1.000	High	-	-		DOC unpub.
1961*	GC	BP	Pukekura	5	Continuous ^{B}	0	-	-	NA	-	-	NA	1.000	High	-	-		DOC unpub.
1962*	GC	BP	Pukekura	4	Continuous ^{B}	0	-	-	NA	-	-	NA	1.000	High	-	-		DOC unpub.
1963*	GC	BP	Pukekura	6	Continuous ^{B}	0	-	-	NA	-	-	NA	1.000	High	-	-		DOC unpub.
1964*	GC	BP	Pukekura	6	Continuous ^{B}	0	-	-	NA	-	-	NA	1.000	High	-	-		DOC unpub.
1965*	GC	BP	Pukekura	7	Continuous ^{B}	0	-	-	NA	-	-	NA	1.000	High	-	-		DOC unpub.
1966*	GC	BP	Pukekura	7	Continuous ^{B}	0	-	-	NA	-	-	NA	1.000	High	-	-		DOC unpub.
1967*	GC	BP	Pukekura	6	Continuous ^{B}	0	-	-	NA	-	-	NA	1.000	High	-	-		DOC unpub.
1968*	GC	BP	Pukekura	8	Continuous ^{B}	0	-	-	NA	-	-	NA	1.000	High	-	-		DOC unpub.
1969*	GC	BP	Pukekura	9	Continuous ^{B}	0	-	-	NA	-	-	NA	1.000	High	-	-		DOC unpub.
1970*	GC	BP	Pukekura	8	Continuous ^{B}	0	-	-	NA	-	-	NA	1.000	High	-	-		DOC unpub.
1971*	GC	BP	Pukekura	8	Continuous ^{B}	0	-	-	NA	-	-	NA	1.000	High	-	-		DOC unpub.
1972*	GC	BP	Pukekura	7	Continuous ^{B}	0	-	-	NA	-	-	NA	1.000	High	-	-		DOC unpub.
1973*	GC	BP	Pukekura	10	Continuous ^{B}	0	-	-	NA	-	-	NA	1.000	High	-	-		DOC unpub.
1974*	GC	BP	Pukekura	7	Continuous ^{B}	0	-	-	NA	-	-	NA	1.000	High	-	-		DOC unpub.

Year	Method	Counted metric	Part site	Reported raw count	Count date	Weeks post μ lay[A]	f	p^b	Ψ^s	Ψ^d	Ψ^p	Ψ^o	π	Acc. category	Reported adjusted count	Reported adjusted metric	Standardised abundance ($y_{i,t}$)	References
1975*	GC	BP	Pukekura	10	Continuous[B]	0	-	-	NA	-	-	NA	1.000	High	-	-		DOC unpub.
1976*	GC	BP	Pukekura	6	Continuous[B]	0	-	-	NA	-	-	NA	1.000	High	-	-		DOC unpub.
1977*	GC	BP	Pukekura	10	Continuous[B]	0	-	-	NA	-	-	NA	1.000	High	-	-		DOC unpub.
1978*	GC	BP	Pukekura	8	Continuous[B]	0	-	-	NA	-	-	NA	1.000	High	-	-		DOC unpub.
1979*	GC	BP	Pukekura	7	Continuous[B]	0	-	-	NA	-	-	NA	1.000	High	-	-		DOC unpub.
1980*	GC	BP	Pukekura	9	Continuous[B]	0	-	-	NA	-	-	NA	1.000	High	-	-		DOC unpub.
1981*	GC	BP	Pukekura	8	Continuous[B]	0	-	-	NA	-	-	NA	1.000	High	-	-		DOC unpub.
1982*	GC	BP	Pukekura	11	Continuous[B]	0	-	-	NA	-	-	NA	1.000	High	-	-		DOC unpub.
1983*	GC	BP	Pukekura	9	Continuous[B]	0	-	-	NA	-	-	NA	1.000	High	-	-		DOC unpub.
1984*	GC	BP	Pukekura	11	Continuous[B]	0	-	-	NA	-	-	NA	1.000	High	-	-		DOC unpub.
1985*	GC	BP	Pukekura	12	Continuous[B]	0	-	-	NA	-	-	NA	1.000	High	-	-		DOC unpub.
1986*	GC	BP	Pukekura	11	Continuous[B]	0	-	-	NA	-	-	NA	1.000	High	-	-		DOC unpub.
1987*	GC	BP	Pukekura	18	Continuous[B]	0	-	-	NA	-	-	NA	1.000	High	-	-		DOC unpub.
1988*	GC	BP	Pukekura	15	Continuous[B]	0	-	-	NA	-	-	NA	1.000	High	-	-		DOC unpub.
1989*	GC	BP	Pukekura	19	Continuous[B]	0	-	-	NA	-	-	NA	1.000	High	-	-		DOC unpub.
1990*	GC	BP	Pukekura	22	Continuous[B]	0	-	0.567[C]	NA	-	-	NA	1.000	High	-	-		DOC Coastal Otago 2026
1991*	GC	BP	Pukekura	15	Continuous[B]	0	-	0.567[C]	NA	-	-	NA	1.000	High	-	-		DOC Coastal Otago 2026
1992*	GC	BP	Pukekura	17	Continuous[B]	0	-	0.567[C]	NA	-	-	NA	1.000	High	-	-		DOC Coastal Otago 2026
1993*	GC	BP	Pukekura	19	Continuous[B]	0	-	0.567[C]	NA	-	-	NA	1.000	High	-	-		DOC Coastal Otago 2026
1994*	GC	BP	Pukekura	20	Continuous[B]	0	-	0.567[C]	NA	-	-	NA	1.000	High	-	-		DOC Coastal Otago 2026
1995	GC	BP	Pukekura	23	Continuous[B]	0	-	0.567[C]	NA	-	-	NA	1.000	High	-	-		DOC Coastal Otago 2026
1996*	GC	BP	Pukekura	21	Continuous[B]	0	-	0.567[C]	NA	-	-	NA	1.000	High	-	-		DOC Coastal Otago 2026
1997*	GC	BP	Pukekura	18	Continuous[B]	0	-	0.567[C]	NA	-	-	NA	1.000	High	-	-		DOC Coastal Otago 2026
1998*	GC	BP	Pukekura	24	Continuous[B]	0	0.458[D]	0.567[C]	NA	-	-	NA	1.000	High	-	-		DOC Coastal Otago 2026
1999*	GC	BP	Pukekura	12	Continuous[B]	0	-	0.567[C]	NA	-	-	NA	1.000	High	-	-		DOC Coastal Otago 2026
2000*	GC	BP	Pukekura	11	Continuous[B]	0	-	0.567[C]	NA	-	-	NA	1.000	High	-	-		DOC Coastal Otago 2026
2001*	GC	BP	Pukekura	20	Continuous[B]	0	-	0.567[C]	NA	-	-	NA	1.000	High	-	-		DOC Coastal Otago 2026
2002*	GC	BP	Pukekura	24	Continuous[B]	0	0.174[D]	0.567[C]	NA	-	-	NA	1.000	High	-	-		DOC Coastal Otago 2026
2003*	GC	BP	Pukekura	34	Continuous[B]	0	0.774[D]	0.567[C]	NA	-	-	NA	1.000	High	-	-		DOC Coastal Otago 2026
2004	GC	BP	Pukekura	17	Continuous[B]	0	0.588[D]	0.567[C]	NA	-	-	NA	1.000	High	-	-		DOC Coastal Otago 2026
2005*	GC	BP	Pukekura	30	Continuous[B]	0	0.655[D]	0.567[C]	NA	-	-	NA	1.000	High	-	-		DOC Coastal Otago 2026
2006*	GC	BP	Pukekura	17	Continuous[B]	0	0.500[D]	0.567[C]	NA	-	-	NA	1.000	High	-	-		DOC Coastal Otago 2026
2007*	GC	BP	Pukekura	15	Continuous[B]	0	0.786[D]	0.567[C]	NA	-	-	NA	1.000	High	-	-		DOC Coastal Otago 2026
2008*	GC	BP	Pukekura	21	Continuous[B]	0	0.400[D]	0.567[C]	NA	-	-	NA	1.000	High	-	-		DOC Coastal Otago 2026
2009	GC	BP	Pukekura	32	Continuous[B]	0	0.563[D]	0.567[C]	NA	-	-	NA	1.000	High	-	-		DOC Coastal Otago 2026
2010	GC	BP	Pukekura	21	Continuous[B]	0	0.762[D]	0.567[C]	NA	-	-	NA	1.000	High	-	-		DOC Coastal Otago 2026
2011	GC	BP	Pukekura	30	Continuous[B]	0	0.700[D]	0.567[C]	NA	-	-	NA	1.000	High	-	-		DOC Coastal Otago 2026
2012	GC	BP	Pukekura	31	Continuous[B]	0	0.548[D]	0.567[C]	NA	-	-	NA	1.000	High	-	-		DOC Coastal Otago 2026
2013	GC	BP	Pukekura	36	Continuous[B]	0	0.694[D]	-	NA	-	-	NA	1.000	High	-	-		DOC Coastal Otago 2026
2014*	GC	BP	Pukekura	32	Continuous[B]	0	0.742[D]	-	NA	-	-	NA	1.000	High	-	-		DOC Coastal Otago 2026
2015*	GC	BP	Pukekura	32	Continuous[B]	0	0.813[D]	-	NA	-	-	NA	1.000	High	-	-		DOC Coastal Otago 2026
2016	GC	BP	Pukekura	35	Continuous[B]	0	0.743[D]	-	NA	-	-	NA	1.000	High	-	-		DOC Coastal Otago 2026

Year	**Method**	**Counted metric**	**Part site**	**Reported raw count**	**Count date**	**Weeks post μ lay**[A]	f	p^b	Ψ^s	Ψ^d	Ψ^p	Ψ^o	π	**Acc. category**	**Reported adjusted count**	**Reported adjusted metric**	**Standardised abundance** $(y_{i,t})$	**References**
2017	GC	BP	Pukekura	38	Continuous [B]	0	0.632 [D]	-	NA	-	-	NA	1.000	High	-	-		DOC Coastal Otago 2026
2018	GC	BP	Pukekura	33	Continuous [B]	0	0.394 [D]	-	NA	-	-	NA	1.000	High	-	-		DOC Coastal Otago 2026
2019	GC	BP	Pukekura	51	Continuous [B]	0	0.529 [D]	-	NA	-	-	NA	1.000	High	-	-		DOC Coastal Otago 2026
2020	GC	BP	Pukekura	45	Continuous [B]	0	0.727 [D]	-	NA	-	-	NA	1.000	High	-	-		DOC Coastal Otago 2026
2021	GC	BP	Pukekura	41	Continuous [B]	0	0.732 [D]	-	NA	-	-	NA	1.000	High	-	-		DOC Coastal Otago 2026
2022	GC	BP	Pukekura	36	Continuous [B]	0	0.694 [D]	-	NA	-	-	NA	1.000	High	-	-		DOC Coastal Otago 2026
2023	GC	BP	Pukekura	49	Continuous [B]	0	0.653 [D]	-	NA	-	-	NA	1.000	High	-	-		DOC Coastal Otago 2026
2024	GC	BP	Pukekura	45	Continuous [B]	0	0.733 [D]	-	NA	-	-	NA	1.000	High	-	-		DOC Coastal Otago 2026
2025*	GC	BP	Pukekura	44	Continuous [B]	0	0.864 [D]	-	NA	-	-	NA	1.000	High	-	-		DOC Coastal Otago 2026
2026*	GC	BP	Pukekura	47	Continuous [B]	0	-	-	NA	-	-	NA	1.000	High	-	-		DOC Coastal Otago 2026

[A] Mean lay date before 1968 = 15 Nov, 1978-2000 = 12 Nov, >2000 = 10 Nov and breeding period is considered ~46 weeks (Robertson 1993, DOC unpub.). [B] Breeding site virtually continuously monitored since its establishment and thus no clear count date apply, and instead breeding attempts are assumed to be recorded at or near laying (DOC unpub.). [C] Reported here but not included in any of the models for other breeding sites as Pukekura breeding success is manipulated to achieve maximum *f* through management (Robetson 2001, Richard et al. 2015) [D] Multi-year average estimated by Richard et al. (2015).

Southern Royal Albatross

Supplementary Table 7. Campbell Island counts of Southern Royal Albatross, including count methods, metrics, and error specifications, as well as subsequent standardised data $y_{i,t}$ expressed in BP at the start of the breeding season (for which superscript numbers refer to equations in main text applied). * Indicates counts not (yet) included in the ACAP database.

Year	Method	Counted metric	Part site	Reported raw count	Count date	Weeks post µ lay^{A}	f	p^{b}	Ψ^{s}	Ψ^{d}	Ψ^{p}	Ψ^{o}	π^{B}	Acc. category	Reported adjusted count	Reported adjusted metric	Standardised abundance ($y_{i,t}$)	References
1958	GC & VPC	BP, AOS & BOG	Campbell I.	2,278	7 Jan-19 Feb	4-11	0.743	-	NA	-	-	-	1.000	Medium	-	-		Westerkov 1963, Dilks & Wilson 1979, Dilks & Grindell 1983
1966*^{C}	GC & VPC	BP, AOS & BOG	Campbell I.	3,216^{C}	Nov-Jan	0-8	0.639^{C}	-	NA	-	-	-	1.000	Unknown (Low)	-	-		Guard 1968, Paul & Surrey 1969, Moore et al. 1997a, Waugh et al. 1997
1969	GC & VPC	BP, AOS & BOG	Campbell I.	4,344	8-26 Jan	5-7^{D}	-	0.510	NA	-	-	-	1.000	Medium	-	-		Taylor et al. 1970, Dilks & Wilson 1979, Waugh et al. 1997
1971*	GC & VPC	BP, AOS & BOG	Campbell I., South of fence	1,709	31 Jan-10 Mar	8-14	0.610	-	-	-	-	-	0.361	Unknown (Low)	-	-		Dilks & Wilson 1979, Moore et al. 1997a
1976	GC & VPC	BP, AOS & BOG	Campbell I.	5,336	12 Dec-14 Feb	2-8^{D}	-	-	NA	-	-	-	1.000	Medium	-	-		Dilks & Wilson 1979, Moore et al. 1997a
1977	GC & VPC	BP, AOS & BOG	Campbell I.	4,906	1 Jan-13 Feb	4-8^{D}	-	-	NA	-	-	-	1.000	Medium	-	-		Dilks & Wilson 1979, Moore et al. 1997a
1978	GC & VPC	BP, AOS & BOG	Campbell I.	4,208	23 Dec-11 Feb	3-10	-	-	NA	-	-	-	1.000	Medium	-	-		Dilks & Dunn 1978, Moore et al. 1997a
1980	GC & VPC	BP, AOS & BOG	Campbell I.	4,575	23 Dec-15 Jan	3-11	-	-	NA	-	-	-	1.000	Medium	-	-		Wilson & Elliott 1981, Moore et al. 1997a
1981	GC & VPC	BP, AOS & BOG	Campbell I.	4,493	29 Dec-7 Feb	4-9	-	-	NA	-	-	-	1.000	Medium	-	-		Wilson & Elliott 1981, Moore et al. 1997a
1983	GC & VPC	BP, AOS & BOG	Campbell I.	4,243	14 Jan-11 Feb	6-10	-	-	NA	-	-	-	1.000	Medium	-	-		Dilks & Grindell 1983, Moore & Moffat 1990, Moore et al. 1997a
1988	GC	BP	Col, Moubray	472	3-8 Jan	4-5	0.744	-	-	-	-	NA	0.089	Medium	-	-		Moore & Moffat 1990
1992	GC	BP	Col, Moubray	534	Early Jan	4-6	0.782	-	-	-	-	NA	0.089	Medium	-	-		Moore et al. 1997a
1993	GC	BP	Col, Moubray	587	1-7 Jan	4-5	-	-	-	-	-	NA	0.089	Medium	-	-		Moore et al. 1997a
1994	GC	BP	Col, Moubray	605	Early Jan	4-6	0.815	-	-	-	-	NA	0.089	Low	-	-		Moore et al. 1997a
1995	GC & VPC	BP, AOS & BOG	Campbell I.	6,308	10 Jan-5 Feb	5-9	0.765	0.520^{E}	NA	ψ^{d}_{GC} =0.967, ψ^{d}_{VPC} = 0.867	ψ^{fail} = 0.943-1.000	-	1.000	Medium	6,939-7,302	BP		Moore et al. 1997ab, 2012, ACAP 2009
1996	GC (& VPC)^{F}	BP	Campbell I.	7,787	4 Jan-6 Feb	5-9	0.769	0.520^{E}	NA	ψ^{d}_{GC} = 0.998, ψ^{d}_{VPC} = 0.720-0.770	ψ^{fail} = 0.960-1.000	-	1.000	Medium	8,075-8,414	BP		Moore unpub., Moore et al. 1997a, 2012, ACAP 2012

Year	**Method**	**Counted metric**	**Part site**	**Reported raw count**	**Count date**	**Weeks post μ lay**[A]	***f***	p^b	Ψ^s	Ψ^d	Ψ^p	Ψ^o	π [B]	**Acc. category**	**Reported adjusted count**	**Reported adjusted metric**	**Standardised abundance ($y_{i,t}$)**	**References**
1997	GC	BP	Col, Moubray, Faye, Paris, Honey	2,121	26 Nov-19 Feb	0-11	0.778	0.520[E]	-	0.996	-	NA	0.257	Medium	8,250-8,560	BP		Moore unpub., ACAP 2012, Moore et al. 2012
1998	GC	BP	Col, Moubray, Faye, Paris, Honey	2,247	Jan-Feb	4-12	0.797	0.520[E]	-	0.990	-	NA	0.257	Medium	-	-		Moore unpub., ACAP 2012, Moore et al. 2012
1999	GC	BP	Col, Moubray, Faye, Paris, Honey	2,323	Dec-Jan	0-8	-	-	-	0.992	-	NA	0.257	Medium	-	-		Moore et al. 2012
2005	GC	BP	Col, Moubray, Faye	1,311	1 Jan-20 Feb	4-11	0.705	-	-	0.997	ψ^{fail} = 0.943	NA	0.163	High	8,300-8,700[G]	BP		Moore et al. 2012
2006	GC	BP	Col, Moubray, Faye	1,184	1 Jan-15 Feb	4-11	0.726	-	-	1.000	ψ^{fail} = 0.880	NA	0.163	High	8,300-8,700[G]	BP		Moore et al. 2012
2007	GC	BP	Col, Moubray, Faye, Paris, Honey	1,916	21 Dec-17 Feb	3-11	0.682	-	-	1.000	ψ^{fail} = 0.943	NA	0.257	High	8,300-8,700[G]	BP		Moore et al. 2012
2008	GC	BP	Col, Moubray, Faye, Paris, Honey	1,987	31 Dec-20 Feb	4-11	0.621	-	-	1.000	ψ^{fail} = 0.907	NA	0.257	High	8,300-8,700[G]	BP		Moore et al. 2012
2009	GC	BP	Col, Moubray, Faye, Paris, Honey	2,204	21 Dec-9 Feb	3-10	-	-	-	-	ψ^{fail} = 0.942	NA	0.257	High	8,300-8,700[G]	BP		Moore et al. 2012
2020	GC	BP	Col	104	12-16 Mar	14	-	-	-	-	(ψ^{fail} = 0.759)[G]	NA	0.025	High	137	BP		Mischler 2020
2023	GC	BP	Col	49[I]	16 Feb	11	-	-	-	-	-	NA	0.012[H]	Medium	-	-		Mischler & Wickes 2023
2024	GC	BP	Col, Moubray, Faye, Paris, Honey	1,480	3 Dec-7 Feb	0-9	0.667	-	-	0.987	-	NA	0.257	High	-	-		Mischler et al. 2024, Fischer & Thompson 2025
2025*	GC	BP	Col, Moubray, Faye, Paris, Honey	1,502	5 Dec-4 Feb	0-9	0.655	-	-	1.000	-	NA	0.257	High	-	-		Mischler et al. 2025, Fischer & Thompson 2025
2026*	GC	BP	Col, Moubray, Faye, Paris, Honey	1,564	14 Dec-22-Jan	1-7	-	-	-	-	-	NA	0.257	High	-	-		Mischler et al. in prep.

[A] Mean lay is ~3 December (Waugh et al. 1997). [B] Proportions estimated based on 2004-08 means. [C] Only a multi-year estimate for 1965-1968 available, here labelled 1966 (Moore et al. 1997b). [D] Weeks since laying directly sourced from Dilks & Wilson 1979 instead of calculating based on reported survey dates. [E] Multi-year estimate available only (Moore et al. 2012). [F] Only a very small section of the overall island was counted using VPCs due to recognition of inadequacies in this count method (Moore et al. 1997a) and thus considered negligible here. [G] Multi-year estimate only reported (Moore et al. 2012). [G] Estimate based on previous counts and thus not include here and instead repeated to enable propagation of uncertainty. [H] Only part of part site counted and subsequently survey effort was used to estimate proportion of part site counted (Mischler & Wickes 2023).

Supplementary Table 8. Enderby Island counts of Southern Royal Albatross, including count methods, metrics, and error specifications, as well as subsequent standardised data $y_{i,t}$ expressed in BP at the start of the breeding season (for which superscript numbers refer to equations in main text applied). * Indicates counts not (yet) included in the ACAP database. **Bold** indicates count selected for inclusion in the data processing framework in scenarios where >1 counts were completed in a year.

Year	Method	Counted metric	Part site	Reported raw count	Count date	Weeks post µ lay^A	f	p^b	Ψ^s	Ψ^d	Ψ^p	Ψ^o	π	Acc. category	Reported adjusted count	Reported adjusted metric	Standardised abundance ($y_{i,t}$)	References
1943*^{B}	GC	BP	Enderby I.	8	?^{C}	?^{C}	-	-	NA	-	-	-	1.000	Unknown (Low)	-	-		Bell 1963, French et al. 2020
1954	GC	BP?	Enderby I.	3	12-23 Mar	14-16	-	-	NA	-	-	NA	1.000	Unknown (Low)	-	-		Falla 1954, Dell 1954, Childerhouse et al. 2003
1963*	GC	BP?	Enderby I.	10	?^{C}	?^{C}	-	-	NA	-	-	NA	1.000	Unknown (Low)	-	-		Taylor 1971, Childerhouse et al. 2003
1966*	GC	BP	Enderby I.	15	Jan	4-8	-	-	NA	-	-	-	1.000	Unknown (Low)	-	-		Taylor 1971, Childerhouse et al. 2003
1973	GC	BP	Enderby I.	17	?^{C}	?^{C}	-	-	NA	-	-	NA	1.000	Unknown (Low)	-	-		Russ 1974, Childerhouse et al. 2003, French et al. 2020
1974*	GC	BP	Enderby I.	20	5-20 Dec	1-3	-	-	NA	-	-	-	1.000	Unknown (Low)	-	-		Russ 1974, Childerhouse et al. 2003
1980*	GC	BP	Enderby I.	16	31 Jan	8	-	-	NA	-	-	NA	1.000	Unknown (Low)	-	-		Mitchell & Ensor 1986, French et al. 2020
1981*	GC	BP	Enderby I.	15	?^{C}	?^{C}	-	-	NA	-	-	NA	1.000	Unknown (Low)	-	-		Bell 1982, Childerhouse et al. 2003
1982*	GC	BP	Enderby I.	16	4 Feb	9	-	-	NA	-	-	NA	1.000	Unknown (Low)	-	-		French et al. 2020
1988*	GC	BP	Enderby I.	33	7-15 Feb	9-11	-	-	NA	-	-	NA	1.000	Unknown (Low)	-	-		Taylor 1988, Childerhouse et al. 2003
1993	GC	BP	Enderby I.	32	Late Dec-Feb	3-12	-	-	NA	-	-	NA	1.000	High	-	-		Childerhouse et al. 2003
1994*	GC	BP	Enderby I.	45	Late Dec-Feb	3-12	-	-	NA	-	-	NA	1.000	High	-	-		Childerhouse et al. 2003
1995*	GC	BP	Enderby I.	52	Late Dec-Feb	3-12	-	-	NA	-	-	NA	1.000	High	-	-		Childerhouse et al. 2003
1996*	GC	BP	Enderby I.	55	Late Dec-Feb	3-12	0.740^D	-	NA	-	-	NA	1.000	High	-	-		Childerhouse et al. 2003
1997*	GC	BP	Enderby I.	47	Late Dec-Feb	3-12	0.740^D	-	NA	-	-	NA	1.000	High	-	-		Childerhouse et al. 2003
1998*	GC	BP	Enderby I.	56	Late Dec-Feb	3-12	0.740^D	-	NA	-	-	NA	1.000	High	-	-		Childerhouse et al. 2003
1999*	GC	BP	Enderby I.	42	Late Dec-Feb	3-12	-	-	NA	-	-	NA	1.000	High	-	-		Childerhouse et al. 2003
2000*	GC	BP	Enderby I.	67	Late Dec-Feb	3-12	-	-	NA	-	-	NA	1.000	High	-	-		Childerhouse et al. 2003
2001	GC	BP	Enderby I.	41	Late Dec-Feb	3-12	-	-	NA	-	-	NA	1.000	High	-	-		Childerhouse et al. 2003

Year	Method	Counted metric	Part site	Reported raw count	Count date	Weeks post μ lay[A]	f	p^b	Ψ^s	Ψ^d	Ψ^p	Ψ^o	π	Acc. category	Reported adjusted count	Reported adjusted metric	Standardised abundance ($y_{i,t}$)	References
2002*	GC	BP	Enderby I.	69	Late Dec-Feb	3-12	-	-	NA	-	-	NA	1.000	High	-	-		Childerhouse et al. 2003
2003	GC	BP	Enderby I.	54	1 Dec-20 Mar	0-15	-	-	NA	-	-	NA	1.000	High	-	-		Wilkinson unpub.
2004	GC	BP	Enderby I.	55	? [C]	? [C]	-	-	NA	-	-	NA	1.000	High	-	-		DOC unpub.
2005	GC	BP	Enderby I.	56	? [C]	? [C]	-	-	NA	-	-	NA	1.000	High	-	-		DOC unpub.
2006	GC	BP	Enderby I.	66	? [C]	? [C]	-	-	NA	-	-	NA	1.000	High	-	-		DOC unpub.
2007	GC	BP	Enderby I.	49	3 Dec-26 Feb	0-12	-	-	NA	-	-	NA	1.000	High	-	-		Chilvers 2007
2008	GC	BP	Enderby I.	64	? [C]	? [C]	-	-	NA	-	-	NA	1.000	High	-	-		DOC unpub.
2009	GC	BP	Enderby I.	53	? [C]	? [C]	-	-	NA	-	-	NA	1.000	High	-	-		DOC unpub.
2010	GC	BP	Enderby I.	57	? [C]	? [C]	-	-	NA	-	-	NA	1.000	High	-	-		DOC unpub.
2011	GC	BP	Enderby I.	38	? [C]	? [C]	-	-	NA	-	-	NA	1.000	High	-	-		DOC unpub.
2012	GC	BP	Enderby I.	77	? [C]	? [C]	-	-	NA	-	-	NA	1.000	High	-	-		DOC unpub.
2013	AC^{heli}	BOG	Enderby I.	74	17 Jan	6	-	-	NA	-	-	ψ^{BOG} = 0.761	1.000	High	54	AOS		Baker & Jensz 2013
	GC	BP	Enderby I.	52	17-31 Jan	6-8	-	-	NA	-	-	-	1.000	High	-	-		
2014	AC^{heli}	BOG	Enderby I.	80	20 Jan	7	-	-	NA	-	-	ψ^{BOG} = 0.768	1.000	High	63	AOS		Baker et al. 2014A
	GC	BP	Enderby I.	52	8-15 Feb	10-12	-	-	NA	-	-	NA	1.000	High	-	-		
2015	GC	BP	Enderby I.	60	28 Jan-16 Mar	8-15	-	-	NA	-	-	NA	1.000	High	-	-		DOC unpub.
2016	GC	BP	Enderby I.	44	Late Dec-Feb	3-12	-	-	NA	-	-	NA	1.000	High	-	-		DOC unpub.
2017	AC^{heli}	BOG	Enderby I.	69	21 Jan	7	-	-	NA	-	-	ψ^{BOG} = 0.851	1.000	High	57	AOS		Baker et al. 2020
	GC	BP	Enderby I.	47	26 Jan	7	-	-	NA	-	-	ψ^{BOG} = 0.839, ψ^{ABA} = 0.904	1.000	High	-	-		
2018	GC	BP	Enderby I.	49	Late Dec-Feb	3-12	-	-	NA	-	-	NA	1.000	High	-	-		DOC unpub.
2019	GC	BP	Part of Enderby I.	29	Late Jan–early Feb	7-10	-	-	-	-	-	NA	0.740 [E]	Low	39	BP		DOC unpub.
2023	GC	AOS	Enderby I.	49	27 Dec	3	-	-	NA	-	-	ψ^{ABA} = 0.959	1.000	High	47	BP		DOC unpub.
2024	GC	BP	Enderby I.	63	17-30 Dec	2-4	-	-	NA	-	-	NA	1.000	High	-	-		DOC unpub.
2025*	GC	BP	Enderby I.	56	19-23 Dec	2-3	-	-	NA	-	-	NA	1.000	High	-	-		DOC unpub.
2026*	GC	BP	Enderby I.	70	19 Dec-13 Jan	2-6	-	-	NA	-	-	NA	1.000	High	-	-		DOC unpub.

[A] Mean lay is ~3 December (Waugh et al. 1997. [B] Only a multi-year estimate for 1941-1945 available, here labelled 1943 (French et al. 2020). [C] For unknown count dates prior to the formalisation of the methodology (Childerhouse et al. 2003) the full range of reported count dates (0-16 post mean laying) is used, after the formalisation of the methodology, the prescribed survey time period (3-12 weeks post mean laying) is used. [D] Multi-year estimate only reported (Childerhouse et al. 2003). [E] Incomplete coverage of the island corrected using the mean distribution of nesting area in 2023 and 2024 (P Frost unpub.).

Campbell Albatross

TBC

Buller's Albatross

Table 10. Hautere | Solander counts of Southern Buller's Albatross (ssp. *bulleri*), including updated count methods, metrics, and error specifications, as well as subsequent standardised data for ACAP IG Trends. Superscript numbers refer to numbered equations in main text applied to standardise counts. * Indicates counts absent from the ACAP database.

Year	Method	Counted metric	Part site	Reported raw count	Count date	Weeks post μ lay^{A}	f	p^{b}	Ψ^{s}	Ψ^{d}	Ψ^{p}	Ψ^{o}	π^{B}	Acc. category	Reported adjusted count	Reported adjusted metric	Standardised abundance $(y_{i,t})$	References
1985	GC	C	Little Solander	143	Late July	26	-	-	-	0.960	$\psi^{fail} = 0.696^{C}$	NA	0.067	Unknown (Low)	205	BP		Cooper et al. 1986, Sagar & Stahl 2005
1996	AC^{heli} & GC & VPC	AOS	Great & Little Solander	?^{D}	15-22 Feb	4-5	0.703	-	-	-	-	$\psi^{BOG} = 0.965$	0.633^{E}	Unknown (Low)	2,625	AOS		Sagar et al. 1999, Sagar & Stahl 2005, Stahl unpub.
2002	AC^{heli} & GC & VPC	BOG	Great & Little Solander	?^{D}	20 Feb-8 Mar	4-7	0.676	-	NA	ψ^{d}_{VPC} = 0.900-0950	-	$\psi^{BOG} = 0.800$ (0.760-0.850)	1.000	Unknown (Low)	4,912 (4,628-5,145	AOS		Sagar & Stahl 2005, Stahl unpub.
2014	AC^{heli}	BOG	Little Solander	182	20 Jan	0	-	-	-	-	$\psi^{lay} = 0.420$	$\psi^{BOG} = 0.970$ $\psi^{ABA} = 0.805$	0.067	Medium	305	AOS		Baker & Jensz 2014B
2016	AC^{heli} & GC & VPC	BOG	Great & Little Solander	6,852^{F}	25-29 Feb	5-6	-	-	NA	$\psi^{d}_{VPC} = 0.950$	-	$\psi^{BOG} = 0.813$ $\psi^{ABA} = 0.821^{G}$	1.000	Medium	5,620	AOS		Thompson et al. 2017
2024*	AC^{heli}	BOG	Great & Little Solander	6,761	9 Mar	7	-	-	NA	-	-	$\psi^{BOG} = 0.969$ $\psi^{ABA} = 0.611^{G}$	1.000	Unknown (Medium)	5,377 (5,234-5,523)	AOS		Frost et al. 2025

[A] Mean lay date used 21 Jan based on "late January in Sagar & Warham (1998). [B] Proportion represented by Little Solander based on average proportion across the full site counts (1996, 2002, 2016, and 2024). [C] Based on a multi-year f estimate covering 1996, 1997, 2002, and 2003 (Sagar & Stahl 2005). [D] Adjusted counts of AOS only reported. [E] Some colonies on Big Solander were missed in 1996 (Sagar & Stahl 2005). [F] Raw counts of BOGs only reported for AC^{heli} counts (86%) of the survey, but not for GC or VPC. [G] ψ^{ABA} reported but not incorporated in the reported estimates due to small sample sizes.

Table 11. Tini Heke | Snares counts of Southern Buller's Albatross (ssp. *bulleri*), including updated count methods, metrics, and error specifications, as well as subsequent standardised data for ACAP IG Trends. Superscript numbers refer to numbered equations in main text applied to standardise counts. * Indicates counts absent from the ACAP database.

Year	Method	Counted metric	Part site	Reported raw count	Count date	Weeks post μ lay^{A}	f	p^{b}	Ψ^{s}	Ψ^{d}	Ψ^{p}	Ψ^{o}	π^{B}	Acc. category	Reported adjusted count	Reported adjusted metric	Standardised abundance $(y_{i,t})$	References
1969	GC & VPC	AOS & BP	North-east Is., Alert Stack	4,024	11-19 Feb	3-4	-	-	-	0.950^{C}	0.929^{C}	-	0.931	High	4,448	AOS & BP		Warham & Bennington 1983, Sagar et al. 1999, Sagar & Stahl 2005
1970*	GC	BP	Mbay	90	?^{D}	3-14^{D}	-	-	-	-	✓; ?	NA	0.014	Unknown (high)	-	-		Sagar & Stahl 2005
1971*	GC	BP	Mbay	83	?^{D}	3-14^{D}	-	-	-	-	✓; ?	NA	0.014	Unknown (high)	-	-		Sagar & Stahl 2005
1972*	GC	BP	Mbay	77	?^{D}	3-14^{D}	-	-	-	-	✓; ?	NA	0.014	Unknown (high)	-	-		Sagar & Stahl 2005
1975*	GC	BP	Mbay	84	?^{D}	3-14^{D}	-	-	-	-	✓; ?	NA	0.014	Unknown (high)	-	-		Sagar & Stahl 2005
1977*	GC	BP	Mbay, Rback	102	?^{D}	3-14^{D}	-	-	-	-	✓; ?	NA	0.019	Unknown	-	-		Sagar & Stahl 2005

Year	**Method**	**Counted metric**	**Part site**	**Reported raw count**	**Count date**	**Weeks post μ lay**^{A}	f	p^b	Ψ^s	Ψ^d	Ψ^p	Ψ^o	π^{B}	**Acc. category**	**Reported adjusted count**	**Reported adjusted metric**	**Standardised abundance** $(y_{i,t})$	**References**
														(high)				
1983*	GC	BP	Mbay	85	?^{D}	3-14^{D}	-	-	-	-	✓; ?	NA	0.014	Unknown (high)	-	-		Sagar & Stahl 2005
1992	GC & VPC	AOS & BP	North-east Is., Alert Stack, Broughton I.	7,683	5-17 Mar	6-8	0.758	-	NA	0.953-0.977^{E}	-	-	1.000	High	-	-		Sagar et al. 1994, Sagar & Stahl 2005
1993	GC & VPC	AOS & BP	N Prom, Mbay	1,326	2-9 Mar	6-7	0.756	-	-	0.976-0.988^{E}	✓; ?	-	0.180	High	-	-		Sagar & Stahl 2005
1994	GC & VPC	AOS & BP	N Prom, Mbay	1,350	2-9 Mar	6-7	0.674	-	-	0.976-0.988^{E}	✓; ?	-	0.180	High	-	-		Sagar & Stahl 2005
1995	GC & VPC	AOS & BP	N Prom, Mbay	1,390	2-9 Mar	6-7	0.682	-	-	0.976-0.988^{E}	✓; ?	-	0.180	High	-	-		Sagar & Stahl 2005
1996	GC & VPC	AOS & BP	N Prom, Mbay	1,258	2-9 Mar	6-7	0.686	-	-	0.976-0.988^{E}	✓; ?	-	0.180	High	-	-		Sagar & Stahl 2005
1997	GC & VPC	AOS & BP	North-east Is., Alert Stack, Broughton I.	8,242	2-14 Mar	5-7	0.761	-	NA	0.956-0978^{E}	-	-	1.000	High	-	-		Sagar & Stahl 2005
1998	GC & VPC	AOS & BP	N Prom, Mbay, Rback	1,460	2-9 Mar	6-7	0.671	-	-	0.976-0.988^{E}	✓; ?	-	0.185	High	-	-		Sagar et al. 1999, Sagar & Stahl 2005
1999	GC & VPC	AOS & BP	N Prom, Mbay, Rback	1,539	2-9 Mar	6-7	0.644	-	-	0.976-0.988^{E}	✓; ?	-	0.185	High	-	-		Sagar & Stahl 2005
2000	GC & VPC	AOS & BP	N Prom, Mbay, Rback	1,504	2-9 Mar	6-7	0.712	-	-	0.976-0.988^{E}	✓; ?	-	0.185	High	-	-		Sagar & Stahl 2005
2001	GC & VPC	AOS & BP	N Prom, Mbay, Rback	1,666	2-9 Mar	6-7	0.735	-	-	0.976-0.988^{E}	✓; ?	-	0.185	High	-	-		Sagar & Stahl 2005
2002	GC & VPC	AOS & BP	North-east Is. Alert Stack	8,165	25 Feb-2 Mar	5-6	0.772	-	-	0.959-0980^{E}	✓; ?	-	0.931	High	8,713	AOS & BP		Sagar & Stahl 2005
2003	GC & VPC	AOS & BP	N Prom, Mbay, Rback	1,724	2-9 Mar	6-7	0.863	-	-	0.976-0.988^{E}	✓; ?	-	0.185	High	-	-		Sagar & Stahl 2005
2004	GC & VPC	AOS & BP	N Prom, Mbay, Rback	1,903	2-9 Mar	6-7	0.727	-	-	0.976-0.988^{E}	✓; ?	-	0.185	High	-	-		Sagar & Stahl 2005
2005	GC & VPC	AOS & BP	N Prom, Mbay, Rback	2,001	Feb-Mar	2-10	-	-	-	0.976-0.988^{E}	✓; ?	-	0.180	High	-	-		Sagar unpub.
2006	GC	BP	Mbay, L & U Punui	289	6-9 Apr	11	-	-	-	-	✓; ?	NA	0.027	High	-	-		Sagar & Thompson 2007
2007	GC	BP	Mbay, L & U Punui	269	4-8 Apr	10-11	-	0.580-0.840^{F}	-	-	✓; ?	NA	0.027	High	-	-		Sagar & Thompson 2007, Francis & Sagar 2012
2008	GC	BP	Mbay, L & U Punui	271	Late Mar-late Apr	8-14	-	-	-	-	✓; ?	NA	0.027	High	-	-		Sagar et al. 2009
2009	GC	BP	Mbay, L & U Punui, Rback	249	6-12 Apr	11-12	-	-	-	-	✓; ?	NA	0.032	High	-	-		Sagar et al. 2009
2010	GC	BP	Mbay, L & U Punui, Rback	227	8-15 Apr	11-12	-	-	-	-	✓; ?	NA	0.032	High	-	-		Sagar et al. 2010

Year	Method	Counted metric	Part site	Reported raw count	Count date	Weeks post μ lay[A]	f	p^b	Ψ^s	Ψ^d	Ψ^p	Ψ^o	π[B]	Acc. category	Reported adjusted count	Reported adjusted metric	Standardised abundance ($y_{i,t}$)	References
2011	GC	BP	Mbay, L & U Punui, Rback	255	Late Mar-late Apr	8-14	-	-	-	-	✓; ?	NA	0.032	High	-	-		Sagar et al. 2012
2012	GC	BP	Mbay, L & U Punui	285	21-27 Apr	13-14	-	-	-	-	✓; ?	NA	0.027	High	-	-		Sagar et al. 2012
2013	GC	BP	Mbay, L & U Punui	241	11-29 Apr	11-14	-	-	-	-	✓; ?	NA	0.027	High	-	-		Sagar 2014
2014	GC & VPC	AOS & BP	North-east Is., Alert Stack, Broughton Is.	8,704	22 Feb – 4 Mar	5-6	-	0.566-0.833[F]	NA	0.962-0.981[E]	-	-	1.000	High	-	-		Sagar 2014, Fu & Sagar 2016
2015	GC	BP	Mbay, L & U Punui	253	23-29 Mar	9-10	-	-	-	-	✓; ?	NA	0.027	High	-	-		Sagar 2015
2016*	GC	BP	Mbay, L & U Punui	241	Late Mar-late Apr	8-14	-	-	-	-	✓; ?	NA	0.027	High	-	-		Sagar et al. 2017
2017	GC	BP	Mbay, L & U Punui	281	3-6 Apr	10-11	-	-	-	-	✓; ?	NA	0.027	High	-	-		Sagar et al. 2017
2019	GC & VPC	AOS & BP	N Prom, W Coast, Rback, E Coast, Broughton I.	3,668	2-10 Mar	6-7	-	-	-	0.976-0.988[E]	-	-	0.469	High	-	-		Thompson & Sagar 2020, Sagar unpub.
2020	GC & VPC	AOS[X] & BP	S Coast[G], Mbay, L & U Punui,	2,668	11-17 Mar	7-8	-	-	-	0.973-0.986[E]	-	-	0.228	High	-	-		Thompson & Sagar 2020, Sagar unpub.
2022	GC	BP	Mbay, L & U Punui	303	27 Mar-10 Apr	9-11	-	-	-	-	✓; ?	NA	0.027	High	-	-		Thompson & Sagar 2022
2023	GC	BP	Mbay, L & U Punui, Rback	269	25 Mar-7 Apr	9-11	-	-	-	-	✓; ?	NA	0.032	High	-	-		Thompson & Sagar 2023
2024	GC	BP	Mbay, L & U Punui	185	7-16 Apr	11-12	-	-	-	-	✓; ?	NA	0.027	High	-	-		Sagar et al. 2024
2025*	GC	BP	Mbay, L & U Punui	227	10-15 Apr	11-12	-	-	-	-	✓; ?	NA	0.027	High	-	-		Sagar et al. 2025

[A] Mean lay date used 21 Jan based on "late January in Sagar & Warham (1998). [B] Proportions based on means calculated using the 1992, 1997, and 2014 full islands counts (Sagar & Stahl 2005, Sagar 2014). [C] Ψ^d and Ψ^p reported but not used to correct counts (Warham & Barrington 1983). [D] Dates unknown so full range during which counts have been conducted used. [E] Ψ^d calculated using the estimate Ψ^d_{VPC} = 0.900-0.950, the assumption that Ψ^d_{GC} = 1.000, and the proportions of each method per count as reported in Thompson & Sagar (2020) with additional insights (P Sagar unpub). [F] Multi-year estimates only reported, and ranges are based on separate estimates of p^b for breeders and non-breeders (Francis & Sagar 2012, Fu & Sagar 2016). [G] Only 72% of the South Coast section was counted (Thompson & Sagar 2020; Sagar unpub.).

Table 12. Motuhara | Fortyfours counts of Northern Buller's Albatross (ssp. *platei*), including updated count methods, metrics, and error specifications, as well as subsequent standardised data for ACAP IG Trends. Superscript numbers refer to numbered equations in main text applied to standardise counts. * Indicates counts absent from the ACAP database.

Year	Method	Counted metric	Part site	Reported raw count	Count date	Weeks post μ lay[A]	f	p^b	Ψ^s	Ψ^d	Ψ^p	Ψ^o	π^B	Acc. category	Reported adjusted count	Reported adjusted metric	Standardised abundance $(y_{i,t})$	References
1972*	GC	BP?	Motuhara	16,000	January	9-13	-	-	-	-	✓; ?	✓; ?	0.985	Unknown (Low)	-	-		Robertson 1991
2008	GC	NS	Motuhara	15,238	13-19 Nov	2-3	-	-	-	-	-	$\psi^{occ} = 0.886$ $\psi^{ABA} = 0.714$	0.985	High[C]	-	-		Scofield et al. 2008, Thompson 2019
2009	GC	NS	Motuhara	14,674	9-11 Nov	1-2	-	-	-	-	$\psi^{fail} = 0.915$	$\psi^{occ} = 0.942$ $\psi^{ABA} = 0.691$	0.985	High[C]	-	-		Fraser et al. 2009A, Thompson 2019
2010	GC	NS	Motuhara	14,185	1-8 Dec	4-5	-	-	-	-	$\psi^{fail} = 0.957$	$\psi^{occ} = 0.917$ $\psi^{ABA} = 0.857$	0.985	High[C]	-	-		Fraser et al. 2010A, Thompson 2019
2017	**AC^{fw}**	BOG	Motuhara + stack 1-4	15,702	23 Nov	3	-	-	NA	-	-	$\psi^{BOG}{}_{AC} = 0.983$, $\psi^{BOG}{}_{GC} = 0.895$, $\psi^{ABA}{}_{GC} = 0.983$	1.000	Medium	13,771 (13,537-14,006)	BP		Baker et al. 2017
	GC	NS	Motuhara + stack 1-4	17,682	5-7 Dec	5	-	-	NA	-	$\psi^{fail} = 0.791$	-[E]	1.000	Medium	13,047	BP		Bell et al. 2017, Baker et al. 2017
2018*	AC^{fw}	BOG	Quadrats 1-5	304	4 Dec	5	-	-	-	-	-[E]	$\psi^{BOG} = 0.974$	0.019	Unknown (High)	296	AOS		Frost 2019
2021*	GC	NS	Quadrats 1-10	647	19-31 Jan	11-13	0.510[F]	-	-	-	-[E]	($\psi^{ABA} = 0.674$[G])	0.038	Unknown (High)	489	BP		Bell 2021, Frost et al. 2021C
2022[H]	GC	NS	Quadrats 1-10	709	29 Jan	13	-	-	-	-	-[E]	-[E]	0.038	High	510	BP		Bell 2022, Frost 2022
2023	GC	NS	Motuhara	15,809	10-12 Dec	6	-	-	-	-	$\psi^{fail} = 0.721$	-[E]	0.985	High	-	-		Bell 2023
2024	GC	NS	Quadrats 1-10	611	18 Feb	16	0.573[I]	-	-	-	$\psi^{fail} = 0.573$	-[E]	0.038	High	322	BP		Bell 2024
2026*	GC & VPC[J]	NS	Motuhara	14,224	28 Nov-1 Dec	4	-	-	-	-	$\psi^{fail} = 0.673$	$\psi^{occ} = 1.000$[K] $\psi^{ABA} = 1.000$[K]	0.985	High	-	-		Bell 2026

[A] Mean lay date used 31 Oct (ACAP 2012). [B] Proportions of quadrats based on means calculated using the 2008, 2009, 2017, 2023, and 2026 full island counts, with additional insights on the offshore stacks from the 2017 count (Fraser et al, 2009A, 2010A, Bell et al. 2017, Bell 2023, 2026). [C] Recorded as *High* accuracy in the ACAP database but here adjusted to Medium due to the lack of *in situ* marking during counts (M Bell pers. comm.) and the fact that the quadrat counts for the same years have also been recorded as *Medium*. [E] Without clear separation between empty and failed nests and explicit statement if statement whether empty nests were occupied or not, assessing Ψ^o is not possible. [F] f estimated using a composite of field-based (Bell 2021) and camera-based (Frost et al. 2021) estimates. [G] Camera-based assessment of ψ^{ABA} but not used in the estimates of BP (Frost et al. 2021). [H] AC^{fw} and AC^{UAV} of quadrats completed as well on 1 Feb but not included here as these counts were completed for comparative purposes, rather than count purposes and thus GC are considered here. [I] f estimated at hatching (Bell 2024). [J] 1.6% of the overall count conducted using VPCs so 1.6% of the reported BP are AOS, but given this small proportion, the overall count is treated as BP (Bell 2026). [K] estimated in the index plots and multiple instances recorded of two eggs being present in nests, indicating that more breeding pairs than nest sites may be present, but due to the nature of probabilities, here treated as 1.000 (Bell 2026).

Table 13. Rangitutahi | Sisters counts of Northern Buller's Albatross (ssp. *platei*), including updated count methods, metrics, and error specifications, as well as subsequent standardised data for ACAP IG Trends. Superscript numbers refer to numbered equations in main text applied to standardise counts. * Indicates counts absent from the ACAP database.

Year	**Method**	**Counted metric**	**Part site**	**Reported raw count**	**Count date**	**Weeks post µ lay^{A}**	***f***	p^{b}	Ψ^{s}	Ψ^{d}	Ψ^{p}	Ψ^{o}	π^{B}	**Acc. category**	**Reported adjusted count**	**Reported adjusted metric**	**Standardised abundance $(y_{i,t})$**	**References**
1972	GC	BP?	Little & Big Sister	2,000	January	9-13	-	-	NA	-	✓; ?	✓; ?	1.000	Low	-	-		Robertson 1991
1996*	GC	BP	Little Sister	565	Late Nov	3-4		-	-	-	-	NA	0.219	Unknown (Low)	-	-		Bell et al. 2018
1997*	GC	BP	Little Sister	636	Late Nov	3-4		-	-	-	-	NA	0.219	Unknown (Low)	-	-		Bell et al. 2018
2005	GC	NS?	Little Sister	200	27 Jan	13		-	-	-	-	-	0.219	Unknown (Low)	-	-		Scofield unpub.
2017	AC^{fw}	BOG	Little & Big Sister	2,692	4 Dec	5	-	-	NA	-	-	$\psi^{BOG} = 0.978$	1.000	Medium	2,366 (2,269-2,464)	BP^{C}		Baker et al. 2017
2018	GC	NS	Little & Big Sister	3,158	30 Nov-4 Dec	4-5	-	-	NA	0.999-0.996	$\psi^{fail} = 0.637-0.752$	$\psi^{occ} \cdot \psi^{ABA} = 0.965$	1.000	Medium	3,158	BP		Bell et al. 2018

^{A} Mean lay date used 31 Oct (ACAP 2012).B Proportions calculated using all counts during which both islands were counted (1972, 2017, and 2018). ^{C} ψ^{ABA} estimated on Motuhara during GCs (Baker et al.2017).

White-capped Albatross

Supplementary Table 14. Disappointment Island counts of White-capped Albatross, including count methods, metrics, and error specifications, as well as subsequent standardised data $y_{i,t}$ expressed in BP at the start of the breeding season (for which superscript numbers refer to equations in main text applied). * Indicates counts not (yet) included in the ACAP database.

Year	Method	Counted metric	Part site	Reported raw count	Count date	Weeks post μ lay[A]	f	p^b	Ψ^s	Ψ^d	Ψ^p	Ψ^o	π^B	Acc. category	Reported adjusted count	Reported adjusted metric	Standardised abundance data ($y_{i,t}$)	References
1973*	GC, VPC, VBC	BOG	Disappointment I.	60,000	15 Feb	13	-	-	NA	0.771 (0.504-0.952)[C]	-	-	1.000	Unknown (Low)	-	-		Robertson 1975, Walker et al. 2020
1985	AC^{heli}	BOG	Disappointment I.	71,799	18 Feb	14	-	-	NA	-	-	$\psi^{BOG} \cdot \psi^{ABA} =$ 0.670-720[D]	1.000	High	50,259	BP		Walker et al. 2021
1993	AC^{heli}	BOG	Castaway Bay	3,740	22 Jan	10	-	-	-	-		$\psi^{BOG} \cdot \psi^{ABA} =$ 0.670-720[D]	0.047[B]	High	-	BP		Walker et al. 2021
2002	AC^{heli}	BOG	Disappointment I.	125,476	21 Feb	14	-	-	NA	-		$\psi^{BOG} \cdot \psi^{ABA} =$ 0.670-720[D]	1.000	Medium	87,833	BP		Walker et al. 2021
2007	AC^{heli}	BOG	Disappointment I.	110,649	16 Dec	4	0.622[E]	-	NA	-	-	$\psi^{BOG} = 0.990$[F]	1.000	High	109,543[G]	AOS		Thompson & Sagar 2008a, Francis 2012, Walker et al. 2021, Baker et al. 2023
2008	AC^{heli}	BOG	Disappointment I.	86,080	13 Dec	4	-	-	NA	-	-	$\psi^{BOG} = 0.995$ ($\psi^{ABA} = 0.810$)[H]	1.000	High	85,650[G]	AOS		Walker et al 2020, Baker et al. 2023
2009	AC^{heli}	BOG	Disappointment I.	91,694	14 Dec	4	-	-	NA	-	-	$\psi^{BOG} = 0.982$ ($\psi^{ABA} = 0.935$)[H]	1.000	High	90,044[G]	AOS		Walker et al 2021, Baker et al. 2023
2010	AC^{heli}	BOG	Disappointment I.	72,275	3 Dec	3	-	-	NA	-	-	$\psi^{BOG} = 0.986$	1.000	High	71,263[G]	AOS		Walker et al 2021, Baker et al. 2023
2011	AC^{heli}	BOG	Disappointment I.	72,635	15 Dec	4	-	-	NA	-	-	$\psi^{BOG} = 0.987$	1.000	High	71,691[G]	AOS		Walker et al 2021, Baker et al. 2023
2012	AC^{heli}	BOG	Disappointment I.	93,752	11 Jan	8	-	-	NA	-	-	$\psi^{BOG} = 0.929$	1.000	High	87,096[G]	AOS		Walker et al 2021, Baker et al. 2023
2013	AC^{heli}	BOG	Disappointment I.	111,312	14 Jan	9	-	-	NA	-	-	$\psi^{BOG} = 0.866$	1.000	High	96,396[G]	AOS		Walker et al 2021, Baker et al. 2023
2014	AC^{heli}	BOG	Disappointment I.	89,552	20 Jan	9	-	-	NA	-	-	$\psi^{BOG} = 0.777$	1.000	High	69,582[G]	AOS		Walker et al 2021, Baker et al. 2023
2015	AC^{heli}	BOG	Disappointment I.	96,864	14 Jan	9	-	-	NA	-	-	$\psi^{BOG} = 0.942$[I] ($\psi^{ABA} = 0.849$-0.851)[H]	1.000	High	91,246[G]	AOS		Walker et al 2021, Baker et al. 2023
2016	AC^{heli}	BOG	Disappointment I.	91,554	13 Jan	8	-	-	NA	-	-	$\psi^{BOG} = 0.901$[I] ($\psi^{ABA} = 0.775$)[H]	1.000	High	82,490[G]	AOS		Walker et al 2021, Baker et al. 2023
2017	AC^{heli}	BOG	Disappointment I.	85,510	19 Jan	9	-	-	NA	-	-	$\psi^{BOG} = 0.900$	1.000	High	76,959[G]	AOS		Walker et al 2021, Baker et al. 2023
2018*	AC^{heli}	BOG	Disappointment I.	95,688	5 Jan	7	0.263[E]	-	NA	-	-	$\psi^{BOG} = 0.892$[J]	1.000	High	85,354[G]	AOS		Rexer-Huber et al. 2019, Walker et al. 2021, Baker et al. 2023, Frost 2026

[A] Mean lay is ~15 Nov. [B] Based on multi-year average proportions calculated from Walker et al. 2021. [C] Estimated through expert elicitation following modified Delphi protocol. [D] Ψ^o based on 1993 ground counts (Walker et al. 2021). [E] Additional f estimates exist for 2006 (0.526; Thompson & Sagar 2008a), 2022 (0.467; Elliott et al. 2023, Frost 2026), and 2023 (0.727, based on chicks only; Frost 2026). [F] ψ^{BOG} based on multi-year average (Baker et al. 2023). [G] Adjusted counts from Baker et al. 2023, additional adjusted counts available in Walker et al. 2021. [H] ψ^{ABA} estimates available in Francis 2012, Parker et al. 2017, and Walker et al. 2021, but not included in Baker et al. 2023, of which the 2008 estimate originates from SW Cape. [I] Additional ψ^{BOG} estimates available in Parker et al. 2017 and Walker et al. 2021 but not included in Baker et al. 2023. [J] Further Ψ^{o} estimates available in Parker et al. 2022 and Elliott et al. 2023.

Supplementary Table 15. South-west Cape (Maukahuka | Auckland Island) counts of White-capped Albatross, including count methods, metrics, and error specifications, as well as subsequent standardised data $y_{i,t}$ expressed in BP at the start of the breeding season (for which superscript numbers refer to equations in main text applied). * Indicates counts not (yet) included in the ACAP database.

Year	Method	Counted metric	Part site	Reported raw count	Count date	Weeks post µ lay[A]	f	p^{b}	Ψ^{s}	Ψ^{d}	Ψ^{p}	Ψ^{o}	π[B]	Acc. category	Reported adjusted count	Reported adjusted metric	Standardised abundance data ($y_{i,t}$)	References
1973*	GC, VPC. VBC	BOG	SW Cape	4,000	Early Feb	12-13	-	-	NA	0.712 (0.397-0.939[B]	-	-	1.000	Unknown (Low)	-	-		Robertson 1975, Walker et al. 2020
1993	AC^{heli}	BOG	SW Cape	3,000	Late Jan – Feb	10-14	-	-	NA	-			1.000	Low	-	-		Robertson & Gales 1998
2007	AC^{heli}	BOG	SW Cape	6,548	16 Dec	4	-	0.680 (0.580; 0.810)	NA	-	-	(ψ^{BOG} = 0.990)[D]	1.000	High	6,483	AOS		Francis 2012, Walker et al. 2021, Baker et al. 2023
2008	AC^{heli}	BOG	SW Cape	4,786	13 Dec	4	0.627	0.680 (0.580; 0.810)	NA	-	-	E_{aba} = 0.810 (ψ^{BOG} = 0.995)[D]	1.000	High	4,762	AOS		Francis 2012, Thompson & Sagar 2008b, Baker et al. 2023
2009	AC^{heli}	BOG	SW Cape	5,264	14 Dec	4	-	0.680 (0.580; 0.810)	NA	-	-	(ψ^{BOG} = 0.982)[D]	1.000	High	5,169	AOS		Francis 2012, Baker et al. 2023
2010	AC^{heli}	BOG	SW Cape	4,161	3 Dec	3	-	0.680 (0.580; 0.810)	NA	-	-	(ψ^{BOG} = 0.986)[D]	1.000	High	4,103	AOS		Francis 2012, Baker et al. 2023
2011	AC^{heli}	BOG	SW Cape	4,370	15 Dec	4	-	-	NA	-	-	(ψ^{BOG} = 0.987)[D]	1.000	High	4,313	AOS		Baker et al. 2023
2012	AC^{heli}	BOG	SW Cape	5,846	11 Jan	8	-	-	NA	-	-	(ψ^{BOG} = 0.929)[D]	1.000	High	5,431	AOS		Baker et al. 2023
2013	AC^{heli}	BOG	SW Cape	6,571	14 Jan	9	-	-	NA	-	-	(ψ^{BOG} = 0.866)[D]	1.000	High	5,690	AOS		Baker et al. 2023
2014	AC^{heli}	BOG	SW Cape	5,542	20 Jan	9	-	-	NA	-	-	(ψ^{BOG} = 0.777)[D]	1.000	High	4,306	AOS		Baker et al. 2023
2015	AC^{heli}	BOG	SW Cape	4,741	14 Jan	9	-	-	NA	-	-	(ψ^{BOG} = 0.942)[D]	1.000	High	4,466	AOS		Baker et al. 2023
2016	AC^{heli}	BOG	SW Cape	4,893	13 Jan	8	-	-	NA	-	-	(ψ^{BOG} = 0.901)[D]	1.000	High	4,409	AOS		Baker et al. 2023
2017	AC^{heli}	BOG	SW Cape	5,436	19 Jan	9	-	-	NA	-	-	(ψ^{BOG} = 0.900)[D]	1.000	High	4,892	AOS		Baker et al. 2023
2018*	AC^{heli}	BOG	SW Cape	5,834	5 Jan	7	-	-	NA	-	-	(ψ^{BOG} = 0.892)[D]	1.000	High	5,204	AOS		Baker et al. 2023
2021*	AC^{UAV}	BOG	East gulch	764	22 Mar	18	-	-	NA	-	-	ψ^{BOG} = 0.955	0.220[B]	High	730	AOS		R. Sagar unpub.

[A] Mean lay is ~15 Nov. [B] Proportion of the east gulch estimated using 2016-2018 AC^{heli} (Baker unpub.). [C] Estimated through expert elicitation following modified Delphi protocol. [D] ψ^{BOG} based on estimates from Disappointment Island.

Supplementary Table 16. Adams Island counts of White-capped Albatross, including count methods, metrics, and error specifications, as well as subsequent standardised data $y_{i,t}$ expressed in BP at the start of the breeding season (for which superscript numbers refer to equations in main text applied). * Indicates counts not (yet) included in the ACAP database.

Year	**Method**	**Counted metric**	**Part site**	**Reported raw count**	**Count date**	**Weeks post μ lay**^{A}	f	p^b	Ψ^s	Ψ^d	Ψ^p	Ψ^o	π	**Acc. category**	**Reported adjusted count**	**Reported adjusted metric**	**Standardised abundance data** $(y_{i,t})$	**References**
1973*	? ^{B}	BOG	Logan Point	200	Early Feb	12-13	-	-	NA	?	-	-	1.000	Unknown (Low)	-	-		Robertson 1975, Walker et al. 2020
1993	AC^{heli}	BOG	Logan Point	100	Late Jan – Feb	10-14	-	-	NA	-	-	-	1.000	Medium	-	-		Robertson & Gales 1998
2008	AC^{heli}	BOG	Logan Point	79	13 Dec	4	-	-	NA	-	-	$(E_{loaf} = 0.995)^C$	1.000	High	79	AOS		Baker et al. 2023
2009	AC^{heli}	BOG	Logan Point	131	14 Dec	4	-	-	NA	-	-	$(E_{loaf} = 0.982)^C$	1.000	High	129	AOS		Baker et al. 2023
2010	AC^{heli}	BOG	Logan Point	132	3 Dec	3	-	-	NA	-	-	$(E_{loaf} = 0.986)^C$	1.000	High	130	AOS		Baker et al. 2023
2011	AC^{heli}	BOG	Logan Point	117	15 Dec	4	-	-	NA	-	-	$(E_{loaf} = 0.987)^C$	1.000	High	115	AOS		Baker et al. 2023
2012	AC^{heli}	BOG	Logan Point	178	11 Jan	8	-	-	NA	-	-	$(E_{loaf} = 0.929)^C$	1.000	High	165	AOS		Baker et al. 2023
2013	AC^{heli}	BOG	Logan Point	215	14 Jan	9	-	-	NA	-	-	$(E_{loaf} = 0.866)^C$	1.000	High	186	AOS		Baker et al. 2023
2014	AC^{heli}	BOG	Logan Point	184	20 Jan	9	-	-	NA	-	-	$(E_{loaf} = 0.777)^C$	1.000	High	143	AOS		Baker et al. 2023
2015	AC^{heli}	BOG	Logan Point	193	14 Jan	9	-	-	NA	-	-	$(E_{loaf} = 0.942)^C$	1.000	High	182	AOS		Baker et al. 2023
2016	AC^{heli}	BOG	Logan Point	176	13 Jan	8	-	-	NA	-	-	$(E_{loaf} = 0.901)^C$	1.000	High	159	AOS		Baker et al. 2023
2017	AC^{heli}	BOG	Logan Point	171	19 Jan	9	-	-	NA	-	-	$(E_{loaf} = 0.900)^C$	1.000	High	154	AOS		Baker et al. 2023
2018*	AC^{heli}	BOG	Logan Point	194	5 Jan	7	-	-	NA	-	-	$(E_{loaf} = 0.892)^C$	1.000	High	173	AOS		Baker et al. 2023

^{A} Mean lay is ~15 Nov. ^{B} Reported as a potential VBC in Roberston (1975) but VPCs may also have been conducted. Unclear if Logan Point can be seen during a VBC. ^{C} ψ^{BOG} based on estimates from Disappointment Island.

Chatham Albatross

Supplementary Table 17. Te Tara Koi Koia | Pyramid counts of Chatham Albatross, including count methods, metrics, and error specifications, as well as subsequent standardised data $y_{i,t}$ expressed in BP at the start of the breeding season (for which superscript numbers refer to equations in main text applied). * Indicates counts not (yet) included in the ACAP database.

Year	Method	Counted metric	Part site	Reported raw count	Count date	Weeks post μ lay[A]	f	p^b	Ψ^s	Ψ^d	Ψ^p	Ψ^o	π^B	Acc. category	Reported adjusted count	Reported adjusted metric	Standardised abundance data ($y_{i,t}$)	References
1965*	VBC	AOS	Te Tara Koi Koia | Pyramid	2,000	17 Oct	6	-	-	NA	0.636 (0.349-0.878)[B]	-	-	1.000	Unknown (low)	2,500	BP		Dawson 1973
1973*	AC^{fw}	AOS	Te Tara Koi Koia | Pyramid	3,965	28 Nov	11	-	-	NA	0.864 (0.693-0.971)[B]	-	-	1.000	Unknown (low)	4,200	BP		Robertson et al. 1991
2000	GC & VPC[C]	NS	Te Tara Koi Koia | Pyramid	5,333	25 Nov-5 Dec	11-13	-	-	NA	-	-	(ψ^{occ} = 0.590)[D]	1.000	High	-	-		Robertson et al. 2003
2001	GC & VPC[C]	NS	Te Tara Koi Koia | Pyramid	5,326	6-10 Dec	13-14	-	-	NA	-	-	(ψ^{occ} = 0.650)[D]	1.000	High	-	-		Robertson et al. 2003
2002	GC & VPC[C]	NS	Te Tara Koi Koia | Pyramid	5,304	30 Nov-9 Dec	12-13	-	-	NA	-	-	(ψ^{occ} = 0.710)[D]	1.000	High	-	-		Robertson et al. 2003
2004*	GC & VPC[C]	NS	Te Tara Koi Koia | Pyramid	5,341	3-12 Dec	12-14	-	-	NA	-	-	(ψ^{occ} = 0.610)[D]	1.000	Unknown (High)	-	-		Robertson et al. 2004
2006	GC & VPC[E]	NS	Te Tara Koi Koia | Pyramid	5,206	28 Jan-13 Feb	20-23	-	-	NA	-	(Ψ^{fail} = 0.931)	(ψ^{occ} = 0.396)	1.000	High	-	-		Fraser et al. unpub.
2007	GC & VPC[E]	NS	Te Tara Koi Koia | Pyramid	5,412	22-28 Jan	19-20	-	-	NA	-	(Ψ^{fail} = 0.987)	(ψ^{occ} = 0.448)	1.000	High	-	-		Fraser et al. unpub.
2008	GC & VPC[E]	NS	Te Tara Koi Koia | Pyramid	5,247	19-29 Nov	10-12	-	-	NA	-	(Ψ^{fail} = 0.960)	(ψ^{occ} = 0.753)	1.000	High	-	-		Scofield et al. 2008
2009	GC & VPC[E]	NS	Te Tara Koi Koia | Pyramid	5,407	22 Nov-7 Dec	11-13	-	-	NA	-	(Ψ^{fail} = 0.967)	(ψ^{occ} = 0.702)	1.000	High	-	-		Fraser et al. 2009B
2010	GC & VPC[E]	NS	Te Tara Koi Koia | Pyramid	5,194	9-12 Dec	13-14	-	-	NA	-	(Ψ^{fail} = 0.970)	(ψ^{occ} = 0.505)	1.000	High	-	-		Fraser et al. 2010B
2011	GC & VPC[E]	NS	Te Tara Koi Koia | Pyramid	5,245	24-30 Nov	11-12	-	-	NA	-	(Ψ^{fail} = 0.973)	(ψ^{occ} = 0.702)	1.000	High	-	-		Fraser et al. 2011
2017	GC & VPC[F]	NS	Te Tara Koi Koia | Pyramid	5,296	9-13 Nov	9-10	-	-	NA	-	(Ψ^{fail} = 0.744)	(ψ^{occ} = 0.966)	1.000	High	-	-		M Bell et al. 2017A
2026*	GC & VPC[G]	NS	Te Tara Koi Koia | Pyramid	5,227	8-13 Nov	9-10	-	-	NA	-	(Ψ^{fail} = 0.666)	-	1.000	High	-	-		Bell 2026

[A] Mean lay is ~7 Sep based on M Bell et al. 2017A. [B] Estimated through a modified Delphi expert elicitation, in which the original value was included as one of the estimated values. [C] 0.04% of the population was counted through VPC (Roberson et al. 2003). [D] Empty nests and failed nests not differentiable. [E] 11.0-11.9% of the population was counted through VPC. [F] 14.0% of the population was counted through VPC. [G] 8.9% of the population was counted through VPC.

Salvin's Albatross

Supplementary Table 18. Moutere Hauriri | Bounty Island counts of Salvin's Albatross, including count methods, metrics, and error specifications, as well as subsequent standardised data $y_{i,t}$ expressed in BP at the start of the breeding season (for which superscript numbers refer to equations in main text applied). * Indicates counts not (yet) included in the ACAP database.

Year	Method	Counted metric	Part site	Reported raw count	Count date	Weeks post μ lay^{A}	f	p^{b}	Ψ^{s}	Ψ^{d}	Ψ^{p}	Ψ^{o}	π^{B}	Acc. category	Reported adjusted count	Reported adjusted metric	Standardised abundance data ($y_{i,t}$)	References
1979	GC^{C}	BP	Moutere Hauriri	76,352	7-20 Nov	9-11		-	NA	-	-	NA	1.000	Low	49,250^{C}	BP		Robertson & van Tets 1982, Amey & Sagar 2013, Thompson 2025
1998	GC	BP	Proclamation I.	3,065	12-16 Nov	10		-	-	>0.990	-	$(\psi^{BOG}\cdot\psi^{ABA}=0.668^{D};\ \psi^{ABA}=0.627^{D})$	0.103	High	-	-		Clark 1998, Amey & Sagar 2013, Thompson 2025
2005	GC	BP	Proclamation I.	2,634	16-23 Nov	10-11		-	-	>0.990	-	$(\psi^{BOG}\cdot\psi^{ABA}=0.579^{D})$	0.103	High	-	-		Amey & Sagar 2013, Thompson 2025
2011	AC^{fw}	BOG	Moutere Hauriri	42,832	12 Oct	5		-	NA	-	-	-^{E}	1.000	High	31,786^{G}	BP		Baker et al. 2014B, Thompson 2025
2012	GC	BP	Proclamation I.	2,211	14 Nov	10		-	-	>0.990	-	$(\psi^{BOG}\cdot\psi^{ABA}=0.622^{D};\ \psi^{ABA}=0.790^{D})$	0.103	Low	-	-		Amey & Sagar 2013, Thompson 2025
2014	AC^{fw}	BOG	Moutere Hauriri	53,893	23 Oct	7		-	NA	-	-	$\psi^{BOG}=0.826^{D}$ $\psi^{ABA}=0.899^{D}$	1.000	High	39,995	BP		Baker et al. 2014B, Thompson 2025
2019	AC^{fw}	BOG	Moutere Hauriri	60,419	25 Oct	7	0.350 (0.230-0.480)^{F}	-	NA	-	-	$\psi^{BOG}=0.716^{G}$ $\psi^{BOG}=0.648^{D}$ $\psi^{ABA}=0.724^{D}$	1.000	High	26,955 (26,626-27,283)	BP		Sagar et al. 2018, Baker & Jensz 2019, Thompson 2025
2020	AC^{UAV}	BOG	Proclamation, Spider, Tunnel Is.	12,684	28 Oct	8	0.350 (0.230-0.480)^{F}	-		-	-	-^{H}	0.272	High	5,962 (5,200-6,595)	BP		Parker & Rexer-Huber 2020, Thompson 2025
2023*	AC^{UAV}	BOG	Moutere Hauriri	69,709	10-15 Nov	5-6	0.350 (0.230-0.480)^{F}	-	NA	-	-	-	1.000	High	-	-		Mattern 2022, Thompson 2025, Mattern
2024*	AC^{UAV}	C	Depot, Tunnel Ruatara, Proclamation, Spider Is.	11,546	31 Jan	21	0.350 (0.230-0.480)^{F}	-	-	-	-	NA	0.777	Medium	-	-		Mattern 2024a, Thompson 2025
2025*	AC^{UAV}	BOG	Moutere Hauriri	50,789	13 Oct	6	0.350 (0.230-0.480)^{F}	-	NA	-	-	$\psi^{BOG}=0.746^{D}$ $\psi^{ABA}=0.903^{D}$	1.000	High	-	-		Mattern 2024b, Thompson 2025

[A] Mean lay date used 4 Sep (Thompson 2025). [B] Proportions based on averages across all full breeding site counts (Thompson 2025). [C] Robertson & van Tets 1979 extrapolation proved challenging and required additional spatial re-analyses (see main text and Thompson 2025). [D] Estimated during ground transects. [E] Ψ^{o} estimate from 2014 used rather than concurrent data.[F] Only Multi-year mean estimates could be derived through daily-survival modelling of remote camera data (Thompson 2025). [G] Estimated from close-up photographs. [H] Ψ^{o} estimate from Sager et al. (2018) used rather than concurrent data.

Supplementary Table 19. Western Chain islets counts of Salvin's Albatross, including count methods, metrics, and error specifications, as well as subsequent standardised data $y_{i,t}$ expressed in BP at the start of the breeding season (for which superscript numbers refer to equations in main text applied). * Indicates counts not (yet) included in the ACAP database. **Bold** indicates count selected for inclusion in the data processing framework in scenarios where >1 counts were completed in a year.

Year	Method	Counted metric	Part site	Reported raw count	Count date	Weeks post μ lay[A]	f	p^b	Ψ^s	Ψ^d	Ψ^p	Ψ^o	π[B]	Acc. category	Reported adjusted count	Reported adjusted metric	Standardised abundance data ($y_{i,t}$)	References
1977	GC	BP	Rima	122	21 Nov	11	-	-	-	-	-	NA	0.333	High	-	-		Sagar 1977, Thompson 2025
1984	GC	C	Toru, Rima	585	Feb	21-25	-	-	NA	-	-	NA	1.000	High	-	-		Miskelly 1984, Thompson 2025
1996	**GC**	BP	Toru	1,021	5 Oct	4	-	-	NA	-	-	NA	0.667	High	-	-		Clark 1996, Thompson 2025
	GC	BP	Rima	189	8 Nov	9	-	-	NA	-	-	NA	0.333	High				Clark 1996, Thompson 2025
2009	GC	BP	Toru, Rima	1,195	6-7, 16 Oct	5-6	-	0.927 (0.662-0.997)[C]	NA	-	-	NA	1.000	High	-	-		Sagar et al. 2011, Thompson 2025
2010	GC	BP	Toru, Rima	1,116	30 Sep, 2 Oct	4	-	0.927 (0.662-0.997)[C]	NA	-	-	NA	1.000	High	-	-		Sagar et al. 2011, Thompson 2025
2011	GC	BP	Toru	780	28-29 Sep	3-4	-	0.927 (0.662-0.997)[C]	-	-	-	NA	0.667	High	-	-		Sagar et al. 2011, Thompson 2025
2015	AC^{heli}	BOG	Toru, Rima	2,307			-	-	NA	-	-	-	1.000	High	1,486	AOS		Baker et al. 2015
	GC	BP	Toru, Rima	1,125	17 Oct	6	-	-	NA	-	-	ψ^{BOG} = 0.667[D] ψ^{ABA} =0.877[D]	1.000	High	-	-		Sagar et al. 2014, Thompson 2025
2026*	GC	BP	Toru	415	1 Nov	8	-	-	-	-	-	NA	0.667	High	-	-		Rexer-Huber et al. in prep.

[A] Mean lay date used 4 Sep (Thompson 2025). [B] Proportion based on average proportion across the full site counts. [C] p^b re-estimated by Thompson (2025). [D] Estimated during ground transects.

Westland Petrel

Supplementary Table 20. Punakaiki counts of Westland Petrel, including count methods, metrics, and error specifications, as well as subsequent standardised data $y_{i,t}$ expressed in BP at the start of the breeding season (for which superscript numbers refer to equations in main text applied). * Indicates counts not (yet) included in the ACAP database.

Year	Method	Counted metric	Part site	Reported raw count	Count date	Weeks post µ lay[A]	f	p^b	Ψ^s	Ψ^d	Ψ^p	Ψ^o	π[B]	Acc. category	Reported adjusted count	Reported adjusted metric	Standardised abundance data ($y_{i,t}$)	References
1974*	GC	AOS	Punakaiki	818	Apr-Jul	0-10	0.390 (0.200; 0.630)[C]	-	-	-	-	✓; ?	0.810	Unknown (Low)	818	AOS		Best & Owen 1976, Freeman & Wilson 2002, Wood & Otley 2013
1975*	GC	AOS	Punakaiki	2,000 (1,000; 5,000)	?[D]	?[D]	0.390 (0.200; 0.630)[C]	-	-	-	-	✓; ?	1.000	Unknown (Low)	2,000 (1,000; 5,000)	AOS		Bartle 1985, Marchant & Higgins 1990, Freeman & Wilson 2002, Wood & Otley 2013
2003 (2002-05; 2010)[E]	GC	NS	Punakaiki	12,843	Oct-Dec	19-26	0.620 (0.542; 0.698)[F]	-	-	-	-	$\psi^{occ} \cdot \psi^{ABA}$ = 0.303 (0.264; 0.342)	0.977	Medium[G]	2,954-5,137	BP		Waugh et al. 2006, Wood & Otley 2013, Waugh & Wilson 2017
2007*	GC	AOS	Punakaiki	5,476 (4,511; 6,443)	15 May - 15 Jun	0-3	-	0.460[G]	-	-	-	ψ^{occ} = 0.435 (0.405; 0.465)[H] (ψ^{ABA} = 0.837)[I]	0.536	Medium[G]	2,385 (2,220; 2,549)	AOS		Waugh & Wilson 2017, Baker et al. 2020
2008*	GC	AOS	Punakaiki	4,718 (3,587; 5847)	17-28 Mar; 12-23 May	0	-	0.460[G]	-	-	-	ψ^{occ} = 0.299 (0.257; 0.341)	0.596	Medium[G]	1,403 (1,085; 1,718)	AOS		Waugh & Wilson 2017, Baker et al. 2020
2011	GC	AOS	Punakaiki	4,334 (3,327; 5346)	17 Jan–3 Feb; 23 May-2 Jun	0-1	-	0.460[G]	-	-	-	ψ^{occ} = 0.546 (0.505; 0.587)	0.693	Medium[G]	2,289 (1,975; 2,628)	AOS		Waugh & Wilson 2017, Baker et al. 2020
2019	GC	BP	Punakaiki	31,306	Jul-Aug	8-14	0.685 (0.469; 0.901)[J]	0.768 (0.670; 0.844)[K]	-	-	-	ψ^{occ} = 0.385 (0.340; 0.500), ψ^{ABA} = 0.480 (0.337; 0.623)[L]	0.886	High[G]	6,223 (5,478; 6,968)	BP		Waugh et al. 2015, 2020

[A] Mean lay is ~23 May.
[B] Proportion calculated based on sub-colonies counted and their population size using information from Wood & Otley (2013) and Waugh et al. (2020).
[C] 1976-1996 average.
[D] Dates of count unknown, and thus date range of the 1974 count was used instead.
[E] Count effort distributed across 2002-2005, with some additional effort as 2010, but information provided in Wood & Otley (2013) is insufficient to disentangle individual survey years and as such 2003 is used here as a midpoint for Wood & Otley (2013).
[F] 1995-2003 average.
[G] Downscaled one accuracy category in the modelling framework to acknowledge the lack of accounting for Ψ^d.
[H] 2007-2014 average.
[I] 2008-2011 average.
[J] ψ^{ABA} considered negligible in Baker et al. (2020).
[K] 2010-2019 average.
[L] 1995-2012 average.
[M] 2015-2019 average.

Black Petrel

Supplementary Table 21. Aotea counts of Black Petrel, including count methods, metrics, and error specifications, as well as subsequent standardised data $y_{i,t}$ expressed in BP at the start of the breeding season (for which superscript numbers refer to equations in main text applied). * Indicates counts not (yet) included in the ACAP database.

Year	Method	Counted metric	Part site	Reported raw count	Count date	Weeks post μ lay^{A}	f	p^{b}	Ψ^{s}	Ψ^{d}	Ψ^{p}	Ψ^{o}	π^{B}	Acc. category	Reported adjusted count	Reported adjusted metric	Standardised abundance data ($y_{i,t}$)	References
1977^{C}	GC	BP	Aotea	500-1,000^{C}	-^{C}	-^{C}	-	-	NA	-	-	-	0.333-0.531^{D}	Unknown (Low)	-	-		Imber 1987
1996	GC	NS	3 census grids	43	?	5-12	0.869	0.719 (0.690-0.742)^{E}	-	-	-	$\psi^{occ} \cdot \psi^{ABA} = 0.535$	0.008^{F}	High	23	BP	NA^{F}	Bell & Sim 2000A, Bell et al. 2025
1997	GC	NS	3 census grids	53	?	5-12	0.686	0.719 (0.690-0.742)^{E}	-	-	-	$\psi^{occ} \cdot \psi^{ABA} = 0.660$	0.008^{F}	High	35	BP	NA^{F}	Bell & Sim 2000A, Bell et al. 2025
1998	GC	NS	3 census grids	52	21 Jan-24 Feb	6-11	0.772	0.719 (0.690-0.742)^{E}	-	-	-	$\psi^{occ} \cdot \psi^{ABA} = 0.673$	0.008^{F}	High	35	BP	NA^{F}	Bell & Sim 2000A
1999	GC	NS	6 census grids	95	25 Jan-28 Feb	7-12	0.708	0.719 (0.690-0.742)^{E}	-	-	-	$\psi^{occ} \cdot \psi^{ABA} = 0.684$	0.015	High	65	BP		Bell & Sim 2000B
2000	GC	NS	9 census grids	118	17 Jan-23 Feb	6-11	0.671	0.719 (0.690-0.742)^{E}	-	-	-	$\psi^{occ} \cdot \psi^{ABA} = 0.695$	0.023	High	82	BP		Bell & Sim 2000C
2001	GC	NS	9 census grids	121	15 Jan-16 Feb	6-10	0.816	0.719 (0.690-0.742)^{E}	-	-	-	$\psi^{occ} \cdot \psi^{ABA} = 0.628$	0.023	High	76	BP		Bell & Sim 2002
2002	GC	NS	9 census grids	124	25 Nov-5 Dec	0	0.763	0.719 (0.690-0.742)^{E}	-	-	-	$\psi^{occ} \cdot \psi^{ABA} = 0.645$	0.023	High	80	BP		Bell & Sim 2003A
2003	GC	NS	9 census grids	130	4-18 Dec	0-2	0.600	0.719 (0.690-0.742)^{E}	-	-	-	$\psi^{occ} \cdot \psi^{ABA} = 0.577$	0.023	High	75	BP		Bell & Sim 2003B
2004	GC	NS	9 census grids	132	1-12 Dec	0-1	0.793	0.719 (0.690-0.742)^{E}	-	-	-	$\psi^{occ} \cdot \psi^{ABA} = 0.583$	0.023	High	77	BP		Bell et al. 2005
2005	GC	NS	Mt Hobson study area (35 ha)	192	?	0-12^{G}	0.750	0.719 (0.690-0.742)^{E}	✓	✓	-	$\psi^{occ} \cdot \psi^{ABA} = 0.575$	0.531	Low^{G}	1,126 (814-1,438)	BP		Bell et al. 2007, 2018
2006	GC	NS	9 census grids	147	1-11 Dec	0-1	0.706	0.719 (0.690-0.742)^{E}	-	-	-	$\psi^{occ} \cdot \psi^{ABA} = 0.626$	0.023	High	92	BP		Bell et al. 2009
2007	GC	NS	9 census grids	148	?	0-2^{G}	0.812	0.719 (0.690-0.742)^{E}	-	-	-	$\psi^{occ} \cdot \psi^{ABA} = 0.649$	0.023	High	96	BP		Bell et al. 2025
2008	GC	NS	9 census grids	149	11-18 Dec	1-2	0.710	0.719 (0.690-0.742)^{E}	-	-	-	$\psi^{occ} \cdot \psi^{ABA} = 0.624$	0.531	High	93	BP		Bell et al. 2011
2009	GC	NS	9 census grids	151	?	0-2^{G}	0.698	0.719 (0.690-0.742)^{E}	-	-	-	$\psi^{occ} \cdot \psi^{ABA} = 0.636$	0.023	High	96	BP		Bell et al. 2025
2010	GC	NS	Mt Hobson study area (35 ha)	298	?	0-12^{G}	0.732	0.719 (0.690-0.742)^{E}	✓	✓	-	$\psi^{occ} \cdot \psi^{ABA} = 0.566$	0.531	Low^{G}	1,010 (698-1,322)	BP		Bell et al. 2010, 2018
2011	GC	NS	9 census grids	153	?	0-2^{G}	0.605	0.719 (0.690-0.742)^{E}	-	-	-	$\psi^{occ} \cdot \psi^{ABA} = 0.627$	0.023	High	96	BP		Bell et al. 2025
2012	GC	NS	9 census grids	154	?	0-2^{G}	0.820	0.719 (0.690-0.742)^{E}	-	-	-	$\psi^{occ} \cdot \psi^{ABA} = 0.578$	0.023	High	89	BP		Bell et al. 2025

Year	Method	Counted metric	Part site	Reported raw count	Count date	Weeks post μ lay[A]	f	p^b	Ψ^s	Ψ^d	Ψ^p	Ψ^o	π[B]	Acc. category	Reported adjusted count	Reported adjusted metric	Standardised abundance data ($y_{i,t}$)	References
2013	GC	NS	Mt Hobson study area (35 ha)	510	?	0-12[G]	0.809	0.719 (0.690-0.742) [E]	✓	✓	-	$\psi^{occ} \cdot \psi^{ABA}$ = 0.567	0.531	Medium [I]	2,587 (1,026-4,148)	BP		Bell et al. 2013, 2018
2014	GC	NS	9 census grids	158	6-13 Dec	0-2	0.685	0.719 (0.690-0.742) [E]	-	-	-	$\psi^{occ} \cdot \psi^{ABA}$ = 0.601	0.023	High	95	BP		Bell et al. 2014
2015	GC	NS	9 census grids	163	6-15 Dec	0-2	0.683	0.719 (0.690-0.742) [E]	-	-	-	$\psi^{occ} \cdot \psi^{ABA}$ = 0.620	0.023	High	101	BP		Bell et al. 2015
2016	GC	NS	9 census grids	166	2-14 Dec	0-2	0.626	0.719 (0.690-0.742) [E]	-	-	-	$\psi^{occ} \cdot \psi^{ABA}$ = 0.645	0.023	High	107	BP		Bell et al. 2016B
2017*	GC	NS	Mt Hobson study area (35 ha)	298	Feb	8-12	0.670	-	✓	✓	-	$\psi^{occ} \cdot \psi^{ABA}$ = 0.582	0.531	Medium [I]	2,427 (1,713-3,140)	BP		Bell et al. 2018
2018	GC	NS	9 census grids	177	12 Jan-9 Feb	5-9	0.636	-	-	-	-	$\psi^{occ} \cdot \psi^{ABA}$ = 0.542	0.023	High	96	BP		Bell et al. 2020
2019	GC	NS	9 census grids [J]	177	7 Jan-13 Feb	4-10	0.696	-	-	-	-	$\psi^{occ} \cdot \psi^{ABA}$ = 0.576	0.023	High	102	BP		Bell et al. 2020
2020	GC	NS	High quality and core medium quality habitat [J]	293	Jan-Feb	4-12	0.715	--	✓	✓	-	$\psi^{occ} \cdot \psi^{ABA}$ = 0.452-0.462	0.900-1.000 [K]	Medium	4,336 (3,770-4,993) [L]	BP		Bell et al. 2020, 2021, 2022A
2021	GC	NS	9 census grids [J]	192	8 Jan-1 Feb	5-8	0.724	-	-	-	-	$\psi^{occ} \cdot \psi^{ABA}$ = 0.604	0.023	High	116	BP		Bell et al. 2022A
2022	GC	NS	9 census grids	195	19 Dec-8 Feb	2-9	0.774	-	-	-	-	$\psi^{occ} \cdot \psi^{ABA}$ = 0.656	0.023	High	128	BP		Bell et al. 2022B
2023	GC	NS	9 census grids	196	28 Nov-5 Dec	0	0.563	-	-	-	-	$\psi^{occ} \cdot \psi^{ABA}$ = 0.607	0.023	High	119	BP		Bell et al. 2023
2024*	GC	NS	9 census grids	198	4-14 Dec, 7-28 Feb	0-12	0.703	-	-	-	-	$\psi^{occ} \cdot \psi^{ABA}$ = 0.611	0.023	High	121	BP		Bell et al. 2024
2025*	GC	NS	9 census grids	200	13-18 Dec, 22 Jan-4 Feb	1-8	0.650	-	-	-	-	$\psi^{occ} \cdot \psi^{ABA}$ = 0.600	0.023	High	120	BP		Bell et al. 2025

[A] Mean lay ~ 7 Dec (Imber 1987, Bell et al. 2025). [B] Proportions for census grids were calculated using the 2019-2021 population estimate as a baseline, assuming that this estimate itself represented ~0.95 of the total population (Bell et al. 2022A), proportions of the 35 ha Mt Hobson study area was calculated using a retrospective estimate of the overall Aotea population based on the proportion of the census grids and the most accurate estimate of the study area (Bell et al. 2018). [C] Based on fieldwork during 1972-1975, 1977, 1979, and 1982-1983 across breeding seasons, and as such, the median year, 1977, was chosen here as the representative year (Imber 1987). [D] estimated using expert judgement (Bell pers. comm.). [E] Only multi-year (1996-2016) estimates available (Zhang et al. 2020). [F] Due to the large uncertainties associated with counts that represent <1% of the breeding site, these counts are not included in the trend modelling (see main text). [G] Initially recorded *High* in the ACAP database but based on comparison with other counts and re-analyses (e.g., Bell et al. 2018), best re-categorised as *Low*. [H] When count date is not available, we assumed that census block counts would take place during Dec and that transect counts took place during Dec-Feb (Zhang et al. 2020). [I] Initially recorded *High* in the ACAP database but based on comparison with other counts and re-analyses (e.g., Bell et al. 2018), best re-categorised as *Medium*. [J] Across 2019-2021, the most robust population estimate was generated (Bell et al. 2022A), which we here assign to the middle year (2020), while we use the census grids and extrapolation to estimate the overall population in the other two years (2019 and 2021), rather than disaggregating the robust overall estimate. [K] Bell et al. (2022A) could not estimate the population in low quality habitat and suggested that <500 BP would remain in the hinterland and as such, we built additional uncertainty into the estimate through π. [L] The truncated, high and core-medium quality habitat estimate is used here (Bell et al. 2022A).

Supplementary Table 22. Hauturu counts of Black Petrel, including count methods, metrics, and error specifications, as well as subsequent standardised data $y_{i,t}$ expressed in BP at the start of the breeding season (for which superscript numbers refer to equations in main text applied). * Indicates counts not (yet) included in the ACAP database.

Year	Method	Counted metric	Part site	Reported raw count	Count date	Weeks post μ lay[A]	f	p^b	Ψ^s	Ψ^d	Ψ^p	Ψ^o	π	Acc. category	Reported adjusted count	Reported adjusted metric	Standardised abundance data ($y_{i,t}$)	References
1977[B] *	GC	BP	Hauturu	50-100	-[B]	-[B]	-	-	NA	-	?	-	0.250-0.500[C]	Unknown (Low)	-	-		Imber 1987
2016	GC	BP	Hauturu	170	28 Apr-19 May	20-23	0.852	-	NA	-	-	$\psi^{occ} \cdot \psi^{ABA} = 0.559$	1.000	Medium	620	BP		Bell et al. 2016A

[A] Mean lay ~ 7 Dec (Imber 1987, Bell et al. 2025). [B] This estimate is based on fieldwork during 1972-1975, 1977, 1979, and 1982-1983 across breeding seasons, and as such, the median year, 1977, was chosen here as the representative year (Imber 1987). [C] estimated using expert judgement (Bell pers. comm.).

References

ACAP. 2009. ACAP Species assessment: Southern Royal Albatross *Diomedea epomophora*. Agreement of Albatrosses and Petrels http://www.acap.aq.

Amey J & Sagar P. 2013. Salvin's albatross population trend at the Bounty Islands 1997-2011; Salvin's albatross population at the Bounty Islands. Conservation Services Programme, Department of Conservation, Wellington, New Zealand.

Baker GB & Jensz K. 2013. Southern royal albatross at Enderby Island – analysis of aerial photographs 2013. Conservation Services Programme, Department of Conservation, Wellington, New Zealand.

Baker GB & Jensz K. 2014A. Gibson's Albatross at Disappointment Island - Analysis of aerial photographs. Conservation Services Programme, Department of Conservation, Wellington, New Zealand.

Baker GB & Jensz K. 2014B. Buller's albatross aerial survey at the Solander Islands 2014. Conservation Services Programme, Department of Conservation, Wellington, New Zealand.

Baker GB & Jensz K. 2019. Aerial survey of Salvin's albatross at the Bounty Islands. Conservation Services Programme, Department of Conservation, Wellington, New Zealand.

Baker GB, Elliott GP, French RK, Jensz K, Muller CG & Walker KJ. 2020. Development of aerial monitoring techniques to estimate population size of great albatrosses (Diomedea spp.). Notornis 67: 321-331.

Baker GB, Hedley G, Cunningham R & Waugh SM. 2020. Estimated population size of the Westland Petrel, 2007-2011. Fisheries New Zealand, Wellington, New Zealand.

Baker GB, Jensz K & Hamer D. 2014A. Southern royal albatross at Enderby Island – analysis of aerial photographs 2014. Conservation Services Programme, Department of Conservation, Wellington, New Zealand.

Baker GB, Jensz K & Sagar P. 2014B. 2013 Aerial survey of Salvin's albatross at the Bounty Islands. Conservation Services Programme, Department of Conservation, Wellington, New Zealand.

Baker GB, Jensz K & Sagar P. 2015. 2014 Aerial survey of Salvin's albatross at The Snares, Western Chain. Conservation Services Programme, Department of Conservation, Wellington, New Zealand.

Baker GB, Jensz K, Bell M, Fretwell PT & Phillips RA. 2017. Seabird population research, Chatham Islands; 2016/17 aerial photographic survey. Conservation Services Programme, Department of Conservation, Wellington, New Zealand.

Baker GB, Jenzs K, Cunningham R, Robertson G, Sagar P, Thompson TR & Double MC. 2023. Population assessment of White-capped Albatross *Thalassarche steadi* in New Zealand. Emu – Austral Ornithology 123: 60-70.

Bartle JA 1985. Report on research on Westland black petrels 1969-83 with an outline of future objectives and a brief summary of management problems. Unpublished report of the National Museum of New Zealand, Wellington, New Zealand.

Bell BD. 1963. Classified notes on birds on and about Auckland Islands. Unpublished report.

Bell BD. 1982: Auckland Island expedition 21.2.82–24.3.82. Wildlife Service, Wellington, New Zealand.

Bell E, Lamb S, Ray S. 2022A. Population trends and breeding population size of black petrels (*Procellaria parkinsoni*) – 2020/2021 operational report. New Zealand Aquatic Environment and Biodiversity Report No. 280. Fisheries New Zealand, Wellington, New Zealand.

Bell E, Ray S & Crowe P. 2021. Population trends, at-sea distribution, and breeding population size of black petrels (*Procellaria parkinsoni*) on Great Barrier Island/Aotea: 2019/2020 operational report. New Zealand Aquatic Environment and Biodiversity Report No. 270. Fisheries New Zealand, Wellington, New Zealand.

Bell E, Ray S, Crowe P, Butler D, Bell M & McArthur N. 2020. Population trends, at-sea distribution, and breeding population size of black petrels (*Procellaria parkinsoni*) on Great Barrier Island/Aotea: 2018/2019 operational report. New Zealand Aquatic Environment and Biodiversity Report No. 246. Fisheries New Zealand, Wellington, New Zealand.

Bell EA & Sim JL. 2000A. Survey and monitoring of black petrels on Great Barrier Island, 1997/98. Conservation Services Programme, Department of Conservation, Wellington, New Zealand.

Bell EA & Sim JL. 2000B. Survey and monitoring of black petrels on Great Barrier Island, 1998/99. Conservation Services Programme, Department of Conservation, Wellington, New Zealand.

Bell EA & Sim JL. 2000C. Survey and monitoring of black petrels on Great Barrier Island, 1999/2000. Conservation Services Programme, Department of Conservation, Wellington, New Zealand.

Bell EA & Sim JL. 2002. Survey and monitoring of black petrels on Great Barrier Island, 2000/01. DOC Science Internal Series 48. Department of Conservation, Wellington, New Zealand.

Bell EA & Sim JL. 2003A. Survey and monitoring of black petrels on Great Barrier Island, 2001/02. DOC Science Internal Series 134. Department of Conservation, Wellington, New Zealand.

Bell EA & Sim JL. 2003B. Survey and monitoring of black petrels on Great Barrier Island, 2002/03. DOC Science Internal Series 135. Department of Conservation, Wellington, New Zealand.

Bell EA & Sim JL. 2005. Survey and monitoring of black petrels on Great Barrier Island, 2003/04. DOC Science Internal Series 213. Department of Conservation, Wellington, New Zealand.

Bell EA, Burgin D, Sim J, Dunleavy K, Fleishman A & Scofield RP. 2018. Population trends, breeding distribution and habitat use of black petrels (Procellaria parkinsoni) - 2016/2017 operational report. New Zealand Aquatic Environment and Biodiversity Report No. 198. Fisheries New Zealand, Wellington, New Zealand.

Bell EA, Lamb S & Maclean C. 2023. Key demographic parameters and population trends of tākoketai/black petrels (*Procellaria parkinsoni*) on Aotea/Great Barrier Island: 2022/23. Conservation Services Programme, Department of Conservation, Wellington, New Zealand.

Bell EA, Lamb S & Ray S. 2024. Key demographic parameters and population trends of tākoketai/black petrels (*Procellaria parkinsoni*) on Aotea/Great Barrier Island: 2023/24. Conservation Services Programme, Department of Conservation, Wellington, New Zealand.

Bell EA, Lamb S & Ray S. 2025. Key demographic parameters and population trends of tākoketai/black petrels (*Procellaria parkinsoni*) on Aotea/Great Barrier Island: 2024/25. Conservation Services Programme, Department of Conservation, Wellington, New Zealand.

Bell EA, Mischler C, Sim JL & Scofield P. 2015. Population parameters of the black petrels (*Procellaria parkinsoni*) on Great Barrier Island (Aotea Island), 2014/15. Conservation Services Programme, Department of Conservation, Wellington, New Zealand.

Bell EA, Mischler C, Sim JL, Scofield P, Francis C, Edward A & Landers T. 2014. At-sea distribution and population parameters of the black petrels (Procellaria parkinsoni) on Great Barrier Island (Aotea Island), 2013/14. Conservation Services Programme, Department of Conservation, Wellington, New Zealand.

Bell EA, Mischler CP, MacArthur N & Sim JL. 2016A. Black petrel (*Procellaria parkinsoni*) population study on Hauturu-o-Toi/Little Barrier Island, 2015/16. Conservation Services Programme, Department of Conservation, Wellington, New Zealand.

Bell EA, Mischler CP, McArthur N, Sim JL, Scofield RP. 2016B. Black petrel (*Procellaria parkinsoni*) population study on Aotea/Great Barrier Island, 2015/16. Conservation Services Programme, Department of Conservation, Wellington, New Zealand.

Bell EA, Sim J, Scofield P, Francis C & Landers T. 2013. At-sea distribution and population parameters of the black petrels (Procellaria parkinsoni) on Great Barrier Island (Aotea Island), 2012/13. Conservation Services Programme, Department of Conservation, Wellington, New Zealand.

Bell EA, Sim JL & Scofield P. 2007. Demographic parameters of the black petrel (Procellaria parkinsoni). DOC Science Internal Series 273. Department of Conservation, Wellington, New Zealand.

Bell EA, Sim JL & Scofield P. 2009. Population parameters and distribution of the black petrel (Procellaria parkinsoni), 2005/06. DOC Science Internal Series 307. Department of Conservation, Wellington, New Zealand.

Bell EA, Sim JL & Scofield P. 2011. Population parameters and distribution of the black petrel (Procellaria parkinsoni), 2007/08. Conservation Services Programme, Department of Conservation, Wellington, New Zealand.

Bell EA, Sim JL, Scofield P & Francis C. 2010. Population parameters o the black petrels (Procellaria parkinsoni) on Great Barrier Island (Aotea Island), 2009/2010. Conservation Services Programme, Department of Conservation, Wellington, New Zealand.

Bell EA, Welch M & Lamb S. 2022B. Key demographic parameters and population trends of tākoketai/black petrels (*Procellaria parkinsoni*) on Aotea/Great Barrier Island: 2021/22. Conservation Services Programme, Department of Conservation, Wellington, New Zealand.

Bell M, Bell D & Boyle D. 2017A. Chatham Island Mollymawk research on Te Tara Koi Koia: November 2016. Conservation Services Programme, Department of Conservation, Wellington, New Zealand.

Bell M, Bell D, Boyle D & Tuanui-Chisholm H. 2017B. Motuhara seabird research: December 2016. Conservation Services Programme, Department of Conservation, Wellington, New Zealand.

Bell M, Bell D, Boyle D & Tuanui-Chisholm. 2018. Rangitatahi Seabird Research: December 2017. Conservation Services Programme, Department of Conservation, Wellington, New Zealand.

Bell M. 2021. Motuhara seabird research: field trip report January 2021. Conservation Services Programme, Department of Conservation, Wellington, New Zealand.

Bell M. 2022. Motuhara seabird research: field trip report January 2021. Conservation Services Programme, Department of Conservation, Wellington, New Zealand.

Bell M. 2023. Motuhara seabird research: field trip report Dec 2022. Conservation Services Programme, Department of Conservation, Wellington, New Zealand.

Bell M. 2024. Motuhara seabird research: field trip report January 2024. Conservation Services Programme, Department of Conservation, Wellington, New Zealand.

Bell M. 2026. Seabird research – Chatham Islands. Conservation Services Programme, Department of Conservation, Wellington, New Zealand.

Best HA & Owen KL 1976. Distribution of breeding sites of the Westland black petrel (*Procellaria westlandica*). Notornis 23: 233 242.

Childerhouse S, Robertson C, Hockly & Gibbs N. 2003. Royal albatross (*Diomedea epomophora*) on Enderby Island, Auckland Islands. DOC Science Internal Series 144.Department of Conservation, Wellington, New Zealand.

Chilvers L. 2007. NZ sea lion research trip, Auckland Islands, November 28th 2006 to February 27th 2007. Conservation Services Programme, Department of Conservation, Wellington, New Zealand.

Clark G, Andrea B, & Amey J. 1998. The "Totorore" Expedition to the Bounty Islands, New Zealand. October 1997 to January 1998 Report. New Zealand Maritime Museum, Auckland, New Zealand.

Clark G. 1996. The “Totorore” expedition to the Snares Western Chain; September 1995 to December 1995. New Zealand Maritime Museum, Auckland, New Zealand.

Cooper WJ, Miskelly CM, Morrison K & Peacock RJ. 1986. Birds of the Solander Islands. Notornis 33: 77-89.

Dawson EW. 1973. Albatross populations at the Chatham islands. Notornis 20: 210–230.

Dell RK 1954. Field notes. ANARE to Enderby Island (Auckland Islands) – Holmlea. MS Papers 2366 297.

Department of Conservation Coastal Otago District Operations. 2026. Pukekura annual report. 2024/25 Season. Department of Conservation, Dunedin, New Zealand.

Dilks PJ & Grindell JM. 1983. Visit to Campbell Island by P.J. Dilks and J.M. Grindell, 11 January - 23 February 1983. Unpublished file report, Ecology Division.

Dilks PJ. 1979: Observations on the food of feral cats on Campbell Island. New Zealand Journal of Ecology 2: 64–66.

Elliot G, Walker K, Rexer-Huber K, Tinnemans J, Long J, Sagar S, Osborne J & Parker G. 2024. Gibson’s wandering albatross: demography, satellite tracking and census. Conservation Services Programme, Department of Conservation, Wellington, New Zealand.

Elliott G & Walker K. 2013. Gibson’s wandering albatross research Adams Island 2013. Conservation Services Programme, Department of Conservation, Wellington, New Zealand.

Elliott G & Walker K. 2014. Gibson’s wandering albatross at Adams Island – population study. Conservation Services Programme, Department of Conservation, Wellington, New Zealand.

Elliott G & Walker K. 2017. Antipodean wandering albatross census and population study 2017. Conservation Services Programme, Department of Conservation, Wellington, New Zealand.

Elliott G & Walker K. 2018. Antipodean wandering albatross census and population study 2018. Conservation Services Programme, Department of Conservation, Wellington, New Zealand.

Elliott G & Walker K. 2019. Antipodean wandering albatross census and population study 2019. Conservation Services Programme, Department of Conservation, Wellington, New Zealand.

Elliott G & Walker K. 2020. Antipodean wandering albatross satellite tracking and population study: Antipodes Island 2020. Conservation Services Programme, Department of Conservation, Wellington, New Zealand.

Elliott G, Waker K, Rexer-Huber K, Tinnemans J, McDonald A, Rawlence T & Parker G. 2025. Gibson’s wandering albatross: drone-based population estimate, demography and at-sea distribution. Conservation Services Programme, Department of Conservation, Wellington, New Zealand.

Elliott G, Walker K, Parker G & Rexer-Huber K. 2016. Gibson’s wandering albatross census and population study 2015/16. Conservation Services Programme, Department of Conservation, Wellington, New Zealand.

Elliott G, Walker K, Rexer-Huber K & Parker G. 2023. White-capped Albatross population study: February 2023. Conservation Services Programme, Department of Conservation, Wellington, New Zealand.

Falla RA. 1954: Field notes. Auckland Islands trip, March 12–23 1954. MS Papers 2366–297.

Fischer JH & Thompson T. 2025. Monitoring ecotourism impacts on Toroa | Southern Royal Albatross breeding success. Department of Conservation, Wellington.

Francis RIC & Sagar PM. 2012. Modelling the effect of fishing on southern Buller’s albatross using a 60-year dataset. New Zealand Journal of Zoology 39: 3-17.

Francis RICC. 2012. Fisheries risks to the population viability of White-capped Albatross *Thalassarche steadi*. Fisheries New Zealand, Wellington, New Zealand.

Fraser M, Henderson G, Robertson CJR & Scofield P. 2011. Population dynamics of the Chatham Albatross at the Pyramid, 19 November – 2 December 2010. Ministry of Fisheries, Wellington, New Zealand.

Fraser M, Bell M, Scofield P & Robertson CJR. 2009A. Population assessment of Northern Buller’s Albatross and Northern Giant Petrel at the Fortyfours. Ministry of Fisheries, Wellington, New Zealand.

Fraser M, Hunt S, Scofield P & Robertson CJR. 2009B. Population dynamics of the Chatham Albatross at the Pyramid, 9 November – 7 December 2008. Ministry of Fisheries, Wellington, New Zealand.

Fraser M, Cameron N, Scofield P & Robertson CJR. 2010A. Population assessment of Northern Buller’s Albatross and Northern Giant Petrels at the Fortyfours, Chatham Islands, 1-8 December 2009. Ministry of Fisheries, Wellington, New Zealand.

Fraser M, Palmer D, Deppe L, Scofield P & Robertson CJR. 2010B. Population dynamics of the Chatham Albatross at the Pyramid, 20 November – 14 December 2009. Ministry of Fisheries, Wellington, New Zealand.

Freeman AND & Wilson K-J. 2002. Westland petrels and hoki fishery waste: opportunistic use of a readily available resource. Notornis 49: 139-144.

French RK, Miskelly CM, Muller CG, Russ RB, Taylor GA & Tennyson AJD. 2020. Birds of Enderby Island, Auckland Islands, New Zealand subantarctic. Notornis 67: 189-212.

Fretwell PT, Scofield P & Phillips RA. 2017. Using super-high resolution satellite imagery to census threatened albatross. Ibis 159: 481-490.

Frost PGH, Baker B, Fischer JH, Sagar PM. 2025. Population survey of southern Buller’s albatross *Thalassarche bulleri bulleri* on the Solander Islands | Hautere, March 2024. Marine Ornithology 53: 361-371.

Frost PGH, Bell MD & Taylor GA. 2021C. Trial-camera assessment of the fates of Northern Royal Albatross and Northern Buller’s Mollymawk chicks: 2021 breeding season, Motuhara. Conservation Services Programme, Department of Conservation, Wellington, New Zealand.

Frost PGH. 2017. Aerial census of Northern Royal Albatross (*Diomedea sanfordi*) fledglings on Rangitatahi (The Sisters) and Motuhara (Forty-fours), July 2017. Conservation Services Programme, Department of Conservation, Wellington, New Zealand.

Frost PGH. 2019. Aerial surveys of Northern Royal Albatross (*Diomedea sanfordi*) on the Chatham Islands: 2017-2018 breeding season. Conservation Services Programme, Department of Conservation, Wellington, New Zealand.

Frost PGH. 2021A. Status of Northern Royal Albatross *Diomedea sanfordi* nesting on the Chatham Islands, December 2020. Conservation Services Programme, Department of Conservation, Wellington, New Zealand.

Frost PGH. 2021B. Numbers of Northern Royal Albatross chicks and Northern Giant Petrel adults on the Chatham Islands, September 2020. Conservation Services Programme, Department of Conservation, Wellington, New Zealand.

Frost PGH. 2022. A Census of Northern Royal Albatross nesting on the Chatham Islands, February 2022. Conservation Services Programme, Department of Conservation, Wellington, New Zealand.

Frost PGH. 2024A. Nesting of Northern Royal Albatross | Toroa *Diomedea sanfordi* on the Chatham Islands: 2022-23 breeding season. Conservation Services Programme, Department of Conservation, Wellington, New Zealand.

Frost PGH. 2024B. Aerial survey of Northern Royal Albatross | Toroa (*Diomedea sanfordi*) populations on the Chatham Islands, December 2023. Conservation Services Programme, Department of Conservation, Wellington, New Zealand.

Frost PGH. 2026. Trail-camera monitoring of White-capped Albatross (*Thalassarche steadi*) on Disappointment Island: 2018, 2022 and 2023) breeding seasons. Conservation Services Programme, Department of Conservation, Wellington, New Zealand.

Fu D & Sagar P. 2016. The 2014 demographic assessment of the Snares islands population of Southern Buller's albatross (*Diomedea bulleri bulleri*). New Zealand Aquatic Environment Biodiversity Report 165. Ministry for Primary Industries, Wellington, New Zealand.

Guard A. 1968. Wildlife breeding locations: albatross distribution. No. I in a series of two unpublished maps drawn from observations by members of the 1964-65-66-67-68 expeditions; fieldwork and research by CG Surrey and D Paull.

Hamilton S, Kemp J, Elliott G, Walker K, Wiltshire A 2000. Monitoring Gibson's wandering albatross; 1999/2000. Conservation Services Programme, Department of Conservation, Wellington, New Zealand.

Imber MJ. 1987. Breeding ecology and conservation of the black petrel (*Procellaria parkinsoni*). Notornis 34: 19–39.

Marchant S & Higgins PJ. 1990. Handbook of Australian, New Zealand and Antarctic Birds. Volume 1: Ratites to ducks. Part A, Ratites to petrels. Oxford University Press, Melbourne, Australia.

Mattern T. 2022. Tawaki Project: Bounty-Antipodes expedition 2022.

Mattern T. 2024a. Tawaki Project: Antipodes-Bounty expedition 2023/24.

Mattern T. 2024b. Tawaki Project: Bounty-Antipodes expedition 2024.

Michler C & Wickes C. 2023. POP2022-11. Campbell Island/Motu Ihupuku Seabird Research & Operation Endurance February 2023. Conservation Services Programme, Department of Conservation, Wellington, New Zealand.

Mischler C, Moore P, Thompson H, Hamilton K, Pryde M. 2025. Campbell Island Seabird Research. Conservation Services Programme, Department of Conservation, Wellington, New Zealand.

Mischler C, Thompson T, Moore P, Philip B & Wickes C. 2024. Campbell Island Seabird Research. Conservation Services Programme, Department of Conservation, Wellington, New Zealand.

Mischler C. 2020. Campbell Island/ Motu Ihupuku Seabird Research; Operation Endurance March 2020. Conservation Services Programme, Department of Conservation, Wellington, New Zealand.

Miskelly CM. 1984. Birds of the Western Chain, Snares Islands 1983-84. Notornis, 31: 209–223.

Mitchell SJ & Ensor PH. 1986. Hooker's sea lion survey, Enderby Island, Auckland Islands, January 1980. In: Penniket A, Garrick A & Breese E. (compilers) Preliminary reports of expeditions to the Auckland Islands Nature Reserve 1973–1984. Reserve Series. Department of Lands and Survey. Wellington, New Zealand.

Moore PJ & Moffat RD. 1990. Research and management projects on Campbell Island 1987-88. Science and Research Internal Report 57. Department of Conservation, Wellington, New Zealand.

Moore PJ, Larsen EJ, Charteris M & Pryde M. 2012. Southern royal albatross on Campbell Island/Motu Ihupuku: solving a band injury problem and population survey, 2004-08. DOC Research and Development Series 333. Department of Conservation, Wellington, New Zealand.

Moore PJ, Scott JJ, Joyce LJ & Peart M. 1997a: Southern royal albatross *Diomedea epomophora epomophora* census on Campbell Island, 4 January–6 February 1996, and a review of population figures. Science and Research Series 101. Department of Conservation, Wellington, New Zealand.

Moore PJ, Waugh SM, West C & Mitchell G. 1997b. Preliminary results of a Southern royal albatross *Diomedea epomophora epomophora* census, Campbell Island, 12 January - 10 February 1995. Science and Research series No. 100. Department of Conservation, Wellington, New Zealand.

Parker G & Rexer-Huber K. 2020. Drone-based Salvin's albatross population assessment: feasibility at the Bounty Islands. Conservation Services Programme, Department of Conservation, Wellington, New Zealand.

Parker G, Sagar P, Thompson D & Rexer-Huber K. 2017. The establishment of a marked population of white-capped albatross to allow estimation of adult survival & other demographic parameters, Disappointment Island, Auckland Islands. Conservation Services Programme, Department of Conservation, Wellington, New Zealand.

Parker GC, Elliott G, Walker K & Rexer-Huber K. 2022. Gibson's albatross and white-capped albatross in the Auckland Islands 2021-2022. Conservation Services Programme, Department of Conservation, Wellington, New Zealand.

Parker GC, Rexer-Huber K, Walker K & Elliott G. 2023. Antipodean wandering albatross population study 2023. Conservation Services Programme, Department of Conservation, Wellington, New Zealand.

Paull D & Surrey G. 1969. Southern royal albatross and giant petrel on Campbell Island over the years 1966, 1967, 1968, 1969. Unpublished nest records and reports, Volumes 1-3.

Rexer-Huber K, Elliott G, Thompson D, Walker K & Parker GC. 2019. Seabird populations, demography and tracking: Gibson's albatross, white-capped albatross and white-chinned petrels in the Auckland Islands 2018-19. Conservation Services Programme, Department of Conservation, Wellington, New Zealand.

Rexer-Huber K, Elliott G, Walker K, Thompson D & Parker GC. 2020. Seabird population research: Gibson's albatross and white-capped albatross in the Auckland Islands 2019-20. Conservation Services Programme, Department of Conservation, Wellington, New Zealand.

Rexer-Huber K, Mattern T, Ellenberg U & Sagar P. In prep. Salvin's Albatross Western Chain population study. Conservation Services Programme, Department of Conservation, Wellington, New Zealand.

Rexer-Huber K, Whitehead E, Parker G, Patterson E, Walker K, Welch J & Elliott G. 2024. Antipodean wandering albatrosses and white-chinned petrels 2024. Conservation Services Programme, Department of Conservation, Wellington, New Zealand.

Rexer-Huber K, Whitehead E, Walker K & Elliott G. 2025. Antipodean wandering albatrosses and white-chinned petrels 2025. Conservation Services Programme, Department of Conservation, Wellington, New Zealand.

Rebergen A. 2000. Royal albatross counts Chatham Islands. Period November 1972-August 1975 and from September 1989-April 2000. Unpublished report. Department of Conservation, Wellington, New Zealand.

Richard Y, Perriman L, Lalas C & Abraham ER. 2015. Demographic rates of northern royal albatross at Taiaroa Head, New Zealand. PeerJ 3: e906.

Robertson CJR & Richdale LE. 1993. The breeding phenology of the Royal Albatross (*Diomedea epomophora sanfordi*) 1937-1974. Conservation Advisory Science Notes No. 48. Department of Conservation, Wellington, New Zealand.

Robertson CJR & van Tets GF. 1982. The status of birds at the Bounty Islands. Notornis 29: 311-336.

Robertson CJR, Bell D & Scofield P. 2003. Population Assessment of the Chatham Albatross at The Pyramid, December 2001. DOC Science Internal Series 91. Department of Conservation, Wellington.

Robertson CJR, Bell D & Scofield P. 2004. Population assessment of the Chatham mollymawk at the Pyramid, September and December, 2003. Unpublished report.

Robertson CJR. 1975. Report on the distribution, status, and breeding biology of the Royal Albatross, Wandering Albatross and White-capped Mollymawk on the Auckland Islands. In Yaldwyn JC (ed). Preliminary Results of the Auckland Islands Expedition 1972-1973. Department of Lands and Survey, Wellington, New Zealand.

Robertson CJR. 1991. Questions on the harvesting of Toroa in the Chatham Islands. Science & Research Series 35. Department of Conservation, Wellington.

Robertson CJR. 1993. Timing of egg laying in the Royal Albatross (*Diomedea epomophora*) at Taiaroa Head 1937-1992. Conservation Advisory Science Notes 50. Department of Conservation, Wellington, New Zealand.

Robertson CJR. 2005. Aerial Photography of Northern Royal Albatross on the Forty-Fours and Sisters Islands, Chatham Islands. Department of Conservation, Wellington, New Zealand.

Robertson G & Gales R. 1998. Albatross biology and conservation. Surrey Beatty & Sons, Chipping Norton, Australia.

Russ R. 1974. Report on activities during the December 1973 trip to Auckland Islands. 5 Dec – 20 Dec. New Zealand Wildlife Service, Wellington, New Zealand.

Sagar P & Thompson D. 2007. The impact of fisheries bycatch on Southern Buller's Mollymawks. Report on the 2006 & 2007 field season.

Sagar P, Charteris M, Parker G, Rexer-Huber K & Thompson D. 2018. Salvin's Albatross: Bounty Island population project – ground component. Conservation Services Programme, Department of Conservation, Wellington, New Zealand.

Sagar P, Rexer-Huber K, Schultz H, Simister K, Thompson D & Parker G. 2025. Population studies of Southern Buller's Albatrosses at Tini Heke | The Snares Islands. Conservation Services Programme, Department of Conservation, Wellington, New Zealand.

Sagar P, Rexer-Huber K, Thompson D & Parker G. 2024. Population studies of southern Buller's albatrosses at Tini Heke / The Snares Islands and Hautere / Solander Islands. Conservation Services Programme, Department of Conservation, Wellington, New Zealand.

Sagar P, Thompson D & Scofield P. 2017. Population study of Southern Buller's Albatross on the Snares. Deepwater Group Ltd. Nelson, Aotearoa New Zealand.

Sagar P, Torres L & Thompson D. 2009. Demography and distribution of Buller's Albatrosses Thalassarche bulleri bulleri: final research report of the 2009 field season. Conservation Services Programme, Department of Conservation, Wellington, New Zealand.

Sagar P, Torres L & Thompson D. 2010. Demography and distribution of Buller's Albatrosses Thalassarche bulleri bulleri: final research report of the 2010 field season. Conservation Services Programme, Department of Conservation, Wellington, New Zealand.

Sagar P, Torres L & Thompson D. 2012. Demography and distribution of Buller's Albatrosses Thalassarche bulleri bulleri: final research report of the 2012 field season. Conservation Services Programme, Department of Conservation, Wellington, New Zealand.

Sagar P, Torres L & Thompson D. 2013. Demography and tracking of Buller's Albatrosses at The Snares, and tracking of Snares Crested Penguins and Rockhopper Penguins from The Snares and Campbel Island respectively: Final research report of the 2013 field season. Conservation Services Programme, Department of Conservation, Wellington, New Zealand.

Sagar P. 2014. Population studies of Southern Buller's Albatrosses on the Snares. Conservation Services Programme, Department of Conservation, Wellington, New Zealand.

Sagar P. 2015. Population study of Southern Buller's Albatrosses on the Snares. Conservation Services Programme, Department of Conservation, Wellington, New Zealand.

Sagar PM & Stahl J-C. 2005. Increases in the numbers of breeding pairs in two populations of Buller's Albatross (*Thalassarche bulleri bulleri*). Emu – Austral Ornithology 105: 49-55.

Sagar PM, Charteris MR & Scofield RP. 2014. Salvin's albatross population size and survival at the Snares Western Chain. Conservation Services Programme, Department of Conservation, Wellington, New Zealand.

Sagar PM, Charteris MR, Carroll JWA & Scofield PR. 2011. Population size, breeding frequency and survival of Salvin's albatrosses (*Thalassarche salvini*) at the Western Chain, The Snares, New Zealand. Notornis 58: 57-63.

Sagar PM, Molloy J, Tennyson AJD & Butler D. 1994. Numbers of Buller's Mollymawks breeding at the Snares Islands. Notornis 41: 85-92.

Sagar PM, Stahl J-C, Molloy J, Taylor GA & Tennyson AJD. 1999. Population size and trends within the two populations of Southern Buller's Albatross *Diomedea bulleri bulleri*. Biological Conservation 89: 11-19.

Sagar PM. 1977. Birds of the Western Chain, Snares Islands, New Zealand. Notornis 24: 178-183.

Scofield P, Fraser M & Robertson CJR. 2008. Population dynamics of the Chatham Albatross at the Pyramid, 19-29 November 2007. Unpublished report.

Scofield P. 2011. Data collection of demographic, distributional, and trophic information on selected seabird species to allow estimation of effects of fishing on populations viability. Ministry of Fisheries, Wellington, New Zealand.

Taylor GA. 1988. Report to the Department of Conservation on an expedition to the Auckland Islands National Reserve, February 1988. Department of Conservation, Wellington, New Zealand.

Taylor GA. 1988. Report to the Department of Conservation on an expedition to the Auckland Islands National Reserve, February 1988. Department of Conservation, Wellington.

Taylor RH. 1971. Influence of man on vegetation and wildlife of Enderby and Rose Islands, Auckland Islands. New Zealand Journal of Botany 9: 225–268.

Taylor RH. Bell BD & Wilson PR. 1970. Royal albatrosses, feral sheep and cattle on Campbell Island. New Zealand Journal of Science 13: 78–88.

Thompson D & Sagar P. 2008a. Annual report 2006/07: A population and distributional study of white-capped albatross (Auckland Islands). Conservation Services Programme, Department of Conservation, Wellington, New Zealand.

Thompson D & Sagar P. 2008b. Annual report 2007/08: A population and distributional study of white-capped albatross (Auckland Islands). Conservation Services Programme, Department of Conservation, Wellington, New Zealand.

Thompson D & Sagar P. 2020. Population studies of southern Buller's albatrosses on the Snares Islands | Tini Heke. Conservation Services Programme, Department of Conservation, Wellington, New Zealand.

Thompson D & Sagar P. 2022. Population studies of southern Buller's Albatross on the Snares. Conservation Services Programme, Department of Conservation, Wellington, New Zealand.

Thompson D & Sagar P. 2023. Population studies of southern Buller's albatrosses on Tini Heke the Snares. Conservation Services Programme, Department of Conservation, Wellington, New Zealand.

Thompson D, Sagar P, Baker B & Jensz K. 2017. Southern Buller's Albatross survey at Solander Islands 2016. Conservation Services Programme, Department of Conservation, Wellington, New Zealand.

Thompson DR. 2019. Data collection of demographic, distributional and trophic information on selected seabird species to allow estimation of effects of fishing on population viability: Synthesis of population and demographic work. New Zealand Aquatic Environment and Biodiversity Report no. 228. Fisheries New Zealand, Wellington, New Zealand.

Thompson T. 2025. Advancing remote monitoring of albatrosses through emerging technologies to inform conservation. MSc thesis. University of Otago, Dunedin, New Zealand.

Walker K & Elliott G. 2002. Population changes and biology of the wandering albatross *Diomedea exulans gibsoni* at the Auckland Islands. DOC Science Internal Series 68. Department of Conservation, Wellington, New Zealand.

Walker K & Elliott G. 2005. Population changes and biology of the Antipodean wandering albatross. Notornis 52: 206-214.

Walker K & Elliott G. 2015. Gibson's wandering albatross population study 2014-15. Conservation Services Programme, Department of Conservation, Wellington, New Zealand.

Walker K & Elliott G. 2022. Antipodean wandering albatross satellite tracking and population study on Antipodes Island in 2021 and 2022. Conservation Services Programme, Department of Conservation, Wellington, New Zealand.

Walker K, Elliott G, Parker GC & Rexer-Huber K. 2023. Gibson's wandering albatross: population study and potential for drone-based while-island census. Conservation Services Programme, Department of Conservation, Wellington, New Zealand.

Walker K, Elliott G, Rexer-Huber K & Parker G. 2017. Gibson's wandering albatross population study and census 2016/17. Conservation Services Programme, Department of Conservation, Wellington, New Zealand.

Walker KJ, Elliott GP, Rexer-Huber K, Parker GC, Sagar PM & McClelland PJ. 2021. Shipwrecks and mollymawks: an account of Disappointment Island Birds. Notornis 67: 213-245.

Warham J & Bell BD. 1979. The birds of Antipodes Island, New Zealand. Notornis 26: 121-169.

Warham J & Bennington SL. 1983. A census of Buller's Albatross Diomedea bulleri at the Snares Islands. Emu 83: 112-114.

Waugh SM & Wilson KJ. Threats and threat status of the Westland Petrel *Procellaria westlandica*. Marine Ornithology 45: 195-203.

Waugh SM, Barbraud C, Adams L, Freeman AND, Wilson K-J, Wood G, Landers TJ & Baker GB. 2015. Modelling the demography and population dynamics of a subtropical seabird, and the influence of environmental factors. The Condor: Ornithological Applications 117: 147-164.

Waugh SM, Barbraud C, Delord K, Simister KLJ, Baker GB, Hedley GK, Wilson K-J & Rands DRD. 2020. Trends in density, abundance, and response to storm damage for Westland Petrels *Procellaria westlandica*, 2007-2019.

Waugh SM, Doherty PF, Freeman AND, Adams L, Wood GC, Bartle JA & Hedley GK. 2006. 2006. Demography of Westland Petrels (*Procellaria westlandica*), 1995–2003. Emu 106: 219-226.

Waugh SM, Sagar PM & Paull D. 1997. Laying dates, breeding success and annual breeding of southern royal albatrosses *Diomedea epomophora* at Campbell Island during 1964–69. Emu 97: 194–199.

Westerskov K. 1963. Ecological factors affecting the distribution of a nesting royal albatross population. Pp. 795–811 in Proceedings of the 13th International Ornithological Congress.

Wilson PR & Elliott GP. 1981. Report on sheep, cattle and royal albatross counts at Campbell Island during 1979/80 and 1980/81: with other biological notes recorded during the 1979/80 visit. Unpublished file report, Ecology Division.

Wood GC & Otley HM. 2013. An assessment of the breeding range, colony sizes and population of the Westland Petrel (*Procellaria westlandica*). New Zealand Journal of Zoology 40: 186–195.j

Zhang J, Bell EA & Roberts JO. 2020. Demographic assessment of black petrels (*Procellaria parkinsoni*) on Great Barrier Island (Aotea Island). New Zealand Aquatic Environment and Biodiversity Report N. 244. Fisheries New Zealand, Wellington, New Zealand.